Upper Cretaceous to Recent plate tectonics, basin formation and tectono-stratigraphy of the Lower Magdalena valley and San Jacinto fold belt of Northwestern Colombia: implications for hydrocarbon systems

Dissertation zur Erlangung des Doktorgrades

im Fachbereich Geowissenschaften der

Freien Universität Berlin

vorgelegt von

Josué Alejandro Mora Bohórquez

Juni, 2018

Erstgutachter: Prof. Dr. Onno Oncken

GeoForschungZentrum, Telegrafenberg, Haus C, Raum 224, 14473, Potsdam

Zweitgutachter: Prof. Dr. Christoph Heubeck

Friedrich-Schiller-Universität Jena, Institut für Geowissenschaften, Burgweg 11, Raum H102, 07749, Jena

Prüfungskommission:

Prof. Dr. Anne Bernhardt (Vorsitz)

Prof. Dr. Onno Oncken

Prof. Dr. Christoph Heubeck

Prof. Dr. Serge Shapiro

Dr. Jörg Giese

Upper Cretaceous to Recent plate tectonics, basin formation and tectono-stratigraphy of the Lower Magdalena valley and San Jacinto fold belt of Northwestern Colombia: implications for hydrocarbon systems

A Dissertation submitted in partial fulfillment of the requirements for the degree:

Doctor of Natural Sciences in the field of Earth Sciences

to the department of Earth Sciences of the Free University of Berlin.

Author:

Josué Alejandro Mora Bohórquez

Place and date of submission:

Berlin, December 15, 2017

Date of Viva Voce/ Defense:

Thursday 7th June, 2018

Abstract

In this thesis I used a regional geological and geophysical dataset to reconstruct the Late Cretaceous to Recent evolution of the Lower Magdalena Valley basin and San Jacinto fold belt of NW Colombia. My detailed interpretations of reflection seismic data and new geochronology analyses reveal that the Lower Magdalena basement is the northward continuation of the basement terranes of the northern Central Cordillera, consisting of Permo-Triassic metasediments, which were intruded by Late Cretaceous granitoids. Structural analyses suggest that the NE-SW trend of basement faults in the northeastern Lower Magdalena is inherited from a Jurassic rifting event, while the ESE-WNW trend in the western part is inherited from a Late Cretaceous to Eocene strike-slip and extension episode. The Upper Cretaceous to lower Eocene sediments preserved in the present day San Jacinto fold belt were deposited in a forearc marine basin formed by the oblique convergence between the Caribbean and the South American plates. A lower to middle Eocene angular unconformity at the top of the San Cayetano sequence, the termination of the activity of the Romeral Fault system and the cessation of arc magmatism are interpreted to indicate the onset of low-angle subduction of the Caribbean plateau beneath South America, which occurred between 56 and 43 Ma. Flat subduction of the plateau has continued to the present and would be the main cause of amagmatic post-Eocene deposition and formation of the Lower Magdalena Valley basin. After the collapse of a pre-Oligocene magmatic arc, late Oligocene to early Miocene fault-controlled subsidence allowed initial infill of the Lower Magdalena with relatively low sedimentation rates. Extensional reactivation of inherited, pre-Oligocene basement faults was crucial for the tectonic segmentation of the basin with the formation of its two depocenters (Plato and San Jorge). Oligocene to early Miocene uplift of Andean terranes made possible the connection of the Lower and Middle Magdalena valleys, and the formation of the most important Colombian drainage system (Magdalena River system). This drainage system started delivering high volumes of sediment in middle Miocene times, as fault-controlled subsidence was gradually replaced by sagging due to increased sedimentary load. Such an increase in sedimentation delivering great sediment volumes to the trench, caused the formation of forearc highs in San Jacinto and of an accretionary prism farther to the west. These results highlight the fundamental role of changes in plate kinematics, of the inherited basement structure and of sediment flux on the evolution of forearc basins such as Lower Magdalena and San Jacinto.

Based on my interpretations and results about the evolution of the Lower Magdalena and San Jacinto, a three-dimensional model of the Lower Magdalena Valley basin was built from seismic and well data, and used to reconstruct the thermal and maturation history of the basin. I reconstructed the stratal architecture of the basin, implemented within the model episodes of uplift and erosion, and built a geothermal gradient map, which was used to construct heat flow maps for 3-D modeling. Model results indicate that the onset of hydrocarbon generation occurred at ~15 Ma (middle Miocene) for upper Oligocene to lower Miocene hydrocarbon source rocks in the northern part of the basin (Plato depocenter), while younger, lower Miocene sources started generating at ~ 9 Ma (middle-late Miocene). Maturation was influenced by sedimentation at very high rates of thick, deep marine to deltaic, Oligocene to upper Miocene sequences. Late Miocene generation was interrupted by shortening and uplift events at Pliocene (4-3 Ma) and Pleistocene times, though it appears to be ongoing in main depocenters. Low to fair source rock quality appears to be compensated by high thicknesses of the Oligocene to lower Miocene sources, which would still be generating below 3,350 m (11,000 ft) in the main pod of active source rock in the northern Lower Magdalena (Plato depocenter). By contrast, the effects of shortening pulses and low heat flow would have inhibited maturation of Oligocene to lower Miocene source rocks in the San Jorge graben of the southern Lower Magdalena, suggesting the need of additional hydrocarbon sources to explain the dry gas occurrences in that part of the basin. Proposed additional sources are pre-Oligocene units preserved in the western San Jorge depocenter, and biogenic generation. The results of this

thesis provide new insights into the controls of plate tectonics and basin evolution on petroleum systems.

(German version of the abstract can be found in *Zusammenfassung*)

Foreword

Throughout the three years undertaken as a PhD candidate I have been able to publish my work as a first author (2 published papers and 2 papers in the final stages of internal review). This PhD thesis is therefore a concatenation of my contributions to this work. I conceived and designed my thesis and did all the writing of the papers and chapters, as well as 79 of the 87 figures. Basement and detrital zircon geochronology and isotope geochemistry analyses were done by Prof. Mauricio Ibáñez-Mejía, at the Arizona LaserChron Center, University of Arizona, U.S.A. Paleo-tectonic reconstructions and measurement of tectonic plate convergence velocitites and obliquities were done by Dr. Eline Le Breton (Freie Universität Berlin). Prof. Dr. Claudio Faccenna (Universita Roma Tre) helped in the paleo-tectonic reconstructions. Dr. Robert Ondrak (GFZ) provided PetroMod software licenses, as well as advise and support on multi-dimensional basin and petroleum system modelling and organic geochemistry. Co-authors who are current and previous colleagues at Hocol S.A. (Bogotá, Colombia) provided ideas and insight, and some of them (M. de Freitas and V. Vélez) also gave their approval for using and publishing Hocol's data. Colleagues at Ecopetrol (Bogotá) provided ideas about the evolution the northern Andes, about basin modelling and also helped with the compilation and regional evaluation of geochemical data in the study area.

Contents

1 Introduction and Motivation

Colombia is a country located in northwestern South America, with coasts in the Caribbean Sea and the Pacific Ocean and with two major morphological domains, the Andean domain to the W and NW, and the Llanos and Amazonian domain to the E and SE (**Figure 1.1**). It has an enormous natural diversity due to its tropical location and to its varied topography and altitudinal range, going from the sea level to almost 6,000 m.a.s.l. Such a diversity is closely related to its geological evolution and configuration which has been the result of the complex interaction of the South American continental plate with the Farallones-Nazca and Caribbean oceanic plates and with the Chocó-Panamá block. While the easternmost part of the country where the South American pre-Cambrian shield is exposed, has remained relatively undisturbed by such interaction, clear evidences of it are observed in the central and western parts where the Andes has been divided into three mountain ranges (Eastern, Central and Western Cordilleras) which have active volcanism (Central Cordillera) and seismicity.

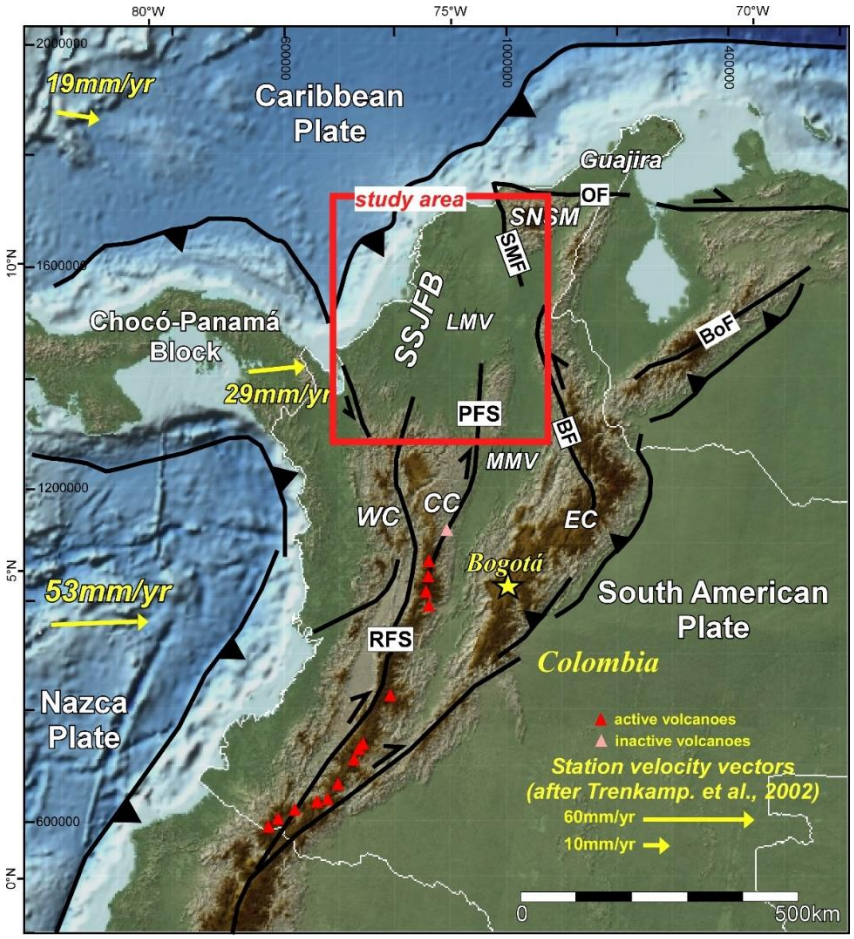

Figure 1.1. Tectonic map of northwestern South America with topography and bathymetry, showing the location of my study area (red square), which includes the Lower Magdalena Valley basin (LMV) and the Sinú-San Jacinto fold belt (SSJFB). Present-day tectonic plate motions are shown in yellow (after *Trenkamp et al., 2002*) and active volcanoes are plotted as red triangles. WC: Western Cordillera; CC: Central Cordillera; EC: Eastern Cordillera; RFS: Romeral Fault System; PFS: Palestina Fault System; BF: Bucaramanga Fault; SMF: Santa Marta Fault; OF: Oca Fault; BoF: Boconó Fault.

In the areas between the Colombian mountain ranges there are around fifteen onshore sedimentary basins preserved, some of which have important hydrocarbon and coal resources and production. As it occurs globally, hydrocarbon exploration has been one of the most important drivers of geological and geophysical data acquisition and basin studies. For this reason, the Colombian basins with more hydrocarbon reserves and production, such as the Llanos and Middle Magdalena Valley, are the best studied and understood in terms of their formation and evolution. However, today the most prolific onshore Colombian basins are relatively well-explored and it appears that the "easy oil" has already been found, making new hydrocarbon discoveries in the onshore basins a much more challenging task. Explorers are then directing their attention to less explored basins which have been less studied and remain poorly understood. Nevertheless, potential hydrocarbon resources in such basins remains uncertain and hydrocarbon exploration implies high risk of failure. Therefore, in order to reduce such risk, there is an urgent need to acquire new data and to carry out updated regional studies focused on understanding the formation and evolution of those basins, and hence their hydrocarbon systems and potential.

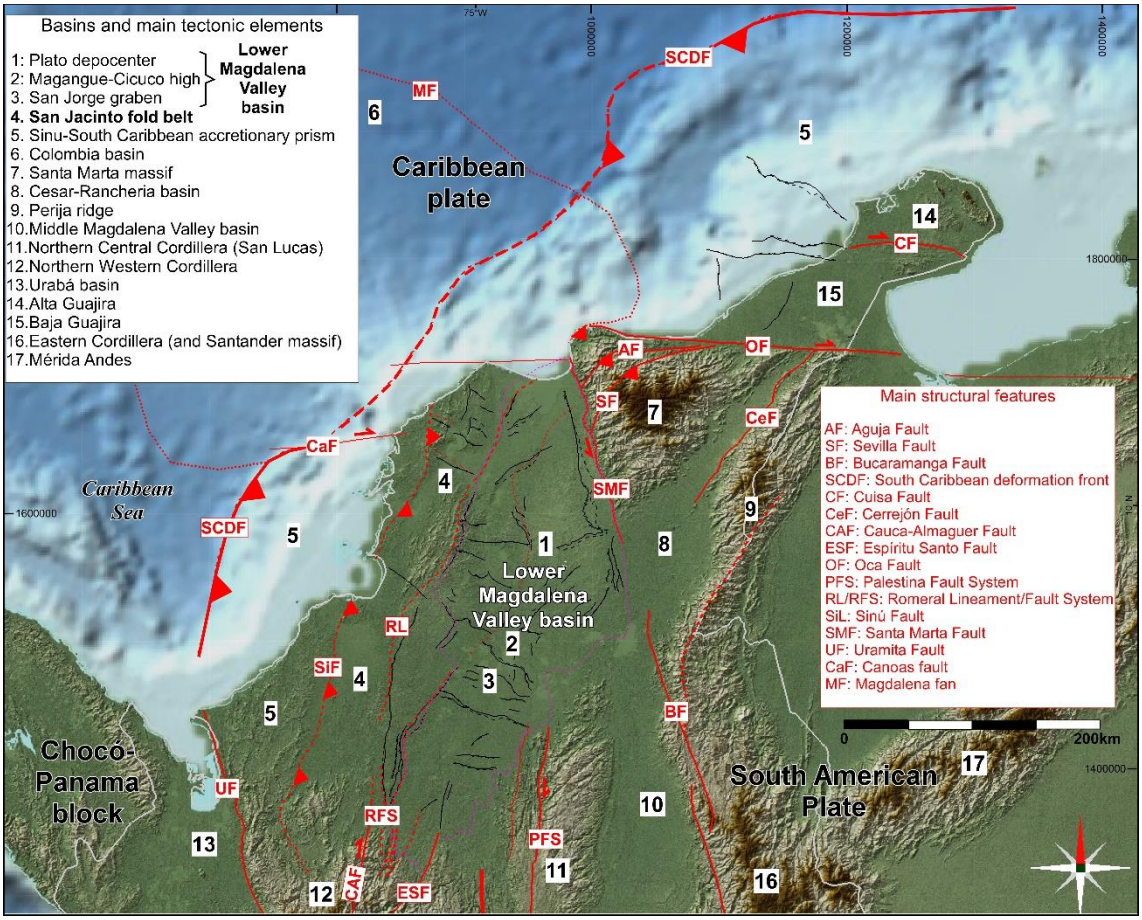

Figure 1.2. Basins and main tectonic elements of northwestern Colombia and the Caribbean. Of relevance for this thesis are numbers 1 to 4, corresponding to the Lower Magdalena Valley basin and the San Jacinto fold belt. Surface faults and lineaments are in red while subsurface faults are in black.

The basins of northwestern Colombia such as Lower Magdalena Valley, Guajira and Sinú-San Jacinto have recently become the focus of renewed hydrocarbon exploration, in spite of the fact that some of the first and oldest wells in Colombia were drilled there in the beginning of the twentieth century. In the last couple of years I have been working on hydrocarbon exploration in two of these basins, the Lower Magdalena Valley basin (LMV) and the San Jacinto fold belt (SJFB, **Figure 1.2**), and I have noticed that they are quite complex in terms of stratigraphy and structure,

and that such a complexity could be the cause of inconsistencies in the previously proposed tectonic and basin models. For example, quite contrasting basin classifications have been proposed for the LMV and SJFB, such as foreland, back-arc, passive margin and more recently as forearc. These contrasting interpretations are clearly showing us that there's a lack of more robust studies which provide a satisfactory explanation of the formation and evolution of those basins. This issue has direct repercussions on our understanding of hydrocarbon systems and therefore on the success of hydrocarbon exploration in these Colombian basins. Therefore, the motivation for carrying out this study comes from hydrocarbon prospectivity standpoint and trying to establish a clearer link between plate tectonics, basins evolution and hydrocarbon prospectivity in NW Colombia. For any company doing hydrocarbon exploration, in order to have a good prospect inventory which will guarantee exploratory success, it is essential to have solid foundations, such as a proper understanding of the plate tectonic history and of the basin formation and evolution. Hence, my thesis will focus on attempting to provide more solid foundations on top of which hydrocarbon exploration activities will hopefully be carried out in a more efficient and successful way.

In order to obtain a better understanding of the formation and evolution of the LMV and SJFB, as well as of the hydrocarbon systems that exist, several questions must be answered such as:

1. What is the structure and age of the basement underneath such basins? How, when, and in which tectonic setting was it formed?
2. How was the paleo-tectonic evolution of NW Colombia and how did it influence the formation and evolution of the SJFB and LMV?
3. What is the current configuration of the convergent margin between the Caribbean and South American plates in NW Colombia?
4. What kind of basins are the SJFB and LMV and which were the mechanisms that controlled their formation and evolution?
5. What are the implications of the plate tectonic and basin evolution of the LMV and SJFB on hydrocarbon systems?

With the objective of answering to these questions, I have reconstructed the evolution of the Lower Magdalena Valley basin and San Jacinto fold belt of northwestern onshore Colombia, using a regional geological and geophysical database kindly provided by Hocol S.A. Such reconstruction provided the input for producing multi-dimensional basin and petroleum system models which will hopefully help in the hydrocarbon prospectivity assessment of the basins. To achieve such a goal I have organized the thesis in such a way that I establish a link between plate tectonics, basin formation and petroleum systems (**Figure 1.3**), trying to set more robust foundations for the hydrocarbon exploration activities focused on play and prospect assessment (upper part of the pyramid in **Figure 1.3**).

1.1 Thesis organization

According to the aforementioned and after providing a summary of the regional geological context (*Chapter 2*), I continue with a study of the basement underneath the Lower Magdalena Valley basin (*Chapter 3*, *Mora et al., 2017a*) , based on the analysis of potential methods, reflection seismic interpretation, well data and sampling, basement U-Pb zircon geochronology and Hf-isotope geochemistry, in order to characterize the basement in terms of structure, age and possible formation mechanisms This study is tackling the first question about the basement underneath the LMV and SJFB, though it has been focused mainly on the LMV, due to the scarcity of basement data in the SJFB. In *Chapter 4*, I present the results of a tectono-stratigraphic study of the pre-Oligocene (Upper Cretaceous to Eocene) sedimentary sequences in the San Jacinto fold belt, in which I also established a link between the deposition of such sequences and the Cretaceous to Eocene plate kinematics and convergence history between the Caribbean oceanic plate and the South American

continental plate (*Mora et al., 2017b*). This chapter is therefore providing answers to questions 2 and 4, about the Late Cretaceous to Eocene paleo-tectonic evolution of NW Colombia. In this chapter I also propose a three-dimensional geometric model of the convergent margin of NW South America and the Caribbean, therefore it is also addressing question 3 about the current configuration of NW Colombia. In *Chapter 5*, I reconstruct the subsidence, sedimentation and paleo-geographic history of the Lower Magdalena Valley forearc basin, calculate how much it was extended, and propose possible mechanisms controlling basin evolution, in the absence of major changes in plate kinematics and within an interpreted flat-slab subduction setting. This chapter is providing answers to questions 2 and 4 by presenting the Oligocene to Recent paleo-geography and facies distribution, paleo-tectonic reconstructions and the analyses of basin subsidence, sedimentation and extension. Based on the previously proposed basin formation and evolution, I constructed a three-dimensional model of the Lower Magdalena Valley basin of NW Colombia from seismic and well data, and the results of such modeling are included as *Chapter 6* of this thesis. This chapter is thus providing answers to question 5 about the implications for petroleum systems in the LMV. The thesis is completed by *Chapter 7* which synthesizes the findings of my PhD and presents the most relevant issues that I consider should be the objective of future research.

1.2 Database and methodology

My thesis is focused in the plate tectonic and basin scale aspects which make up the foundation of the hydrocarbon exploration pyramid depicted in **Figure 1.3**. It is based to a great extent on my detailed interpretation and mapping in two-way-time (TWT) of reflection seismic data provided by my employer, Hocol S.A. Approximately 30,000 km of 2-D seismic and more than 3,000 km^2 of 3-D seismic were interpreted and tied to around 250 exploratory and stratigraphic wells in both the LMV and SJFB (**Figure 1.4**). However, I also had access to several seismic lines and a few exploratory wells located in offshore areas, which were very important for the interpretation in the boundary between the oceanic Caribbean plate and the continental South American plate. The 2D-seismic database includes numerous surveys acquired by oil and gas companies during different exploratory phases since the 60s, hence there's a wide variety of seismic data quality. Seismic data quality and density is much higher in the LMV than in the SJFB and most of this seismic has been pre-stack time-migrated by specialized processing companies. Seismic interpretation was carried out in a regional project in the software Petrel v. 2013 (Schlumberger), in which the seismic surveys were positioned and tied using a datum (mean sea level) and a replacement velocity (2,000 m/sec). Well data including electrical logs, lithological and biostratigraphic tops, was loaded into the project and tied to the seismic data by constructing synthetic seismograms. The Petrel project which I used for this thesis was created at Hocol's offices in Bogota, and data loading and quality checking was carried out by Hocol exploration staff. However, I personally quality-checked and adjusted data when necessary and I also loaded new data into the project as it became available.

I downloaded seismicity data from the study area from the Colombian Earthquake Network (Red Sismológica Nacional, http://seisan.sgc.gov.co/RSNC/) and plotted it both in map and section view, together with the seismic interpretation and maps. A total of 14,081 events were obtained, corresponding to earthquakes with Mw 1 to 9, recorded from June 1, 1993 to November 26, 2015. Additionally, I compiled the available focal mechanism solutions from published sources (*Pennington, 1981*; *Malave and Suarez, 1995*; *Corredor, 2003*; *Ekstrom et al., 2005*; *Cortes and Angelier, 2005*) and plotted them together with the structural models.

I also compiled all the available surface geology maps (e.g. *Gomez et al., 2007*; *Gomez et al.,2015*; *Ecopetrol/ICP, 2014*) and also had access to potential methods data (air gravity and magnetics acquired by *Lithosphera (2010*). In the San Jacinto fold belt, where older pre-Oligocene units are cropping out and deformation is intense, it was crucial to tie the seismic and well data to the geological maps. I also participated in a couple of field trips in several areas of San Jacinto in order

to directly see and study the units which I was interpreting in the subsurface and to collect samples for different kinds of analyses.

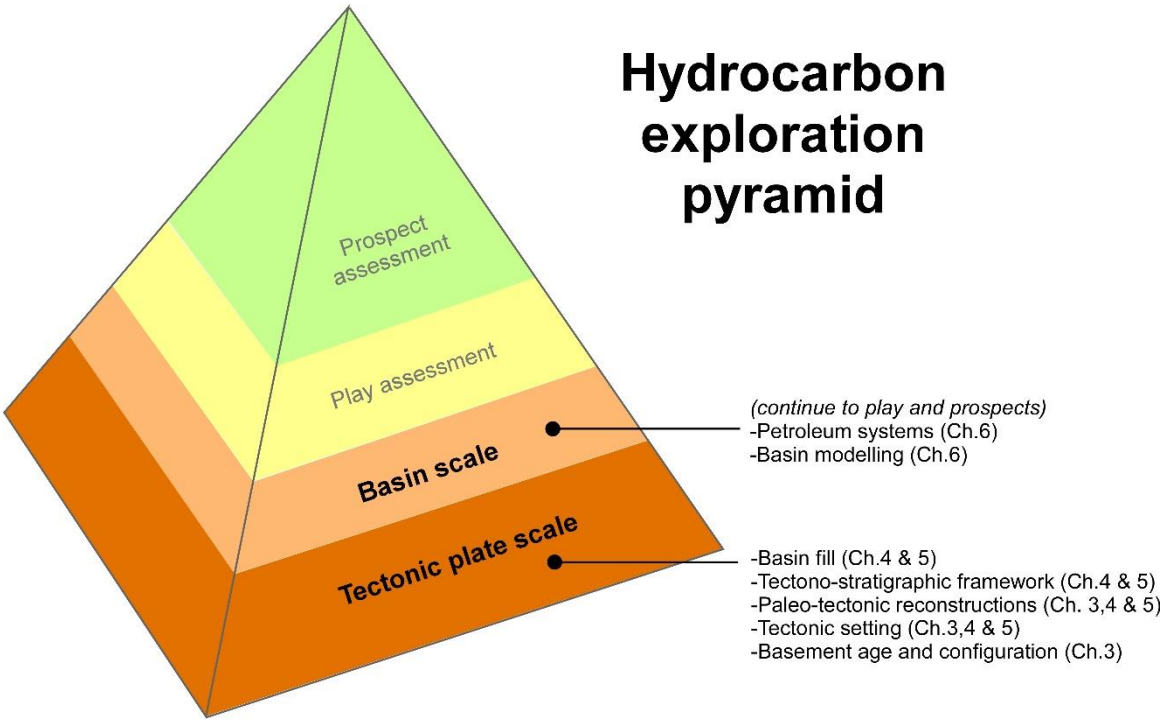

Figure 1.3. Methodology of my PhD thesis, which is finally intended to provide solid foundations for the hydrocarbon exploration activities in NW Colombia. In order to have a good prospect inventory which will guarantee exploratory success, it is essential to have solid foundations, such as a proper understanding of the plate tectonic history and of the basin formation and evolution. The exploration pyramid was inspired in Shell's Play-based exploration guide available in the internet.

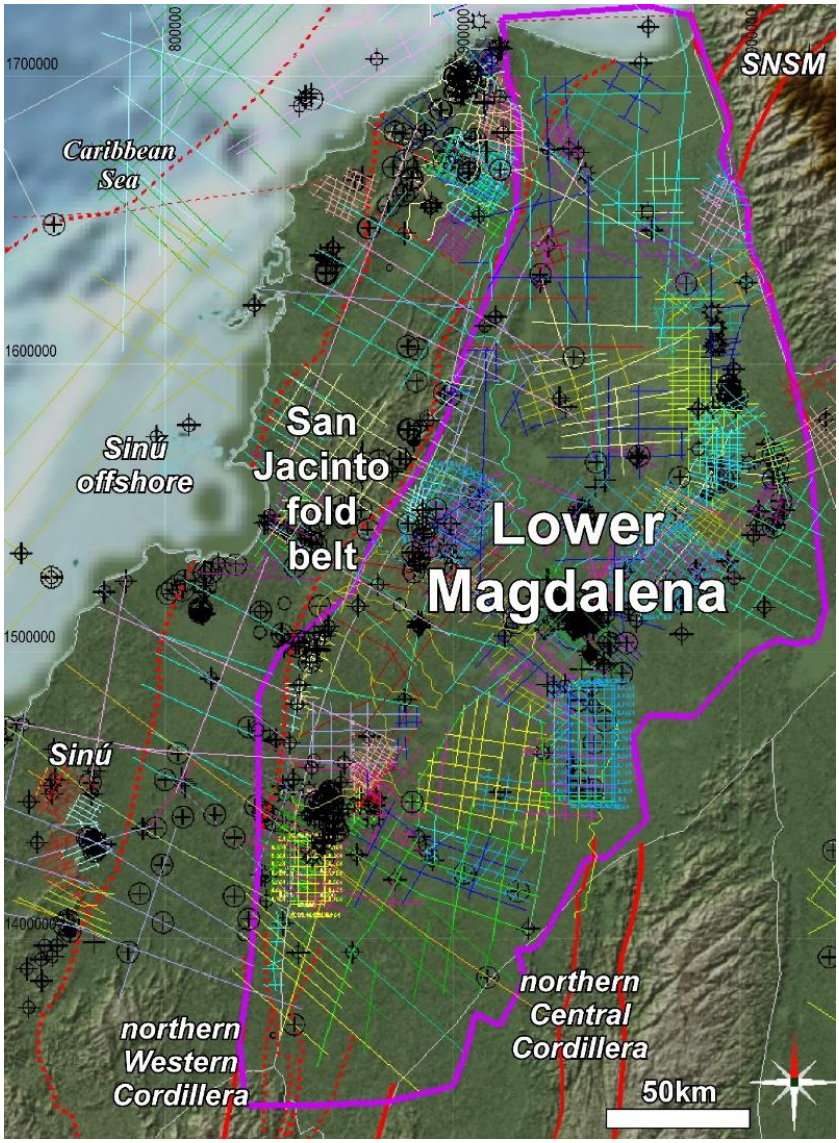

Figure 1.4. Reflection seismic and well database used for this study, provided by Hocol S.A. Colors represent different seismic surveys, wells are shown in black circles with crosses and 3D surveys are shown as rectangular grids. Magenta polygon is the limit of the LMV and red lines are major faults. SNSM: Sierra Nevada de Santa Marta.

2 Geological setting and previous studies

2.1 General aspects of the study area

The complex interaction of the Nazca, Caribbean and South American plates since Cretaceous times has created the extremely varied tectonic, geological and geomorphological configuration of Colombia that we see today (**Figure 1.1** and **Figure 1.2**). To the center and south of the country, where the main influence has been the interaction of the Farallones/Nazca and South American plates, and more recently the Chocó-Panamá block, the Andes mountains are divided into three ranges or cordilleras (Western, Central and Eastern) which are separated by two inter-mountain fluvial valleys (Cauca and Magdalena). The Central and Eastern Cordilleras are considered to be autochthonous terranes rooted in continental crust, while the Western Cordillera is considered an allochthonous terrane rooted in oceanic crust (*Duque-Caro, 1979*), which is thought to have accreted during the Mesozoic along the Romeral Fault System (*Cediel et al., 2003*). In the northern part of the country, where the influence of the Caribbean plate has been much more important, the Central and Western cordilleras terminate as they plunge to the north and get progressively buried under Tertiary sediments of the Sinú-San Jacinto fold belts and Lower Magdalena Valley basin.

There are two prominent mountain ranges in northern Colombia that are separate from the Andes and which divide different Tertiary basins. The highest one is the triangular-shaped Sierra Nevada de Santa Marta (SNSM) or Santa Marta massif, with elevations of 5,700 m.a.s.l., which separates the Sinú-San Jacinto fold belts and the Lower Magdalena Valley basin in the southwest from the Guajira basins in the northeast (**Figure 1.2**). The second prominent mountain range of northern Colombia is the Sierra de Perijá or Perijá ridge, which is located to the east of the Santa Marta massif and marks the eastern boundary of the Cesar-Ranchería basin. The Perijá ridge can reach elevations of more than 3,200 m.a.s.l. and is forming part of the political limit with Venezuela to the east. Southwest of the Sierra de Santa Marta and north of the Central Cordillera, there's a wide topographic depression that temporarily accumulates the sediment and water discharge from two of Colombia's main rivers, Magdalena and Cauca, forming the present-day Lower Magdalena Valley. The Sinú-San Jacinto fold belts are located west of the Lower Magdalena and they exhibit some uplifted areas with elevations above 500 m.a.s.l. This geomorphology is reflecting the undeformed structure of the Lower Magdalena basin versus the deformed structure of the Sinú-San Jacinto fold belts, which in fact comprises two separate fold and thrust belts with different structural styles (Sinú and San Jacinto, *Duque-Caro, 1979*; **Figure 1.2**). The northernmost portion of Colombia is the Guajira Peninsula, located to the northeast of the Sierra de Santa Marta and which comprises two separate basins, the northern one called Alta Guajira, with some low altitude topographic elevations (>500 m.a.s.l.), and the southern one called Baja Guajira which is mostly flat. In the Colombian offshore areas, there are two main geomorphological elements, the South Caribbean Deformed Belt that is adjacent to the coast and the deep Colombian basin farther to the northwest.

2.2 Geological setting

2.2.1 Studies in offshore areas

The Caribbean and northwestern Colombia offshore areas have been the studied by numerous researchers using a wide range of tools. Some of the first studies used seismic refraction and reflection profiles in the Western Caribbean and the Colombian basin, to conclude that crustal rocks are twice as thick as the average oceanic crust (*Ewing et al., 1960*). Seismic basement-related horizons (called "A" and "B") were interpreted and then correlated with wells of the Deep Sea Drilling Project (DSDP), concluding that the oceanic basement consists of basaltic sills overlain by Late Cretaceous sediments (*Edgar et al., 1971*). *Houtz and Ludwig (1977)* computed seismic velocities and layer depths from air gun/sonobuoy profiles made along the Colombian Basin and

concluded that the crustal structure of the basin is a complex arrangement of basement ridges and interposed basins that is masked by an overburden of thick, flat-lying sediments. In the eighties, *Bowland and Rosencrantz (1988)* studied the upper crustal structure of the western Colombian basin using multichannel seismic reflection profiles and concluded that this basin is underlain by a large oceanic plateau. These studies provided approximate crustal thicknesses in the Colombian basin which went from 10.1 km close to the Colombian coast, to 17.9 km to the north towards the Hess Escarpment.

2.2.2 About the origin of the Caribbean Plate

Concerning the origin and evolution of the Caribbean, there are two main interpretations, one proposes a "Pacific" origin for the Caribbean plate, implying that it has drifted long distances to its present position between the Americas (e.g. *Burke, 1988*; *Pindell and Kennan, 2009*), while the other one proposes an "in situ" origin for the plate, implying that it formed to the west of its present position but still between the two Americas (e.g. *Meschede and Frisch, 1998*; *James, 2006*). Though the debate continues, the "Pacific" interpretation is more robust and appears to be more widely accepted, considering that it is implemented in the most recent global paleo-tectonic reconstruction models (e.g. *Boschman et al., 2014*; *Matthews et al., 2016*).

2.2.3 About the existence of a subduction zone in NW Colombia

Another topic of debate has been the existence of a subduction zone in NW Colombia, considering that it is an area with low seismicity and without an active volcanic arc. In spite of few studies proposing that there is no subduction in this area (e.g. *Rossello and Cossey, 2012*), there are abundant studies which have used different methodologies to identify subducting slabs beneath NW Colombia, supporting a Caribbean subduction beneath NW South America. For instance, after the study carried out by *Pennington (1981*), in which he identified two subducting slabs beneath Colombia (Bucaramanga in the north and Cauca in the south, upper panel in **Figure 2.1**), later studies have identified subducting slabs with different geometries and interpreted origins (e.g. *Van der Hilst and Mann, 1994*; *Malave and Suarez, 1995*; *Taboada et al., 2000*; *Corredor, 2003*; *Cortes and Angelier, 2005*; *Zarifi et al., 2007*; *Vargas and Mann, 2013*; *Yarce et al., 2014*; *Chiarabba et al., 2015*; *Syracuse et al., 2016*). *Bernal et al., (2015 a, b and c*) carried out one of the most recent studies in the Lower Magdalena and San Jacinto areas of NW Colombia, in which they provide earthquake, tomographic, seismic reflection and gravity evidence for a shallowly-dipping subduction zone beneath northwest Colombia. Displacement vectors of the tectonic plates (e.g. *Trenkamp et al., 2002*; *Symithe et al., 2015*) also support a nearly-orthogonal convergence between the Caribbean and South American plates (**Figure 1.1**), in agreement with subduction.

2.2.4 Basement types and boundaries beneath the Lower Magdalena and San Jacinto

The nature and thickness of the crust and basement beneath the Lower Magdalena and San Jacinto is another matter of debate. *Duque-Caro (1979*) proposed that the basement in the San Jacinto fold belt, west of the Romeral Fault System, is of oceanic affinity while the basement beneath the Lower Magdalena, east of Romeral, is of continental affinity. *Cerón et al. (2007*) concluded that geophysical data do not support a northern extension of the oceanic-type basement beneath the Sinú-San Jacinto foldbelts, since gravity modelling demonstrated the localized effect of the scattered outcrops of oceanic rocks. Therefore, the basement beneath the Sinú-San Jacinto foldbelts would not be of the same composition of the basement in the Western Cordillera, and they propose a transitional continental basement (attenuated continental crust) for these foldbelts. *Cerón et al. (2007)* also calculated the depth of the Moho discontinuity in northwestern Colombia and obtained depth estimates of the oceanic Moho of 20-25 km and of the continental Moho from 27 to 45 km, with the deepest values under the Eastern Cordillera of Colombia.

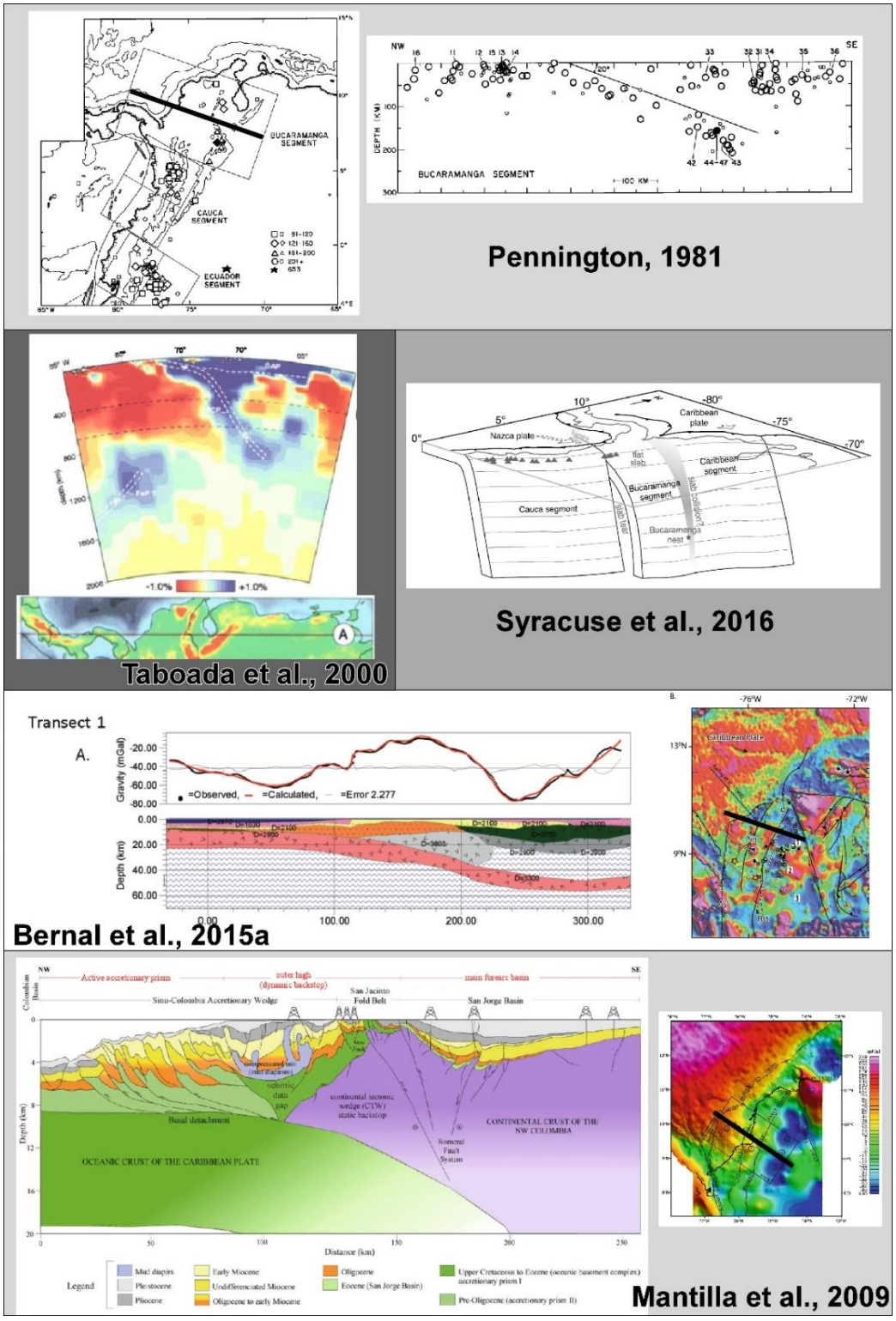

Figure 2.1. Selection of relevant figures from previous research on the tectonic configuration of NW Colombia. Upper panel shows a map with the two subducting slabs proposed and a section along the Bucaramanga slab (*Pennington, 1981*); below I show a tomographic section from *Taboada et al. (2000*), the three-dimensional configuration of NW Colombia interpreted by *Syracuse et al. (2016*) and a gravity model constructed by *Bernal et al., 2015a*; in the lower part, the major tectonic features of NW Colombia, interpreted by *Mantilla et al., 2009* from seismic and gravity data are shown.

According to *Mantilla (2007*) and *Mantilla et al. (2009*), the Colombian Caribbean margin displays morphological and tectonic characteristics of a typical accretion-dominated subduction complex (**Figure 2.1**). The 3D gravity modelling suggests that the Caribbean plate is approximately 11 km

thick and that it is subducting beneath northwestern Colombia at a low angle of about 5° in an east to southeast direction. The 3D gravity and magnetic modelling also supports the presence of an oceanic "basement complex" (mixture of basalts and sediments) underlain by a continental tectonic wedge which belongs to the overriding South American plate. Hence, they also conclude as *Cerón et al. (2007),* that the emplacement of oceanic affinity rocks over continental basement resulted from the offscraping and backthrusting of Caribbean material onto the continental margin during the initiation of the oblique subduction of Caribbean crust beneath northwest South America. The existence of the continental tectonic wedge beneath the oceanic "basement" complex in the San Jacinto Foldbelt would be indicating that the Romeral Fault System does not represent a paleo-suture or tectonic boundary between oceanic crust to the west and continental crust to the east. The results of 3D gravity and magnetic modelling by *Mantilla (2007*) and *Mantilla et al. (2009*) suggest that the Romeral Fault System originated within the block of continental crust on which the San Jacinto Fold Belt was formed.

In my thesis I follow the "Pacific" origin interpretation and I will provide new insights into the existence of a subduction zone and into basement age and configuration in the Lower Magdalena Valley basin and San Jacinto fold belt of NW Colombia (Chapters *3* and *4*).

2.2.5 Tectonic Provinces in Northern Colombia

Previous studies have subdivided Colombia into different tectonic provinces or terranes, based mainly on the age, origin and evolution of the basement and sedimentary infill and on the tectonic boundaries, which generally consist of a major fault system (*Etayo et al, 1983*; *Toussaint and Restrepo, 1994*; *Cediel et al., 2003*). The differences within these tectonic subdivisions reflect the complexity of the geology and the constant need for more geological information.

Etayo et al. (1983) subdivided the whole country into 24 terranes, eight of which are in northern Colombia, while *Toussaint and Restrepo (1994*) made a different and simpler subdivision in what they called "Suspect Terranes of Colombia", and decided to use names of native Colombian tribes for each terrane (**Figure 2.2**). According to their work, northern Colombia would comprise mainly three terranes, the Chibcha terrane to the east, with continental para-autochthonous basement which was accreted to the paleo-continent during the Late Paleozoic (*Ordoñez and Pimentel, 2002*), the Tahamí terrane in the center, representing the westernmost province with continental nature and the Calima terrane to the west, which corresponds to an oceanic basement province. *Ordoñez and Pimentel (2002*) later modified Toussaint and Restrepo's original division by proposing a new terrane called Panzenú, due to the basement differences compared to the Tahamí terrane farther south.

Cediel et al. (2003) then proposed a series of tectonic realms for what they called the Northern Andean Block, which comprises Toussaint and Restrepo's allochthonous and para-autochthonous terranes (**Figure 2.2**). They divided this block into several realms, four of which are forming northern Colombia. These are the Central Continental Sub-Plate realm which includes the Eastern Cordillera and most of the Central Cordillera, the Maracaibo Sub-Plate realm which includes Perijá, Cesar, Lower Magdalena and Sierra Nevada de Santa Marta, the Western Tectonic Realm which consists of all the allochthonous terranes made of oceanic crust (including the Caribbean Terrane which contains Sinú and San Jacinto), and the Guajira-Falcón Composite terrane which includes the Guajira basins. The Central Continental Sub-Plate realm is considered to have an old Grenvillian terrane called Chicamocha, which is included in the Chibcha terrane of *Toussaint and Restrepo (1994*), as well as the Triassic-Jurassic San Lucas and Ibagué blocks with their dioritic to granodioritic batoliths and associated volcanics. However, *Cediel et al. (2003*) include in this realm a terrane they call Cajamarca-Valdivia, which is basically equivalent to the Tahamí terrane of *Toussaint and Restrepo (1994*). As seen in **Figure 2.2**, the proposal by *Cediel et al. (2003*) is much more detailed but also much more complex.

Though the previously described are the main subdivisions in tectonic terranes in northern Colombia, it is expected that the numerous petrologic and geochonologic studies which have been carried in recent years will allow the proposal of updated models of tectonic terranes in northern South America. In this thesis I use new basement data to propose correlations of the basement underneath the LMV with surrounding outcropping basement terranes (Chapter 3).

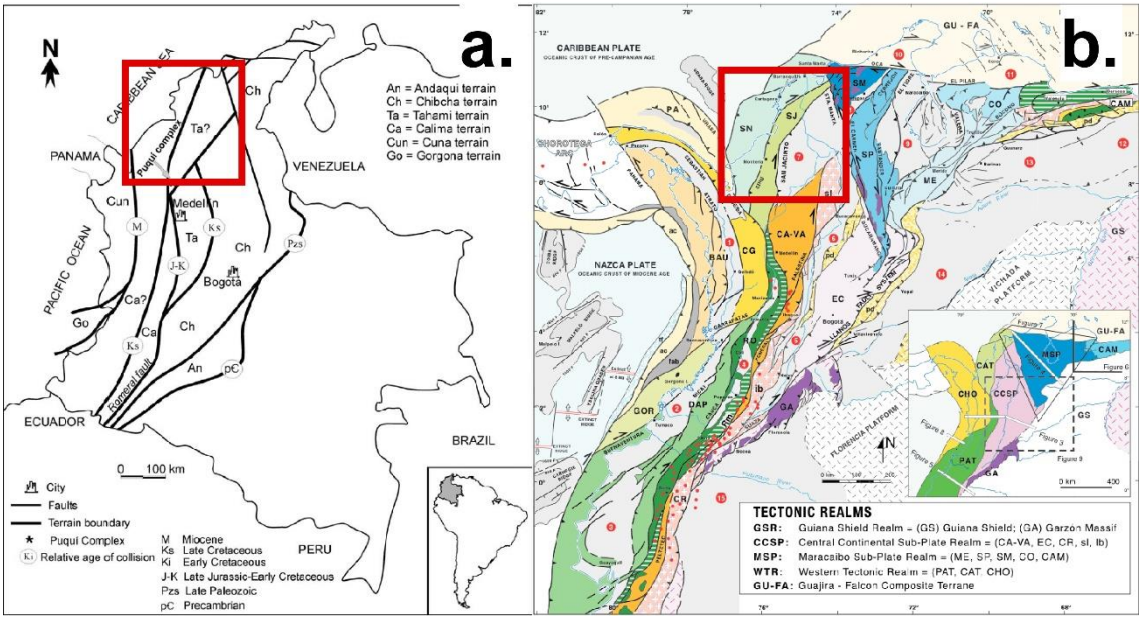

Figure 2.2. a) Proposal of tectonic terranes by *Toussaint and Restrepo (1994*), modified by *Ordoñez and Pimentel (2002);* b) lithotectonic and morphostructural map of NW South America from *Cediel et al. (2003*). The red square shows the study area of this thesis.

2.2.6 Previous studies of the Lower Magdalena and Sinú-San Jacinto provinces

The present-day Lower Magdalena and Sinú-San Jacinto provinces have been classified in different and quite contrasting ways, an indication of both the complexity of the area and of the poor understanding of its geology.

Macellari (1995) proposed their formation in a foreland setting which resulted from the overthrusting of Caribbean-arc rocks, while *Flinch (2003*) proposed a back-arc classification of the Lower Magdalena. The accretionary model proposed by *Duque-Caro (1979*) was accepted and adopted by the *ICP (2000*) and by *Flinch (2003*), whereas *Caro and Spratt (2003*) proposed that the San Jacinto fold belt was a rift with active extensional faults from the Upper Cretaceous to the Eocene and that it was inverted during Pliocene to Pleistocene times. According to *Ladd et al. (1984),* the Lower Magdalena and Sinú-San Jacinto are all forearc basins, and *Mantilla (2007*), *Mantilla et al. (2009*) and *Bernal et al. (2015 a, b and c*) propose that the forearc basin is the Lower Magdalena, with the San Jacinto fold belt as the present-day forearc high, and the Sinú fold belt as the accretionary wedge.

Strike-slip and tectonic block rotation have also been proposed as formation mechanisms for basins such as the LMV. One way of assessing possible tectonic block rotation is by doing paleomagnetic analyses but unfortunately, in northwestern Colombia there are very few of such studies. According to previous studies, petrochemical and paleomagnetic data of oceanic volcanic rocks in the

Caribbean terranes (Kerr et al., 1996a; MacDonald and Opdyke, 1972, in *Cediel et al., 2003*) indicate that they are allochtonous. Paleomagnetic data for the Coniacian Finca Vieja Formation in the San Jacinto terrane indicate a provenance to the southwest (J. Brock and H. Duque, personal comm., 1986, in *Cediel et al., 2003*). This would be supported by the petrochemical analyses of Kerr et al. (1996b, in *Cediel et al., 2003*)), which suggest that the volcanic sequences of the Pacific Dagua-Piñón terrane and the "southern Caribbean" basalts in general, belong to the same volcanic province.

The model of transrotational basins of *Nilsen and Sylvester (1995*), in which tectonic blocks undergo rotation under the influence of limiting stike-slip faults, has been applied to some basins in South America such as the Ecuador forearc model proposed by *Daly (1989*). In Colombia, such block rotation models were first proposed by *ICP (2000*), which interpreted that the depocenters in the Lower Magdalena area were initially formed as transrotational basins. *Montes et al. (2010*) later used a generalized basement map by *Cerón et al. (2007*) to calculate extension in the Lower Magdalena and relate it to major rotation of the Santa Marta massif. However, the conclusions of the work by *Bernal et al. (2015c*) did not agree with the proposal of such major block rotations. One of the objectives of this thesis is to use my regional database to propose and discuss mechanisms of basin formation, as well as more robust basin classifications (Chapters *4* and *5*).

2.3 Brief background on hydrocarbon exploration and previous regional studies in the Lower Magdalena and San Jacinto

2.3.1 Historical background and older studies

In the final chapter of my thesis (*Chapter 6*), I carry out three-dimensional basin modelling, in order to better understand the petroleum systems in the area and to help to reduce the risk in hydrocarbon exploration. For this reason, I think it is worth highlighting that historically it was in northwestern Colombia where the first hydrocarbons were exploited in the country, though the first reports of petroleum in Colombia come from the Spanish "conquistadores" in the Middle Magdalena valley. The historical archives with the initial hydrocarbon drilling and exploration history in Colombia are found in a few publications such as *Anderson (1926*). According to internet archives and old publications, in 1869, during the construction of railways in the area of Puerto Colombia, located west of the important coastal city of Barranquilla, the workers reported a constant strong petroleum odor and sudden gas-related explosions. Experts were sent to check the area and in 1884, with the aid of foreign geologists, several artesian wells were drilled to depths of around 100 feet, producing gas and light oil (42°API) at rates of 50 barrels per day. It thus appears that the first official oil wells that were drilled in Colombia were called "Las Perdices-1" and Las "Perdices-1A", apparently operated by a company called Atlantic Oil. Co and which were drilled to depths between 754 and 1,705 feet (230 to 520 m), producing 60 barrels of light oil per day. In the following years, several Perdices wells were drilled (Perdices-2 to 14) and though small quantities of oil and gas were found, the final results were considered uncommercial (*Anderson, 1926*; **Figure 2.3**).

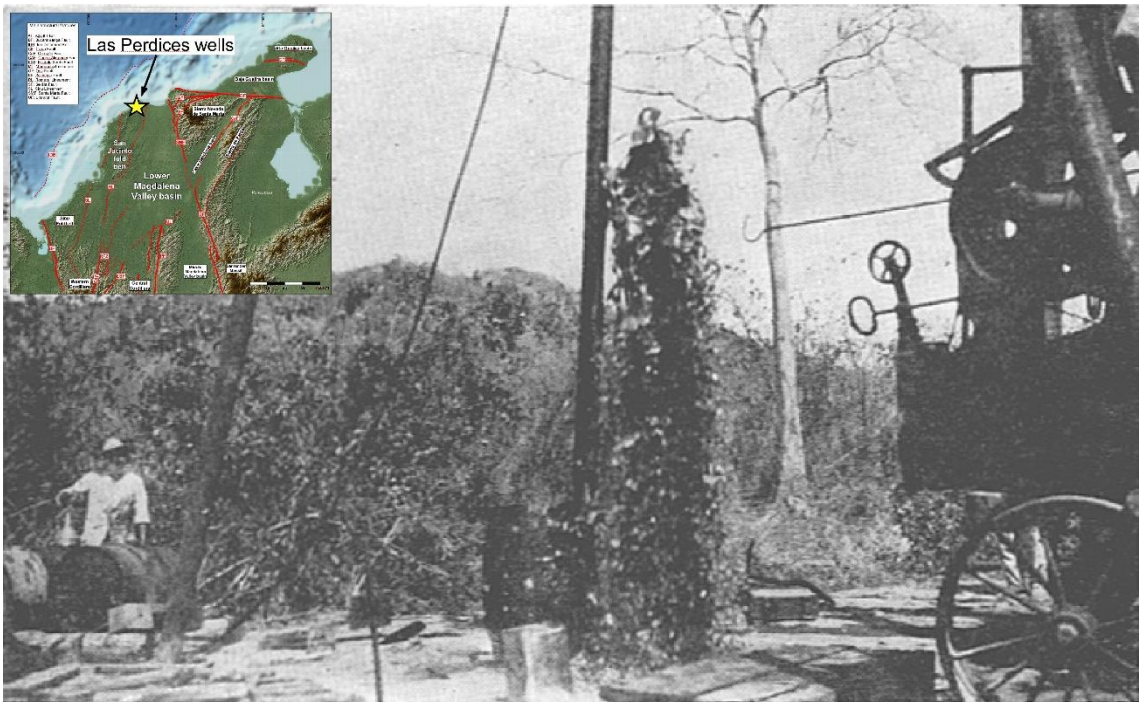

Figure 2.3. Flowing oil well near Puerto Colombia, northern San Jacinto fold belt, May 1922. Photo taken from *Anderson (1926*). Location of the well in the northern San Jacinto fold belt, is depicted in the inset.

After the initial exploration campaigns, other companies started drilling in different areas of the Colombian coastal plains but it was only until 1943 when the first commercial discovery in the LMV was made with the "El Difícil-1" well (Shell) that found gas and condensate in Lower Miocene carbonates. Subsequent discoveries occurred in 1956 when the Colombian Petroleum Company (Colpet) discovered the Cicuco field and in the sixties and seventies when other fields such as Jobo-Tablón, Sucre, Coral and Boquete were discovered. The latest discoveries in the study area were La Creciente gas field in 2006, Bonga and Mamey gas fields in 2011-2012 (Hocol) and the Nelson and other gas discoveries near the old Jobo-Tablón fields. However, it must be noted that all the commercial discoveries have been made in the Lower Magdalena Valley while in the San Jacinto and Sinú fold belts only sub-commercial hydrocarbon production has been obtained.

Until the sixties, most of the geological information of the Sinú-San Jacinto and Lower Magdalena areas came from oil industry exploration reports. Hence, Hermann Duque-Caro (*Duque-Caro, 1979*; *1984*; *1991*) was one of the first independent researchers to propose a definition of tectonic provinces and stratigraphic sequences in the Colombian Caribbean. While working with the Colombian Geological Survey (Ingeominas), Duque-Caro combined field work in the Lower Magdalena, Sinú and San Jacinto with some available subsurface data, mainly from seismic and wells, to propose a tectonostratigraphic configuration and evolution of the Colombia Caribbean, so his work has been an enormous contribution to the geological knowledge of northwestern Colombia. *Duque-Caro (1979*) divided the Lower Magdalena and Sinú-San Jacinto area into an unfolded, stable region or platform to the east (Lower Magdalena), underlain by continental crust and a folded, unstable region or geosyncline to the west (Sinú-San Jacinto), underlain by oceanic crust. As the limit between these two distinct geological provinces, he proposed the extension to the north of the Romeral Fault, which was defined farther south by *Barrero et al. (1969*), as the contact between the accreted oceanic terranes in the west and the continental terranes in the east. *Duque-Caro (1979*) also defined the Sinú Lineament as the boundary between the San Jacinto belt to the east and the Sinú belt to the west (**Figure 1.2**). He also suggested that the margin of

northwestern Colombia has grown by successive westward accretion of the San Jacinto and Sinú belts from the Late Cretaceous to the Pliocene.

2.3.2 More recent exploration activities and regional studies

Several oil and gas companies have carried out integrated regional hydrocarbon evaluation studies in the Lower Magdalena and Sinú-San Jacinto areas. The Gulf E&P Company (*Aleman, 1983*) carried out a geological and hydrocarbon evaluation of the northwest of Colombia, including stratigraphy, tectonics and hydrocarbon potential. Three years later, *Beroiz et al. (1986*) of the Chevron Petroleum Company did a regional hydrocarbon evaluation of northwest Colombia which included structure and tectonics, stratigraphy, petroleum geology and prospectivity. Later on, as part of the Lower Magdalena Valley Technical Evaluation Agreement, *Hocol (1993*) carried out another regional study which included stratigraphy and basin development, structural geology and hydrocarbon habitat. In 1995, a joint regional study of the Sinú-San Jacinto basin was done between Ecopetrol and the Earth Sciences and Resource Institute (ESRI) of the Universities of South Carolina and Utah in the USA while in 1996, the petroleum systems of the Lower Magdalena Basin were initially characterized by another joint study between Ecopetrol and Petrobras (*Petrobras/Ecopetrol, 1996*).

In the year 2000, the Colombian Petroleum Institute (ICP) finished a regional evaluation of the Lower Magdalena Valley Basin (*ICP, 2000*) integrating a big seismic and well database with outcrop data and the results of lab analyses. The study proposed the tectono-stratigraphic evolution of the basin, defined several tectonostratigraphic regions and also evaluated hydrocarbon systems and prospectivity. This study based its paleogeographic reconstructions mainly on the work by *Duque-Caro (1979*) and according to them the formation of the LMV occurred as transrotational basins or depocenters, limited by normal faults, which were formed due to the tectonic stresses in north-western Colombia. Total (*Flinch, 2003*) also did a regional prospectivity evaluation of the area and proposed a structural evolution of the Sinú-Lower Magdalena area of northern Colombia. He also subdivided the area into the same provinces proposed by *Duque-Caro (1979*), separated by the Romeral Fault System. However, he classified the Plato-San Jorge Basin (Lower Magdalena) as a back-arc basin filled by Oligocene to Pliocene sediments, without providing evidence of the existence or location of an Oligocene to Pliocene magmatic arc.

With creation of the National Hydrocarbons Agency of Colombia (ANH) in 2003, new geological activities were carried out mainly in the Sinú-San Jacinto areas, such as the acquisition of regional 2D-seismic lines, drilling of stratigraphic wells which recovered cores that were later described and analyzed (*ANH/U. Caldas, 2009*), geological mapping (*ATG/ANH, 2009*) and other studies. Such activities were aiming to provide more information in terms of geology and petroleum systems to estimulate hydrocarbon exploration in the area. Following several years of field work with the Colombian Geological Survey, *Guzman et al. (2004*) and *Guzman (2007*) studied in detail the stratigraphy of the San Jacinto fold belt, and their results included a big database of micropaleontological data.

An important part of what I have done in this thesis relates to tying the surface geology and outcrop studies with the subsurface data and with my reflection seismic intepretations; I consider that in the absence of outcrops of the units buried in the LMV, such an integration between the surface and the subsurface geology is necessary and provides new insights into the tectono-stratigraphy of the Lower Magdalena and San Jacinto areas (Chapters *4* and *5*). Furthermore, one of the most valuable uses of the paleo-tectonic reconstructions, basin models, and the tectono-stratigraphic framework which I built, was their implementation in the three-dimensional basin and petroleum system model I constructed. The different scenarios I have tested in each of the model simulations will certainly have important implications for petroleum systems and will hopefully be a valuable tool for hydrocarbon exploration in these basins of NW Colombia.

3 Structure And Age Of The Lower Magdalena Valley Basin Basement, Northern Colombia: New Reflection-Seismic And U-Pb-Hf Insights Into The Termination Of The Central Andes Against The Caribbean Basin

This chapter is a reformatted version of a Journal of South American Earth Sciences paper (*Mora et al., 2017a*). Supplementary figures have been placed in *Appendix A.*

Citation: Mora, J.A., Ibáñez-Mejía, M., Oncken, O., De Freitas, M., Vélez, V., Mesa, A. and Serna, L. 2017a. Structure and Age of the Lower Magdalena Valley Basement, Northern Colombia: New reflection-seismic and U-Pb-Hf Insights into the termination of the Central Andes against the Caribbean Basin. Journal of South American Earth Sciences 74, 1-26. http://dx.doi.org/10.1016/j.jsames.2017.01.001

Abstract

Detailed interpretations of reflection seismic data and new U-Pb and Hf isotope geochemistry in zircon reveal that the basement of the Lower Magdalena Valley basin is the northward continuation of the basement terranes of the northern Central Cordillera, and thus that the Lower Magdalena experienced a similar pre-Cenozoic tectonic history as the latter. New U-Pb and Hf analyses of zircon from borehole basement samples retrieved in the basin show that the southeastern region consists of Permo-Triassic (232-300 Ma) metasediments, which were intruded by Late Cretaceous (75-89 Ma) granitoids. In the northern Central Cordillera, west of the Palestina Fault System, similar Permo-Triassic terranes are also intruded by Late Cretaceous felsic plutons and display ESE-WNW-trending structures. Therefore, our new data and analyses prove not only the extension of the Permo-Triassic Tahamí-Panzenú terrane into the western Lower Magdalena, but also the along-strike continuity of the Upper Cretaceous magmatic arc of the northern Central Cordillera, which includes the Antioquia Batholith and related plutons. Hf isotopic analyses from the Upper Cretaceous Bonga pluton suggest that it intruded new crust with oceanic affinity, which we interpret as the northern continuation of a Lower Cretaceous oceanic terrane (Quebradagrande?) into the westernmost Lower Magdalena. Volcanic andesitic basement predominates in the northwestern Lower Magdalena while Cretaceous low-grade metamorphic rocks that correlate with similar terranes in the Sierra Nevada de Santa Marta and Guajira are dominant in the northeast, suggesting that the Tahamí-Panzenú terrane does not extend into the northern Lower Magdalena. Although the northeastern region of the Lower Magdalena has a similar NE-SW fabric as the San Lucas Ridge of the northeastern Central Cordillera and the Sierra Nevada de Santa Marta, lithologic and geochronologic data suggest that the San Lucas terrane terminates to the north against the northeastern Lower Magdalena, as the Palestina Fault System bends to the NE. The NE-SW trend of basement faults in the northeastern Lower Magdalena is probably inherited from the Jurassic rifting event which is responsible for the conspicuous fabric of surrounding terranes outcropping to the east of the Palestina Fault System, while the ESE-WNW trend in the western Lower Magdalena is inherited from a Late Cretaceous to Eocene strike-slip and extension episode that is widely recognized in the western Andean forearc from Ecuador to Colombia.

Keywords: Lower Magdalena Valley, San Jacinto fold belt, Caribbean, reflection seismic, basement, U-Pb and Hf isotope Geochronology.

3.1 Introduction

The Lower Magdalena Valley basin is an Oligocene to recent basin of northwestern Colombia, located between two basement massifs, the Central Cordillera and the Sierra Nevada de Santa Marta (**Figure 3.1**). It is considered to be a forearc basin associated with the northern Colombia subduction complex, where the oceanic crust of the Caribbean Plate subducts towards the ESE beneath the continental crust of the South American plate (*Mantilla, 2007*; *Mantilla et al., 2009*; *Bernal et al., 2015a*; *Syracuse et al., 2016*). The basin lies between the inactive magmatic arc of the northern Central Cordillera in the SE and the forearc high and the Southern Caribbean accretionary prism to the west. The nature of the substratum of modern forearc basins such as the Lower Magdalena remains a matter of controversy, primarily because the basin floor is buried under a thick cover of post-Oligocene forearc sediments (*Dickinson and Seely, 1979*; *Dickinson, 1995*). Despite several researchers having considered the basement beneath the Lower Magdalena to be related to the continental basement exposed in the Central Cordillera and Sierra Nevada de Santa Marta (*Duque-Caro, 1979*; *Reyes et al., 2000*; *Montes et al., 2010*), the paucity of basement data from the Lower Magdalena has precluded the development of robust arguments in support of such correlations. However, because the Lower Magdalena Valley basin holds important hydrocarbon reserves at different stratigraphic levels (*ICP, 2000*), the last two decades have seen a considerable increase in exploratory drilling and geophysical tools applied to this basin such as gravimetry, magnetics and reflection seismic. These new data have provided valuable information about the basement structure of the Lower Magdalena and have allowed improved regional correlations, structural evaluation and mapping to be conducted (*Reyes et al., 2000*; *Cerón et al., 2007*; this study). In spite of the numerous oil exploration wells that have reached the Lower Magdalena basement during the past few decades, very few and localized analyses have been carried out to provide robust geochronologic and geochemical constraints on the type and age of the basement that underlies it (*Montes et al., 2010*; *Silva et al., 2016*). Considering the unique location of the Lower Magdalena in northwestern South America, where several tectonic plates have been complexly interacting through time, new information about its basement structure, type and age is relevant to understanding the formation and evolution of this important hydrocarbon-producing basin in Colombia.

The aim of this paper is to present new information on the structure and age of the basement of the Lower Magdalena Valley basin, including detailed structural-depth maps obtained from seismic reflection data, as well as new geochronological constraints from zircon U-Pb analyses and source characterization through zircon Hf isotope geochemistry. The new subsurface maps and U-Pb-Hf information presented here, coupled with the extensive published literature on the age and structure of the Central Cordillera and Sierra Nevada de Santa Marta, allowed us to develop improved geological correlations between the Lower Magdalena basement and its surrounding massifs. These results are evaluated within a regional plate-tectonic framework, and their implications for Late Cretaceous paleo-tectonic reconstructions of northern South America and the circum-Caribbean region are discussed. This basement study will have important implications for future research focusing on Cenozoic tectonics and the formation and evolution of the Lower Magdalena Valley basin and of the San Jacinto fold belt.

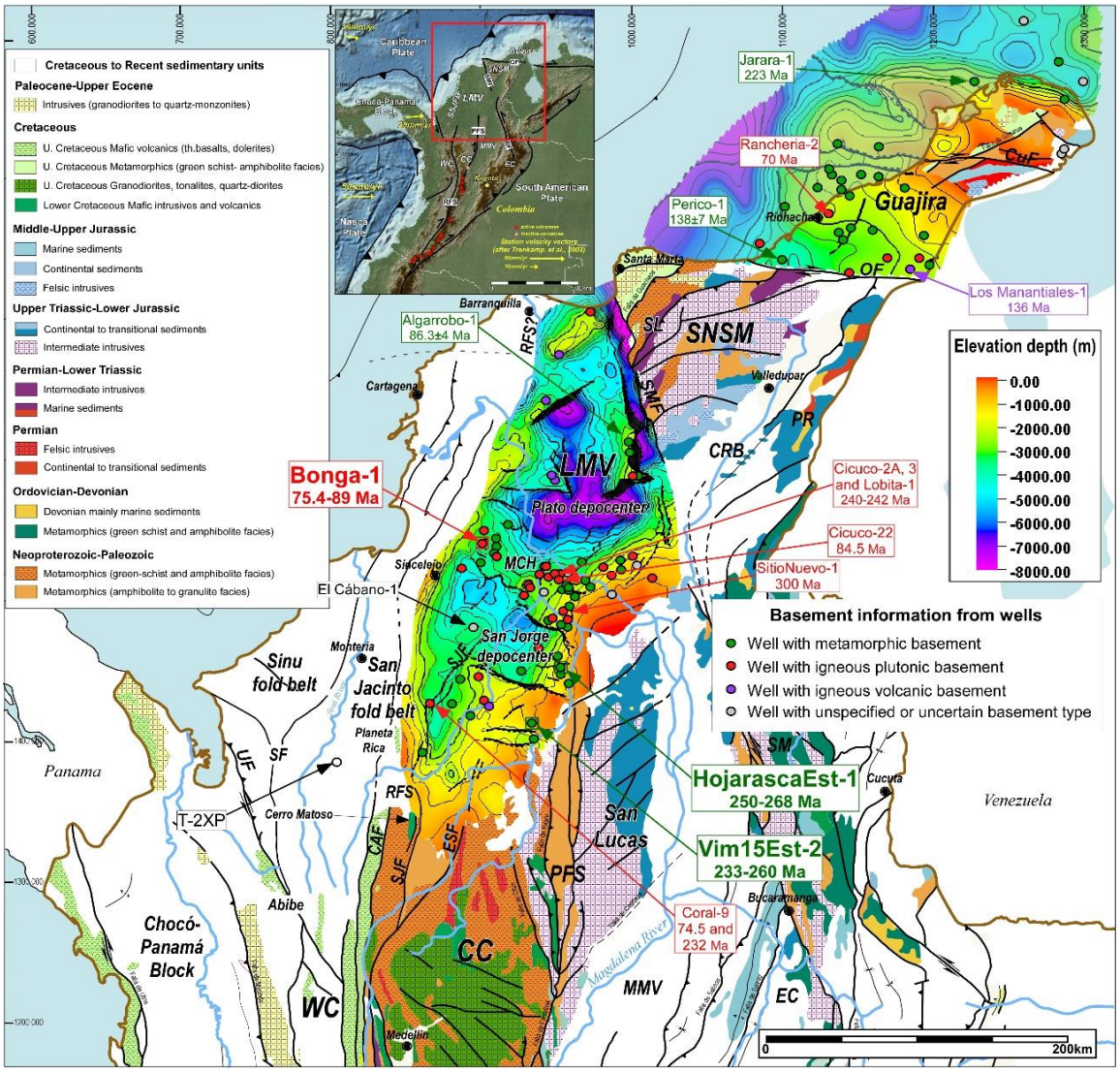

Figure 3.1. Geological map of northern Colombia (*Gomez et al., 2007*), highlighting basement terranes and pre-Tertiary sedimentary units and integrating subsurface basement maps in depth (meters) of the LMV and Guajira. Colored circles are wells that drilled into the basement and have basic rock descriptions; previous and new geochronological data from the basement is depicted. CAF: Cauca-Almaguer fault; ESF: Espiritu Santo fault; SJF: San Jerónimo Fault; PFS: Palestina Fault System; UF: Uramita Fault; SF: Sinu fault; SMF: Santa Marta fault; SL: Sevilla Lineament; OF: Oca Fault; CuF: Cuisa Fault; CRB: Cesar-Rancheria basin; PR: Perijá Ridge; EC: Eastern Cordillera; SNSM: Sierra Nevada de Santa Marta; MMV: Middle Magdalena Valley basin. Inset: Tectonic map of northwestern South America with topography and bathymetry, showing the location of the Lower Magdalena Valley basin (LMV) and the Sinú-San Jacinto fold belt (SSJFB). Present-day tectonic plate motions are shown in yellow (after *Trenkamp et al., 2002*). WC: Western Cordillera; CC: Central Cordillera; EC: Eastern Cordillera; RFS: Romeral Fault System; PFS: Palestina Fault System; BF: Bucaramanga Fault; SMF: Santa Marta Fault; OF: Oca Fault.

3.2 Geological framework and previous studies.

The present-day configuration of northern South America is the end result of a complex interaction between several tectonic plates and blocks, which include the Nazca, Caribbean and South American plates and the Chocó-Panamá block (inset in **Figure 3.1**). Around the latitudes of south and central Colombia (0˚-5˚N), where the main tectonic driver has been the interaction of the Nazca and South American plates, the Andes Mountains are divided into three ranges or cordilleras (Western, Central and Eastern) which are separated by two inter-mountain fluvial valleys (Cauca and Magdalena). The basement of the Central and Eastern Cordilleras is considered to be comprised

mostly of autochthonous terranes rooted in continental crust, while the Western Cordillera (WC) is considered allochthonous and constituted of oceanic crust. A major suture zone, called the Romeral Fault System (RFS), is separating the Central and Western Cordilleras and within the fault system there are several allochthonous terranes (e.g. Quebradagrande and Arquía), which would represent an oceanic arc, a mid-oceanic ridge or an ensialic marginal basin (*Toussaint and Restrepo, 1994*; *González, 1980*; *Nivia et al., 2006*). *Bayona et al. (2011*) and *Cardona et al., (2012*) have also proposed that there was a younger Upper Cretaceous intra-oceanic arc, formed between 88 and 73 Ma, which collided against the NW South American margin in latest Cretaceous to early Paleocene times and that it is represented by localized and poorly preserved serpentinized peridotites outcropping in northern Central Cordillera and southern LMV. The oceanic domains of the WC are thought to have accreted during the Mesozoic, along the RFS (*Barrero et al., 1969*; *Barrero, 1979*; *Etayo et al., 1983*; *Restrepo and Toussaint, 1988*; *Cediel et al., 2003*). In the northern part of the country, where the influence of the Caribbean plate and collision of the Chocó-Panamá block has continued into the Cenozoic, the Central and Western cordilleras terminate as they plunge to the north and are progressively buried under Tertiary sediments of the Lower Magdalena Valley basin (LMV) and the Sinú and San Jacinto fold belts. The LMV is limited to the east and northeast by the left-lateral, strike-slip Santa Marta-Bucaramanga fault system, composed of the Santa Marta fault system (SMF) in the north and of the Bucaramanga Fault system (BF) in the south (**Figure 3.1**). While a basement high (Cáchira) in the northernmost Central Cordillera (CC) is separating the LMV from the Middle Magdalena Valley basin (MMV), the Santa Marta-Bucaramanga fault system is separating it from the Cesar-Ranchería (CR) Basin and from the Sierra Nevada de Santa Marta (SNSM, **Figure 3.1**). To the southeast and south, the LMV is limited by the northernmost termination of the CC, the Palestina Fault System (PFS) and the San Lucas Ridge. Its western boundary has been considered to be the inferred extension to the north of the trace of the RFS (Romeral Lineament, *Duque-Caro, 1979*), which would be separating this basin from the deformed Sinú-San Jacinto fold belt in the west. As described in previous studies (*Duque-Caro, 1979*; *1984*; *ICP, 2000*; *Cerón et al., 2007*), the main morphological features of the basement underneath the LMV are the Plato and San Jorge depocenters, which are separated by a NW-SE-trending high called the Magangué-Cicuco High (MCH, **Figure 3.1**). The formation of the basement architecture under the LMV has been related to strike-slip tectonics (transrotational basins, *ICP, 2000*), large-scale clockwise rotation (*Montes et al., 2010*) and forearc extension (*Mantilla et al., 2009*; *Bernal et al., 2015c).*

3.2.1 Basement data from outcrop studies

Surrounding the LMV, there are three main litho-tectonic provinces in which basement rocks are exposed (**Figure 3.1**): the northern WC, the northern CC including the San Lucas ridge, and the SNSM. In the northernmost WC, there are scattered outcrops of oceanic basement rocks. In the Serranía de Abibe, basic agglomerates, gabbros and basalts are reported (*ICP, 2000*) while in the Planeta Rica area, ultrabasic rocks and basalts are exposed (**Figure 3.1**). The Planeta Rica outcrops were studied by *Dueñas and Duque-Caro (1981*) and they comprise the Planeta Rica peridotites and the Nuevo Paraíso basalts. Basaltic lavas and agglomerates of the Ojo Seco Formation yielded a minimum age of 83 Ma (Campanian, Cáceres, 1978, in *ICP, 2000*) but the dating method is not specified in *ICP (2000*). Farther south, in the Cerro Matoso area, there are nickel mineral exploitations derived from the near-surface alteration of the peridotites, producing laterites enriched in nickel and iron (*Gleeson et al., 2004*). These rocks are considered to represent the northernmost extension of the allochthonous oceanic crust terranes, which were accreted to the paleo-continental margin during the Late Jurassic and Early Cretaceous. These terranes have been grouped by *Toussaint and Restrepo (1994*) in the Calima Terrane, located to the west of the RFS, and in the Quebradagrande and Arquía Complexes which are located within the RFS (*Nivia et al., 2006*, *Villagómez et al., 2011a*). Based on provenance studies, *Cardona et al. (2012*) have discussed the affinity of the basement in some areas close to the limit between the San Jacinto fold belt and the LMV.

There are four main groups of crystalline igneous-metamorphic rocks in the northern CC (*Clavijo, 1996, Ordoñez et al., 1999*; *Ordóñez and Pimentel, 2002*; *Vinasco et al., 2006*; *Clavijo et al., 2008, Restrepo et al., 2011*; *Villagómez et al., 2011a*). The oldest group comprises Meso- to Neoproterozoic high-grade metamorphic rocks which outcrop in the San Lucas Ridge of the northeastern CC and are part of the Chibcha terrane (*Toussaint and Restrepo, 1994*; *Cuadros et al., 2014*), while the second group comprises Paleozoic to Triassic, medium to high-grade metamorphic and igneous rocks (Puquí and La Miel units of the Tahamí-Panzenú Terrane, *Ordoñez and Pimentel, 2002*, *Villagomez et al., 2011a*), unconformably overlain by metasedimentary and meta-igneous rocks of the Middle to Late Triassic Cajamarca Group (*Villagómez et al., 2011a*). The third major group of basement rocks in the northern CC consists of Jurassic granitoids and related volcanics, exposed mainly along the San Lucas Ridge (*Clavijo, 1996*; *Clavijo et al., 2008*). The fourth group comprises mid to Late Cretaceous granitoids such as the Antioquia Batholith and the Córdoba Pluton; the Antioquia Batholith is the largest calc-alkaline intrusion in the northern CC and it comprises mainly granodiorite and tonalite (*Ordóñez & Pimentel, 2002*). U-Pb in zircon ages of the batholith were obtained by *Ibáñez-Mejía et al. (2007*; 88-83Ma) and by *Villagómez et al., (2011a*; 93-87 Ma), confirming that the construction of this major composite pluton took place between the Cenomanian and the Santonian. The emplacement of these calc-alkaline plutons is thought to be related to Late Cretaceous subduction of Proto-Caribbean oceanic crust below the South American Plate (*Villagómez et al., 2011a*). In the study area, *Toussaint and Restrepo (1994*) defined two main basement terranes, separated by the PFS: an older one (Chibcha) to the east, including the San Lucas Ridge, and a younger one (Tahamí) to the west. *Cediel et al. (2003*) proposed a different name for the Tahamí terrane (Cajamarca-Valdivia), also limited to the east by the PFS. Considering the later re-definition by *Ordóñez and Pimentel (2002*), we will use in this paper the name "Tahamí-Panzenú" for the terrane that lies between the Chibcha and the Calima terranes. The correlations and proposed along-strike continuation of these terranes towards the north beneath the LMV basin will be further discussed below.

The SNSM has been divided into three southwest-northeast-trending geological provinces, separated by major fault zones (*Tschanz et al., 1974*). The southeastern Sierra Nevada province is the largest, highest and oldest in the SNSM and has a core of Proterozoic granulites, anorthosites and gneisses (*Cordani et al., 2005*, *Cardona et al., 2006*). These Grenvillian-age rocks were later intruded by Jurassic felsic plutons and covered by volcano-sedimentary sequences including spilitic rocks to the south. This province correlates with the Chibcha terrane of *Toussaint and Restrepo (1994*) and is limited to the NW by the Sevilla Lineament (SL). The Sierra Nevada province overthrusts the Sevilla province to the northwest, which consists of Paleozoic mafic gneisses and schists, intruded by Permian-Late Triassic syntectonic granitoids and Paleogene granites (*Tschanz et al., 1974, Cardona et al., 2006*; *2010a*). The northwestern province, which is also the youngest one, is the Santa Marta province which comprises two Upper Cretaceous to Paleogene metamorphic belts: the coastal belt consisting of green schists and phyllites and the inner belt which comprises mica-schists and amphibolites. These two belts are separated by undeformed Paleogene granitoids of the Santa Marta Batholith (58-44 Ma K-Ar age, *Tschanz et al., 1974*). The Santa Marta province has been also considered an oceanic terrane, proposed to have accreted to the Sevilla province in Late Cretaceous or early Paleogene times (*Cardona et al., 2010b*).

3.2.2 Basement data from the subsurface

Previously available data (*ICP, 2000*; *Cerón et al., 2007*) has shown the basement underneath the LMV to consist mainly of igneous and metamorphic rocks of broad continental affinity, quite similar to those described in the northern CC and in the SNSM. The majority of wells drilled a basement consisting of felsic igneous rocks (granitoids) and low-grade metamorphic/metasedimentary rocks, mainly phyllites and schists (**Figure 3.1**). A recent study by *Silva et al. (2016*) provided more information about the nature of the basement in the LMV which was incorporated in **Figure 3.1**. *Silva et al. (2016*) report felsic plutonic rocks in the Alejandría-1 well (granodiorite) and in the Chilloa-1 and Coral-9 wells (monzogranites), while mafic plutonic

rocks were reported in the northern LMV (quartzdiorites to diorites in Medialuna-1 and Salamanca-1) and in the eastern Magangué high (gabbros-pyroxenites in SitioNuevo-1).

Concerning the age of the LMV basement, there are very few geochronological analyses available to date. The first geochronological study was conducted by *Pinson et al. (1962*), which sampled the Cicuco-3 well and obtained a K-Ar age of 110 Ma from a biotite. *Montes et al. (2010*) reported zircon U-Pb crystallization ages between 239 to 241 Ma for similar granitoids from the Cicuco-3 borehole and two other exploratory wells in the Magangué-Cicuco basement high (i.e., Cicuco-2A and Lobita-1 wells); based on these results, *Montes et al. (2010*) suggested that the cooling age reported by *Pinson et al. (1962*) does not approximate the crystallization age for these granitoids, but instead has been partially reset during a later Cretaceous re-heating event. *Silva et al. (2016*) provided the most recent geochronological and geochemical data from the basement in the LMV. A U-Pb (zircon) age of 300 Ma (Carboniferous-Permian boundary) was obtained from the cored gabbros recovered in the SitioNuevo-1 well, while a syenogranite core recovered in the Cicuco-22 well, yielded an age of 84.6 Ma (Santonian). Ditch cuttings of monzogranites recovered from the Coral-9 well yielded two U-Pb ages, an old one of 232 Ma (Middle Triassic) and a young one of 74.5 Ma (Campanian). Both *Montes et al. (2010*) and *Silva et al. (2016*) related the basement in the central part of the LMV to that of the CC and SNSM.

Farther west from the Cicuco area, chloritic schists considered to be the basement in the El Cábano-1 well were analyzed by *Thery et al. (1977*), who obtained an isochron age of 62 ± 2 Ma using the Rb-Sr method. However, these ages probably correspond to pre-Oligocene highly foliated sediments, since seismic data shows that some reflectors below their "basement" reflector most likely correspond to pre-Oligocene sedimentary sequences. *Tschanz et al. (1974*) reported a cooling age of 86.3 ± 4 Ma (K-Ar whole rock) in phyllitic schists found in ditch cuttings from the Algarrobo-1 well in the eastern LMV, and proposed a correlation with schists outcropping in the northwestern part of the SNSM (Santa Marta terrane); however, it is still uncertain whether this K-Ar date approximates the age of metamorphism for the basement schists, or if in turn it was also affected by a younger re-heating event similarly to the Cicuco-3 granitoids discussed above.

3.3 Methods

3.3.1 Subsurface basement mapping and integration with well and seismicity data

For this study, we used Hocol's 2D and 3D-seismic database in the LMV (**Figure 3.2**) which consists of more than 30,000 linear km of 2D-seismic, approximately 1,000 km^2 of 3D-seismic, data from nearly 90 exploratory and stratigraphic wells including e-logs, sample analyses and reports, air gravity and magnetic data acquired by Hocol and the Colombian National Hydrocarbons Agency (ANH), remote sensing data and available surface geology maps and reports. The 2D-seismic database includes numerous surveys acquired by oil and gas companies during different exploratory phases since the 60s, so there is a wide variety of seismic data quality. Most of this seismic has been pre-stack time-migrated by specialized processing companies. The air gravity and magnetics data, acquired and processed by a specialized company (*Lithosphera Ltda, 2010*), provided initial information about the basement configuration. Seismic interpretation and mapping was carried out using Schlumberger's Petrel software provided by Hocol S.A. The top of the acoustic basement was tied to the seismic using available sonic logs and check-shots, and its interpretation was generally not difficult as the impedance contrast between the crystalline basement and the overlying sediments produces a continuous, high-amplitude reflector. Once we interpreted and mapped the basement in the LMV and built 3D-models in two-way-time (TWT), we used the well data to construct regional pseudovelocity maps, which are average velocity maps to the top of the basement. These pseudovelocity maps were used to depth-convert the 3D-model of the LMV. The geometry of the basement under the LMV was also analyzed by identifying

different fault families according to their trends and relating them to similar outcrop patterns in surrounding terranes. Fault and lineament trends were measured from available geological maps, mainly the Geological Map of Colombia (*Gómez et al., 2007*). After dividing the individual faults into fault families with similar trends and styles, each family was plotted in a rose diagram using the Stereonet free software (*Allmendinger, 2013*; *Cardozo and Allmendinger, 2013*) and with bins set to 20 degrees. Representative seismic cross-sections were interpreted in order to unravel the tectonostratigraphic evolution of the LMV and San Jacinto fold-belt.

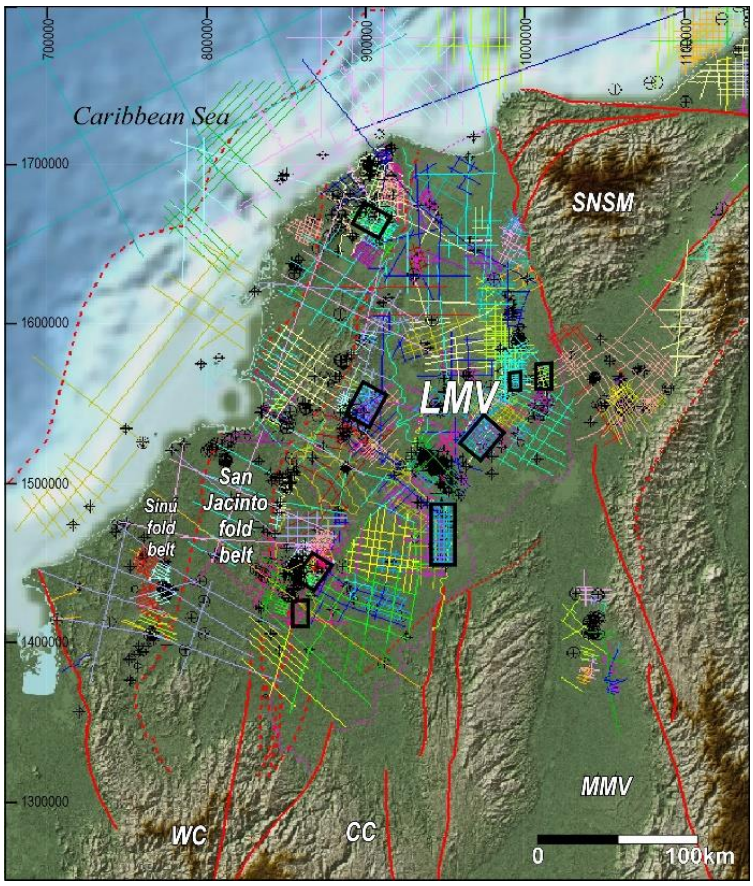

Figure 3.2. Reflection seismic and well database used for this study, provided by Hocol S.A. Colors represent different seismic surveys, wells are shown in black circles with crosses and 3D surveys are shown in thick black rectangles. Abbreviations as in Figure 3.1.

All the exploratory and stratigraphic wells that reached the basement were selected and subdivided according to the type of basement they found, highlighting those with geochronological analyses from previous studies and also from this study (**Figure 3.1**; see below). The described samples, which are mostly ditch cuttings, were subdivided into four basement types, namely metamorphic, igneous intrusive, igneous volcanic and unspecified/uncertain. The well data, colored by basement type and including the available geochronological data, were plotted against the seismic and gravimetric basement maps, the magnetic intensity maps and the surface geology in order to correlate the basement of the LMV to surrounding terranes. The patterns and relationships that were found from these plots are discussed in forthcoming sections. In addition, we also compiled the available earthquake and seismicity data from the study area, in order to characterize the main faults and structural features in terms of seismic activity and kinematics. Seismicity data from the study area was downloaded from the Colombian Earthquake Network (Red Sismológica Nacional, http://seisan.sgc.gov.co/RSNC/) and plotted both in map and section view, together with the seismic interpretation and maps. A total of 14,081 events were obtained, corresponding to

earthquakes with Mw 1 to 9, recorded from June 1, 1993 to November 26, 2015. Additionally, we compiled the available focal mechanism solutions from published sources (*Pennington, 1981*; *Malavé and Suárez, 1995*; *Corredor, 2003*; *Ekstrom et al., 2005*; *Cortés and Angelier, 2005*) and plotted them together with our structural models.

3.3.2 Zircon U-Pb Geochronology and Hf Isotope chemistry

In order to expand the existing geochronological dataset for the basement of the LMV and further support interpretations made from the structure, we selected eight samples from deep exploratory and stratigraphic wells that drilled through the basement to be processed for zircon geochronology and Hf isotope geochemistry. Two stratigraphic wells from the southern LMV and one exploratory well from the western part of a basement high (Magangué-Cicuco High; MCH) were selected (**Figure 3.1** and **Table 3.1**). Three core samples were analyzed from the metamorphic basement drilled in the VIM15 Est-2 stratigraphic well in the southeastern part of the basin. Five ditch cutting samples were analyzed from the basement in the HojarascaEst-1 stratigraphic well in the eastern part of the San Jorge depocenter and from the Bonga-1 exploratory well, located in the western MCH.

Well	Latitude N d°m's"	Longitude W d°m's"	Basement depth (MD in ft)	Type of sample	Reported lithology	Age Ma	Method	Source
Algarrobo-1	N 10°07'59.7"	W 74°09'1.69"	8327	cuttings	Phyllitic schists	86.3 ±4	K-Ar whole rock	Tschanz et al., 1974
Cicuco-2A	N 9°16'24.78"	W 74°38'53.07"	7872	cuttings	Granitoid	241.6±3.9	U-Pb zircon	Montes et al., 2010
Cicuco-3	N 9°17'38.58"	W 74°38'51.94"	8200	cuttings	Granitoid	241.6 ± 3.1	U-Pb zircon	Montes et al., 2010
Lobita-1	N 9°17'20.84"	W 74°40'18.49"	8200	cuttings	Biotite granite	239.6 ± 2.9	U-Pb zircon	Montes et al., 2010
Bonga-1	N 9°30'16.9"	W 75°04'11.20"	10816	cuttings	Granitoid	75.4 - 89.2	U-Pb zircon	This study
HojarascaEst-1	N 8°42'38.13"	W 74°35'19.95"	5228	cuttings	Qtz-mica-schists,quartzites and gneisses	234 ± 5	U-Pb zircon	This study
Vim15Est-2	N 8°21'46.01"	W 74°46'45.18"	3087	core	phyllite, sericitic slate and tremolitic schist	233 ± 4	U-Pb zircon	This study
Cicuco-22	N 9°15'9.35"	W 74°36'5.03"	8227	core	Granodiorite	84.5	U-Pb zircon	Silva et al., 2016
Sitionuevo-1	N 9°03'34.63"	W 74°35'35.41"	5307	core	Gabbro/pyroxenite	300 ± 1.3	U-Pb zircon	Silva et al., 2016
Coral-9	N 8°28´45.31"	W 75°25´9.39"	10267	cuttings	Monzogranite	74 and 232	U-Pb zircon	Silva et al., 2016

Table 3.1. Summary of geochronological data of the basement of the LMV, including our new U-Pb (zircon) data.

Zircons were separated from cores and cuttings using standard gravimetric and magnetic techniques. Prior to crushing, all samples were soaked in a strong organic solvent and thoroughly rinsed with water in order to remove any external contamination to the cores and cuttings caused by residual drilling mud. In the case of cuttings, samples were sieved with a 1 mm mesh and only the larger and similarly-looking rock fragments retained by the mesh were processed for zircon separations in order to minimize potential contamination by cavings. Zircon crystals were randomly mounted in epoxy resin and polished to expose an internal surface prior to laser ablation – inductively coupled plasma – mass spectrometry (LA-ICP-MS) measurements. Alongside each sample, fragments of the Sri Lanka (SL2) natural zircon crystal (564 Ma; *Gehrels et al., 2008*) were mounted for use as the U-Pb primary reference material, and fragments of Mud Tank ($^{176}Hf/^{177}Hf$= 0.282507; *Woodhead and Hergt, 2005*), FC-1 ($^{176}Hf/^{177}Hf$= 0.282183; *Fisher et al., 2014*) and R-33 ($^{176}Hf/^{177}Hf$= 0.282764; *Fisher et al., 2014*) were used as reference material for Hf isotopic compositions.

Analytical procedures for the U-Pb and Yb-Lu-Hf isotopic measurements followed the methods described in *Cecil et al. (2011)*; all analyses were conducted in a Nu Plasma multicollector-ICP-MS instrument coupled to a Photon Machines Analyte-G2 laser ablation system using static collection mode at the Arizona LaserChron Center, University of Arizona. In brief, for U-Pb geochronology, isotopes ^{238}U, ^{232}Th, ^{208}Pb, ^{207}Pb and ^{206}Pb were measured simultaneously in Faraday collectors whereas $^{204}(Pb+Hg)$ and ^{202}Hg were measured in discrete-dynode ion-multipliers. Instrumental inter-element and isotopic fractionations affecting the measured $^{206}Pb/^{238}U$ and $^{207}Pb/^{206}Pb$ compositions were corrected by a standard-sample bracketing approach using the Sri Lanka reference crystal, which was measured once or twice every five unknowns, and normalizing all data with respect to its known ID-TIMS values (*Gehrels et al., 2008*). For Yb-Lu-

Hf measurements, all masses from 171 to 180 were measured simultaneously on ten Faraday cups equipped with 3 x 10^{11} Ω resistors. Hafnium mass fractionation was corrected using an exponential law with respect to a $^{179}Hf/^{177}Hf$ value of 0.7325 (*Patchett and Tatsumoto, 1981*). Ytterbium mass fractionation was corrected using a $^{173}Yb/^{171}Yb$ value of 1.129197 (*Vervoort et al., 2004*) and a session-specific $^{176}Yb/^{173}Yb$ bias correction factor derived from the measurement of high-Yb natural and synthetic zircon crystals (see *Ibanez-Mejia et al., 2015* for details). All $^{176}Hf/^{177}Hf$ compositions reported here are relative to a Mud Tank value of 0.282507 (see *Fisher et al., 2014b*); this reference crystal was analyzed once or twice every ~15 unknowns during our session. Additionally, the reference crystals FC-1 and R-33 were also analyzed in repeated occasions throughout the session in order to monitor the accuracy of the Hf mass-bias and Yb interference corrections. These crystals are particularly well suited for the latter, owing to their relatively high HREE concentrations with respect to other widely available reference zircons and the average composition of natural crystals. We obtained mean values of 0.282167 ± 58 (2 S.D., n= 56, MSWD= 1.5) and 0.282725 ± 62 (2 S.D., n= 78, MSWD= 0.7) for FC-1 and R-33, respectively, which are accurate with respect to their reference solution-MC-ICP-MS values within quoted uncertainties.

3.4 Results

In this section we present the configuration and age of the basement of the LMV from four main sources of information, potential methods (air gravity and magnetics), two and three-dimensional reflection seismic, seismicity and isotope geochronology. We start by describing the broad regional basement morphology, as interpreted from potential methods (air gravity and magnetics, **Figure 3.3**) and continue with the more detailed structure, interpreted from reflection-seismic data and tied to the exploratory and stratigraphic wells (**Figure 3.4**). We then present the isotope geochronology data which was used to date the basement and to understand its origin and finally, we integrate seismicity data from public sources to constrain the tectonic and geodynamic setting of the basin.

3.4.1 Potential Methods

The broad basement morphology of the LMV, as interpreted from air gravity and magnetic intensity maps is show in **Figure 3.3**. In the Total Bouguer gravity anomaly map (**Figure 3.3**a), the most notorious basement lows are marked by negative anomalies with gravity values of less than -75 mGal, while the most prominent positive gravity anomaly occurs in the SNSM, where values of more than +175 mGal were obtained. The SNSM is a very high (>5,000 m) basement massif that is not in isostatic equilibrium (*Case and MacDonald, 1973*). While the gravity data provided a much broader image of the basement morphology, the data from the total magnetic intensity reduced to the pole (TMIRP, **Figure 3.3**b) shows more localized concentrations of highly-magnetic rocks which correspond to basement highs or to elongated features related to major fault zones, as will be discussed farther on. It appears that the high magnetic anomalies are related to basement rocks which have been described as felsic or mafic, occurring at shallow levels, as also interpreted by *Silva et al (2016*). According to the seismic and well data, these highs are all found at depths between 1500 and 3500 meters, which is much shallower than the estimated Curie Point Depth for northern Colombia (30-55 km, *Vargas et al., 2015*), therefore the basement still preserves its magnetic properties. The magnetic data shows an alignment of basement highs in the northwestern LMV, close to the RFS, defining a NE-SW-trending fringe. This fringe that could be limited to the east by the northward extension of the San Jerónimo fault (SJF, **Figure 3.3**), appears to be formed by volcanic rocks, which may relate to a different basement terrane.

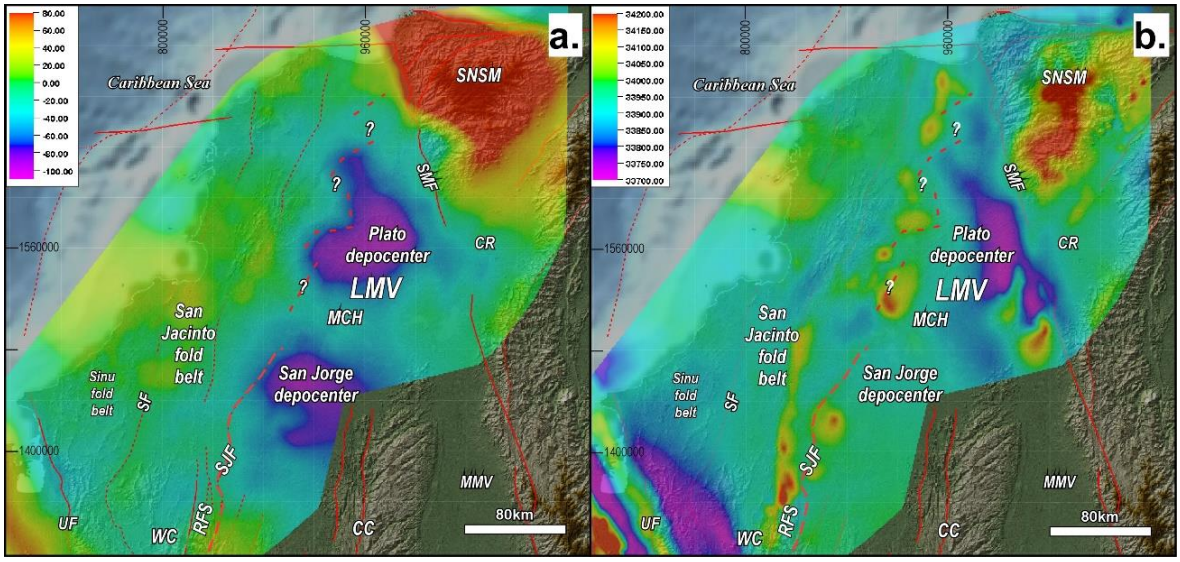

Figure 3.3. Air gravity and magnetics data from northern Colombia, acquired by *Lithosphera (2010*) for Hocol and the ANH. a. Total Bouguer anomaly, scale from -80 to 80 mGal; b. Total magnetic intensity reduced to the pole (TMIRP) with scale from 33700 to 34200. LMV: Lower Magdalena Valley basin; MCH: Magangue-Cicuco High; SF: Sinu fault; RFS: Romeral Fault system; SJF: San Jerónimo fault; WC: Western Cordillera; CC: Central Cordillera; UF: Uramita Fault; MMV: Middle Magdalena Valley basin; CR: Cesar-Rancheria basin; SMF: Santa Marta fault; SNSM: Sierra Nevada de Santa Marta.

3.4.2 Reflection seismic and well data

The structure of the basement underneath the LMV, as interpreted from reflection seismic data, is presented both in map and cross-section view and both in TWT and depth (**Figure 3.4** to **Figure 3.7**). The depth-structural map of the continental crystalline basement of the LMV obtained from detailed seismic mapping is shown in **Figure 3.4**. When comparing the Bouguer anomaly map with the depth-converted top basement map of the LMV, a very good match can be seen in terms of basement configuration. The southeastern boundaries of the LMV are the PFS and the basement outcrops of the northernmost CC, while the boundaries in the northeast are the Santa Marta Fault (SMF) and the SNSM. The SMF is forming the eastern limit of a NW-trending pull-apart basin limited in the west by the Algarrobo Fault. The western limit of the LMV has been considered the northward extension of the RFS (*Duque-Caro, 1979, 1984*), which would be separating the basin from the San Jacinto deformed belt to the west. However, based on reflection seismic data (**Figure 3.6** and section 3 in **Figure 3.7**), we have interpreted an east-verging fault splay in the southwestern LMV, which correlates at the surface with the San Jerónimo fault (SJF, **Figure 3.3** and **Figure 3.4**) and appears to correspond to the southwestern limit of the continental affinity basement of the LMV, as will be discussed in forthcoming sections.

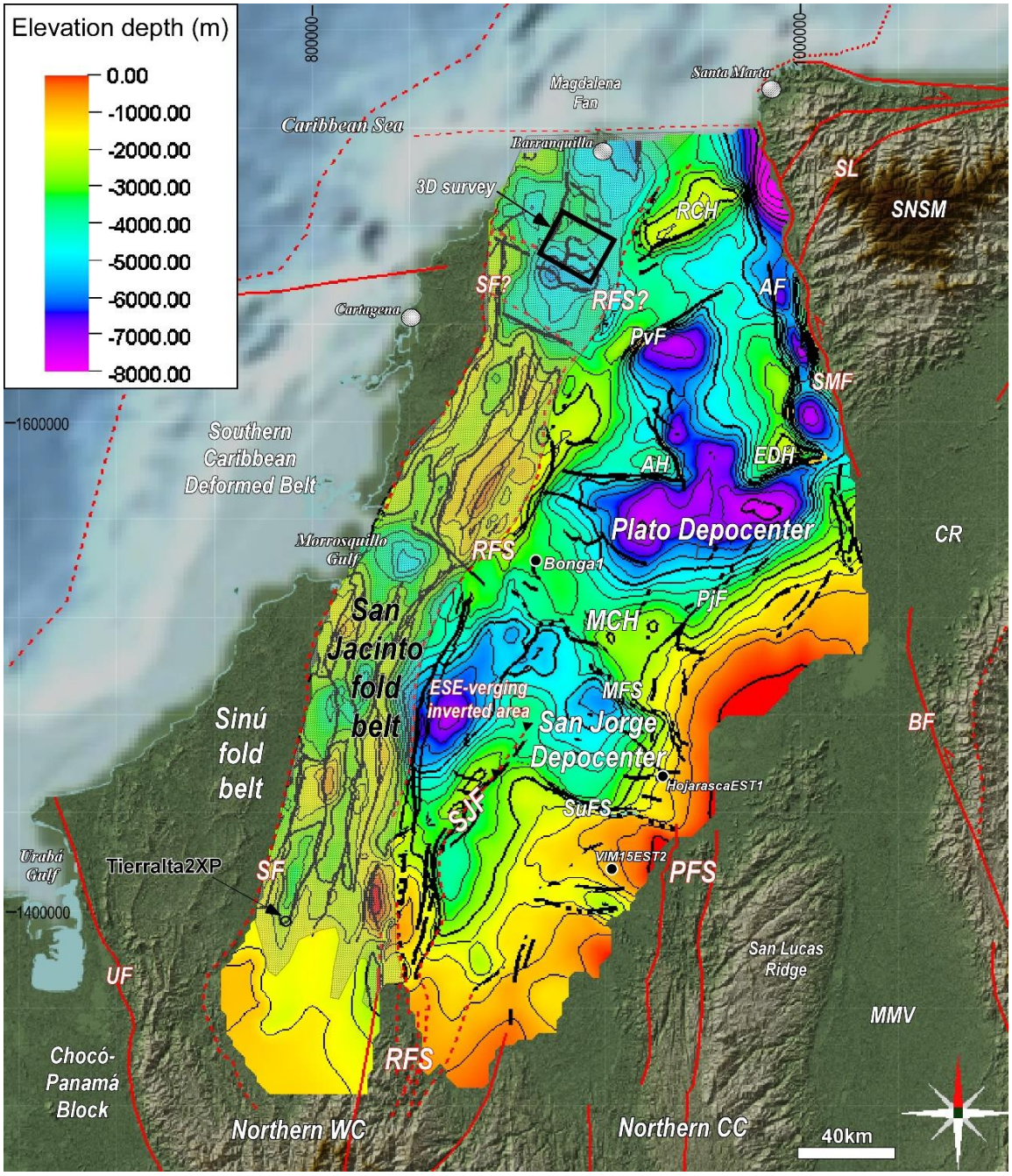

Figure 3.4. Structural depth-model (elevation in meters) of the top of the basement of the LMV and San Jacinto fold belt, showing the main morphological and structural elements. RFS: Romeral Fault system; PFS: Palestina Fault system; SJF: San Jerónimo Fault; MCH: Magangué-Cicuco High; PjF: Pijiño Fault; AH: Apure High; EDH: El Dificil High; PvF: Pivijay Fault; RCH: Remolino-Ciénaga High; BF: Bucaramanga Fault; SMF: Santa Marta Fault; SL: Sevilla Lineament; UF: Uramita Fault; SF: Sinu Fault; CR: Cesar-Ranchería basin; MMV: Middle Magdalena Valley basin; SNSM: Sierra Nevada de Santa Marta.

It must be noted that the basement interpretation and mapping has good control with wells and seismic within the LMV, while in the San Jacinto fold belt, we do not have any basement control. To interpret Cretaceous to Eocene sequences in the fold belt, we used several exploratory wells from the northern part of the fold belt and four stratigraphic wells recently drilled by the National Hydrocarbons Agency in the southern part of the belt (e.g. T-2XP, **Figure 3.1** and **Figure 3.4**). Concerning the possible base of the Cretaceous sequence, we had to tie the seismic to the outcrops, especially to those where the Cretaceous succession appears to be nearly complete, such

as the Arroyo Cacao section (*ICP, 2000*). Based on seismic-outcrop ties, we interpreted a possible base of the Cretaceous sequence in San Jacinto (**Figure A 1**), in order to produce the map shown in **Figure 3.4**. The similarities between the basement interpretation and the gravity expression of the basement in the San Jacinto belt suggest that our interpretation is reasonable. From several regional composite cross-sections that were built to analyze the three-dimensional basement structure, we present two representative geo-seismic sections in TWT that show the LMV-basement structure along the strike and dip (**Figure 3.5**). The area from which we recovered basement samples for U-Pb and Hf analyses (Bonga-1 well) is shown in the same figure, in which a prominent topographic feature in the basement (Magangué cone) that may correspond to a volcanic edifice can be seen. The area in which the Bonga basement samples were taken shows diffuse seismic reflectors below the interpreted "basement" reflector, which suggest the occurrence of pre-"basement" (pre-Oligocene) sequences below. A regional profile crossing the San Jorge depocenter is presented in **Figure 3.6**, showing our interpretation of the top of the subducting oceanic slab and its correlation with the subduction megathrust beneath the Sinú and San Jacinto fold belts and western Lower Magdalena. This TWT interpretation was used to obtain the depth map of the top of the oceanic slab in the study area. In the same figure we also highlight the interpreted structure of the deep San Jacinto fold belt and the RFS, including the eastern splay which we correlate with the San Jerónimo fault (SJF). This east-verging splay has been up-warped due to compression and inversion (see **Figure A 2**), and it is here considered to represent the eastern boundary of an oceanic affinity terrane, as will be discussed farther on. The integration in cross-section view of the depth-converted basement model and the gravity and magnetics data is shown in **Figure 3.7**, in which four dip-sections and one strike-section are displayed to highlight the gravimetric and magnetic expression of basement morphology. Gravity and magnetics data seem to highlight not only the basement highs but also the interpreted extension to the north of the SJF, suggesting a change in basement type.

Regarding the main morphological features of the basement underneath the LMV, the Plato depocenter in the north consists of a wide, nearly E-W-trending low in its southern part and a small depocenter in the north, in the downthrown block of an important NE-SW-trending fault (Pivijay fault, PvF, **Figure 3.4**). In these low areas the basement is probably found at depths of more than 7 km (23 thousand feet) and sections 1 and 5 of **Figure 3.7** show the respective gravimetric response. A stratigraphic well (called ANH-Plato Profundo) was recently drilled by the National Hydrocarbons Agency in this depocenter down to a depth of more than twenty-thousand feet (>6 km), without reaching the basement. Two structural highs are surrounding the Plato depocenter, the El Dificil High to the NE and the Apure High to the NW. The El Dificil High is limited to the E by the Algarrobo-Santa Marta strike-slip fault system, which has created a very deep pull-apart basin that has been filled with thick Miocene to Quaternary deposits. In the northernmost portion of the basin, though the seismic coverage is not good, gravity and magnetic data confirm the occurrence of a NE-SW-trending structural high called here the Remolino-Ciénaga High. Oil exploration wells have reported a volcanic basement in the southwestern part of this high, while plutonic rocks were recovered in the northeast. The Apure high, where two exploratory wells (Apure-1 and Apure-2) have reached and sampled the basement (**Figure 3.1**), also has volcanic andesitic rocks and seems to be defining a volcanic basement province in the northernmost LMV. By contrast, the block of the El Dificil high consists of a low-grade metamorphic basement (schists and phyllites) which have been related to similar rocks outcropping in the northwestern SNSM (*Campbell, 1968*; *Tschanz et al., 1974*). However, granodiorites were recently reported in the Alejandría-1 well, located in the El Dificil high (*Silva et al., 2016*). Most of these basement highs have a clear expression in magnetic data (TMIRP), which shows positive anomalies on top of them (**Figure 3.3** and **Figure 3.7**).

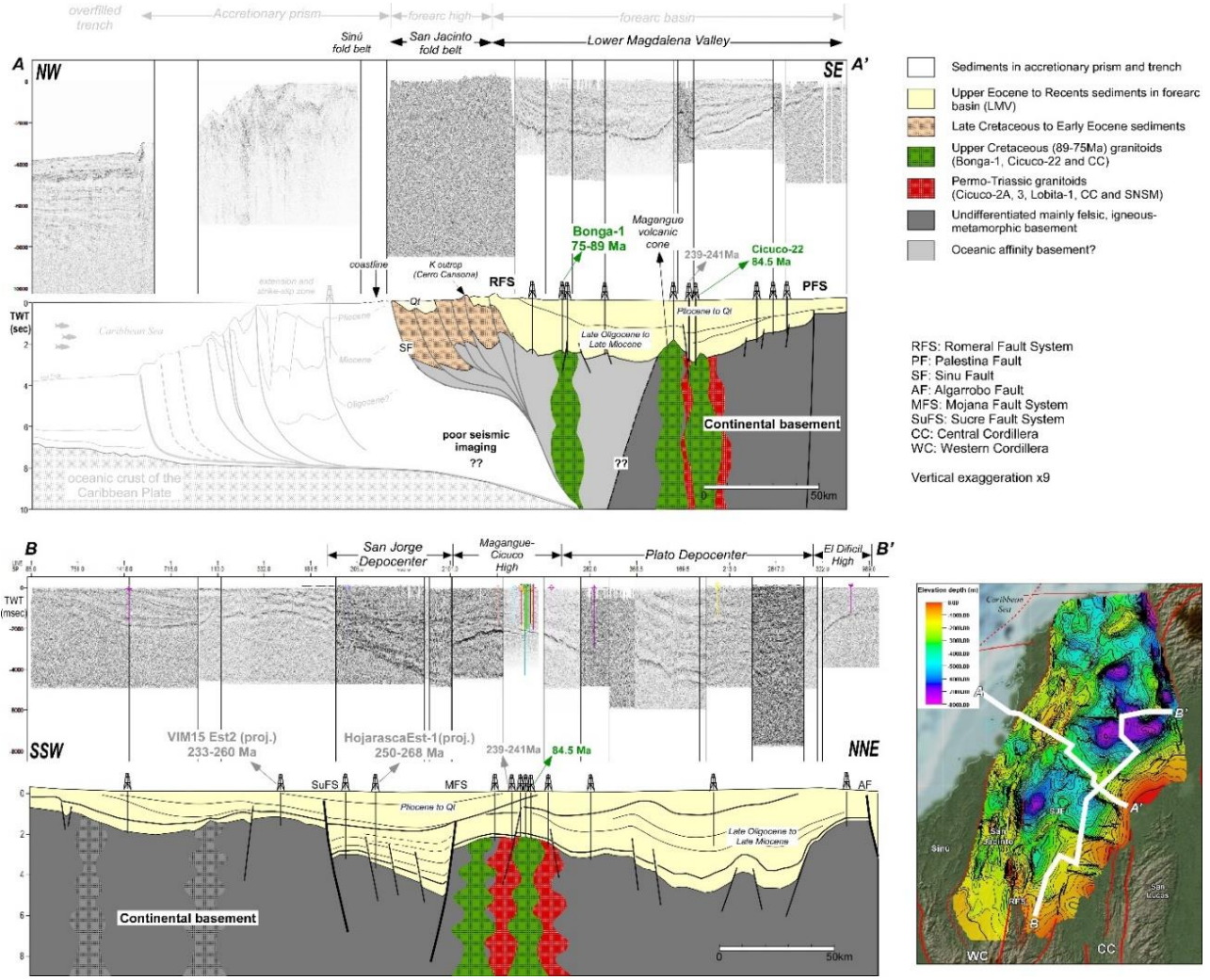

Figure 3.5. Regional composite two-way-time reflection seismic lines and respective interpretations showing the time-structure of the LMV in both dip (section A-A') and strike-direction (section B-B'), and the location of the wells analyzed in this work. Vertical exaggeration is x9.

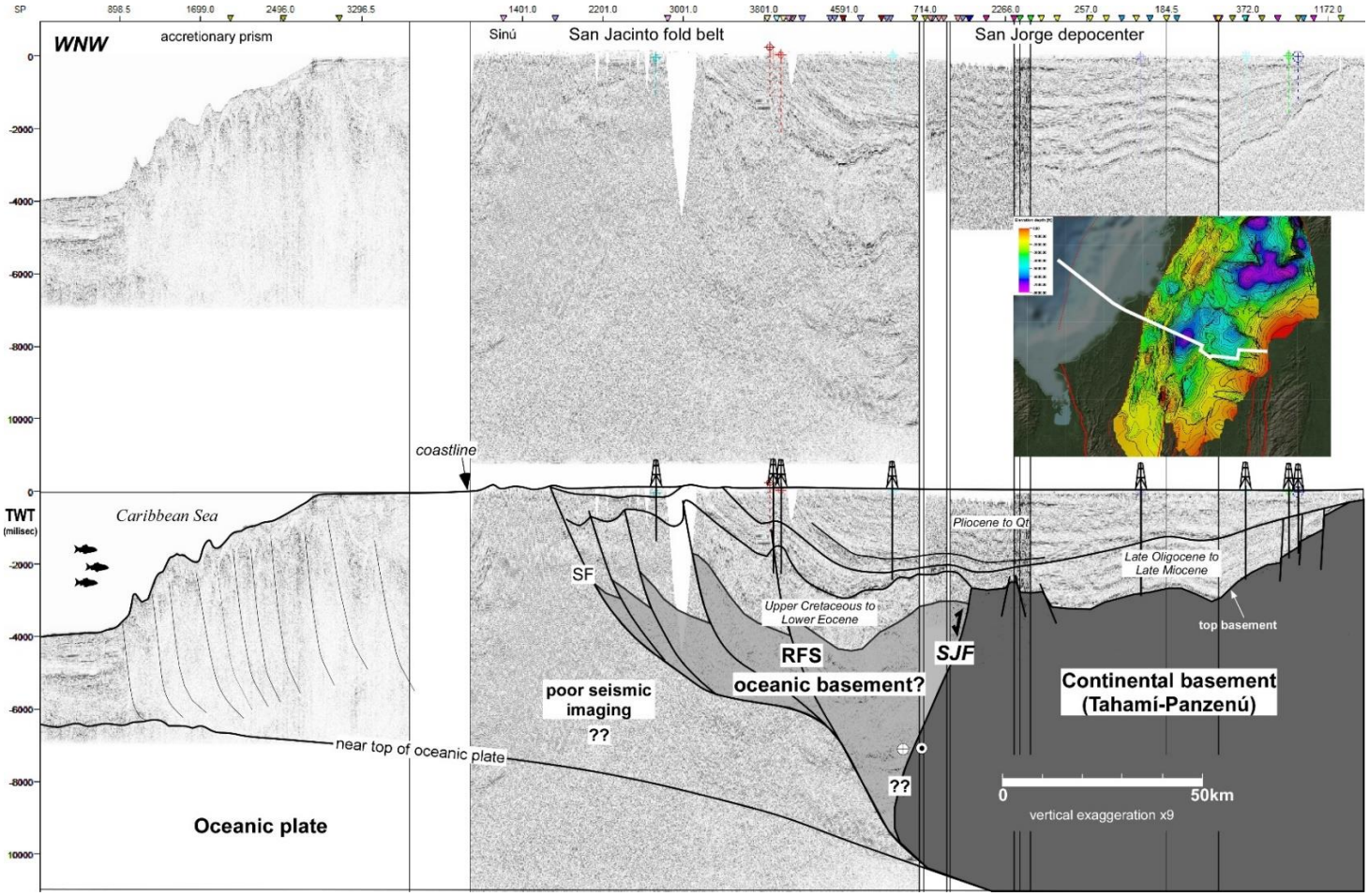

Figure 3.6. Regional cross-section from the accretionary prism in the WNW to the San Jorge depocenter in the ESE, showing the interpreted top of the subducting oceanic slab and the seismic expression of the RFS, including the southeast-verging SJF andthe southern LMV.

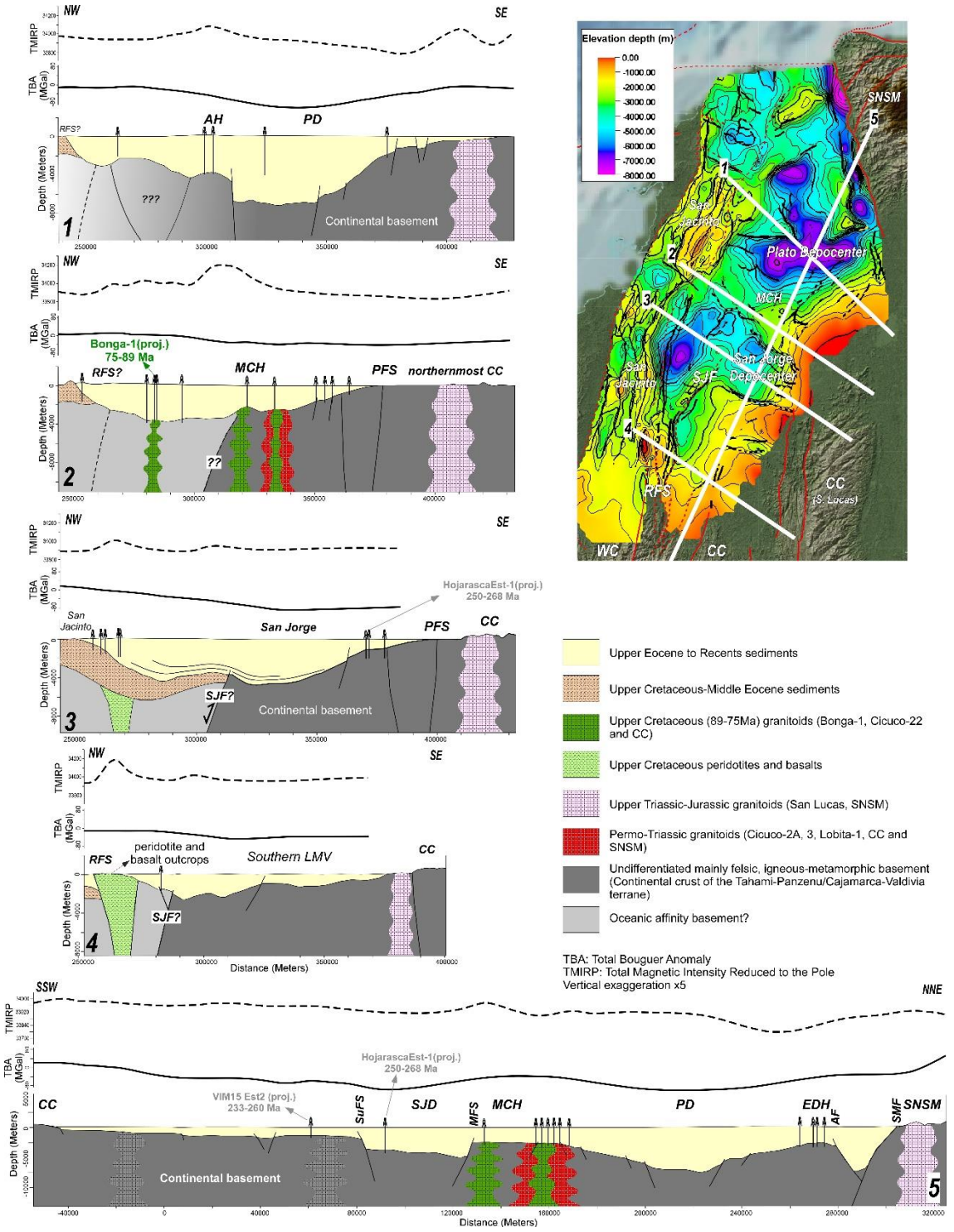

Figure 3.7. Structural cross-sections in depth of the LMV, showing the basement structure of the LMV and its gravimetric and magnetic response. TBA: Total Bouguer Anomaly with scale between - -80 and 80 Mgal; TMIRP: Total magnetic intensity reduced to the pole, with scale between 33700 and 34200. Vertical exaggeration is x5.

The SE-NW-trending Magangue-Cicuco High (MCH) also has a very clear expression in both gravity and magnetic data. In fact, well-developed gravimetric and magnetic anomalies occur on top of this high (**Figure 3.7**) and relate to what appears to be a volcanic cone. Concerning the rock types, the most complete basement database comes from this high because the area has been

drilled by numerous wells and several oil and gas fields have been found (e.g. El Dificil, Cicuco, Boquete, etc., see https://epis.anh.gov.co). The predominant basement rock types are felsic plutonic (e.g., granites, granodiorites, diorites, quartzdiorites) and metamorphic (e.g., metasediments, schists, phyllites, quartzites and gneisses, **Figure 3.1**), though gabbros and pyroxenites were recently reported in the SitioNuevo-1 well, in the eastern part of the high (*Silva et al., 2016*).

The San Jorge depocenter, located south of the MCH, is an ESE-WNW-trending graben bordered by two main fault systems, the Mojana Fault System in the north and the Sucre Fault System in the south (**Figure 3.4**, **Figure 3.5** and **Figure 3.7**). In the bottom of this graben, the basement can be found at depths of more than 5 km (17 thousand feet). South of this depocenter there are some minor and shallower structures, such as an E-W-trending graben located near the VIM15 Est-2 well and other nearly N-S-trending faults, which are related to the northern CC fabric. Rock types from drill holes show a predominance of a low- to medium-grade metamorphic basement in the southeastern LMV, probably related to metamorphic units outcropping in the northernmost CC (*Gómez et al., 2007*). However, a few wells drilled igneous plutonic and volcanic rocks which generally correlate with basement highs that also have a clear expression in both seismic and TMIRP data (**Figure 3.3**).

3.4.3 Fault families

Detailed seismic mapping of the basement underneath the LMV shows that the fault pattern is much more complex than previously considered. We divided the basement faults into four fault families according mainly to their trend and also to their age, and found that these families define two structural regions in the LMV: a western region with a dominant ESE-WNW-trending fault family and a northeastern region with a dominant NE-SW-trending family (**Figure 3.8**). The oldest fault family (family 1, green traces in **Figure 3.8**) comprises normal faults trending NE-SW (40-60°) and includes the southern El Difícil fault, the Pivijay Fault and the fault that limits the Remolino-Ciénaga High to the south. This fault family appears to be slightly older than family 1 because it became active in Late Eocene (?) to Oligocene times, as suggested by seismic data. These faults have very similar trends compared to the notorious lineaments in the northern CC (San Lucas Range) and also in the Sierra Nevada de Santa Marta (SNSM, **Figure 3.8**).

The second fault family (family 2, red traces in **Figure 3.8**) comprises extensional faults which exhibit subtle strike-slip and inversion deformation affecting the sedimentary infill and which have an ESE-WNW-trend (265-320°). This family includes the Mojana and Sucre fault systems which are limiting the San Jorge depocenter, as well as the southern Apure fault and other faults that mark the northern limit of the Magangué-Cicuco High (**Figure 3.4** and **Figure 3.8**). Seismic and well data show that these faults are affecting a felsic igneous plutonic, andesitic volcanic and metamorphic basement and that they became active as extensional faults in Late Oligocene to early Miocene times (**Figure 3.5**). The trends of this family are similar to those observed in the CC farther south, where they are affecting Permo-Triassic granitoids and the Late Cretaceous Antioquia Batholith (**Figure 3.8**).

The third fault family (orange traces in **Figure 3.8**) trends SSE-NNW (330-360°) and corresponds to the Algarrobo fault, a trans-tensional strike-slip fault, and to the northern Apure fault. This trend implies ENE-WSW-oriented extension, which allowed the formation of the Algarrobo pull-apart depocenter and part of the Plato depocenter. The activity of this fault family probably began in early Oligocene times but the age of the oldest sediments in the Algarrobo pull-apart basin is unknown. The fourth and least important fault family in the LMV (blue traces in **Figure 3.8**) comprises normal faults with subtle inversion and a NNE-SSW-orientation (0-30°), hence implying an ESE-WNW-oriented extensional component.

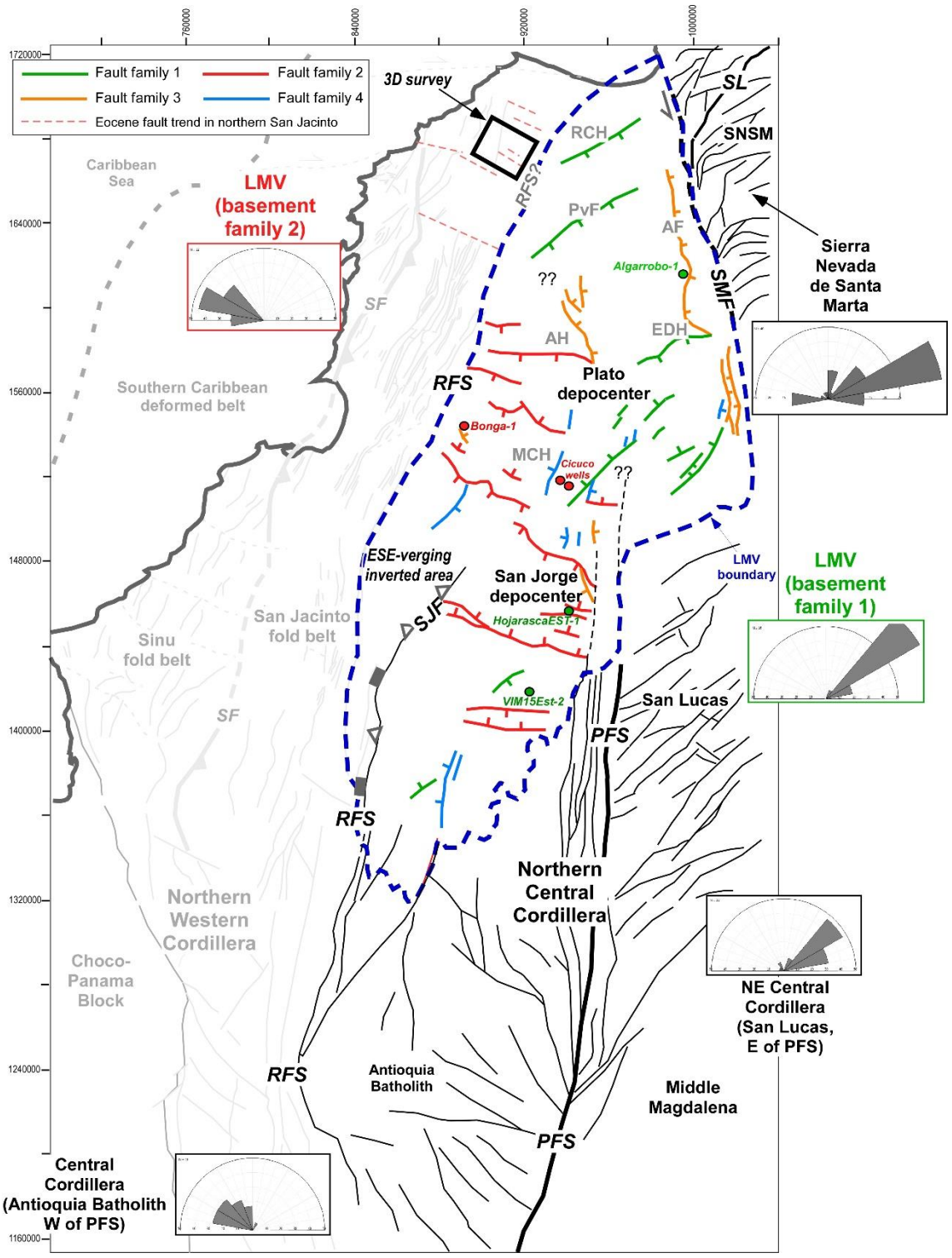

Figure 3.8. Structural fabric of the basement terranes in northwestern Colombia (northern CC, western SNSM and LMV). Surface faults and lineaments were drawn from the Geological Map of Colombia (*Gomez et al., 2007*) and subsurface fault families were interpreted and drawn from our basement depth-models. In all rose diagrams, the bin size was set to 20 degrees. Light gray features drawn in the Sinú and San Jacinto fold belts are Neogene to recent structures.

Neogene to Recent, E-W and SE-NW contraction has obscured the original Cretaceous to Paleogene structural fabric in most of the San Jacinto fold belt, except for the northernmost area, where NW-SE-trending Eocene extensional features that influenced sedimentation have been recently interpreted (*Mora et al., 2013* and **Figure 3.8**). For this reason, most of the structures exposed in the San Jacinto and Sinú fold-belts are Pliocene to recent folds and faults mapped in geological maps (light gray features in **Figure 3.8**, *Gómez et al., 2007*). **Figure 3.4** and **Figure 3.8** also show how deformation of the San Jacinto fold belt extended farther to the east in the southern LMV, as shown by the east-verging splay that inverted an area just west of the San Jorge depocenter. Geological maps of the northern CC (*Gómez et al., 2007*) show that this splay appears to represent the northern extension of the San Jerónimo fault (SJF, mapped by *Gómez et al., 2007* as Santa Rita Fault), which marks the boundary between the Tahamí-Panzenú terrane to the east and an oceanic terrane called Quebradagrande Complex (*Nivia et al., 2006*) to the west.

3.4.4 Zircon U-Pb geochronology and Hf isotope geochemistry

In the eastern MCH, *Montes et al. (2010*) reported Middle Triassic (Ladinian) granitoids in the Cicuco and Lobita wells, while *Silva et al. (2016*) reported uppermost Carboniferous to lowermost Permian gabbros and pyroxenites in the SitioNuevo-1 well, and Middle Triassic monzogranites in the Coral-9 well. The samples that we recovered in this study come from the eastern San Jorge depocenter (Hojarasca Est-1) and from the southeastern LMV (VIM15 Est-2). These were classified petrographically as quartz-mica schists and quartzites in Hojarasca and as tremolitic schists and sericitic slates in VIM15. Detrital zircon U-Pb dates from these low-grade metasediments indicate a Middle to Upper Triassic maximum depositional age for their sedimentary protoliths (**Figure 3.9**), estimated to 234 ± 5 Ma (n= 4, MSWD= 0.7) for Hojarasca and 233 ± 4 Ma for VIM15 (n= 4, MSWD= 0.7) based on the youngest group of zircons that define an equivalent population at 2σ (e.g., *Dickinson and Gehrels, 2009*). The age spectra retrieved for both localities is dominated by zircons with early Permian to Middle Triassic crystallization ages, with subdued older populations in the early Paleozoic (Cambrian-Ordovician) and the Meso- and Neoproterozoic. A comparison with the known age distributions of pre-Jurassic basement domains in NW South America reveals that these detrital zircon age populations are most similar to the igneous and detrital zircon U-Pb ages found in the basement of the CC and the SNSM (**Figure 3.9**, see references in figure caption), thus strongly suggesting a close paleogeographic connection. This provenance interpretation is also supported by the Hf isotopic compositions of the Permo-Triassic grains found in Hojarasca and VIM15 (**Figure 3.11**), which closely match the existing data from the "Cajamarca" group granitoids and gneisses exposed that are exposed along the CC (*Cochrane at al., 2014*).

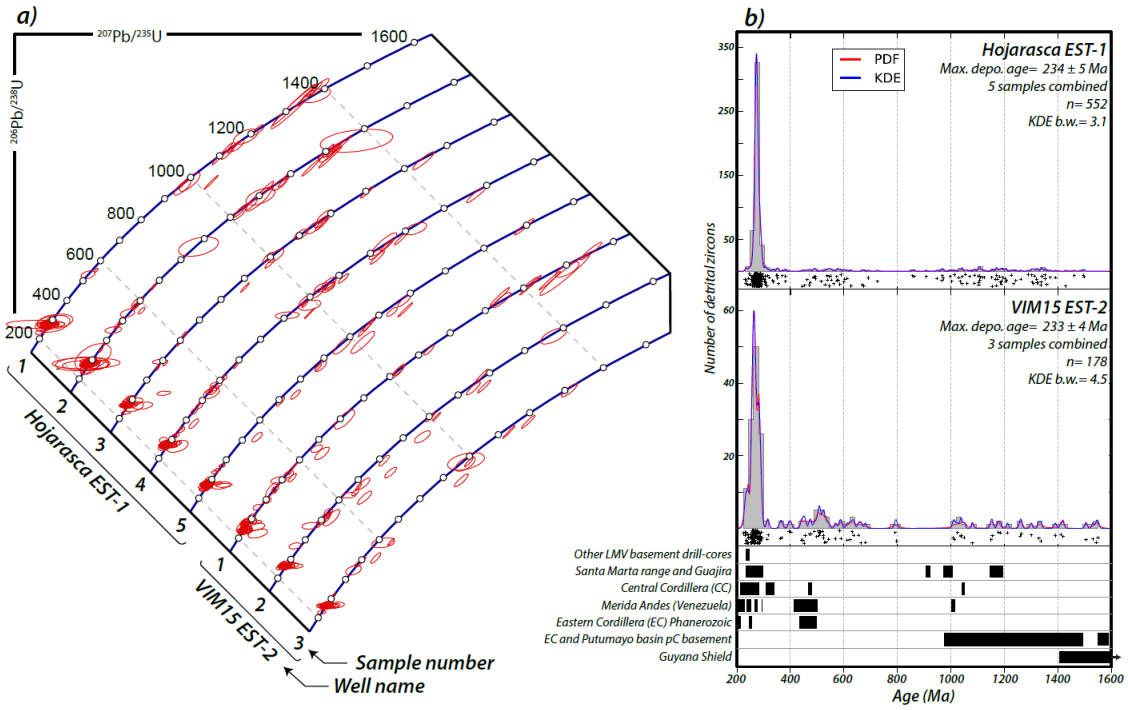

Figure 3.9. a) Concordia diagrams for the zircon U-Pb age data obtained from basement samples of the VIM15Est-2 and HojarascaEst-1 wells. b) Probability Density Function (PDF) and Gaussian Kernel Density Estimate (KDE) curves for detrital zircon age spectra of the Hojarasca and VIM15 basement metasediments. Reference basement ages for possible source terranes were compiled using the data of *Cordani et al. (2005)*, *Vinasco et al. (2006)* , *Cardona et al. (2010a)* , *Cardona et al. (2010b)* , *Horton et al. (2010)* , *Restrepo-Pace and Cediel (2010)* , *Weber et al. (2010)* , *Ibanez-Mejia et al. (2011)* , *Leal-Mejia (2011)* , *Villagomez et al. (2011a)* , *Cochrane et al. (2014)*, *Ibanez-Mejia et al. (2015)* , *Van der Lelij et al. (2016)*.

However, the basement in the LMV not only comprises Permo-Triassic igneous and metamorphic rocks but also Upper Cretaceous felsic intrusives , as evidenced by the age obtained in the basement sample of the Bonga-1 well. In this well, located in the western part of the MCH (**Figure 3.1** and **Figure 3.5**), we recovered samples of a granitic basement that yielded zircon U-Pb ages in the range of 76 to 89 Ma (Coniacian-Campanian). Interestingly, three cutting samples taken from a depth interval between ~3299 and 3303 m in the Bonga-1 well and processed for zircon geochronology all yielded bi-modal age distributions (**Figure 3.10**), defining two clear populations ca. 76 Ma and 88-89 Ma. Considering that the samples were taken from drill cuttings, the occurrence of two populations suggests that they may represent two different magmatic events, an old one with a Coniacian age (88-89 Ma) and a younger one with a Campanian age (75-76 Ma). However, based on the absence of textural observations, the relationship between these two apparent magmatic pulses is difficult to ascertain. Despite this complexity, the new results from the Bonga-1 well clearly indicate that magmatism in this portion of the LMV basement was ongoing for this time interval in the Upper Cretaceous as has been observed in other parts of the basin; for instance, a granite sample from the Cicuco field in the MCH was dated as Santonian (Aleman, 1983, in *ICP, 2000*), while a recent study by *Silva et al., 2016,* provided a similar age (84.5 Ma, U-Pb in zircon) for the granodioritic basement in the Cicuco-22 well in the eastern MCH. Another Late Cretaceous age was reported in the Coral-9 well (74.5 Ma, *Silva et al., 2016*).

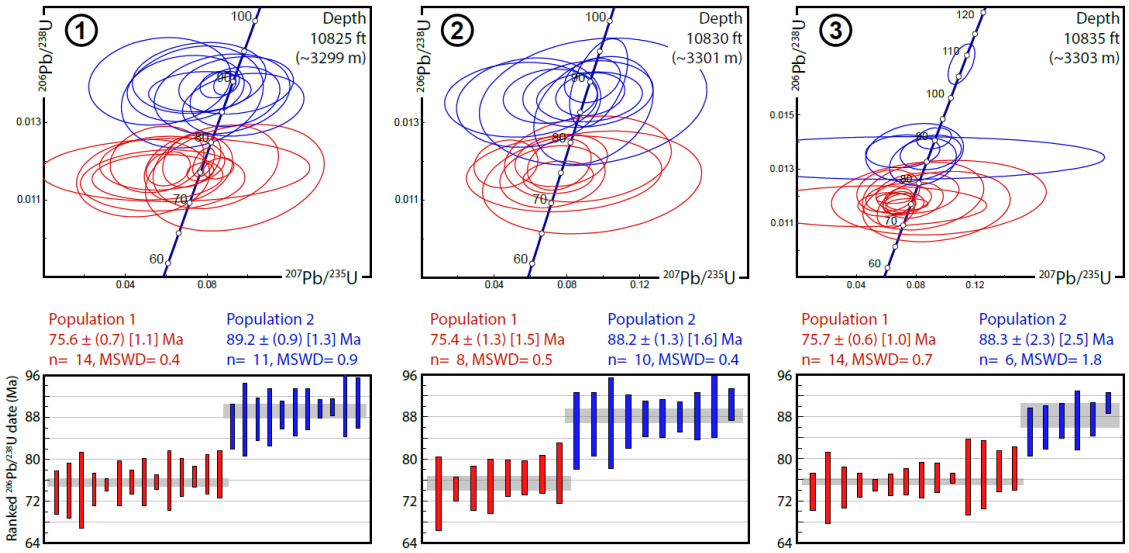

Figure 3.10. Summary of U-Pb (zircon) age data from the three basement samples of the Bonga-1 well.

In addition to the new U-Pb results for the Bonga-1 well, the Hf isotopic compositions of the dated zircons also indicate a rather juvenile affinity for this portion of the LMV basement (**Figure 3.11**). Several analyses conducted in two of the Bonga samples yield εHf(t) values in excess of +10 and up to +15, which exceed the values typical for arc-related crust (*Dhuime et al., 2011*) and overlap with a depleted mantle-like composition (*Vervoort and Blichert-Toft, 1999*). Although the intra-sample variability for each one of the two analyzed age populations exhibits a dispersion in initial $^{176}Hf/^{177}Hf(t)$ values that exceeds the external reproducibility of our reference zircon crystals (i.e., MT and R33; **Figure 3.11**), possibly indicating some interaction with and incorporation of older crustal components, these Hf results evidence that the Bonga magmatism has a very clear juvenile mantle source. In contrast, samples from the VIM15 and Hojarasca wells discussed above yield much lower εHf(t) values, mostly ranging between +4 and -8, thus indicating a much older crustal source for the preceding magmas from which these detrital zircons crystallized.

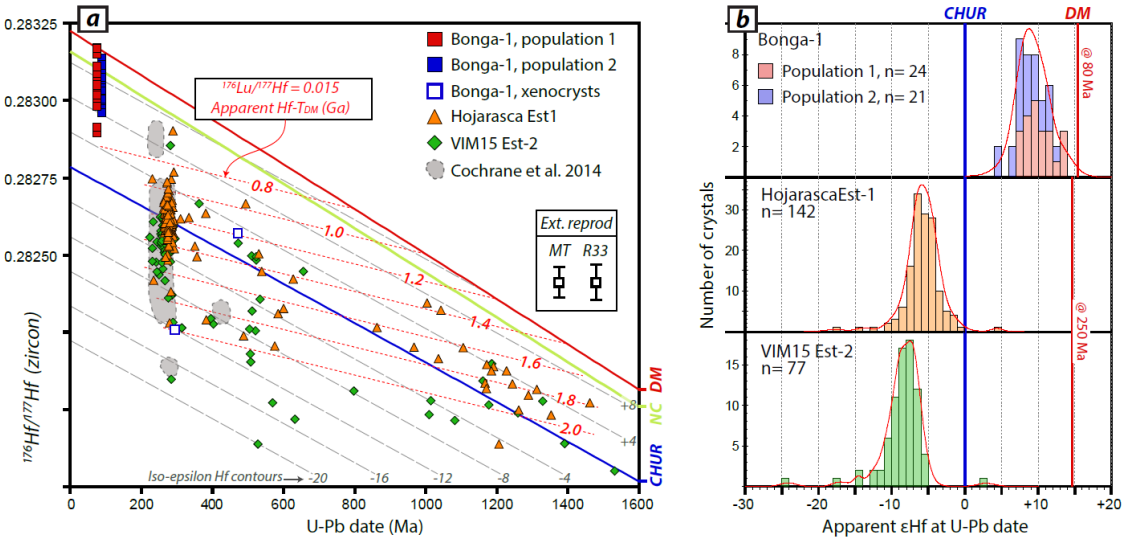

Figure 3.11. Hf isotope compositions of zircon from all drill hole samples analyzed in this study, shown in a) $^{176}Hf/^{177}Hf(i)$ vs. apparent $^{206}Pb/^{238}U$ age space, and b) as histograms of apparent initial εHf at age of zircon crystallization. Field for 'Cajamarca Complex' zircon compositions (gray shaded area) after *Cochrane et al. (2014)*. Chondritic uniform reservoir (CHUR) values from *Bouvier et al. (2008)*. New Crust (NC) model for the Hf isotopic

composition of arc-crust from *Dhuime et al. (2011*). Model composition for the depleted mantle (DM) was calculated from the juvenile crust data of *Vervoort and Blichert-Toft (1999*).

3.4.5 Seismicity data

The Colombian Caribbean margin, southwest of the SNSM, is a remarkably aseismic area (**Figure 3.12**). The LMV and Sinú-San Jacinto fold belts exhibit very few scattered shallow (<70 km) and low magnitude (<4 Mw) events and seismicity increases notoriously and deepens towards the Bucaramanga intermediate seismicity nest (BN) in the southeast. Within the study area, the very few available focal mechanism solutions correspond to shallow events (< 60 km, beachballs in black) while only one solution corresponds to an intermediate depth event (118 km, beachball in red). Solutions close to the SNSM (*Malavé and Suárez, 1995*; *Cortés and Angelier, 2005*) coincide with strike-slip displacement related to the SMF- Algarrobo pull-apart basin and with thrusting of the massif towards the NW. However, other important fault zones, such as the Romeral Fault System, San Jeronimo Fault, Palestina Fault System and the Sevilla Lineament do not show seismic activity, suggesting that they are currently inactive structures. One focal mechanism solution by *Corredor (2003)* is probably related to the Sucre fault system, which limits the San Jorge depocenter in the south. This solution is in agreement with the ESE-WNW fault trend and indicates a left-lateral strike-slip displacement. Solutions by *Ekstrom et al. (2005*) in the limit with the Chocó-Panamá block in the southwest clearly show a sinistral strike-slip displacement related to the Uramita Fault.

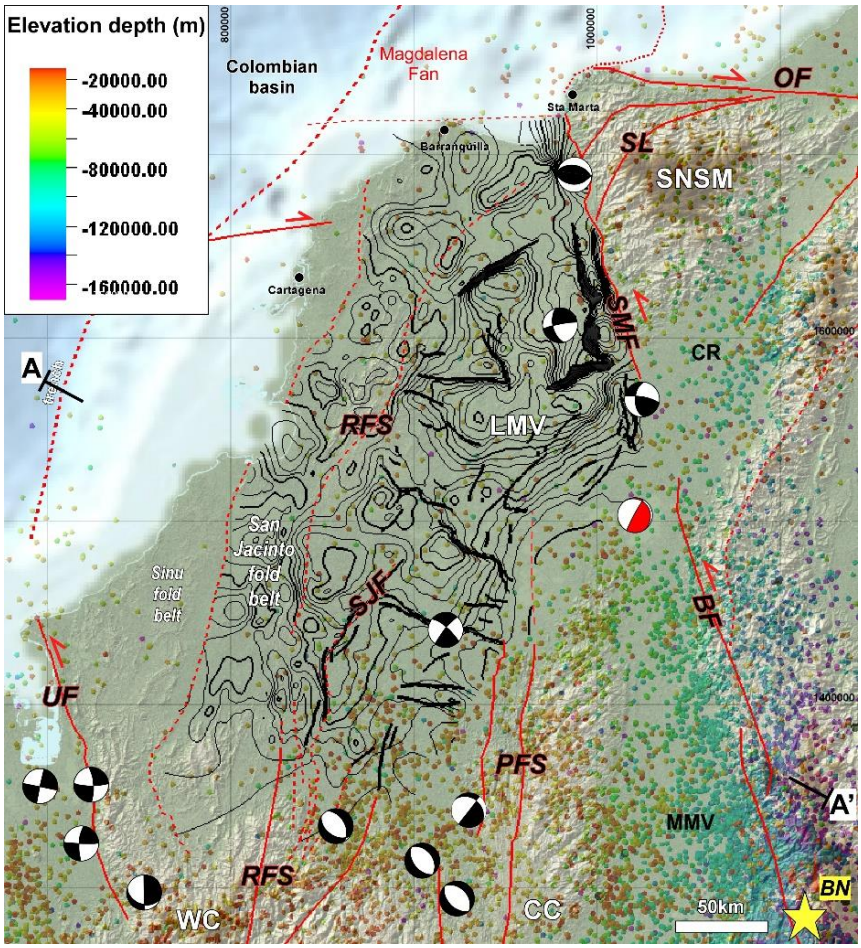

Figure 3.12. Earthquake and seismicity data obtained from the Colombian Seismological Network, plotted with the basement depth-structure of the LMV and with available focal mechanism solutions. Dots are earthquakes that have been colored according to depth. Black beach balls are shallow (<60 km) solutions and the red beachball is the only solution deeper than 60 km. BN: Bucaramanga seismicity nest. SCDB: Southern Caribbean deformed belt.

We interpreted and mapped the near top of the subducting oceanic plate under the Sinú-San Jacinto fold belt, which connects with a megathrust that can be imaged in some of the regional seismic lines (**Figure 3.6** and **Figure A 1**). Using stacking processing velocities from reflection seismic data, we depth-converted the interpreted subduction megathrust and plotted it with the earthquake and seismicity data in cross sections (**Figure 3.12** and **Figure 3.13**).

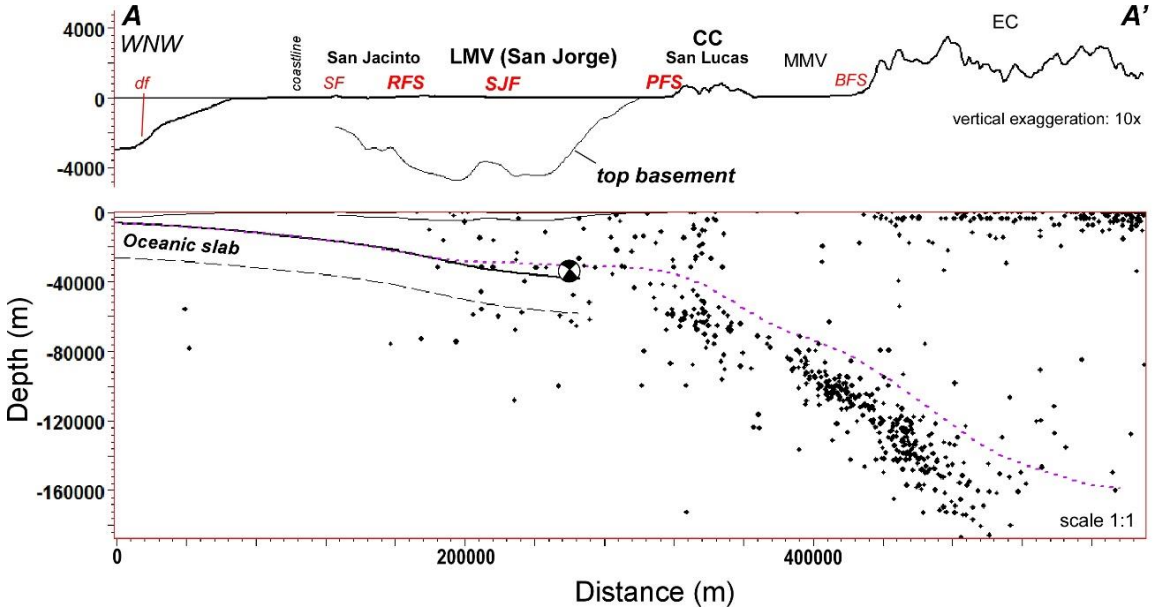

Figure 3.13. Regional profile A-A' (location in **Figure 3.12**), integrating seismicity, earthquake focal mechanism solutions, topography and basement depth-structure of the southern LMV. The flat slab under the LMV, obtained from reflection-seismic interpretations, shows a good match with the interpreted top of the steeper Bucaramanga slab (pink dotted line). The bend or inflection between the flat slab under the LMV and the steeper slab to the east, coincides with the surface trace of the Palestina Fault System (PFS). The base of the accretionary prism (df=deformation front) and the coastline are also indicated.

3.5 Discussion

3.5.1 LMV basement structure and fault families

In most of the recent studies, it has been proposed that the basement of the LMV displays a simple radial pattern which can be easily used to explain the extension observed in the LMV as a result of clockwise block rotation (*Montes et al., 2010*; *Bayona et al., 2011*; *Ayala et al., 2012*; *Cardona et al., 2014*). However, our detailed interpretation of seismic data shows that the basement in the LMV is affected by extensional faults which display a different and more complex pattern, compared to the previously interpreted, simple radial pattern. A detailed comparison of the previous and our new basement interpretation shows that the faults of Family 1 (in green in **Figure 3.8**) which are bounding important basement highs, are not reported, while some of the reported NW-SE-trending faults are not visible in seismic data (see Figure 12 in *Montes et al., 2010*). The observed differences are expected considering the very different databases that were used in both studies. The subdivision of basement faults in families with different orientations and possibly different origin (**Figure 3.8**),

and the integration of the basement structure in depth with the geology of surrounding areas (**Figure 3.1**) allows us to further delineate more robust correlations in terms of terranes defined by structural trends, rock ages and types. Concerning structural trends, the Palestina Fault System appears to be separating two basement areas with different rock types and ages (**Figure 3.1** and **Figure 3.8**), and affected by faults and lineaments that exhibit markedly different structural trends. While the Upper Cretaceous Antioquia Batholith, located W of the Palestina Fault System, is affected by SE-NW-trending structures, the San Lucas Ridge, located to the E of the fault system, exhibits very clear NE-SW-trending lineaments (**Figure 3.8**).

The NE-SW trend of fault family 1, which occurs to the east of the Palestina Fault System, is very conspicuous in areas where the Chibcha terrane is outcropping, such as the San Lucas Ridge and the SNSM (*Ordóñez and Pimentel, 2002*; *Gómez et al., 2007*; *Clavijo et al., 2008*), where Triassic-Jurassic volcano-sedimentary sequences covered older rocks. Jurassic volcano-sedimentary rocks and red beds of northwestern South America were deposited in a series of NE-SW-trending grabens such as the El Indio, Morrocoyal, Bocas, Girón and La Quinta, which made part of the Bolivar Aulacogen of *Cediel et al. (2003*) that was formed during a Jurassic rifting phase (*Maze, 1983*; *Cediel et al., 2003*; *Pindell and Kennan, 2009*). In fact, the Jurassic structural fabric strongly influenced Cretaceous and later sedimentation and deformation (*Cooper et al., 1995*), hence the conspicuous NE-SW structural trend that is seen today in several terranes of northern Colombia had its origin in a widespread rifting episode. Considering its location just between these terranes (**Figure 3.8**), it is probable that the northeastern LMV basement was also affected by such Jurassic extension episode and subsequently, we argue that the NE-SW trend of fault family 1 is probably inherited from the older Jurassic fabric.

The fault family in the western LMV (family 2) has an ESE-WNW trend which is also observed in the south, where Permo-Triassic and Cretaceous terranes exposed in the northern CC (**Figure 3.8**). Subduction of the Caribbean plate underneath northern South America started in late Paleocene times (*Bayona et al., 2008*; *Cardona et al., 2011*), allowing the formation of several forearc basins along western Ecuador and Colombia. We have reflection-seismic evidence from several parts of the San Jacinto fold belt (**Figure 3.2** and **Figure A 3**), to propose that the origin of this fault family relates to a Paleocene to Eocene extensional and strike-slip episode which occurred in the western Andean forearc from Ecuador to Colombia. Recently acquired three-dimensional seismic data in the northern San Jacinto fold belt (**Figure A 3**) shows very clear, Middle to Late Eocene extensional faulting which also appears to control sedimentation (*Mora et al., 2013*). This ESE-WNW trend is also seen in some regional two-dimensional seismic lines in the westernmost LMV which were interpreted and mapped in this study (**Figure 3.8**) and in the pre-Oligocene units of the Jobo-Tablón area. Furthermore, a similar structural trend affecting Eocene deposits has been reported farther south, in the Ecuadorian forearc. *Daly (1989*) studied the Tertiary evolution of the forearc basins of Ecuador and concluded that during the Middle to Late Eocene, the Piñón and Cayo forearc basement was extensively faulted and the major structural pattern of today established. Such pattern comprises ESE-WNW trending extensional faults, which controlled the deposition of the Eocene flysch and which were formed due to clockwise block rotation between two major dextral strike-slip faults. This model is similar to the transrotational basin model proposed by the *ICP (2000*) for the LMV.

The faults in family 3, which are far from the Santa Marta Fault, could also be inherited basement features corresponding to a conjugate set of Jurassic extensional faults, as seen in other Colombian basins (*De Freitas et al., 2003*). However, the Santa Marta-Bucaramanga Fault System is also considered to be an old Proterozoic to Paleozoic feature (*Cediel et al., 2003*), hence the faults in family 3 which are parallel to it may also have a Paleozoic overprint. Finally, fault family 4 which is nearly parallel to the trend of the Palestina Fault System, may also relate to older pre-Mesozoic features which were later compressed and inverted in Neogene to Recent times.

3.5.2 Permo-Triassic units

According to the revision of basement outcrop studies in surrounding areas, we argue that the Permo-Triassic basement ages and rock types best correlate with the Late Paleozoic-Triassic Tahamí-Panzenú terranes in the northern CC (*Ordóñez and Pimentel, 2002*; *Villagómez et al., 2011a)* and with the Permo-Triassic Sevilla province of the SNSM (*Tschanz et al., 1974*; *Cardona et al., 2006*; *2010b*). However, recent studies have highlighted the necessity of studying and mapping in more detail the different units that occur within the Tahamí-Panzenú terranes (*Villagómez et al., 2011a*). Regarding the paleo-tectonic setting for the northern CC and LMV, while the Permian to earliest Triassic magmatism within NW South America is thought to have formed in a compressional setting during the final amalgamation of western Pangaea (*Spikings et al., 2015),* sedimentary rocks of the Cajamarca complex were deposited later in the Triassic, possibly during subsidence associated with Pangea's disassembly (*Villagómez et al., 2011a*; *Cochrane et al., 2014*). The new detrital zircon U-Pb ages from the metasedimentary basement of the LMV presented here span the proposed transition from the compressional magmatic arc phase to the extensional collapse of the CC terranes; however, no clear evidences for a systematic shift in the $^{176}Hf/^{177}Hf(t)$ compositions of zircon associated to this major tectonic transition can be discerned from our data. Based on the good match between our results and those obtained by Cochrane et al. (2014) (**Figure 3.11**), it is likely that the zircons found in the schists, slates and quartzites of the LMV basement originated from the Permian-Triassic basement exposed in the CC, originally formed in a magmatic arc product of the east-dipping subduction of the Pacific slab under the proto-Andean South American margin.

3.5.3 Hypothesis about Late Cretaceous magmatism in the LMV

The presence of Cretaceous igneous bodies in the basement of the LMV, which is widely documented in the northern CC, had only been loosely mentioned in old industry reports (Aleman, 1983, in *ICP, 2000*). The data obtained from the Cicuco-22 well (*Silva et al., 2016*) and our new Coniacian-Campanian crystallization ages from the Bonga-1 granitoid confirm the continuity to the north of the Upper Cretaceous magmatic arc in the northern CC, which includes important plutons like the Antioquia Batholith (88-83 Ma, *Ibáñez-Mejía et al., 2007* and 93-87 Ma, *Villagómez et al., 2011a*), the Sabanalarga Batholith (89.9±0.8 to 98.2±3.5 Ma, *Rodriguez et al., 2012*) and the Córdoba pluton (79.7 Ma, *Villagómez et al., 2011a*). *Leal (2011*) also reports K-Ar ages for vein-related dikes at the Segovia-Remedios mining district in the northern CC, between 84±3 and 88±3 Ma, which are very close to the ages obtained by *Silva et al.(2016*) for the Cicuco intrusive.

Geochemical analyses of the Upper Cretaceous Cicuco intrusive suggested that this granitoid is related to a subduction environment and corresponds to calc-alkaline magmas, interpreted to be emplaced in a continental Andean-type crust (*Silva et al., 2016*). In fact, *Silva et al. (2016*) proposed the existence of an Upper Cretaceous (Campanian) intra-continental magmatic arc, which they called the "Magangué Magmatic Arc". However, our new Bonga Hf isotopic data indicate a clear juvenile component, with limited evidence for significant contamination with older continental crust (**Figure 3.11**). Furthermore, the highly positive Bonga εHf values obtained here are in contrast with the less radiogenic values obtained for the Late Cretaceous granitoids of the northern CC such as the Antioquia Batholith (*Restrepo et al., 2007*). Considering these observations, and taking into account the proximity of the Bonga granitoid to the Romeral Fault System, we consider that there are two hypothesis about the origin of the pluton. The first one is that the Bonga pluton intruded a previously accreted oceanic terrane possibly located within the Romeral System, which may correspond to the northern continuation of the Quebradagrande Complex (*Nivia et al., 2006*). The second one is that the pluton formed within an allochthonous intra-oceanic arc which collided against the Permo-Triassic continental margin in latest Cretaceous to early Paleocene times (*Bayona et al., 2011*; *Cardona et al., 2012*).

3.5.3.1 Intrusion into a previously Accreted Oceanic Terrane (Quebradagrande)

Concerning the hypothesis of the origin of the Bonga pluton as an intrusion into a previously accreted oceanic terrane such as the Quebradagrande Complex (*Nivia et al., 2006*), a similar situation is reported much farther south with the Córdoba pluton, which consists of granodiorites with dates ca. 80 Ma (U-Pb zircon) that are intruding the Quebradagrande Complex (*Villagómez et al., 2011a).* In the western flank of the Central Cordillera, the Berriasian-Albian Quebradagrande Complex consists of unmetamorphosed to greenschist gabbros, diorites, basalts, andesites and tuffs, covered by marine and terrestrial sediments and the igneous rocks are considered to have been formed in an island arc that fringed the continental margin (*Nivia et al., 2006*; *Pindell and Kennan, 2009*; *Villagómez and Spikings, 2013*). In that area, the complex is limited from the Tahamí terrane to the west by the San Jerónimo fault (SJF, *Nivia et al., 2006*), which is an eastern splay of the RFS. The northernmost outcrop of the Quebradagrande Complex is located just east of the Cerromatoso area where serpentinized peridotites are exploited for iron-nickel minerals (*Gómez et al., 2007*; *Gleeson et al., 2004*). *Altamira and Burke (2015*) have related the Quebradagrande Complex to the Great Arc of the Caribbean defined by *Burke (1988*).

We consider the east-verging splay of the Romeral Fault System that we mapped in the southwestern LMV to represent the northern extension of the San Jerónimo fault, which was locally reactivated in the Miocene (**Figure 3.1**, **Figure 3.4**, **Figure 3.6** and **Figure 3.7**). This splay extends farther north into the western San Jorge depocenter, where it is clearly imaged in reflection seismic data (**Figure 3.6** and **Figure A 2**). Though west of the San Jerónimo Fault the basement has not been drilled, well and reflection seismic data show that Upper Cretaceous to lower Eocene units are preserved only to the west of this fault, suggesting that it has been a major tectono-stratigraphic limit. In the northwestern CC, a similar Upper Cretaceous succession is preserved (Nutibara and Urrao units, *Rodriguez et al., 2010*) in tectonic blocks with a core of oceanic affinity units, such as the Quebradagrande and Barroso (*Rodriguez et al., 2010*). The San Jerónimo Fault can be continued to the north until it reaches the Mojana Fault System and the southern Magangue-Cicuco High (**Figure 3.4** and **Figure 3.8**). In the Magangue-Cicuco High, there is no clear evidence of a major basement fault that was reactivated in Tertiary times. However, reflection seismic data in La Creciente gas field of the western part of the high, shows seismic packages below the base of the Oligocene sequence, which were interpreted by *Arminio and Yoris (2006*) as pre-Paleogene, Jurassic syn-rift sequences. This area is only twelve kilometers south of the Bonga well, so it is possible to consider that instead of Jurassic sequences, those pre-Oligocene packages that are seen in several seismic lines in the western Magangue-Cicuco High may represent the Quebradagrande Complex or related Lower Cretaceous oceanic units. It is then possible that the fault system that is bounding the complex to the east also continues into the Magangue-Cicuco High, though its trace is difficult to see with the available reflection seismic data.

Magnetics and gravity data also appear to support the occurrence of a different basement province in the westernmost LMV, apparently limited by the San Jerónimo Fault (**Figure 3.3**). In cross-section, there is an increase in the total Bouguer anomaly and in the TMIRP in the western LMV, coinciding with the interpreted trace of this fault (**Figure 3.7**). This interpretation allows extending the Quebradagrande Complex tectonic fringe much farther to the north, into the western Magangue-Cicuco High, where the Bonga pluton is located. Furthermore, north of the Bonga pluton, the few data that are available from drill holes indicates that the northwestern LMV is a volcanic basement province, with andesites reported in the Apure High (AH), in the footwall of the Pivijay Fault, and with the andesites-diorites reported in the Remolino-Ciénaga High (PvF and RCH, **Figure 3.1** and **Figure 3.4**). Consequently, it is also possible that the Quebradagrande Complex and related terranes extend even farther to the north and make up most of the basement of the westernmost LMV.

3.5.3.2 Intra-oceanic arc magmatism

Though our new Hf isotopic data evidences some interaction with old crust, it is also compatible with an origin of the Bonga pluton within a younger, Upper Cretaceous intra-oceanic arc which collided with the older continental crust of NW South America in latest Cretaceous to early Paleocene times (*Bayona et al., 2011*; *Cardona et al., 2012*). According to *Cardona et al. (2012*), the record of events extracted from coarse clastic rocks in the San Jacinto fold belt includes the formation and approach of an allochthonous Upper Cretaceous intra-oceanic arc active from 88 Ma until 73 Ma (Coniacian to Campanian). Such arc would have collided against the continental margin after 73 Ma, but before late Paleocene times. *Cardona et al. (2012*) consider that remnants of the accreted arc and the substrate of the San Jacinto fold belt include scarcely studied, weathered volcanic rocks associated to the Cretaceous sediments of the Cansona Formation, and some limited serpentinized remnants exposed in the southeastern segment of the belt. In other words, they interpret the serpentinized peridotites which crop out in the Cerromatoso area (*Gleeson et al., 2004*; *Gomez et al., 2007*) and which have a characteristic magnetic signature (**Figure 3.4**), as the remnants of the accreted intra-oceanic arc. Considering the only reported but not very reliable age for the serpentinized peridotites in the southern San Jacinto belt (83 Ma; Cáceres, 1978, in *ICP, 2000*), this hypothesis also seems feasible, though new geochronological analyses of these rocks are required. Based on gravity modelling, *Mantilla et al. (2009)* and *Bernal et al., (2015a*) suggest that the accretion or off-scraping of ultramafic material in the westernmost LMV did not happen evenly along the margin and that ultramafic bodies were accreted in some areas, while in others thick sedimentary basins are resting directly on top of continental crust. Our new Hf isotopic data from the Bonga pluton reveal an isotopically juvenile affinity for this domain, possibly indicating a lack of old continental crust at this concrete location of the westernmost LMV. However, as seen in geological maps in the western CC, the Romeral Fault System comprises an extremely irregular and highly deformed area in which the involved allochthonous terranes can be very narrow or considerably wide, thus it is possible that a similar configuration also exists in the basement of the westernmost LMV (**Figure 3.14**). We are also aware of the fact that the basement of the LMV may have experienced varied degrees of erosion in different localities, hence the predominance of volcanic versus plutonic rocks in a certain areas could just be related to differential exhumation and not necessarily imply the existence of different basement terranes. Nevertheless, much more geological, geophysical and geochronologic data are needed in order to define the configuration of the Romeral Fault System and its relationship with the LMV in more detail to what is attempted here.

3.5.4 Correlations between the LMV basement and San Lucas, the SNSM and Guajira

The San Lucas Ridge of the northeastern CC (Chibcha terrane), comprises three major litho-tectonic units (*Clavijo et al., 2008*) which do not seem to match the lithologies and ages reported from the basement of the northeastern LMV. Therefore, the new data presented here do not support the extension of the Chibcha terrane into the northeastern LMV. We thus consider that the basement exposed in the San Lucas ridge terminates to the north against the northeastern LMV, while the Palestina Fault System bends to the NE (**Figure 3.14**a).

There is a good correlation between the basement terranes exposed in the San Lucas Ridge (Chibcha terrane) and the Sierra Nevada province of the SNSM (*Tschanz et al., 1974* and **Figure 3.14**a). However, while the faults and lineaments in the San Lucas Ridge display trends of 40-60°, lineaments affecting the Sierra Nevada terrane are trending 60-80°. If the two terranes share a similar origin, this difference in structural trend would be partly explained by a clockwise rotation of 20° of the SNSM block, not very different from the one proposed by *Montes et al. (2010*). Permo-Triassic terranes in the basement of the LMV correlate with the Sevilla province of the SNSM, but there is no evidence of Late Cretaceous magmatism in this massif. *Tschanz et al. (1974*) correlated the Upper Cretaceous green schists that outcrop in the northwestern SNSM massif with the green

schists that were recovered in the Algarrobo-1 well, located in the northeastern LMV (El Dificil High), which yielded a K-Ar age of 86 Ma (Santonian). However, this terrane does not seem to correlate with the Tahamí-Panzenú or with the Chibcha terranes to the south, suggesting that the northeastern LMV may be part of a different and younger terrane (**Figure 3.14**a). Several Late Cretaceous metamorphic complexes including the Santa Marta schists (*Cardona et al., 2010b*) have shown both a continental margin origin in their protoliths and high-pressure metamorphism which spans between ca. 90 and 70 Ma (*Weber et al., 2010*). *Cardona et al. (2010b*) propose that the protoliths of the Santa Marta schists were formed in an allocthonous terrane within a back-arc setting or at the transition between the intra-oceanic arc and the Caribbean oceanic crust.
Few studies have been carried out to understand the origin and evolution of the basement in the Guajira area. The fact that the basement in the Guajira peninsula does not show a preferential arrangement or pattern in terms of basement structure, lithology and age (*Londoño et al., 2015* and this work), makes it very difficult to propose more robust correlations between the basement terranes in the Guajira area and the basement in the SNSM and northern LMV.

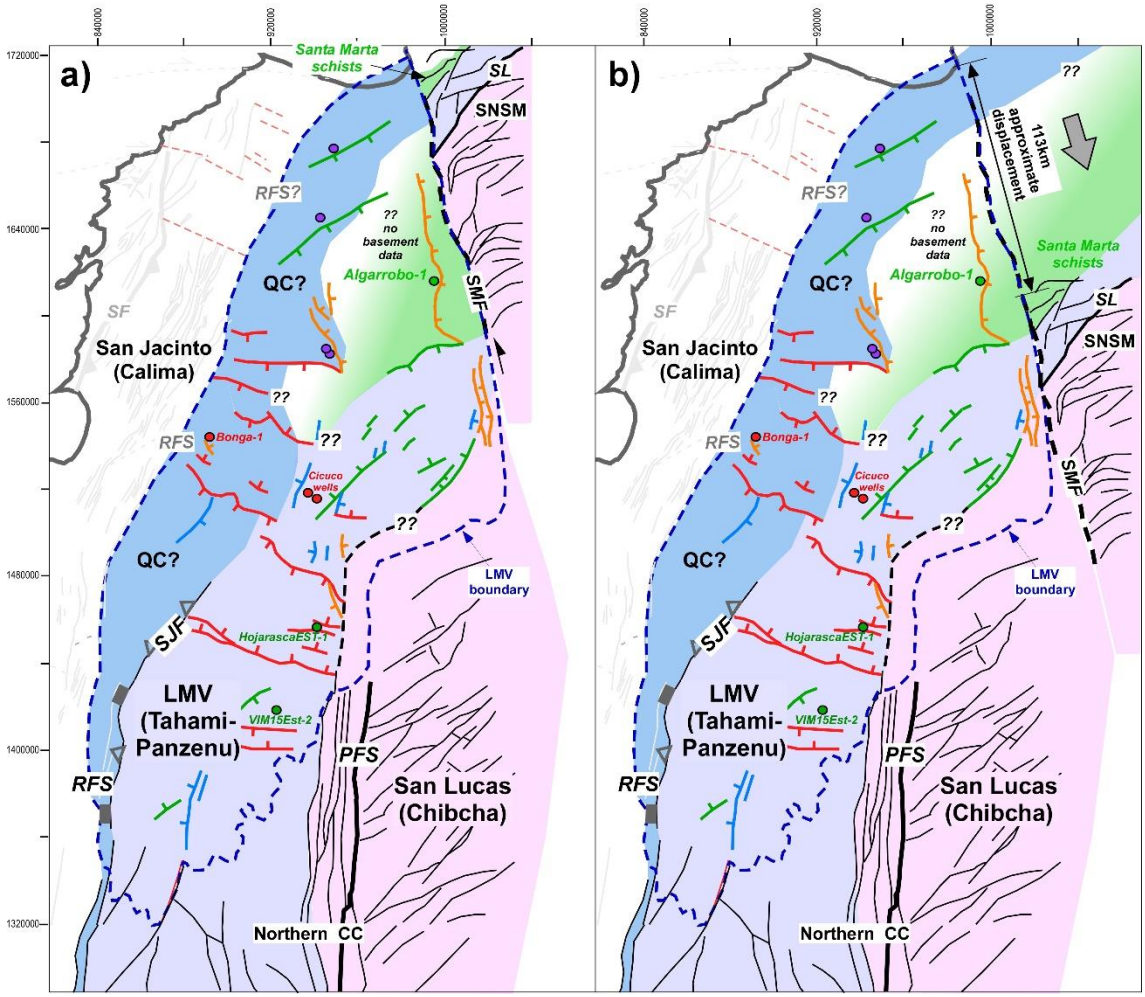

Figure 3.14. a). Interpreted basement terranes in the LMV and surrounding massifs. b). Tectonic reconstruction of the basement terranes in the study area by restoring the left-lateral displacement along the SMBF. Chibcha terrane is in pink, Tahamí-Panzenú in lavender, Quebradagrande Complex (QC) in blue, and Calima is white. Upper Cretaceous, low-grade metamorphic terranes in LMV (El Difícil and Algarrobo) and in the northwestern SNSM are colored in green. SL: Sevilla lineament; SJF: San Jerónimo fault.

3.5.5 Formation of the basement architecture and fabrics in the LMV

The basement architecture of northwestern Colombia was built from Cretaceous to middle Eocene times and resulted in the formation of two major suture zones, the Romeral and the Palestina Fault Systems (*Restrepo and Toussaint, 1988*; *Cediel et al., 2003*). According to *Toussaint and Restrepo (1994*) these sutures separate three main tectonic terranes which they called Calima, Tahamí-Panzenú and Chibcha, which we have extended to the north, into the LMV and San Jacinto fold belt, as shown in **Figure 3.14**a. From reflection seismic shown here (**Figure 3.5** to **Figure 3.7**, **Figure 3.12** and **Figure A 2**), earthquake and outcrop data, we propose that the activity of the Romeral Fault System extended until middle Eocene times and since then, it has become mostly inactive (**Figure 3.12**). The San Jerónimo Fault, which makes part of the Romeral System, shows a minor reactivation in late Oligocene to Miocene times in the southwestern LMV (**Figure A 2**). Though the Palestina Fault System lacks seismic coverage, outcrop studies report that this fault system was active until the Upper Cretaceous (*Feininger, 1970*). The open-source archive of active faults for northwest South America (*Veloza et al., 2012*) shows that while the PFS in the San Lucas Ridge evidences some compressive and left-lateral displacement, the only active faults in the study area appear to be localized NNE-trending thrusts in the northern San Jacinto fold belt. This means that the basement of the LMV became stable since early Miocene times, except for local and subtle fault reactivations. By contrast, the Santa Marta-Bucaramanga Fault System (SMBF in **Figure 3.14**) which was also active in the Cretaceous, has been reactivated several times during the Cenozoic and continues to be active today, as shown by neo-tectonic and seismicity studies (*Cediel et al., 2003; Veloza et al., 2012*; *Jimenez et al., 2014* and **Figure 3.13**).

Considering the scarcity of kinematic indicators in basement and Cretaceous rocks of the LMV and San Jacinto, it is difficult to reconstruct the pre-Eocene kinematic regimes. However, based on previous studies and our new data and interpretations, we propose that the basement fabric in the LMV and San Jacinto fold belt was formed by two main, regional tectonic processes (**Figure 3.15**): 1) Jurassic rifting and 2) Late Cretaceous to Middle Eocene oblique convergence of the Caribbean and South American plates, producing large-scale, dextral strike-slip displacement, arc-parallel extension due to displacement partitioning, and clockwise block rotation. We have already proposed that a Jurassic rifting and extension phase could have formed the oldest, NE-SW-trending fault family of the northeastern LMV. Concerning the ESE-WNW-trending fault of the central and western LMV, which has also been identified in the San Jacinto fold belt, we propose that it is also an inherited fabric which was formed due to a Late Paleocene to Middle Eocene regional extensional and strike-slip tectonic episode. According to paleo-tectonic reconstructions (*Müller et al., 1999; Kennan and Pindell, 2009*; *Villagómez et al., 2011a*; *Boschman et al., 2014*), it appears that from Late Cretaceous to Middle Eocene times, convergence between the Caribbean-South American was mostly oblique, giving rise to intense, right-lateral, strike-slip deformation along the western Ecuador and Colombia forearc. Studies dealing with displacement partitioning in obliquely convergent plate-boundary zones, such as the Aleutians and Sumatra, have related high obliquities with the existence of lateral displacements along one or more strike-slip faults, parallel to the plate boundary (*Jarrard, 1986*; *Ave-Lallemant and Oldow, 1988*; *McCaffrey, 1992*; *Ave-Lallemant, 1996).* Furthermore, *Ave Lallemant and Oldow (2000*) proposed that deformation associated with displacement partitioning is characterized by spatially segregated domains of contraction and transcurrent motion together with a significant component of arc-parallel extension. Taking into account the paleo-tectonic reconstructions, it is then likely that in the northwestern South American obliquely convergent margin, displacement was partitioned into a major trench-parallel, strike-slip component and into an arc-parallel extensional component, as well as a minor compressional component. Major right-lateral, strike-slip displacement has been documented for the Romeral and Palestina fault systems in pre-Oligocene times (*Cediel et al., 2003*), and we consider that an additional, outer, strike-slip feature (paleotrench?), which could correspond to the present-day Sinú fault, would have also accommodated important dextral displacement in those times (**Figure 3.15**). The ESE-WNW-trending extensional faults of family 2 could have been formed by extension parallel to the NNE-SSW-trending magmatic arc that existed between the northern CC and the

SNSM. This oblique convergence and right-lateral strike-slip setting would have also caused clockwise rotation of fault-bounded blocks, as proposed by *Daly (1989*) in the Ecuadorian forearc and by *Kodama et al. (1993*) in northern Japan. The inherited pre-Oligocene basement fabric was later reactivated during the late Oligocene and early Miocene, allowing the formation and infill of the LMV.

ICP (2000) previously related the formation of the LMV to clockwise block rotation in a trans-rotational basin setting, which would have been active since the Oligocene. Our data and interpretations do not support such proposal because the main suture zones (Romeral and Palestina) became inactive after the Middle Eocene. Concerning the model of vertical-axis, clockwise rotation of the Santa Marta Massif proposed by *Montes et al. (2010*) to explain the formation of the LMV, we do not discard that clockwise rotation of large tectonic blocks such as the Santa Marta massif could have influenced Neogene extension, but our basement maps do not agree with the simple, fan-shaped basement-fault geometry on which they base their model. While seismic data show that localized fault-controlled extension and subsidence occurred in late Oligocene to early Miocene times (*Bernal et al., 2015c*), most of the Miocene to Pliocene subsidence that allowed very thick sedimentary sequences to fill the basin, appears to be related to sagging (e.g. section B-B', **Figure 3.5**).

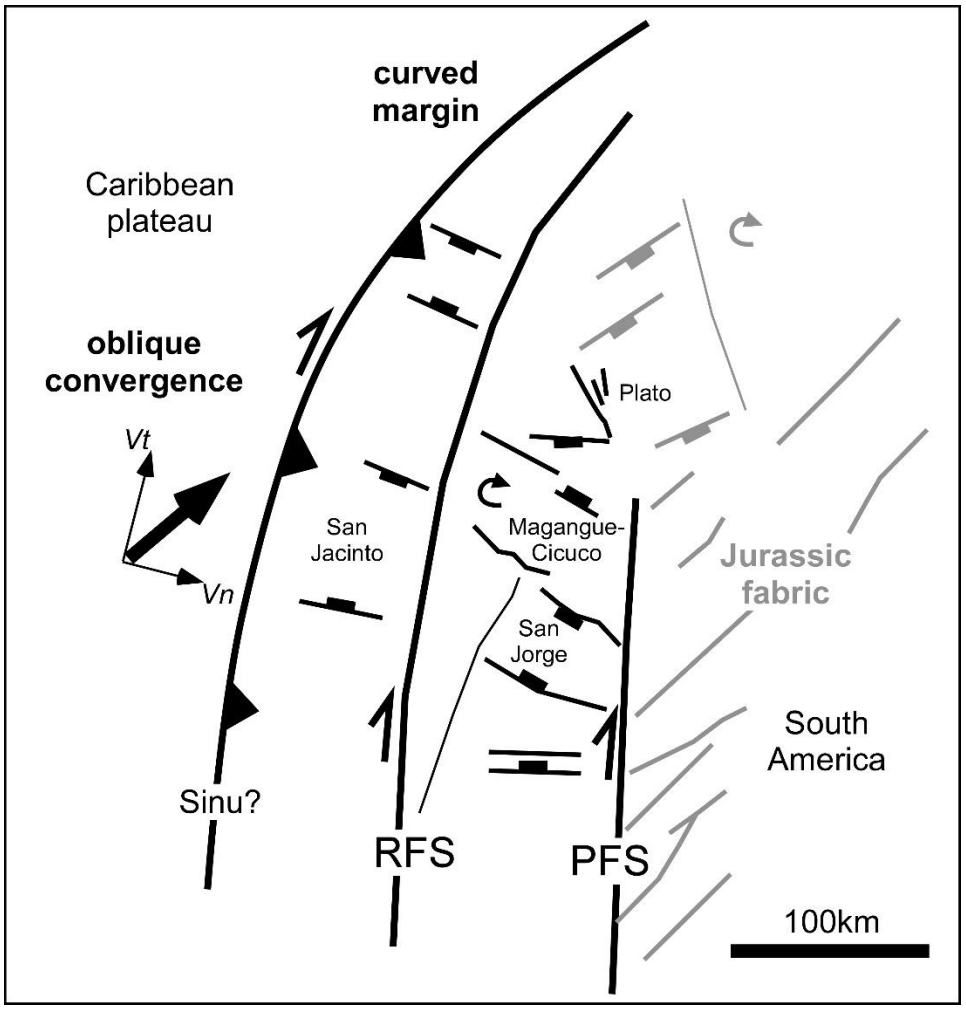

Figure 3.15. Sketch illustrating the proposed mechanisms of formation of the basement architecture in the LMV and San Jacinto areas of northernwestern Colombia, which acted during Late Cretaceous to Middle Eocene times. RFS: Romeral Fault System; PFS: Palestina Fault System; Vn: displacement vector component normal to the plate margin; Vt: displacement vector component parallel to the margin.

3.5.6 Basement terrane reconstruction.

In this work we confirm the extension of the Tahamí-Panzenú terrane to the north into the LMV and we propose that an oceanic terrane which could correspond to the Quebradagrande Complex or to a younger Upper Cretaceous, allochthonous intra-oceanic arc, also extends in the western LMV, while the San Lucas (Chibcha) terrane terminates against the northeastern LMV (**Figure 3.14**a). This mapping of terranes allows us to reconstruct, in much more detail than in previous studies, the possible tectonic configuration of the northern CC and SNSM prior to the left-lateral strike-slip movement that the Santa Marta Fault System experienced since Paleogene times (**Figure 3.14**b). This reconstruction illustrates the possible pre-Eocene basement architecture of the northwestern Colombian margin, showing in more detail the configuration of the three tectonic terranes defined by *Toussaint and Restrepo (1994*) and the possible configuration of an oceanic terrane (QC?), which is considered to lie within the Romeral Fault System (*Villagómez et al., 2011a*). Juxtaposition of the Santa Marta schists of the northwestern SNSM with the El Difícil High of the northeastern LMV suggests that the SNSM has been displaced to the NNW approximately 113 km, which is in agreement with previous estimates ranging from 100 to 115 km in magnitude (*Tschanz et al., 1974*; *Kellogg, 1984*; *Boinet et al., 1989*). The eastward displacement of the Caribbean plate relative to northern South America, together with the left-lateral strike-slip along the Santa Marta fault system, were responsible for the tectonic erosion and removal of a great part of the Tahamí-Panzenú terrane and of the entire Quebradagrande Complex and Calima terranes from the northern part of the present-day SNSM tectonic block (**Figure 3.14**).

Though we consider that the LMV shares the same basement terranes with the northern CC and possibly with the SNSM, clearly these tectonic provinces have had very different Cenozoic histories: the northern CC and the SNSM were strongly uplifted, while the area of the LMV subsided in two main depocenter areas. Recently measured crustal thicknesses (*Poveda et al., 2015*; *Bernal et al., 2015a*) show that the crust is thin under the LMV and coastal Caribbean terranes (24-35 km), including the SNSM (30 km), while it is much thicker in the northern CC (52-58 km). Based on paleo-tectonic reconstructions (*Kennan and Pindell, 2009*; *Boschman et al., 2014*), we consider that oblique convergence between the Caribbean and the South American plate, the curved shape of the margin and the basement fabric of the LMV and Sinú-San Jacinto fold belt all favored continued extension, crustal thinning and subsidence in the area since Paleogene times, contrasting with the intense compression, exhumation and uplift in the northern CC and SNSM. There also appears to be much more Cretaceous to Eocene magmatism in the CC and SNSM, which would have also contributed to form a thicker crust. However, the mechanisms which caused the extensional reactivation of older inherited basement features and clockwise block rotation since Oligocene times remain poorly understood and are beyond the scope of this contribution.

3.5.7 Late Cretaceous Paleogeography

As previously discussed, we consider that there are two main hypothetical, geodynamic scenarios for the LMV and San Jacinto fold belt in late Cretaceous (Coniacian-Campanian) times. The first hypothesis is illustrated in **Figure 3.16**, and considers that the Bonga pluton intruded a previously accreted oceanic terrane such as the Quebradagrande Complex, in Coniacian to Campanian times. According to this hypothesis, the proto-Caribbean plate was being subducted under the South American plate (*Pindell and Kennan, 2009*, *Villagómez et al., 2011a*, *Spikings et al., 2015*) and the latter was made up by the Proterozoic to Permo-Triassic Tahami-Panzenú and Chibcha terranes. The Upper Cretaceous subduction complex had a magmatic arc represented by the Bonga and Cicuco plutons but while the Cicuco pluton intruded old continental crust of the Tahamí-Panzenú terrane (*Silva et al., 2016*), the Bonga pluton, located farther to the west, intruded a dominantly oceanic terrane (Quebradagrande?) where continental crust was absent or extremely attenuated. The forearc basement was probably formed by accreted or off-scraped peridotite blocks and other oceanic basement units of the Calima terrane, and was covered by marine organic-rich shales,

limestones and cherts of the Cansona Formation of Coniacian to Maastrichtian age (*Duque-Caro, 1979; 1984*; *1991*; *Guzman, 2007*). According to this model, sediment source areas for the Cansona Formation were located towards the arc to the E and SE, with proximal, shallow marine sedimentation taking place closer to the source areas, while in the trench axis, deeper marine sedimentation occurred. The Bonga pluton was probably located approximately 250 km to the east of the trench, the average distance of volcanic arcs from trenches in present-day subduction zones (*Tatsumi and Eggins, 1995*). However, the present-day location of the Bonga pluton only 170 km away from the trench suggests that significant erosion of the older forearc has occurred in the last ~80 Ma. Though subduction erosion (*Clift and Vannucchi, 2004*) may have been partially responsible for such important erosion, Latest Cretaceous and Paleogene collision of allochthonous terranes along the main dextral strike-slip sutures would be also to blame for shaping the present-day configuration the western margin of the LMV. Farther to the east of the Palestina Fault System, in the back-arc areas, Santonian-Campanian sedimentation took place in a marine platform, low-energy setting, represented by the bituminous black shales of the La Luna Formation and equivalent units (*Erlich et al., 2003*).

The second hypothesis ascribes the formation of the Bonga pluton between 89 and 75 Ma to an allochthonous intra-oceanic arc, which collided with the Permo-Triassic margin of South America in latest Cretaceous to early Paleocene times (*Bayona et al., 2011*; *Cardona et al., 2012*). This hypothesis implies that in Late Cretaceous times there was a west-dipping subduction of the proto-Caribbean plate beneath the Caribbean plate, which allowed the formation of an intra-oceanic arc in the leading edge of the Caribbean plate (*Burke, 1988*; *Pindell and Kennan, 2009*; *Kennan and Pindell, 2009*). However, the recent report of an Upper Cretaceous magmatic arc (Magangue arc represented by the Cicuco pluton of 84.5 Ma; *Silva et al., 2016*), located just 60 km SE of the Bonga pluton, is an evidence in favor of a coetaneous, intra-continental east-dipping subduction setting. Hence, this hypothesis would imply that during the Upper Cretaceous, there were two simultaneous but opposite-dipping subduction zones: to the west, there was a west-dipping subduction zone with an intra-oceanic arc in which the Bonga pluton was emplaced, while to the east there was an east-dipping intra-continental subduction zone, which led to the emplacement of the Cicuco and related plutons in the northern CC, as shown in Figure 10E of *Villagómez et al., (2011a*). The block diagram in Figure 13 of *Cardona et al. (2012*), depicts the Late Cretaceous formation of the Bonga pluton within an intra-oceanic arc above a west-dipping subduction, but it does not take into account the formation of the coeval Cicuco and other related intra-continental plutons (e.g. Antioquia). Carrying out further geochronologic and paleomagnetic analyses to oceanic-affinity rocks outcropping in the boundary between the southern LMV and San Jacinto fold belt will help to clarify the doubts about the Upper Cretaceous geodynamic setting of this area of NW Colombia.

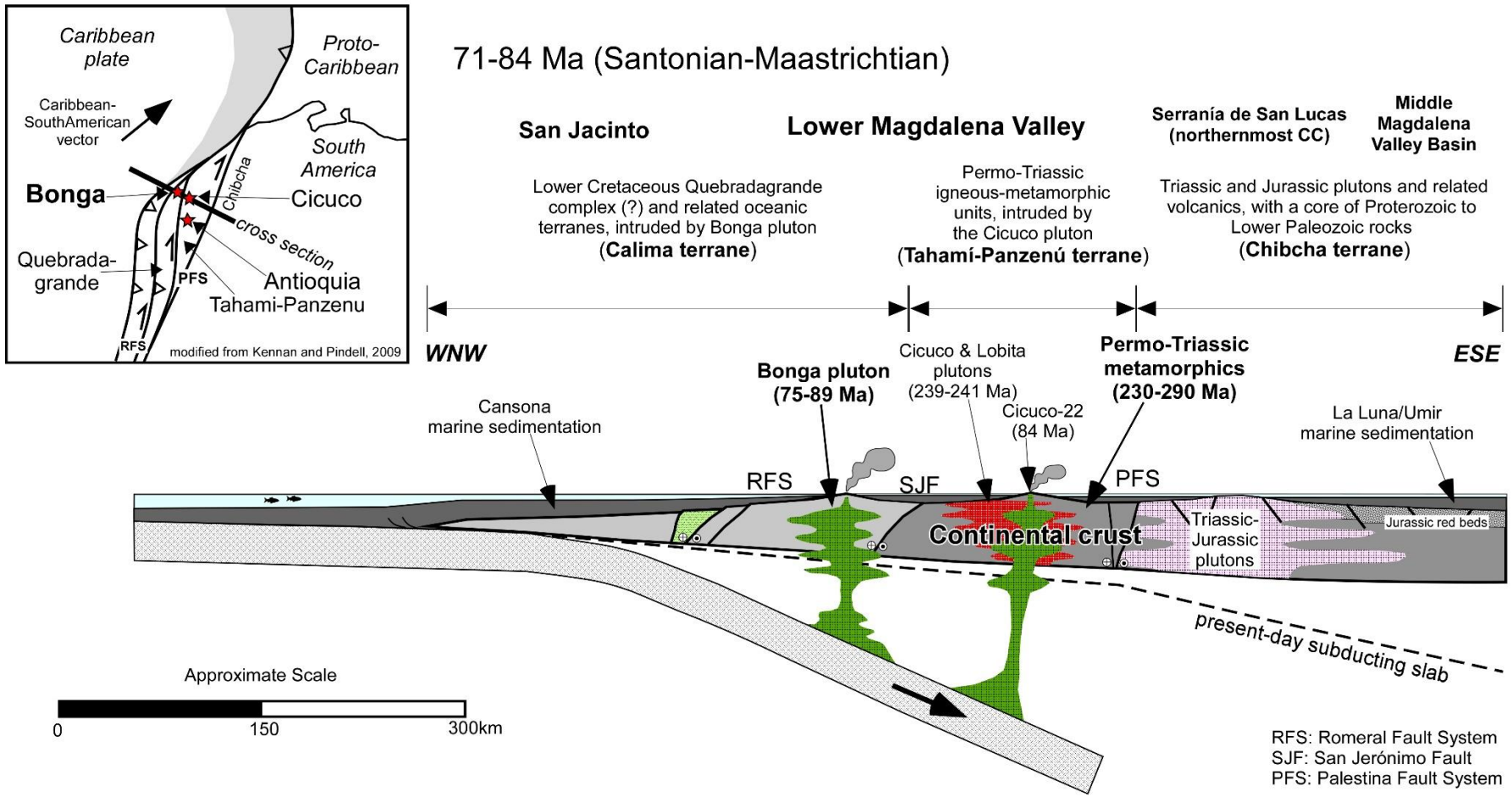

Figure 3.16. Plate-tectonic reconstruction of northern South America and the Caribbean, for Coniacian -Campanian times (based on *Kennan and Pindell, 2009*), and hypothetical cross–section with the interpreted geodynamic setting at the Bonga pluton location.

3.5.8 Final Considerations about the present-day tectonic configuration

Our results obtained from seismic interpretation show that the oceanic plate is being subducted under the Sinú-San Jacinto fold belt and LMV at a very low angle, dipping 5 to 9° to the SE. This flat-slab geometry extends for a distance of 250 to 300 km, measured from the base of the deformation front until the top of the slab reaches an approximate depth of 40 km. There is a fair correlation of our shallow top of the subducted slab with the intermediate-depth seismicity data farther to the east, suggesting the existence of a bend in the slab, approximately coinciding with the Palestina Fault System (**Figure 3.13** and dashed line in **Figure 3.16**). East of this bend, intermediate-depth seismicity is imaging the Bucaramanga slab (*Pennington,1981*), which shows a nearly S-N-trend (N5-10°E), dips between 23 and 30° to the ESE and reaches depths of 160 km near the Bucaramanga seismicity nest. Our interpretation of the configuration of the oceanic subducted slab in the study area is in agreement with *Bernal et al. (2015a*), who also identified a very-low-angle slab below the LMV and San Jacinto.

According to the previous interpretation and assuming the hypothesis illustrated in **Figure 3.16**, the present-day geodynamic configuration of NW Colombia is thus very different from the Coniacian-Campanian configuration, implying an overall migration of the subduction complex to the SE. An intriguing aspect of the present-day configuration of the subduction complex is that, based on the well-supported interpretation that there is ongoing subduction of the Caribbean plate beneath northern South America (*Mantilla et al., 2009, Bernal et al., 2015a*), a magmatic arc above the slab would normally be expected at the point where it reaches depths close to 100 km. This occurs in the limits between the Middle Magdalena Valley basin and the Eastern Cordillera where there is currently no magmatic arc. Hence, further research has to be carried out to explain the absence of a magmatic arc in this region of northwestern Colombia.

3.6 Conclusions

Detailed interpretations of reflection seismic data and new U-Pb and Hf isotope geochemistry in zircon confirm that the basement of the Lower Magdalena Valley basin is the northward continuation of the basement terranes of the northern Central Cordillera, thus the Lower Magdalena experienced a similar pre-Tertiary tectonic history as the latter. Using a regional-scale geological and geophysical database, we characterized the basement underneath the Lower Magdalena in terms of structure and age, and correlated it with surrounding outcropping terranes. Gravity, magnetics and reflection seismic data show that the basement underneath the Lower Magdalena Valley basin exhibits a notorious structural compartmentalization and an irregular morphology, which resulted from tensional stresses that acted in different orientations. While gravity data shows a broad picture of the morphology, magnetics data allows the identification of more localized (magnetic) basement highs and fault zones. Detailed seismic mapping reveals that the basement structure of the Lower Magdalena is much more complex than previously considered and that it comprises two regions of different fault trends, a western region with a dominant ESE-WNW-trending fault family and a northeastern region with a NE-SW-trending family. The most important structural features in the Lower Magdalena are the Plato and San Jorge depocenters, which are separated by the Magangué-Cicuco basement high. Estimated basement depths in these depocenters range from more than 24 thousand feet (>7 km) in Plato and more than 17 thousand feet (>5 km) in San Jorge.

New geochronological data prove the extension into the Lower Magdalena Valley basin not only of the Permo-Triassic terrane (232-300 Ma, Tahamí-Panzenú), but also of the Upper Cretaceous (75-89 Ma) magmatic arc of the northern Central Cordillera, confirming the along-strike continuity to the north of the arc which includes the Antioquia and Sabanalarga plutons. These Permo-Triassic and Upper Cretaceous basement terranes exhibit mainly NW-SE-trending faults and lineaments in outcrop and in the subsurface. Hf isotopic analyses from the Bonga Upper Cretaceous

pluton suggest that the preceding melts were mantle-derived and possibly intruded young crust with oceanic affinity, which we interpret as the northern continuation of the Lower Cretaceous Quebradagrande Complex underneath the westernmost segment of the LMV. In the northern LMV, volcanic basement of andesitic composition predominates towards the west while Cretaceous low-grade metamorphic rocks that correlate with similar terranes in the Sierra Nevada de Santa Marta and Guajira are dominant in the east, suggesting that the Tahamí-Panzenú terrane does not extend into the northern Lower Magdalena. There is a notorious similarity in structural trend between the terranes exposed in the San Lucas Ridge (Chibcha terrane) to the east of the Palestina Fault System and the interpreted subsurface structures in the northeastern Lower Magdalena. However, rock litho-types and geochronologic data do not entirely support the extension of the San Lucas (Chibcha) terrane into the northeastern Lower Magdalena. We thus consider that the Chibcha terrane terminates to the north against the northeastern Lower Magdalena, as the Palestina Fault System appears to bend to the NE. The NE-SW trend of basement faults in the northeastern Lower Magdalena is probably inherited from the Jurassic rifting event which is responsible for the conspicuous fabric of surrounding terranes outcropping to the east of the Palestina Fault system, while the ESE-WNW trend in the western Lower Magdalena is inherited from a Late Cretaceous to Eocene, extension and dextral strike-slip episode, which has been recognized in the western Andean forearc from Ecuador to Colombia. Our interpretations confirm previous tectonic correlations between the northern Lower Magdalena Valley basin and the Sierra Nevada de Santa Marta and agree with a left-lateral strike-slip displacement of ~113 km along the Santa Marta-Bucaramanga fault system since the Paleocene.

4 Linking Late Cretaceous to Eocene tectono-stratigraphy of the San Jacinto fold belt of NW Colombia with Caribbean plateau collision and flat subduction

This chapter is a reformatted version of a Tectonics paper (*Mora et al., 2017b*). Supplementary text and figures have been placed in *Appendix B*.

Citation: Mora, J.A., Oncken, O., Le Breton, E., Ibáñez-Mejía, M., Faccena, C., Veloza, G., Vélez, V., De Freitas, M., Mesa, A., 2017b. Linking Late Cretaceous to Eocene tectono-stratigraphy of the San Jacinto fold belt of NW Colombia with Caribbean plateau collision and flat subduction. Tectonics, 36, 1-36. doi: 10.1002/2017TC004612

Abstract

Collision with and subduction of an oceanic plateau is a rare and transient process that usually leaves an indirect imprint only. Through a tectono-stratigraphic analysis of pre-Oligocene sequences in the San Jacinto fold belt of Northern Colombia, we show the Late Cretaceous to Eocene tectonic evolution of northwestern South America upon collision and ongoing subduction with the Caribbean plate. We linked the deposition of four forearc basin sequences to specific collision/subduction stages and related their bounding unconformities to major tectonic episodes. The Upper Cretaceous Cansona sequence was deposited in a marine forearc setting in which the Caribbean plate was being subducted beneath northwestern South America, producing contemporaneous magmatism in the present-day Lower Magdalena Valley basin. Coeval strike slip faulting by the Romeral wrench fault system accommodated right-lateral displacement due to oblique convergence. In Latest Cretaceous times, the Caribbean plateau collided with South America marking a change to more terrestrially-influenced marine environments characteristic of the upper Paleocene to lower Eocene San Cayetano sequence, also deposited in a forearc setting with an active volcanic arc. A lower to middle Eocene angular unconformity at the top of the San Cayetano sequence, the termination of the activity of the Romeral Fault system and the cessation of arc magmatism are interpreted to indicate the onset of low-angle subduction of the thick and buoyant Caribbean plateau beneath South America, which occurred between 56 and 43 Ma. Flat subduction of the plateau has continued to the present and would be the main cause of amagmatic post-Eocene deposition.

Keywords: San Jacinto fold belt, Lower Magdalena Valley, tectono-stratigraphy, Caribbean, reflection seismic, flat-slab subduction, U-Pb and Hf isotope Geochronology.

4.1 Introduction

The northwestern margin of South America has experienced a complex Cretaceous to Recent tectonic history which involves subduction of the Caribbean plate and later collision of the Caribbean oceanic plateau, causing accretion of oceanic terranes in some areas or the subduction of the plateau in others (*Cediel et al., 2003*; *Restrepo et al., 2009*; *Villagómez et al., 2011a*; *Bayona et al., 2012; Spikings et al., 2015*; *Mora et al., 2017a*). While oceanic terrane accretion and later subduction of the Farallón and Nazca plates has been better studied in central-western Colombia (*Pennington, 1981*; *Van der Hilst and Mann, 1994*; *Taboada et al., 2000*; *Corredor, 2003*; *Zarifi et*

al., 2007; *Vargas and Mann, 2013*; *Chiarabba et al., 2015*; *Syracuse et al., 2016*), collision, accretion and subduction of the Caribbean plateau remain poorly understood in northwestern Colombia. This is caused by the lack of good-quality geological and geophysical information and by the low seismicity of the area, which has made very difficult to image the lithospheric configuration of the NW Colombia convergent margin.

In this study we present a tectono-stratigraphic analysis of the San Jacinto fold belt of northwestern Colombia and propose correlations of the interpreted tectono-stratigraphic sequences and their bounding unconformities with specific tectonic and geodynamic settings, as deduced from the interpretation of reflection-seismic, earthquake and seismicity data. The San Jacinto fold belt (**Figure 4.1** and **Figure 4.2**) is a west-verging fold and thrust belt in which an Upper Cretaceous to lower Eocene marine basin has been preserved (*Duque-Caro, 1979*; *1984*; *1991*; *Flinch, 2003*; *Guzman, 2007*) and it has remained poorly studied due to the structural complexity, poor outcrops, few drill holes and widely-spaced and low-quality reflection seismic data. However, it is an area of NW Colombia in which Cretaceous to Eocene sedimentary sequences are well-preserved, hence its importance for pre-Oligocene tectono-stratigraphic and plate-tectonic studies. Furthermore, in the past decade the National Hydrocarbons Agency of Colombia (ANH- Agencia Nacional de Hidrocarburos) made important efforts to acquire new information in the San Jacinto fold belt by drilling stratigraphic boreholes and acquiring new geophysical data, including air gravity (Bouguer anomaly), magnetics and reflection-seismic data. This has been complemented by new well and seismic data acquired by oil and gas companies doing hydrocarbon exploration in the area.

Taking advantage of the recently acquired data in the area, we have revised and updated Upper Cretaceous to Eocene tectono-stratigraphic framework of the San Jacinto fold belt, which has been integrated to surrounding basins in order to identify the main regional sequences and unconformities in northwest Colombia. The tectono-stratigraphic analysis included new seismic interpretations and maps, outcrop and well log correlations, biostratigraphy, organic geochemistry and sedimentary provenance analyses through detrital zircon U-Pb geochronology and Hf isotope geochemistry. In order to look for correlations between our defined sequences, unconformities and major regional tectonic events such as collision/subduction of the Caribbean oceanic plateau, we used reflection-seismic, earthquake and seismicity data, including our own interpretations and maps, as well as previous published work on lithospheric imaging of northwestern South America. Based on previous studies and on the results of our new data and analyses, we also propose a present-day geometric model of the lithospheric configuration of NW Colombia.

4.2 Geological Setting

The San Jacinto fold belt (SJFB) is located in northwestern South America, close to the northern end of the western South American convergent margin (**Figure 4.1**). However, convergence in the study area does not involve the Nazca plate, but instead it involves the Caribbean plate, which is separated from the Cocos and Nazca plates by the Panama-Chocó block (inset in **Figure 4.1**). It has been proposed that this area is characterized by the slow and flat-slab subduction of the Caribbean oceanic plate beneath South America, forming the Bucaramanga and Caribbean flat slabs imaged and described by several researchers (*Pennington, 1981*; *Van der Hilst and Mann, 1994*; *Taboada et al., 2000*; *Zarifi et al., 2007*; *Chiarabba et al., 2015*; *Bernal et al., 2015a; Syracuse et al., 2016*). Slow and flat-slab subduction would be the cause of the low seismicity and of the lack of a magmatic arc in northwestern Colombia (inset in **Figure 4.1**).

The SJFB is a SW-NE trending terrane which makes up part of the subduction complex of northwestern Colombia (*Mantilla, 2007*; *Mantilla et al., 2009*) and is located between an Oligocene to Recent forearc basin to the east (Lower Magdalena Valley basin-LMV, **Figure 4.1**) and the Miocene to Recent accretionary prism to the west (Sinú-Southern Caribbean deformed belt; *Duque-Caro, 1979*; *Mantilla et al., 2009*; *Bernal et al., 2015b*). According to *Mantilla et al. (2009*), the SJFB represents the fossilized part of the accretionary prism of the northwest Colombia subduction complex, which today acts as dynamic backstop. It is formed by three discontinuous ranges or

anticlinoria, called by *Duque-Caro (1979*) from south to north, San Jerónimo, San Jacinto and Luruaco (**Figure 4.1**). Pre-Oligocene sedimentary units exposed in this fold belt have been considered the northward extension of the Western Cordillera of Colombia (*Barrero et al., 1969*; *Duque-Caro, 1979*; *Cediel et al., 2003*) and have been related to an oceanic-type basement. The Romeral Fault System (RFS), which is also considered to continue from the south to form the eastern boundary of the SJFB, appears to be separating the oceanic to transitional basement under the belt from the felsic continental basement of the South American crust which floors the LMV in the east (*Duque-Caro, 1979*; *Flinch, 2003*; *Mora et al., 2017a*). The RFS makes part of a ~2000 km long tectonic suture that extends from Ecuador (Peltetec Fault). There is general consensus about the large-scale right-lateral strike-slip movement that occurred along this fault zone during the Cretaceous, causing the juxtaposition of allochthonous oceanic terranes against Central Cordillera basement blocks (*Cediel et al., 2003*; *Villagómez et al., 2011a*; *Spikings et al., 2015*). The northern extension of the RFS has also been an important tectono-stratigraphic feature as shown by the different stratigraphic successions preserved on both sides of the fault system (**Figure 4.2**). In the SJFB, west of the RFS, there are Upper Cretaceous to Eocene sedimentary units which are not preserved in the LMV to the east (*Duque-Caro, 1979*; *1984*) and which will be the focus of the tectono-stratigraphic analysis performed in this study.

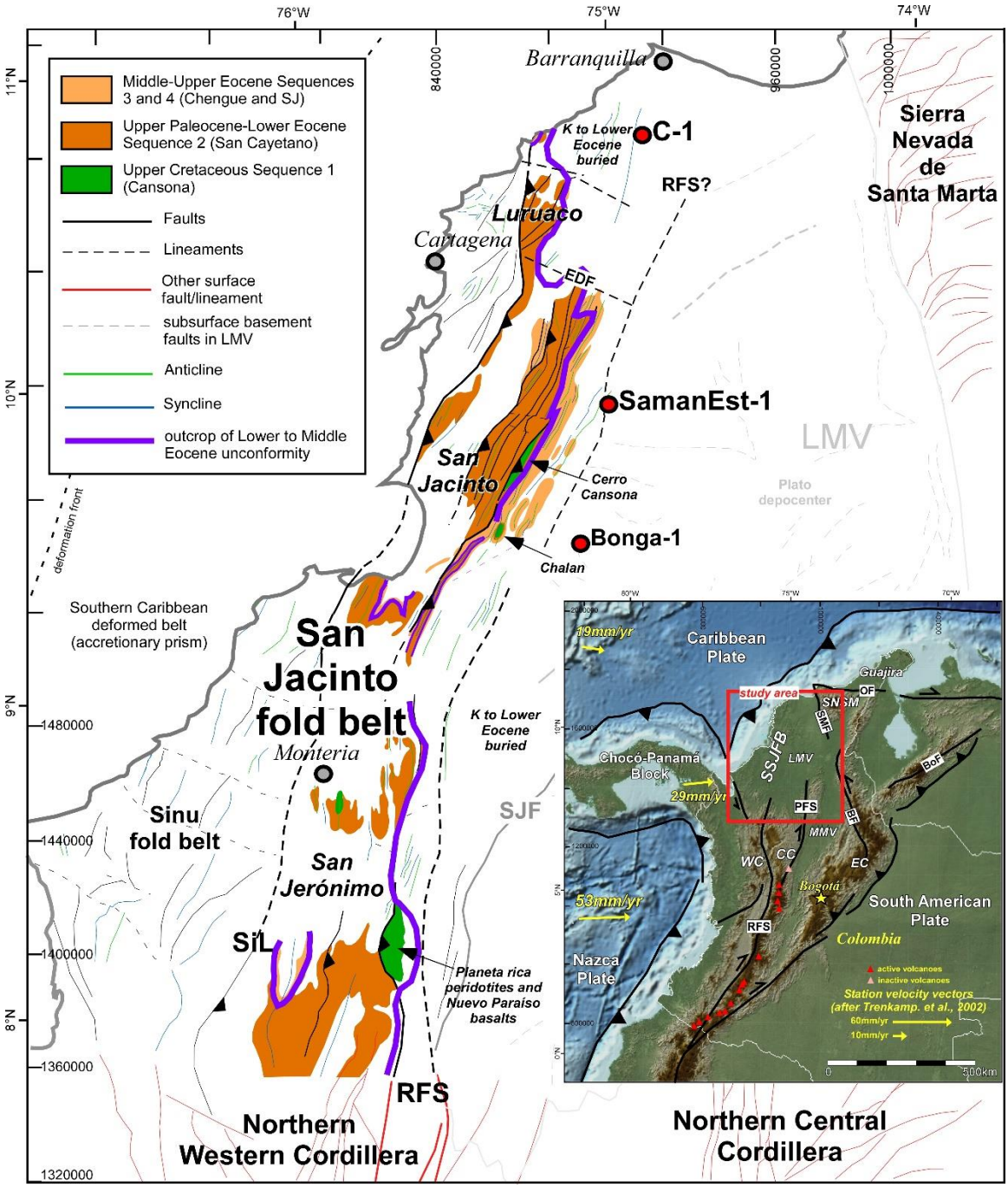

Figure 4.1. Geological map of the San Jacinto fold belt, highlighting outcrops of Cretaceous to Eocene units and showing major structural and morphologic features. RFS: Romeral Fault System; SJF: San Jerónimo Fault; SiL: Sinu Lineament; EDF: El Dique Fault. Based on *Gomez et al. (2007*). Inset: Tectonic map of northwestern South America with topography and bathymetry, showing the location of the Lower Magdalena Valley basin (LMV), the Sinú-San Jacinto fold belt (SSJFB), and the active volcanoes. Present-day tectonic plate motions are shown in yellow (after *Trenkamp et al., 2002*). WC: Western Cordillera; CC: Central Cordillera; EC: Eastern Cordillera; RFS: Romeral Fault System; PFS: Palestina Fault System; BF: Bucaramanga Fault; SMF: Santa Marta Fault; OF: Oca Fault; BoF: Bocono Fault.

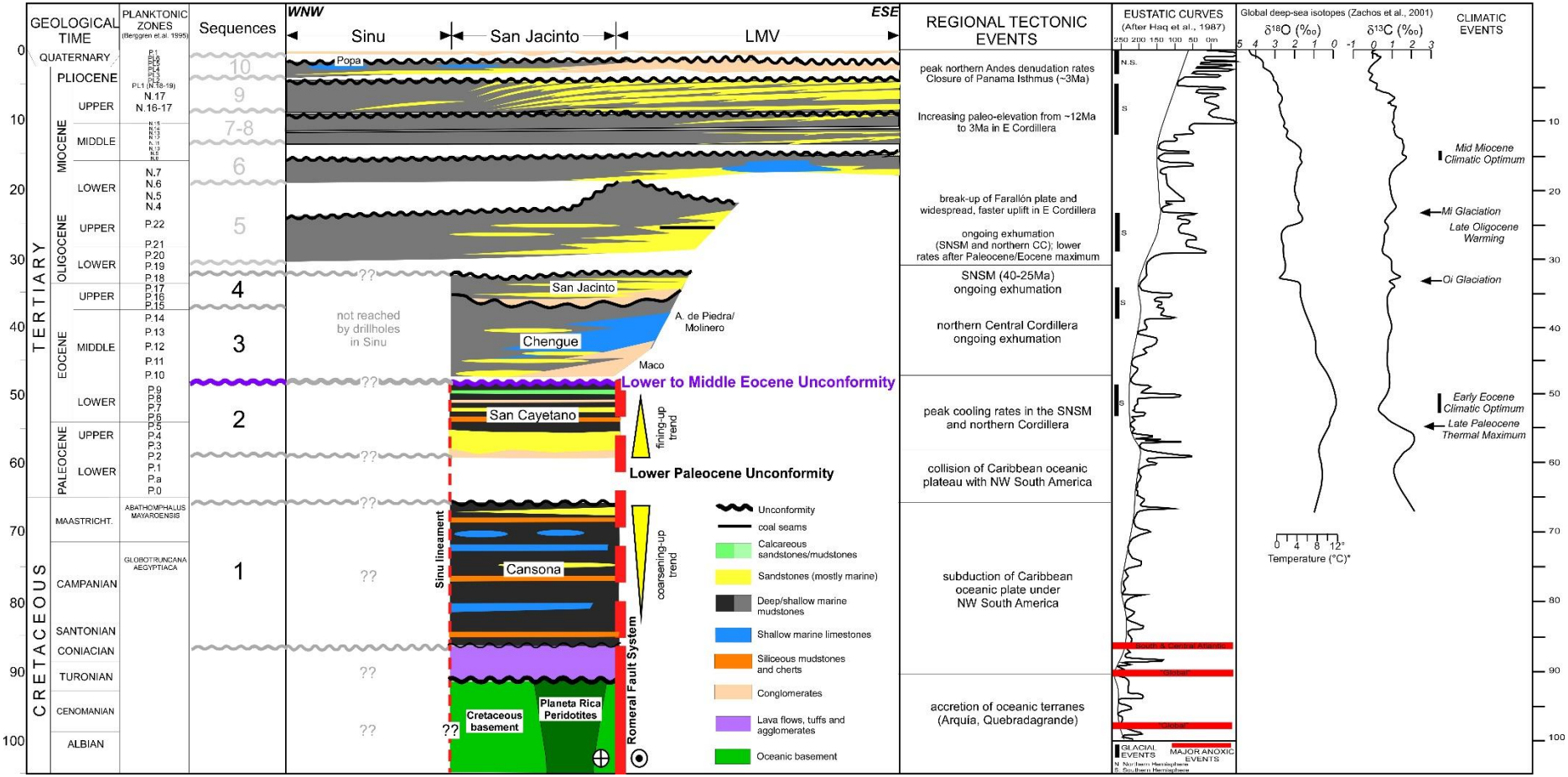

Figure 4.2. WNW-ESE-trending chronostratigraphic chart of the Sinú, San Jacinto and Lower Magdalena areas, based on different sources (*Hocol, 1993*; *ICP, 2000*; *Guzman, 2007*) and adjusted with our recent analyses of well and outcrop samples. Biostratigraphy is based on numerous papers and industry reports by *Duque-Caro (1979*, *1984*, *1991*, *2000*, *2001*, *2011a* to *2014*), tectonic events are after *Villagómez et al. (2011a* and *b*), *Parra et al. (2012*), *Saylor et al. (2012*), *Mora et al. (2013*a), *Caballero et al. (2013a, b*), *Mora et al. (2015*), *De La Parra et al. (2015),* while the eustatic curves are from *Haq et al. (1987*) and the climatic events from *Zachos et al. (2001*).

4.2.1 The Basement of the San Jacinto fold belt (SJFB)

Basement information in the SJFB comes from localized outcrops located in the southernmost SJFB, close to the northern Western Cordillera (WC), and from a couple of reports from old drill holes which have a high degree of uncertainty, suggesting the predominance of mafic and ultramafic rocks (**Figure 4.2**). These Upper Cretaceous mafic and ultramafic rocks have been related to allochtonous, accreted oceanic terranes (*Cediel et al., 2003*; *Villagómez et al., 2011a*). From gravity modelling, the basement under the SJFB is considered to be thinned-continental to transitional, with localized mafic allochthonous blocks (*Cerón et al., 2007*; *Mantilla et al., 2009*; *Bernal et al., 2015a*). However, recent Hf isotope geochemistry of a pluton in the western Lower Magdalena valley (Bonga pluton, *Mora et al., 2017a*) suggests that it intruded a young crust of possible oceanic affinity, such as the Quebradagrande and related terranes which have been studied farther south, within the RFS between the Central and Western Cordilleras.

4.2.2 Upper Cretaceous to lower Oligocene stratigraphic units

Several researchers used the name "Cansona" to refer to the Upper Cretaceous strata that outcrop in the "Cerro Cansona" area of the San Jacinto Anticlinoria (**Figure 4.2**; *Duque-Caro, 1972*; *Duque-Caro et al., 1996; Guzman et al., 2004*). The Cretaceous strata in the SJFB consists of a volcano-sedimentary succession with a predominantly volcanic lower part and an upper part consisting of organic-rich and calcareous mudstones, limestones and cherts with few quartzarenites (*Aleman, 1983*; *Clavijo and Barrera, 1999*; *Guzman, 2007*), deposited in marine environments.

Upper Paleocene to lower Eocene rocks have been described in outcrops and drill holes all along the SJFB (*Guzman, 2007*; **Figure 4.2**). They comprise a fining-upward succession of polymictic conglomerates and litharenites towards the base and gray siltstones and mudstones with minor chert and limestone interbeds (*Guzman et al., 2004*; *Guzman, 2007*). Though several names have been proposed for this succession, the most common name is "San Cayetano" (**Figure 4.2**, *Chenevart, 1963*; *Guzman et al., 2004*; *Guzman, 2007*). Interpretations of its depositional environment range from deep marine turbiditic fans (*Duque-Caro, 1972*; *Aleman, 1983*; *Guzman, 2007*), turbiditic to distal deltaic (*Geosearch Ltda., 2006*) and fan deltas (*ATG-ANH, 2009*). The lower contact with the Upper Cretaceous Cansona sequence has been described as unconformable (*Duque-Caro, 1979*; *Guzman et al., 2004*; *Guzman, 2007*).

An angular middle Eocene unconformity separates the upper Paleocene to lower Eocene San Cayetano deposits from polymictic conglomerates, lithic sandstones, red algae limestones and mudstones of middle to upper Eocene age, which have received different names depending on the lithology and locality (*Guzman et al. 2004*: *Guzman, 2007*). For simplicity, the sedimentary succession of middle to upper Eocene age will be called here Chengue (**Figure 4.2**, *Guzman et al., 2004*; *Guzman, 2007*). The conglomeratic facies were deposited in fan deltas and related submarine slope deposits (*Guzman, 2007*), while the limestone facies were deposited in shallow marine carbonate platforms (*Guzman et al., 2004*).

Sandstones, conglomerates and mudstones of upper Eocene to lower Oligocene age are locally preserved in the SJFB and unconformably overlying the middle to upper Eocene rocks of the Chengue unit (*Guzman et al., 2004*; *Guzman, 2007*). These clastic deposits have been called San Jacinto Formation (**Figure 4.2**) and were deposited in proximal deltaic fans (*Guzman et al., 2004*; *Guzman, 2007*), while upper Eocene carbonate deposits which occur in the central and southern SJFB have been called the Toluviejo Formation (*Guzman et al., 2004).* The lower and upper contacts of this unit are unconformities (*Alemán, 1983*; *Guzman et al., 2004*; *Guzman, 2007*). Upper Oligocene to Recent deep marine to deltaic and continental units have been partially eroded in the SJFB but have been well preserved farther to the east, where they have filled the younger Lower Magdalena Valley basin (**Figure 4.2** and **Figure 4.4**).

4.3 Methodology

4.3.1 Construction of the tectono-stratigraphic framework

We interpreted in two-way-time (TWT) more than 3,000 km of 2D-reflection-seismic, which were tied to more than 40 wells that have been drilled in the San Jacinto fold belt (**Figure 4.3**) and to the outcropping units. We identified and defined four Upper Cretaceous to lower Oligocene tectono-stratigraphic sequences separated by major unconformities (**Figure 4.2** and **Figure 4.4**, *Text B1*), which according to *Catuneanu et al. (2009*) correspond to "depositional sequences". Sequence 1 comprises Upper Cretaceous deposits of the Cansona unit, Sequence 2 consists of upper Paleocene to lower Eocene strata of the San Cayetano unit, Sequence 3 comprises middle to upper Eocene rocks of the Chengue Group and Sequence 4 consists of upper Eocene to lower Oligocene deposits of the San Jacinto unit. The lack of more detailed data for this study makes very difficult the identification of sequence stratigraphic surfaces other than subaerial unconformities, and hampers the proposal of systems tracts (*Catuneanu et al., 2009*).

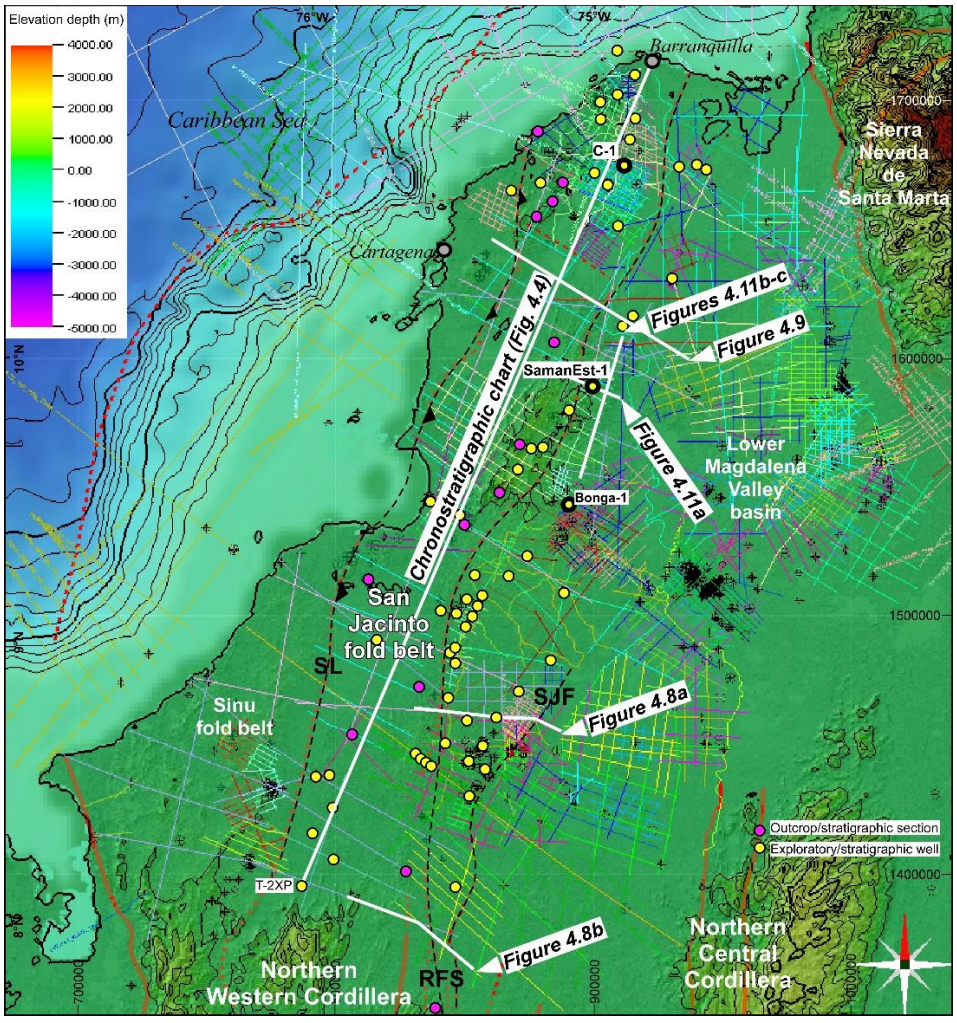

Figure 4.3. Reflection seismic and well database used for this study, provided by Hocol S.A. Colors represent different seismic surveys, the wells used in this study are shown in yellow and outcrops in pink. Location of **Figure 4.4** and of seismic sections in **Figure 4.8** to **Figure 4.11** are shown in white. Exact location of lines in **Figure 4.10** is not shown due to confidentiality.

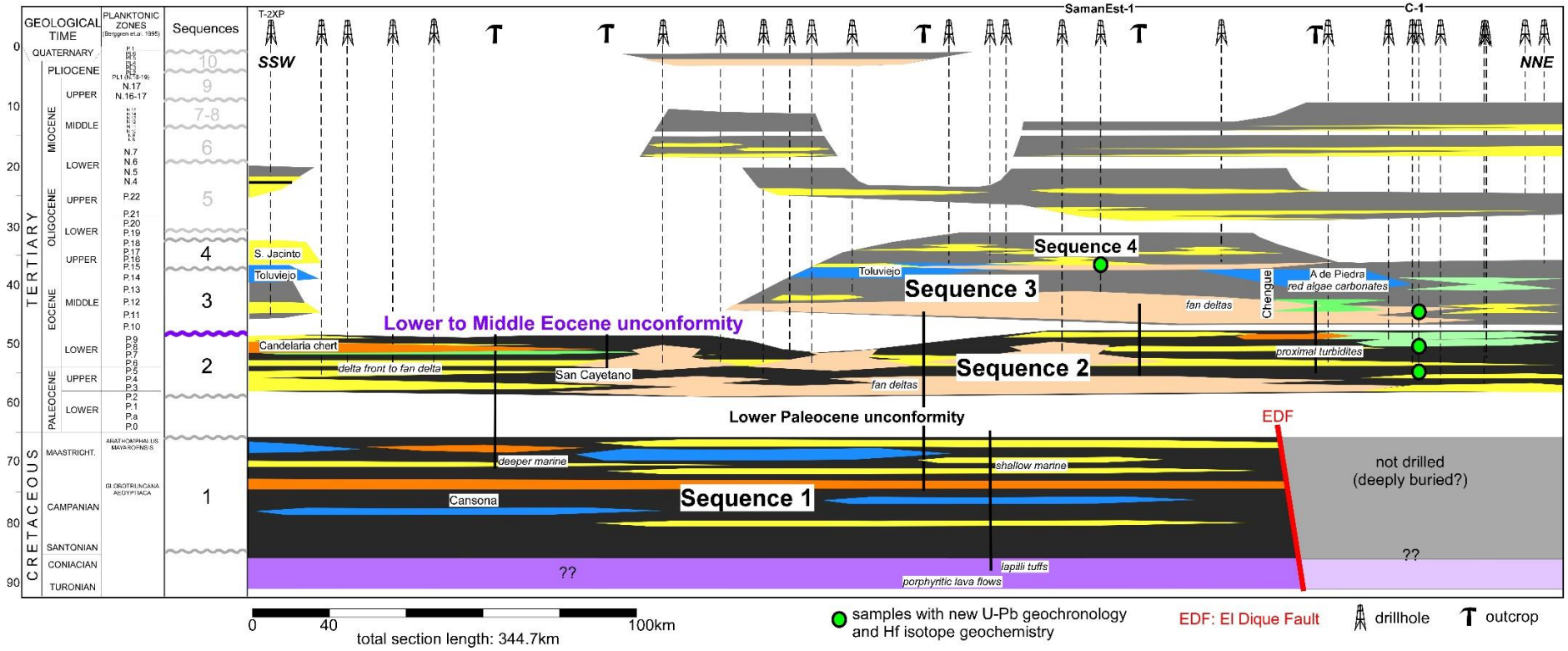

Figure 4.4. SSW-NNE-trending chronostratigraphic chart along the strike of the San Jacinto fold belt, built with available well and outcrop data, showing the studied tectono-stratigraphic sequences. Wells with new geochronology analyses are highlighted and the lithology legend is the same as in **Figure 4.2**.

4.3.2 Detrital zircon U-Pb Geochronology and Hf Isotope Geochemistry

In order to expand the geochronological dataset for the pre-Oligocene strata in the SJFB and for correlations with basement units in northern Colombia, samples (cuttings) for petrography and detrital zircon U-Pb and Hf isotope analyses were recovered from two wells located in the northern half of the SJFB. Six samples from upper Paleocene to upper Eocene units (San Cayetano and Chengue) were collected in the C-1 well, located in the northern San Jacinto fold belt, while two more samples from an upper Eocene to lower Oligocene unit (San Jacinto) were collected in the SamanEST-1 well, located farther south, close to the boundary between the SJFB and the LMV (**Figure 4.3** and **Figure 4.4**). The SamanEST-1 well is located 50 km to the north of the Bonga-1 well, which found granitic basement of Coniacian to Campanian age (*Mora et al., 2017a*). The U-Pb geochronology and Hf isotope geochemistry detrital zircon analyses were done at the Arizona LASERCHRON Laboratory and the detailed methodology is presented in *Text B2*. The stratigraphic succession in both wells was dated by *Duque-Caro (2013 a, b*).

4.3.3 Seismicity data

We also compiled the available earthquake and seismicity data from the study area, not only to characterize the main faults and structural features in terms of seismic activity and kinematics, but also to try to image the lithospheric structure of the subduction zone in the study area. Seismicity data from the study area was downloaded from the Colombian Earthquake Network (Red Sismológica Nacional, http://seisan.sgc.gov.co/RSNC/) and plotted both in map and section view, together with the seismic interpretation and maps. A total of 14,081 events were obtained, corresponding to earthquakes with Mw 1 to 9, recorded from June 1, 1993 to November 26, 2015. We interpreted and mapped the near top of the subducting oceanic plate under the SJFB, which connects with a megathrust that can be imaged in some of the regional seismic lines, as shown in *Mora et al., 2017a* (**Figure A 1**). Using stacking processing velocities from reflection seismic data, we depth-converted the interpreted subduction megathrust and plotted it with the earthquake and seismicity data in cross sections (**Figure B 1**). Further procedures followed to construct our maps and plots are described in *Text B3*.

4.4 Results

4.4.1 Stratigraphic framework

The general characteristics of the identified and studied tectono-stratigraphic sequences are presented in **Table 4.1** and the detailed descriptions are found in *Text B1*. Though our tectono-stratigraphic framework is mostly based on previous research, it was built after incorporating a great deal of recent regional drill hole, seismic and outcrop data and interpretations.

4.4.1.1 Sequence 1 (Cansona-Upper Cretaceous)

The oldest, 2nd-order sequence is of Coniacian to Maastrichtian age (see *Text B1*) and comprises the bituminous shales, cherts and limestones of the Cansona unit. Biostratigraphic data compiled by *Duque-Caro (2000, 2001*) and *Guzman (2007*) show an absence of lower Paleocene planktonic foraminiferal zones (P.0 to P.2) in the SJFB, indicating the existence of a regional unconformity which marks the upper limit of this sequence (**Figure 4.4**). The Cansona sequence appears to show a general coarsening- and shallowing-upward pattern (*Guzman, 2007*), similar to the pattern

displayed in other Upper Cretaceous successions of northern Colombia (*Villamil, 1999*), all of which are in agreement with the global eustatic curve of *Haq et al. (1987*, **Figure 4.2**).

Sequence	Lithostratigraphic Unit	Planktonic foram zones (Berggren et al., 1995; Blow, 1969)	Age	Thickness and other characteristics	Facies and depositional environments
4	San Jacinto	P.15 to P.20	upper Eocene to lower Oligocene	Highly variable facies and thicknesses, average thickness of 342 m but drilled ~1000 m in the Saman stratigraphic well	Exhibits clastic (San Jacinto) and calcareous (Toluviejo) facies
unconformity		*absence of P.14 to P.16*	*upper Eocene*		
3	Chengue	P.10 to P.14	middle to upper Eocene	Highly variable facies and thicknesses; original syn-depositional fabric comprises ESE-WNW and NNE-SSW-trending extensional faults; onlaps the basement to the ESE; thicknesses range from 150 m in paleohighs to >1000 m in low areas	Exhibits clastic syn-tectonic deposits (Maco, Pendales), and local with development of carbonates in possible paleohighs (Arroyo de Piedra)
unconformity		*absence of P.9 to P.10*	*lower to middle Eocene*		
2	San Cayetano	P.3 to P.9	upper Paleocene to lower Eocene	Original fabric comprises ESE-WNW and NNE-SSW-trending extensional faults; thicknesses of > 2000 m in wells in the north and ~1600 m in stratigraphic sections	General fining-upward trend, but notorious lateral facies variations; interpreted depositional environments range from turbidites in the north and south, to fan deltas in the central part of the fold belt
unconformity		*absence of P.0 to P.2*	*lower Paleocene*		
1	Cansona		Coniacian to Maastrichtian	Original syn-depositional fabric affected by west-verging deformation of the San Jacinto fold-belt; thickness uncertain but would be ~762 m in the most complete stratigraphic section (Cacao)	Shows a general coarsening and shallowing-upward pattern, deep marine environments interpreted; seismic expression is not clear, though locally presents high amplitude, parallel and continuous reflectors

Table 4.1. Main characteristics of the studied Upper Cretaceous to Eocene tectono-stratigraphic sequences in the San Jacinto fold belt. More information, detailed descriptions and sources of biostratigraphic, petrographic and organic geochemistry reports are found in *Text B1*.

4.4.1.2 Sequence 2 (San Cayetano-upper Paleocene to lower Eocene)

This is also a 2nd-order sequence which has been dated as upper Paleocene to lower Eocene (planktonic foraminiferal zones P.3 to P.9, see *Text B1*). The late Paleocene was characterized by a high global sea level (eustatic curves in **Figure 4.2**, *Haq et al., 1987*), which could have influenced the onset and extension of San Cayetano sedimentation. Biostratigraphic data shows that there is a big hiatus in the center of the SJFB, where the lower Eocene is missing, while to the north the section is more complete and the contact with the overlying sequence appears to be a disconformity (**Figure 4.4** and **Table 4.1**).

4.4.1.3 Sequence 3 (Chengue-middle to upper Eocene)

A middle to upper Eocene, 2nd-order sequence corresponds to the Chengue Group, defined by the P.10 to P.14 planktonic foraminiferal zones of middle to late Eocene age (*Text B1*). Biostratigraphy indicates that the unconformity between Sequences 2 (San Cayetano) and 3 (Chengue) corresponds to the P.9 to P.10 foraminiferal zones, implying a time interval of 46 to 51 Ma which includes the limit between the lower and middle Eocene. This syn-tectonic sequence has been eroded in the southern part of the SJFB and is more preserved in the northern part (**Figure 4.4**).

4.4.1.4 Sequence 4 (San Jacinto-upper Eocene to lower Oligocene)

This locally preserved 2nd-order sequence comprises the siliciclastic San Jacinto unit and the calcareous Toluviejo unit (**Figure 4.2** and **Figure 4.4**), which according to biostratigraphic studies (*Duque-Caro, 1979*; *Guzman et al., 2004*; *Guzman, 2007*) are defined by the P.15 to P.20 planktonic foraminiferal zones of upper Eocene to lower Oligocene age.

4.4.2 Detrital zircon U-Pb geochronology and Hf isotope geochemistry

The detrital zircon U-Pb geochronology of samples of upper Paleocene to Eocene samples (Sequences 2 to 4, **Figure 4.5**) shows three clear provenance peaks: a main Upper Cretaceous (70-88 Ma, Coniacian-Maastrichtian) peak, a secondary peak of Permo-Triassic age (230-250 Ma) which is less evident in the SamanEST-1 well, and a minor Albian-Cenomanian peak (~100 Ma). However, the Paleocene to Middle Eocene samples also evidence both lower Paleozoic and Proterozoic provenance. Therefore, detrital zircon U-Pb geochronology indicates that the upper Paleocene to lower Oligocene sediments of Sequences 2 to 4 were mostly sourced from Upper Cretaceous and Permo-Triassic basement blocks.

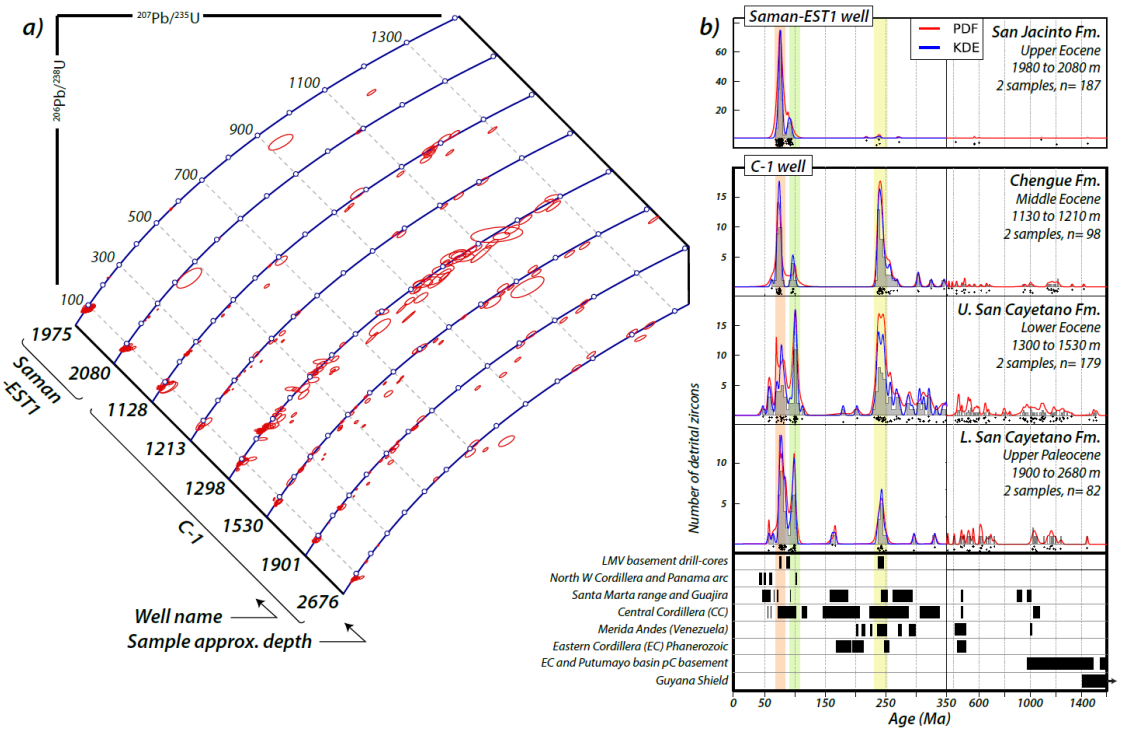

Figure 4.5. Results of detrital zircon U-Pb geochronology in samples of wells C1 and SamanEST-1. Reference basement ages for possible source terranes were compiled using the data of *Cordani et al. (2005*), *Vinasco et al. (2006*) , *Ibañez-Mejia et al. (2007*); *Cardona et al. (2010a*) , *Cardona et al. (2010b*) , *Horton et al. (2010*) , *Montes et al. (2010); Restrepo-Pace and Cediel (2010*) , *Weber et al. (2010*) , *Ibanez-Mejia et al. (2011*) , *Leal-Mejia (2011*) , *Villagomez et al. (2011*a) , *Cardona et al. (2012*); *Cardona et al. (2014*); *Cochrane et al. (2014*), *Ibanez-Mejia et al. (2015*) , *Montes et al. (2015*); *Spikings et al. (2015*); *Weber et al. (2015*); *Van der Lelij et al. (2016*); *Mora et al. (2017a).*

Hf isotopic data shows that the three dated detrital zircon populations (Coniacian-Maastrichtian, Albian-Cenomanian and Permo-Triassic) are related to different magmatic sources (**Figure 4.6**). While the Coniacian-Maastrichtian zircons would be related to a juvenile mantle source, the older Albian-Cenomanian and Permo-Triassic zircons have much lower εHf(t) values, indicating a much older crustal source. Furthermore, in the SamánEST-1 well there are two sub-populations within

the Upper Cretaceous Coniacian-Maastrichtian population (**Figure 4.6**c), and both overlap quite well with the compositions of the Bonga pluton (*Mora et al., 2017a*), located 50 km to the south (**Figure 4.3**). The Permo-Triassic Hf isotopic compositions from the C-1 well also show a good match with the Hf compositions of the Permo-Triassic basement in the HojarascaEST-1 and VIM15Est-2 wells (*Mora et al., 2017a*) and with data from previous studies (*Cochrane et al., 2014*; *Cardona et al., 2012*).

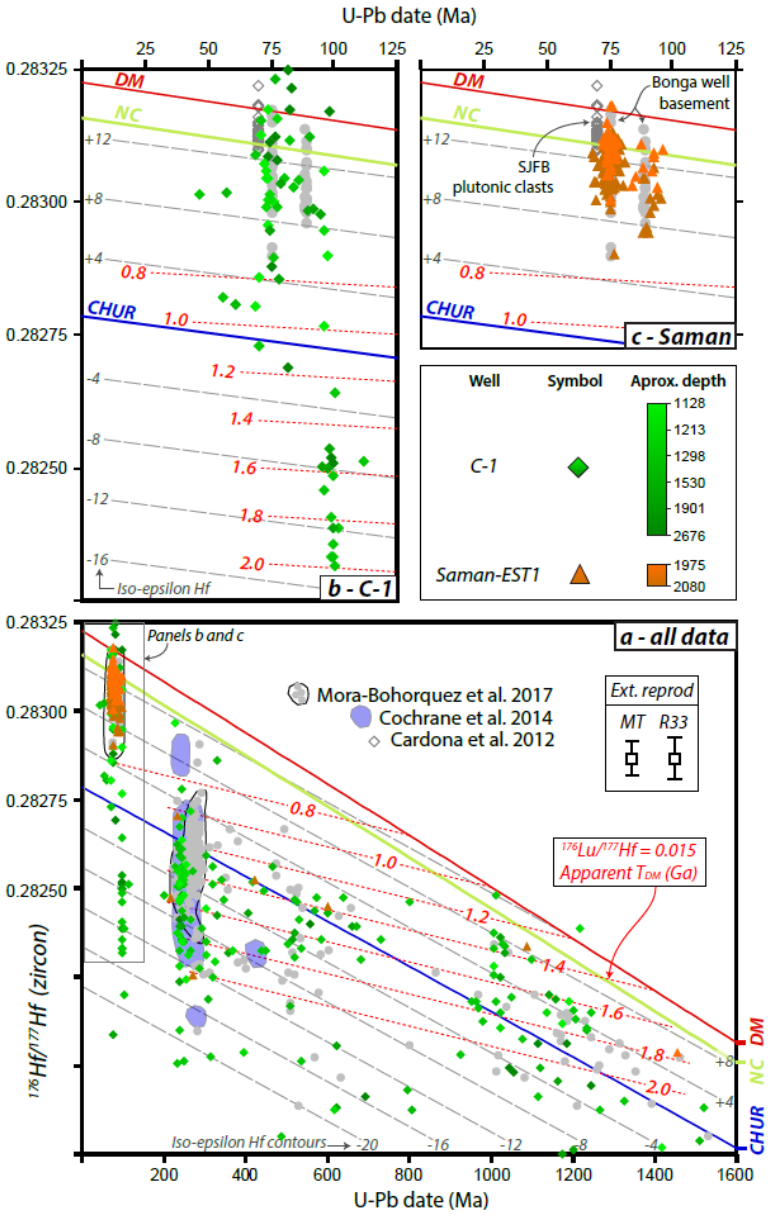

Figure 4.6. Results of detrital zircon Hf isotope geochemistry in samples of wells C1 and SamanEST-1. Good matches with basement data from *Mora et al. 2017a, Cochrane et al. 2014* and *Cardona et al. 2012* suggest a link between the analyzed pre-Oligocene sedimentary units and the Permo-Triassic and Upper Cretaceous basement terranes in the LMV and northern CC.

4.4.3 Seismic stratigraphy and facies

Seismic characterization of each sequence is not an easy task considering the structural deformation, a not very dense reflection-seismic coverage with poor to locally fair quality, partial erosion and notorious along-strike facies and thickness changes of the sequences. Though the present-day SJFB is the result of at least two contraction and inversion tectonic pulses, which have obscured the original Cretaceous to Eocene structural fabric (**Figure 4.7**), in this study we document two areas in which pre-Oligocene sequences have remained deeply buried and in which their original structural fabric has been better preserved. The first area, in the southeastern SJFB, is located between the San Jerónimo anticlinorium to the west and the SJF to the east (section 3, **Figure 4.7**), while the second area is the northernmost portion of the SJFB, located to the northeast of the Luruaco anticlinorium (section 1, **Figure 4.7**). In cross section it can be seen that Sequences 1 and 2 are mostly restricted to the western side of the RFS, and would be limited to the east by the San Jerónimo Fault (SJF). Sequences 3 and 4 extend farther to the east and probably into the LMV, where equivalent deposits would be preserved in the hanging wall of major extensional faults and in the deepest part of the Plato depocenter.

Reflection seismic imaging of the Upper Cretaceous Sequence 1 is very poor, hence it is very difficult to characterize it in terms of seismic facies and seismic stratigraphic relationships. The base of the sequence does not have a clear expression in the seismic data (**Figure 4.8** and **Figure 4.9**), suggesting the absence of an acoustic impedance contrast. This is in agreement with the few descriptions of the basal portion of the sequence that report a transitional lower contact, which includes interbedded marine sediments and volcanic deposits. Imaging is extremely poor at shallow levels in which seismic facies are mainly transparent, with only local and discontinuous, east-dipping, high-amplitude parallel reflectors that appear to form the steep flanks of west-verging thrust blocks (**Figure 4.8**). The upper contact with Sequence 2, which has been described in outcrops as an unconformity, is very difficult to identify in the seismic data. However, in the syncline located west of the San Jorge depocenter (**Figure 4.8**a), we interpret an angular unconformity which may correspond to the contact between Sequences 1 and 2. Seismic data also suggests that Sequence 1 gets thinner to the east, either by erosion related to the lower to middle Eocene unconformity or by stratigraphic thinning of the sequence probably towards more proximal areas.

A poor seismic imaging of Sequence 2 has been obtained in the southern SJFB (**Figure 4.8**b), where Sequences 1 and 2 appear as folded strata, which are separated from younger post-lower Eocene sequences by an angular unconformity. Farther north, in the syncline preserved to the west of the San Jorge depocenter (**Figure 4.8**a), Sequence 2 shows a divergent pattern with fanning towards the west and onlap towards the east, against the underlying Sequence 1. Such geometry would be related to sedimentation in very inclined surfaces, typical of slope deposits such as those interpreted in nearby outcrops. In the northern SJFB, Sequence 2 appears as a series of ESE-dipping high amplitude and low frequency reflectors that have been interpreted as extensional rotated fault blocks (**Figure 4.10**b). Detailed mapping of such structures showed that they are forming two sets of extensional faults, one with a SSW-NNE orientation and the second one with a WNW-ESE orientation (*Mora et al., 2013*). The upper contact of Sequence 2 is an angular unconformity, which has been imaged in several seismic sections (**Figure 4.7** to **Figure 4.10**). Considering the age of Sequences 2 and 3, the approximate age of the unconformity is marked by the planktonic zones P.9 to P.10, corresponding to the limit between the lower and middle Eocene (**Figure 4.2** and **Figure 4.4**). As seen in the seismic cross-sections (**Figure 4.7** to **Figure 4.11**), the activity of the RFS, including the SJF, has been sealed by the lower to middle Eocene unconformity, and the eastward tilting of the whole fold belt has been caused by a deeper and younger major fault that probably extends to the deformation front of the accretionary prism, in offshore areas much farther to the west.

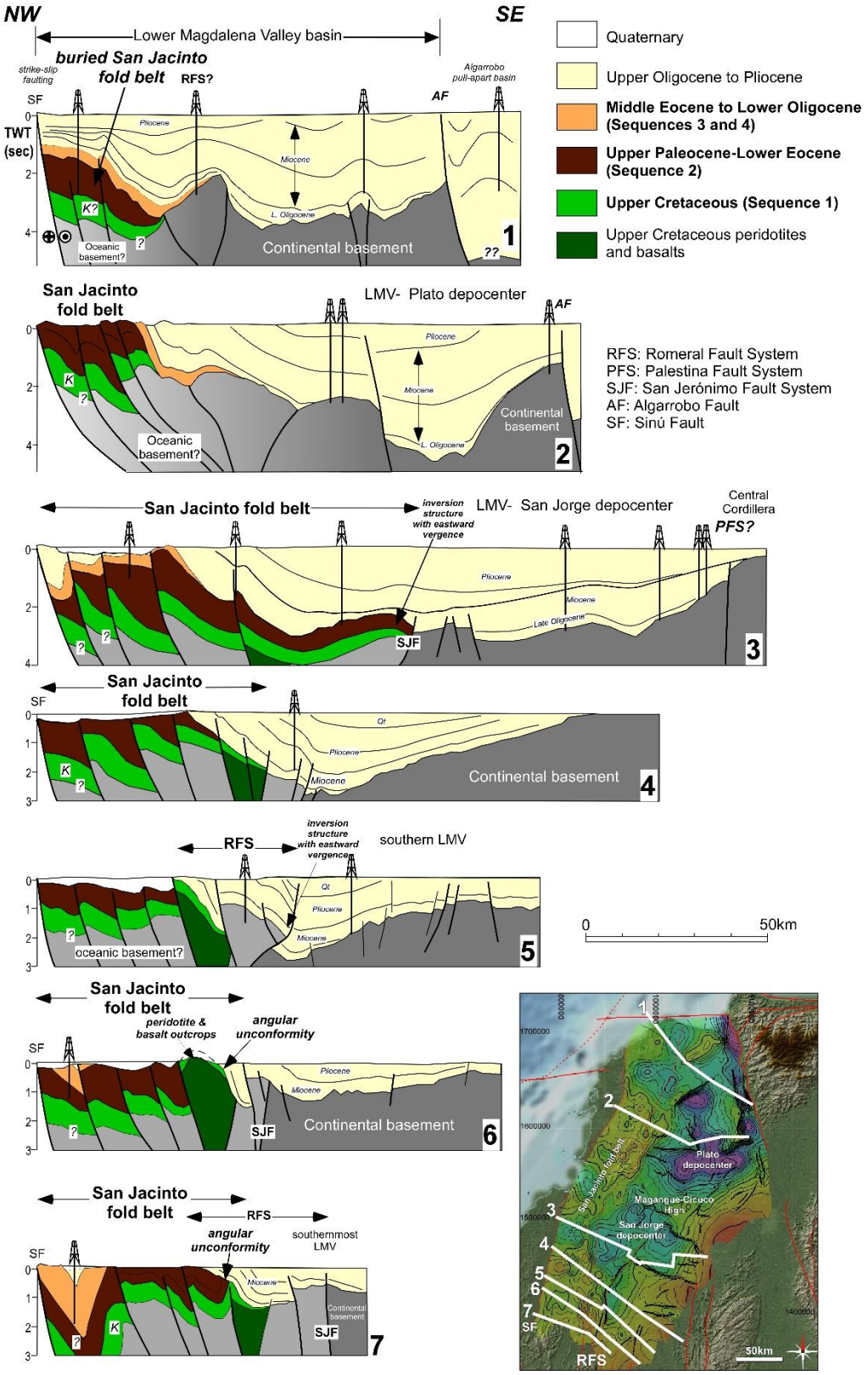

Figure 4.7. NW-SE-trending geo-seismic cross-sections in two-way-time (TWT), showing the along-strike variation in structure of the SJFB, LMV and RFS, and highlighting tectono-stratigraphic relationships among the studied sequences. The SJFB exhibits more contraction and shortening in the central and southern areas, whereas in the north (section 1), where pre-Oligocene units are buried, it displays much less contraction. The activity of the RFS also decreases from S to N. SF: Sinu Fault; SJF: San Jerónimo Fault; PFS: Palestina Fault System; AF: Algarrobo Fault.

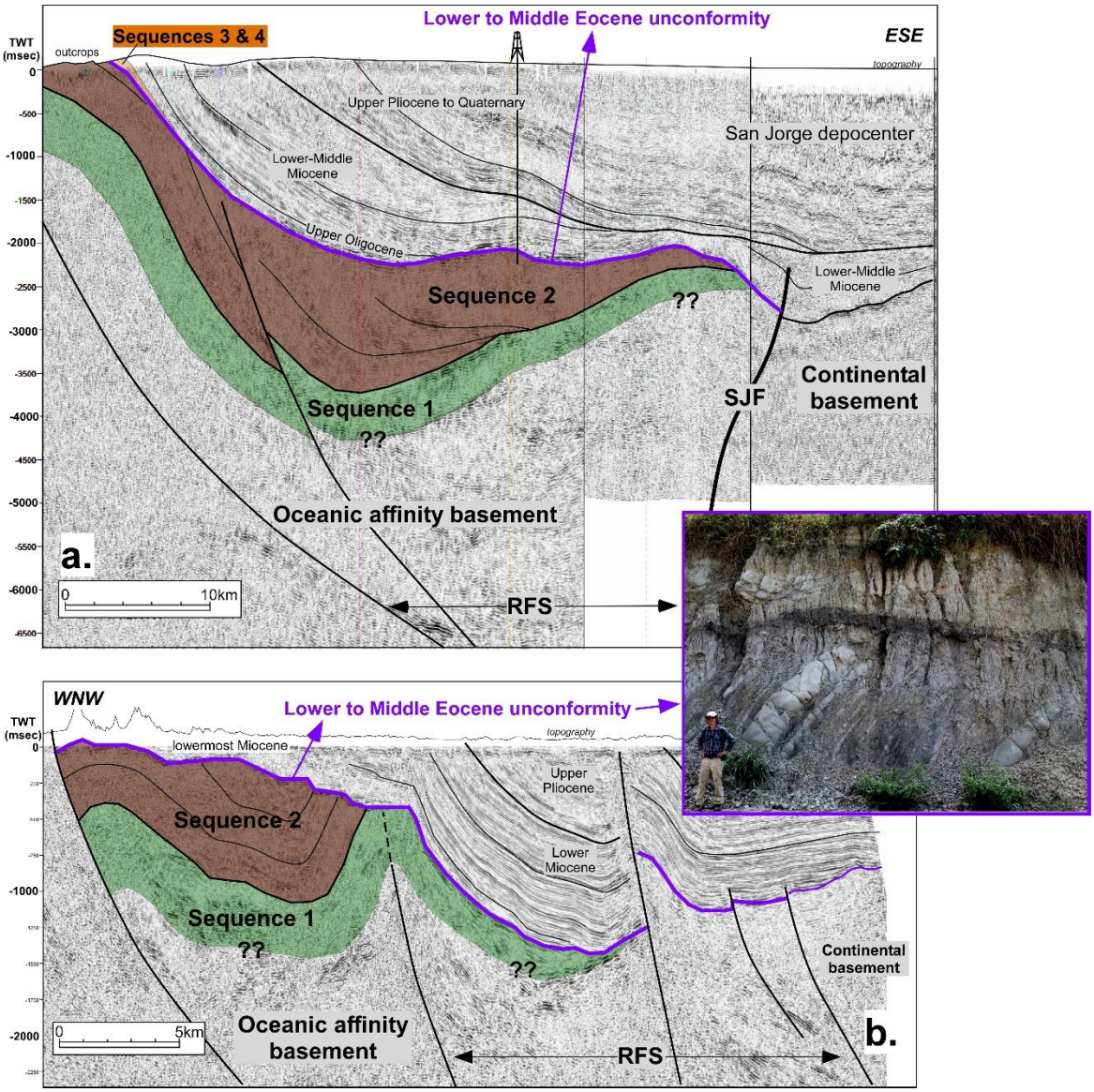

Figure 4.8. TWT-seismic lines showing the interpreted structure of the RFS and SJFB in the southern part of the study area and the seismic and outcrop expression of the impressive, lower to middle Eocene unconformity above sequences 1 and 2. The San Jerónimo Fault (SJF) in the southern SJFB appears to be responsible for the presence of pre-Oligocene units towards the east, into the southern LMV. Location of the sections is shown in **Figure 4.3** and uninterpreted versions of the seismic lines are included as supplementary material (**Figure B 2**).

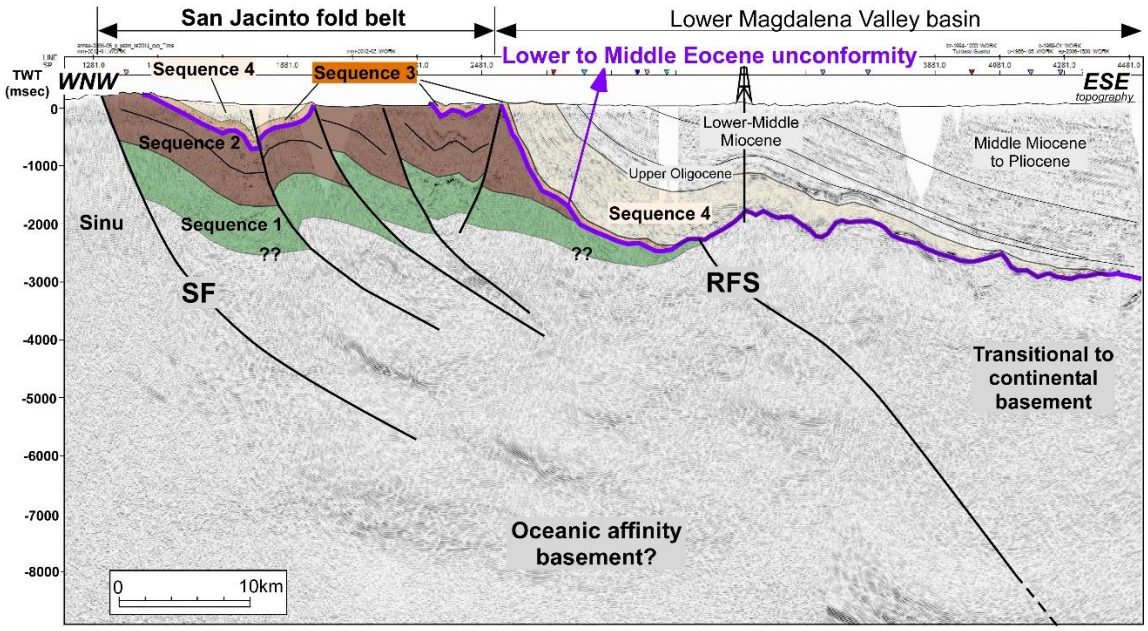

Figure 4.9. TWT-seismic line showing the interpreted structure of the northern San Jacinto anticlinorium and of the northwestern LMV, highlighting the pre-Oligocene tectono-stratigraphic sequences. Thick deposits of Sequence 4, drilled by the SamanEST-1 well, have sealed the RFS, which would only be responsible for slight folding. Main deformation of the SJFB is related to the activity of the Sinu Fault (SF) and other deeply-rooted structures which appear farther to the W, in the Sinú fold belt. The location of the section is shown in **Figure 4.3** and an uninterpreted version of the seismic line is included as supplementary material (**Figure B 3**).

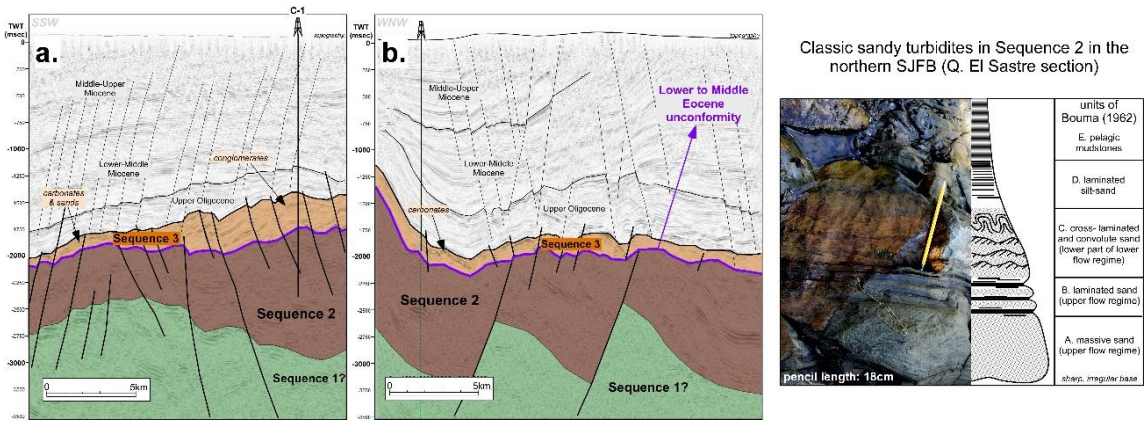

Figure 4.10. TWT-seismic lines showing the interpreted structure of the northernmost SJFB. Extensional structures are well preserved in this area, in contrast to the central and southern areas of the fold belt where compression and strike-slip deformation is predominant. The seismic lines show how Sequence 3 delimits a lower structural domain (Sequences 1 to 3) from an upper structural domain. An example of a classic sandy turbidite, occurring in Sequence 2 and described in a stratigraphic section in the northern SJFB, is also shown. Sequence 4 is not preserved in this area. Line in Figure 4.10a is a strike line, trending approximately from NE to SW, while the line in Figure 4.10b is a dip line, trending approximately from SE to NW. The lines are located close to the C-1 drill hole in the northern SJFB, but due to confidentiality, the exact location of the lines cannot be provided.

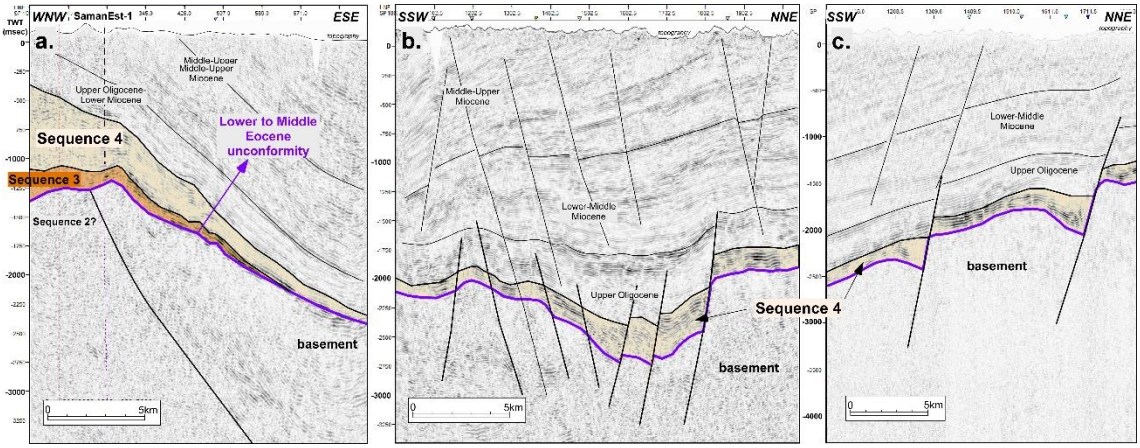

Figure 4.11. TWT-seismic lines in the central to northern SJFB (eastern San Jacinto anticlinorium) showing the onlap of Sequences 3 and 4 against the basement to the ESE, sealing the RFS (Figure 11a). Figures 4.11b and c show the interpreted syn-extensional deposits of Sequence 4 preserved in extensional faults trending ESE-WNW. Location of the sections is shown in **Figure 4.3** and uninterpreted versions of the seismic lines are included as supplementary material (**Figure B 5**).

Sequence 3 is best preserved in the northern SJFB where it has also been well imaged by 2D and 3D-seismic data (**Figure 4.10**) and has been drilled by wells such as the C-1. This sequence has notorious lateral thickness and facies changes. In the northern SJFB, Sequence 3 is also affected by extensional faults (**Figure 4.10**), which, when mapped in detail with 3D-seismic, were found to have two main, probably inherited structural trends, a SSW-NNE trend and a WNW-ESE trend (*Mora et al., 2013*). The carbonates tend to be preserved in areas interpreted as paleo-highs, while conglomerates appear to occur in low areas (**Figure 4.10**). In the eastern San Jacinto anticlinoria, seismic packages with medium to high amplitude and frequency reflectors have fossilized the RFS and are onlapping the basement towards the east (**Figure 4.11**a). Sequences 3 and 4 thus represent the onset of landward-stepping sedimentation in the area after the lower to middle Eocene tectonic, uplift and erosional event. The lower contact of Sequence 3 is a clearly imaged angular unconformity, while the upper contact is also unconformable with upper Oligocene strata in the northern SJFB (**Figure 4.10**) and with upper Eocene to lower Oligocene strata of Sequence 4 (**Figure 4.11**a).

Sequence 4 exhibits high thicknesses in the axis of a syncline in which the T-2XP was drilled (section 7, **Figure 4.7**). This sequence is also imaged in seismic data in the central-eastern part of the San Jacinto anticlinoria, where the Samán stratigraphic well was drilled (**Figure 4.1**, **Figure 4.7**/section 2 and **Figure 4.11**a). However, in this area, Sequences 3 and 4 were deposited on top of the basement and show moderate to high amplitude, medium to high frequency reflectors, which are divergent towards the west and onlap older units at low angles towards the ESE (**Figure 4.9** and **Figure 4.11**a). Seismic lines oriented parallel to the belt's strike (**Figure 4.11**b and c) show that the clastic deposits of Sequence 4 are also affected by the WNW-ESE extensional fault family that is affecting Sequence 3 in the north.

4.4.4 Seismicity data and paleo-tectonic reconstructions

4.4.4.1 Present-day lithospheric configuration of the convergent margin in NW South America

We used the publicly available seismicity data and data from previous research (e.g. *Bezada et al., 2010*) to study the present-day geometry and configuration of the subduction zone of NW Colombia. We constructed a depth map of the top of the subducted oceanic slab beneath South

America and a cross-section depicting its geometry and the configuration of the subduction zone of NW Colombia (**Figure 4.12** and **Figure 4.13**). The detailed description of the construction of the map and cross-section is included in *Text B3* and **Figure B 1**.

The study area is characterized by a low seismicity, with very few scattered, shallow (< 70 km) and low magnitude (< 4 Mw) events (*Mora et al., 2017a*), and there are no focal mechanism solutions in the San Jacinto fold belt. Although it seems to be a seismically inactive area, some neo-tectonic fault activity has been identified by Veloza et al. (2012) in the northern part of the belt.

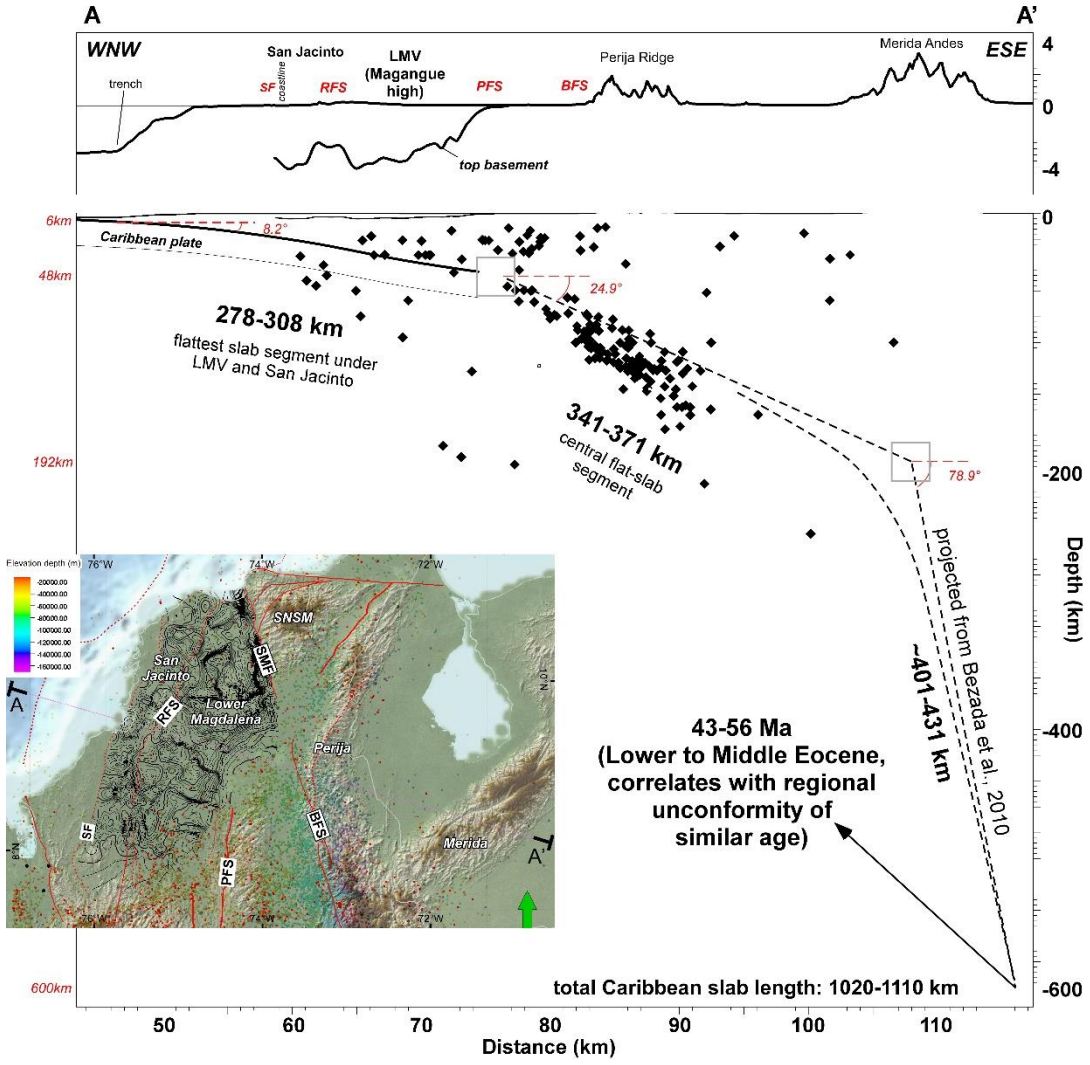

Figure 4.12. Regional WNW-ESE-trending cross-section showing the configuration of the subducted Caribbean oceanic plate, as interpreted from reflection-seismic mapping for the shallowest part, intermediate-depth seismicity for the central part and from published tomography data (*Bezada et al., 2010*) for the deepest part of the cross-section. The top of the basement under the LMV from reflection-seismic mapping and the topography are also displayed. Gray squares represent the uncertainty (± 15 km) in the horizontal and vertical measurements. This cross-section is located farther to the north of the cross-section presented by *Mora et al. (2017a*, their Figure 13). We highlight the end of the subducted slab at a depth of ~600 km, which would have entered the trench in early to Middle Eocene times, assuming convergence velocities shown in **Table 4.2**. Further explanations in the text.

The Caribbean plate subducted beneath NW South America appears to be formed by three different slab segments, separated by kinks or bends (**Figure 4.12**): a northwestern shallow and very flat slab segment, a central intermediate-depth and flat-slab segment (the "Caribbean" flat-slab of *Syracuse et al., 2016*), and a southeastern deep and very steep slab segment imaged by *Bezada et al. (2010*). The three slab segments could have different geometries, thicknesses and physical properties, as deduced from deep drilling (DSDP), reflection-seismic imaging, tomography data

and water depths in the Colombia and Venezuela basins (*Leroy et al., 1996*; *Mauffret and Leroy, 1997*, *Driscoll and Diebold, 1999*; *Magnani et al., 2009*; *Kroehler et al., 2011*). In general, the Colombian Basin to the west is composed of an oceanic plateau with thicknesses between 10 and 18 km (*Bowland and Rosencrantz, 1988*), while north of Colombia, in the area of the Beata Ridge (**Figure 4.13**), the plateau appears to be thicker (*Kroehler et al., 2011*). Slab segments with specific physical and chemical properties would then have specific buoyancy properties, which could explain such changes in dip.

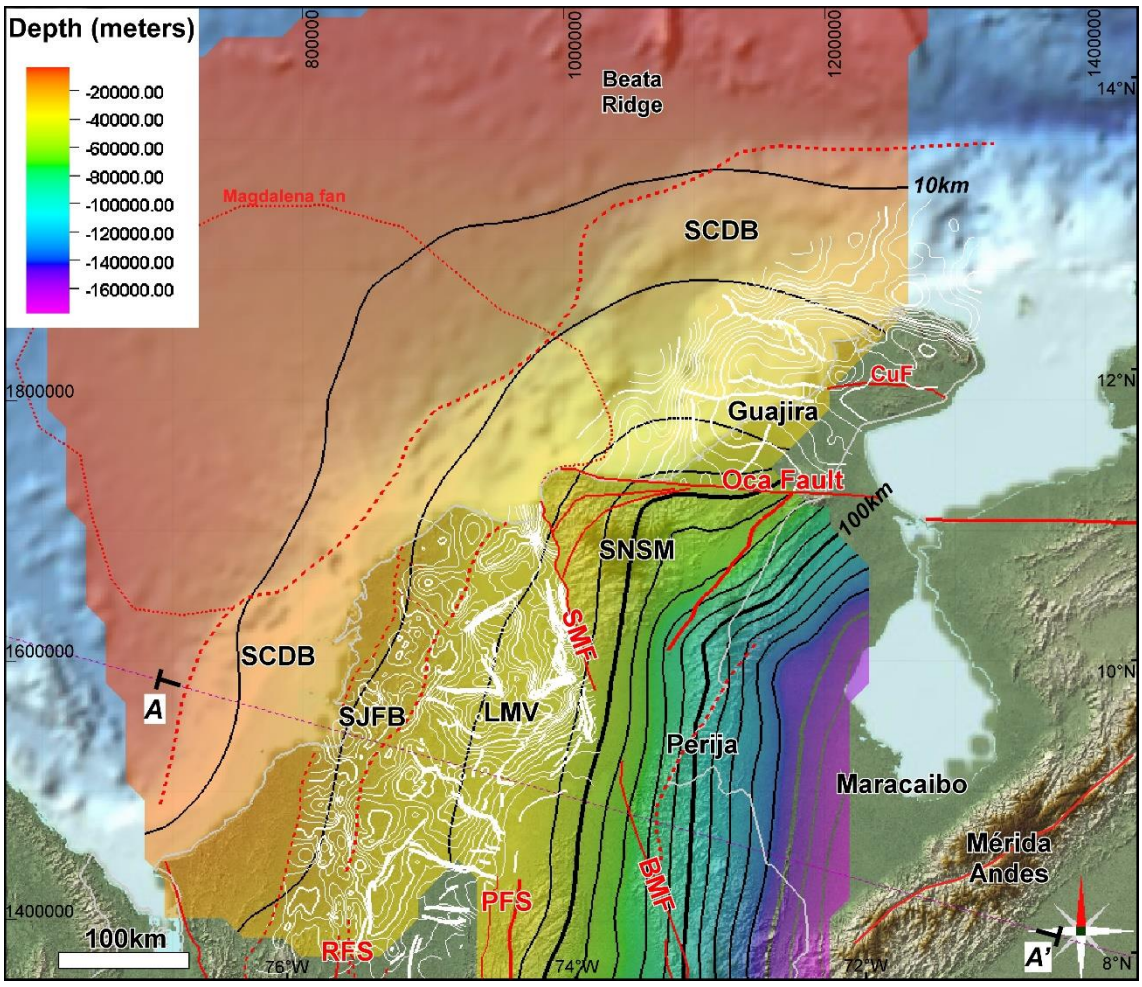

Figure 4.13. Integrated depth map in meters of the top of the oceanic Caribbean plate (in colors) which has been subducted under NW South America since early to middle Eocene times. Note the change in dip of the slab in the location of the Palestina Fault System (PFS) and how it changes its strike as it approaches the Oca Fault. The white contours are the depth structure of the basement below the LMV, SJFB and Guajira basins. SCDB: South Caribbean deformed belt (red dashed lines); RFS: Romeral Fault System; SMF: Santa Marta fault; BMF: Bucaramanga fault; SNSM: Sierra Nevada de Santa Marta.; CuF: Cuisa fault. Further details about the construction of this map and the related cross-section (**Figure 4.12**) are found in the supplementary *text B3* and in **Figure B 1**.

The previously described segmented slab geometry of the subducted Caribbean plate does not seem to continue to the north of the Oca-El Pilar-San Sebastian Fault System. In the Guajira Peninsula of northernmost Colombia, seismic interpretations and gravity modelling (*Londoño et al. 2015* and this study) show that the Caribbean plate is being subducted at low angle beneath the Southern Caribbean deformed belt. Farther to the east, in northern Venezuela, wide-angle reflection seismic and tomography data (*Magnani et al., 2009*; *Bezada et al., 2010*) show that the boundary between northern South America and the southern Caribbean plate is dominated by strike-slip tectonics related to the Oca-El-Pilar-San Sebastián fault system (OEPFS) and the Caribbean plate is clearly

imaged at shallow levels in the block to the north of the fault system. Seismicity also changes abruptly from the southern block of the OEPFS, where the Wadati-Benioff zone is clearly imaged by intermediate depth seismicity, to the northern block of the fault system, where only isolated and shallow seismic events occur (*Syracuse et al., 2016* and section 2 in **Figure B 1**).

Based on the steep descent of the Caribbean plate under Maracaibo and the Mérida Andes, previous researchers have proposed that there should be a tear in the Caribbean plate (*Masy et al., 2011*; *Bezada et al., 2010*; *Levander et al., 2015*), which would be separating the steeper dipping Caribbean slabs, located to the south of the OEPFS, from the shallow Caribbean plate that has been imaged north of the same fault system. Using data from previous research and our new depth map of the shallow subducted Caribbean oceanic segment under the San Jacinto fold belt, Lower Magdalena Valley basin and the Perijá Ridge (**Figure 4.13**), we propose a new interpretation of the three-dimensional plate tectonic configuration of northern Colombia and western Venezuela (**Figure 4.14**). This interpretation implies that the boundary between northern South America and the Caribbean plate consists of two tears or subduction-transform edge propagator (STEP, *Govers and Wortel, 2005)* faults instead of only one. The difference is that the STEP fault previously proposed by *Govers and Wortel (2005*) is tearing the Atlantic/South American plate in the area of the Paria seismicity cluster, at the eastern end of the OEPFS in northeastern Venezuela (*Russo et al., 1993*), while the newly proposed STEP fault would be tearing the Caribbean plate in an undefined area of the western OEPFS, probably close to the Sierra Nevada de Santa Marta (SNSM, **Figure 4.14**). This means that the Oca-San Sebastián-El Pilar dextral fault system is the tear fault that limits the Caribbean and South American/Atlantic plates at crustal and mantle levels. Our observations are in agreement with *Levander et al. (2015*) who propose that the southern Caribbean plate boundary is a complex strike-slip fault system bounded by oppositely vergent subduction zones.

4.4.4.2 Upper Cretaceous to Eocene paleotectonic reconstructions

It is expected that the onset of subduction of the irregular Caribbean plateau had an important effect on the upper plate and that this effect should be recorded in the sedimentary basins in the area. We used the free software package GPlates (version 2.0.0, www.gplates.org; *Boyden et al., 2011*) and two paleo-tectonic models available for this area (*Boschman et al., 2014* and *Matthews et al., 2016* from the GPlates database) to perform Late Cretaceous to Eocene paleo-tectonic reconstructions (**Figure 4.15**). Our reconstructions show the motion of the Caribbean plate relative to a fixed South American plate but it is important to highlight that plate tectonic processes between the Caribbean and the Americas were driven by relatively fast, westward motion of North and South America, while the Caribbean plate has remained nearly stationary since the Eocene (*Müller et al., 1999*).
Using average plate convergence velocities of the Caribbean plate relative to South America over the last 45 Ma, we calculated for both models the geological time when each of the three subducted slab segments of the Caribbean plate imaged along cross-section A-A' (**Figure 4.12**) entered the trench (**Table 4.2**). The age of entrance in the trench of the whole Caribbean slab (total length of 1065 ± 15 km) ranges from lower Eocene (c. 56 ± 2 Ma) to middle Eocene (c. 43 ± 2 Ma) depending on the model used (*Boschman et al. 2014* or *Matthews et al. 2016*, respectively). Equivalence of the obtained age of entrance in the trench of the Caribbean slab with the identified unconformities in the stratigraphic succession in the SJFB (also shown in **Figure 4.12**) will be discussed in forthcoming sections.

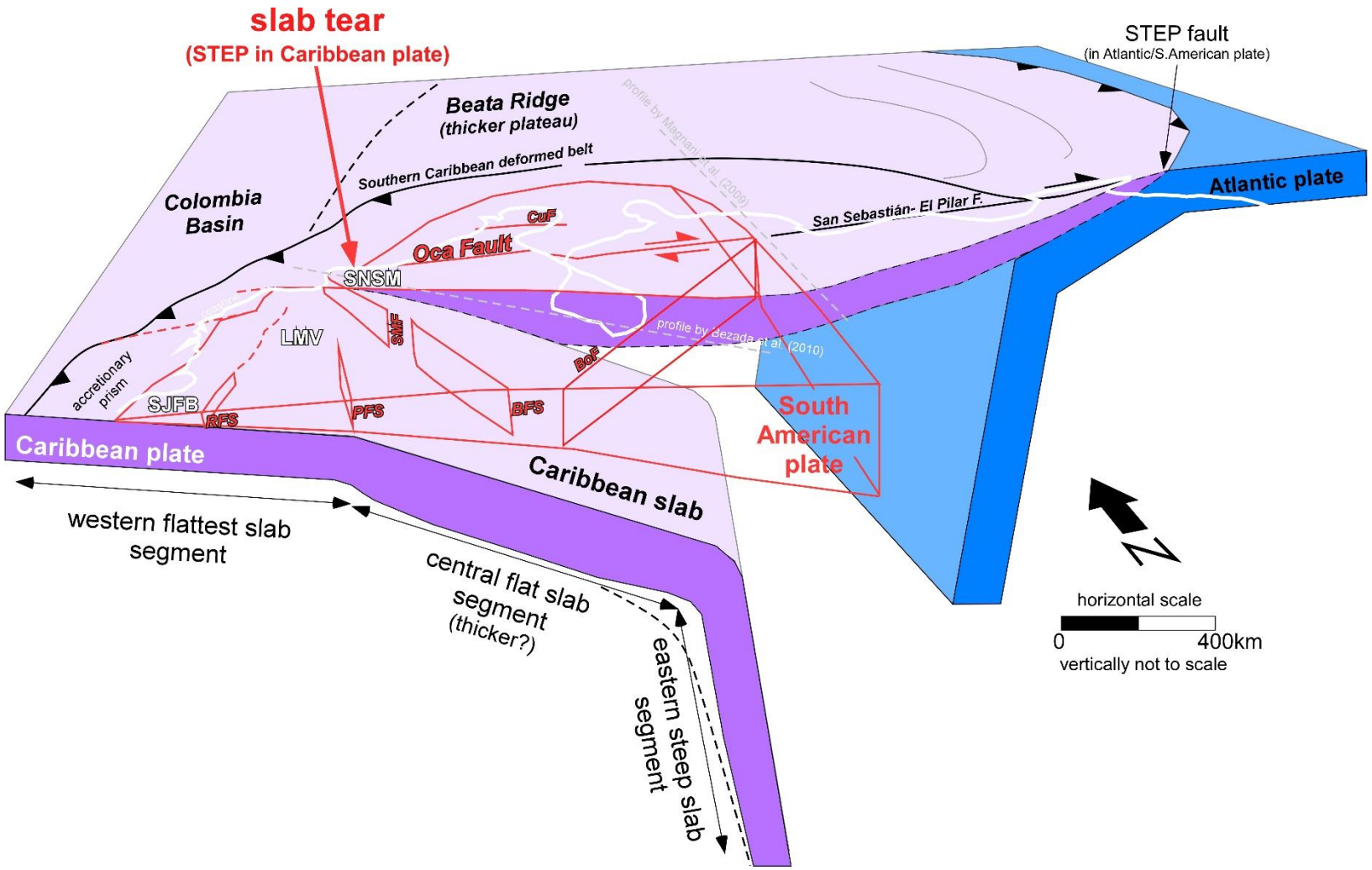

Figure 4.14. Proposed three-dimensional lithospheric configuration of NW South America, as interpreted from shallow reflection-seismic mapping, intermediate-depth seismicity and deep tomographic imaging from previous studies (e.g. *Bezada et al., 2010*); according to our interpretation, there would be a slab tear or STEP fault (subduction transform edge-propagator, *Govers and Wortel, 2005*) in the Caribbean plate, probably represented in the upper crust by the western tip of the Oca-El Pilar-San Sebastián dextral fault system (OEPFS).

	Slab segment length (km) (± 15 km error)	Calculated age of slab entrance in the trench using mean plate velocities over the last 45 Ma	
		Boschman et al. 2014 19 mm/yr	Matthews et al. 2016 25 mm/yr
Western flat slab segment under SJFB and LMV	278-308	14.6-16.2 Ma	11.1-12.3 Ma
Central intermediate-depth flat slab segment	341-371	18-19.5 Ma	13.6-14.8 Ma
Eastern deepest and steepest slab segment	401-431	21.1-22.7 Ma	16-17.2 Ma
Western plus Central flat slab segments	619-679	32.6-35.7 Ma	24.8-27.2 Ma
All three slab segments	1020-1110	53.7-58.4 Ma (56 ± 2 Ma)	40.8-44.4 Ma (43 ± 2 Ma)
*Slab length by Van Benthem et al. (2013)**	900	47,4 Ma	36 Ma

** they interpret three slab segments, each one 300 km-long*

Table 4.2. Compilation of the slab segment lengths, convergence velocities and ages of entrance in the trench of each slab segment shown in **Figure 4.12**. We calculated average velocities over the last 45 Ma according to each of the two available models (*Boschman et al., 2014* and *Matthews et al., 2016*). Using such velocities and the measured lengths of each slab segment, we could calculate the time at which each segment entered the trench. From these calculations, we found that the ~1000 km-long Caribbean slab entered the trench in early to middle Eocene times (shaded in gray), coinciding with regional unconformities identified in the San Jacinto fold belt.

4.5 Discussion

4.5.1 Late Cretaceous to Eocene paleo-tectonic reconstructions and kinematics

In the debate about the origin and evolution of the Caribbean oceanic plate, two main models have been proposed, an in situ model which implies a short migration of the Caribbean to its present position *(James, 2006*) and a Pacific model which proposes an eastern Pacific origin of the plate and a long-distance migration (*Pindell, 1993*; *Kennan and Pindell, 2009*; *Boschman et al., 2014*). The Pacific model appears to be the most robust and more widely accepted, though the migration distances of the terranes in northwestern Colombia, which show an oceanic affinity remain poorly constrained. Using the Gplates free software and the models of *Boschman et al. (2014*) and *Matthews et al. (2016*), we present modified paleo-tectonic reconstructions for the most relevant time slices for this study (**Figure 4.15**). Based on the model by *Boschman et al. (2014*), we calculated that the maximum northwestward displacement of the allochthonous oceanic (Caribbean) terranes west of the RFS was ~1077 km between 90 and 65 Ma, which can be subdivided into 691 km from 90 to 75 Ma and 386 km from 75 and 65 Ma. This means that most of the northwestward displacement of the allochthonous Caribbean terranes occurred in Late Cretaceous times, along the RFS and PFS. We also calculated the tectonic convergence velocity and obliquity curves for the Caribbean-South American margin and plotted them with the identified tectono-stratigraphic unconformities in the SJFB and with the main tectonic events studied in the

literature (**Figure 4.16**). The obliquity was calculated as the angle between the plate displacement vector and the orthogonal to the strike of the SW-NE South American plate boundary, as defined by *Philippon and Corti (2016*).

Convergence obliquities where much higher in Late Cretaceous to early Eocene times and they notoriously decreased in middle Eocene times (50 to 40 Ma) in both models (**Figure 4.16**), while velocities decrease earlier in the model by *Matthews et al. (2016*) and later (45 Ma) in the model by *Boschman et al. (2014*). The lower Paleocene unconformity, which would be the expression of the collision of the Caribbean oceanic plateau, appears to be related to a velocity reduction according to the model by *Matthews et al. (2016*). The lower to middle Eocene unconformity fits with a significant decrease in convergence obliquity and velocity (*Boschman et al. 2014*) and several major tectonic events, such as the end of the strike-slip activity of the RFS and PFS, the cessation of arc magmatism in NW Colombia and the onset of strike-slip displacement of the OEPFS (*Gomez, 2001*; *Vence, 2008*).

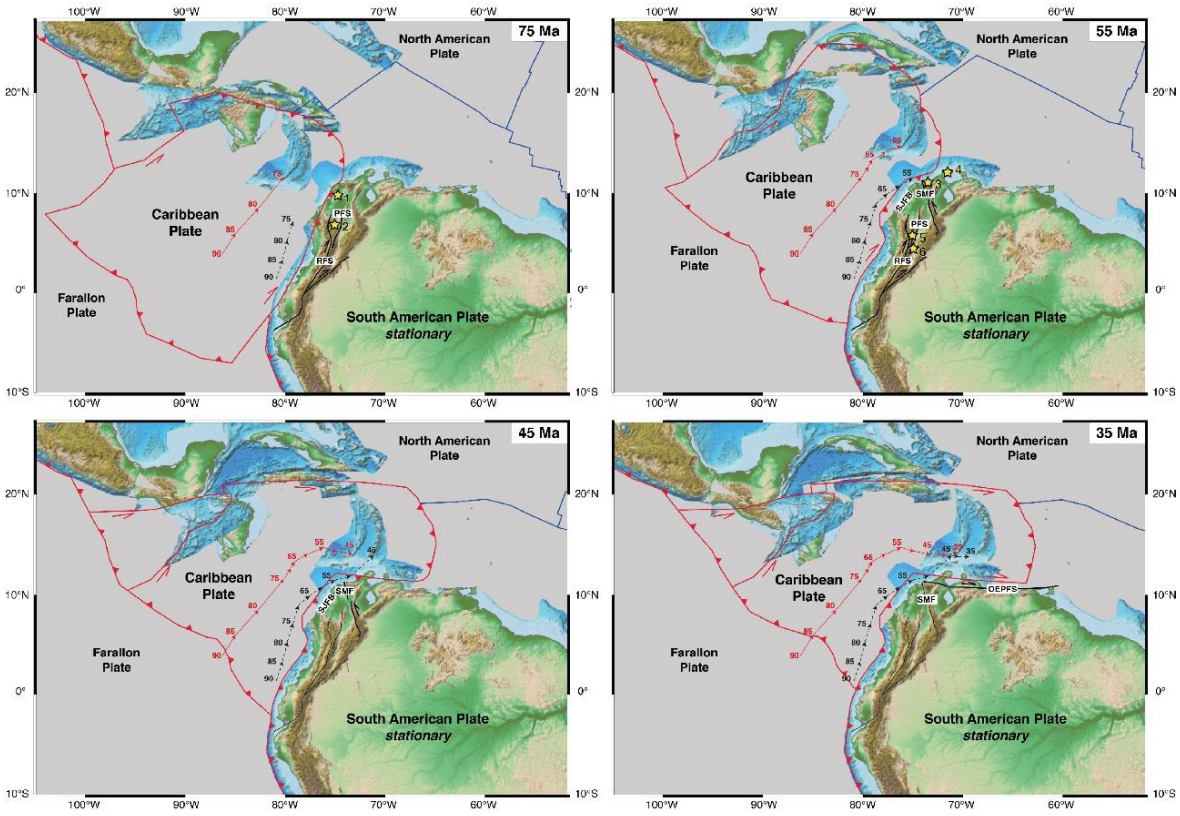

Figure 4.15. Paleo-tectonic reconstructions at 75, 55, 45 and 35 Ma, illustrating the displacement of the Caribbean plate relative to fixed South America and the major change in convergence obliquity, which occurred between 55 and 45 Ma. The displacement vectors of the Caribbean plate relative to South America are shown in red arrows according to the model of *Matthews et al. (2016*, GPlates database) and in black dashed arrows according to *Boschman et al. (2014*). The plate boundaries (spreading ridges in blue, subduction and transform zones in red) and continent polygons are from *Matthews et al. (2016*). The main fault zones of NW South America are labelled and drawn in thick black lines when active. Yellow stars indicate active magmatic arcs in our studied area: 1. Bonga and Cicuco plutons, 2. Antioquia Batholith, 3. Santa Marta Batholith and related plutons, 4. Parashi pluton, 5. Sonsón Batholith, 6. El Bosque Batholith (from *ANH, 2011*a; *Cardona et al. 2011*; *Bayona et al., 2012*; *Cardona et al.,* 2014; *Bustamante et al., 2017*). The northwestward motion of allochthonous oceanic terranes (up to ~1077 km between 90 and 65 Ma, in *Boschman et al. 2014*), accreted to western Colombia along major suture zones such as the right-lateral RFS in Late Cretaceous to Paleogene times, is not shown here. Since 50 Ma, c. 1000 km of Caribbean oceanic crust were subducted below South America. See the text for further discussion.

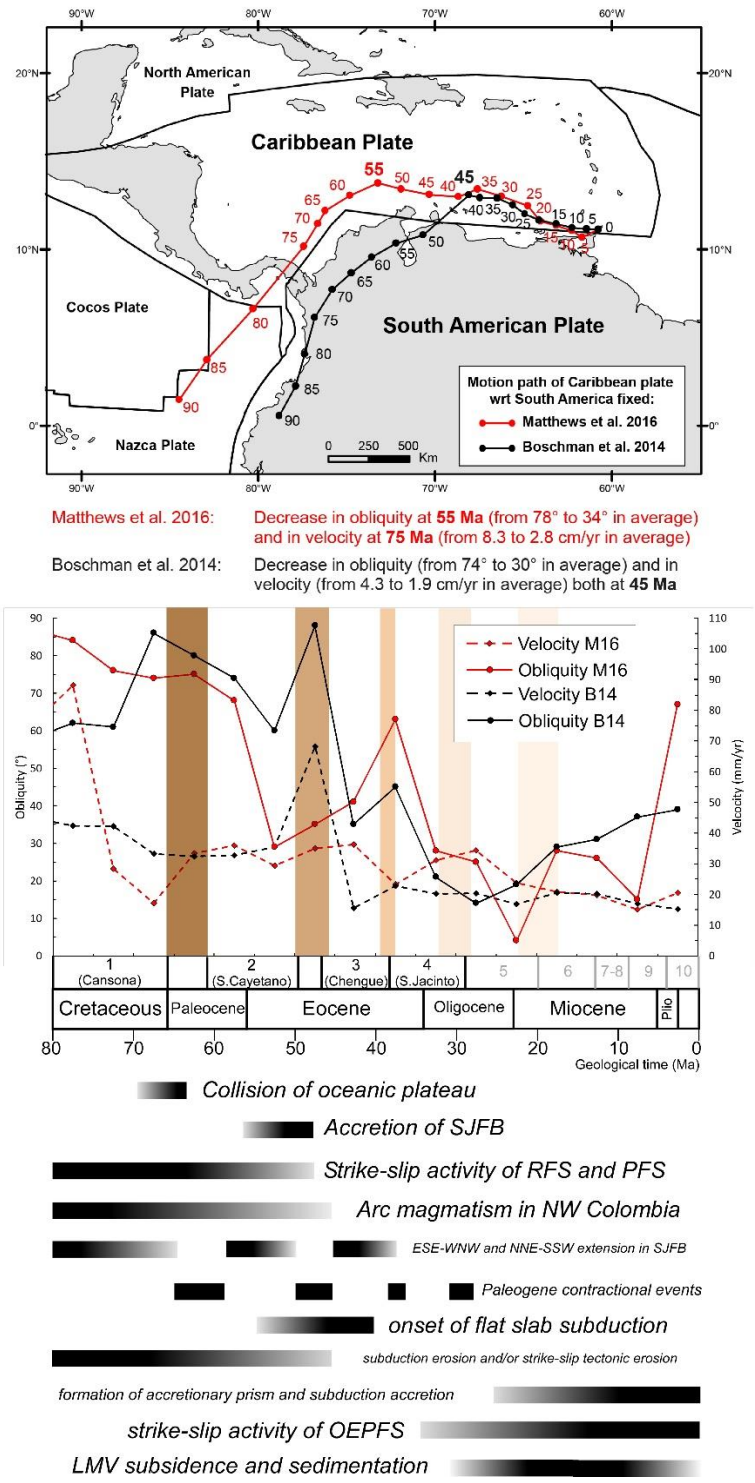

Figure 4.16. Evolution of Late Cretaceous to present-day tectonic plate convergence velocity and obliquity compared with major tectonic events and tectono-stratigraphic unconformities. The upper panel shows the displacement vectors of the Caribbean plate relative to a fixed South American plate, since 90 Ma, according to two different paleo-tectonic models (*Boschman et al. 2014* in black, B14; *Matthews et al. 2016* in red, M16). The central panel shows the changes in plate convergence velocity and obliquity with time for both models, compared with the pre-Oligocene tectono-stratigraphic sequences and unconformities (vertical bars of brown shades) and major tectonic events (black horizontal bars in the lower panel). We calculated velocities and obliquities in time-steps of 5 Ma, hence the points in the graph represent the middle of each time interval. The identified Paleogene unconformities correlate with major tectonic events such as the Late Cretaceous to early Paleocene collision of the Caribbean plateau and the Eocene onset of Caribbean flat-slab subduction. See text for further discussion.

4.5.2 Late Cretaceous forearc basin (89 to 75 Ma, Coniacian to Campanian)

From the available information, it appears that during Late Cretaceous times, a forearc basin existed SW of the study area, with an intra-continental, magmatic arc to the east (called the Magangué Arc by *Silva et al., 2016*, **Figure 4.15**), formed by the east-dipping subduction of a "normal" thickness, Caribbean oceanic plate under South America (*Villagómez et al., 2011a*). Magmatism affected both continental and accreted oceanic crust (the Quebradagrande terrane or a younger, allochthonous intra-oceanic arc) and supplied abundant mafic and felsic, volcaniclastic material to the proximal parts of the basin. Recent petrography analyses (see *Text B1*) support a Late Cretaceous magmatic arc setting in which there was also some sediment supply from more distal and older terranes, such as the Tahami-Panzenú and Chibcha terranes of the eastern LMV and northern CC (*Mora et al., 2017a*). *Gómez et al. (2005*), *Restrepo et al. (2009*) and *Caballero et al. (2013b*) used apatite fission track thermochronology to propose that uplift of the CC and the San Lucas ridge began since Late Cretaceous times (Campanian-Maastrichtian), consequently these were potential source areas, which provided sediments to surrounding basins such as the SJFB. However, according to *Boschman et al (2014*) paleo-tectonic reconstructions, at 90 Ma the SJFB would have been as far as ~1077 km to the SW of its present location, hence it would have been sourced by Permo-Triassic and Cretaceous terranes located much farther south within the proto-Central Cordillera. Nevertheless, several researchers (e.g. *Kennan and Pindell, 2009*) have suggested that the Tahami-Panzenu terrane, located between the RFS and the PFS, is para-autochthonous and that it also moved from the southwest along its limiting dextral fault systems. This would mean that the sedimentary sources and the San Jacinto basin always moved parallel to each other, thus explaining the good match we obtained in terms of provenance. Outcrop and the very few well data show that sedimentation in the area of the present day SJFB occurred in a marine shelf in which proximal marine environments occurred in the central area (San Jacinto) while deeper marine environments occurred in the south.

4.5.3 Latest Cretaceous-early Paleocene collision of the Caribbean oceanic plateau

It has been proposed that in the Latest Cretaceous to early Paleocene times, the Caribbean oceanic plateau collided with northwestern South America (*Cediel et al., 2003*, *Pindell et al., 2005*, *Bayona et al., 2012*). Paleo-tectonic reconstructions (*Pindell and Kennan, 2009*; *Spikings et al., 2015*) suggest that at this time, the Caribbean plate moved towards the NE relative to the North and South American plates and started to occupy space between them. *Villagómez et al. (2011b*) and *Caballero et al. (2013b)* used apatite fission track thermochronology to identify an exhumation pulse in the San Lucas ridge and southernmost SNSM during early Paleocene times (**Figure 4.15**) which they relate to the collision of the Caribbean Plateau with northwestern South America. We consider that the absence of lower Paleocene deposits in northwestern Colombia (planktonic zones P.0 to P.2., 65 to 61Ma) and the unconformity that has been reported in outcrops between Sequence 1 (Cansona) and Sequence 2 (San Cayetano, **Figure 4.16**) are the expression of a regional shortening event which took place in latest Cretaceous to early Paleocene times, and which would be related to the collision of the Caribbean plateau. The notorious decrease in convergence velocity between 75 and 70 Ma, according to *Matthews et al. (2016*) could also be related to this collision event.

4.5.4 Late Paleocene to early Eocene forearc basin

After the early Paleocene shortening episode, forearc extension and subsidence resumed, but it is not clear if at that time the Caribbean plateau was already being subducted under South America

(*Bayona et al., 2012*; *Bustamante et al., 2017*), or if early Paleogene magmatism is more related to the final subduction stage of the "normal" thickness Caribbean plate. For the deposition of Sequence 2, our integration of outcrop and well data throughout the San Jacinto fold belt shows that mud-rich and mixed sand-mud, proximal turbidite systems (sensu *Richards, 2001*) were predominant in the north and south, while sand and gravel-rich turbidite systems prevailed in the central part.
Reflection-seismic data from the central and northern SJFB shows that during sedimentation of Sequence 2 (late Paleocene to early Eocene), the area experienced WNW-ESE-oriented extension (*Mora et al., 2013*; *Mora et al., 2017a*). However, in the northern SJFB, reported lithologies are mainly fine-grained and no facies changes related to the activity of extensional faults have been documented. In the central part of the fold belt, Sequence 2 shows onlap patterns towards the east and fanning towards the west, suggesting sedimentation in steep slopes. We consider that the origin of the WNW-ESE-trending faults that affect Sequence 2 relates to forearc extension due to oblique convergence between the Caribbean and South American plates, as proposed by *Daly (1989*) in the Ecuador forearc. However, *Mora et al. (2017a*) suggested that subduction erosion (*Clift and Vanucchi, 2004)* occurred in the margin in Late Cretaceous times, hence Late Cretaceous to Paleogene subsidence and extension in the forearc could have also been related to subduction erosion.

New petrography data (*Text B1*) shows that detrita of Sequence 2 come from similar tectonic regions that sourced Sequence 1, including a magmatic arc and older continental basement blocks. Recent analyses of drill hole samples in the San Jacinto fold belt (*Sarmiento et al., 2016*) provide more evidence of volcanic activity during late Paleocene to early Eocene times. According to *Cardona et al. (2011*), the San Cayetano sandstones fall within the transitional to dissected arc fields of *Dickinson (1985*), in agreement with *Ecopetrol/ICP (2014*).

Our new U-Pb geochronology and Hf isotope geochemistry results clearly show a main provenance from Upper Cretaceous magmatic arcs and a secondary provenance from Permo-Triassic igneous terranes such as those documented in the Tahamí-Panzenú terrane of the eastern LMV and northern CC (*Mora et al., 2017a*). Furthermore, a very good match is seen between the Hf isotope geochemical compositions of the detrital zircons in the C-1 well and the compositions of both the Coniacian-Campanian Bonga pluton zircons and the Permo-Triassic metamorphic basement zircons from the Hojarasca and VIM15 wells reported by *Mora et al. (2017a*). This suggests that the upper Paleocene-lower Eocene sediments of Sequence 2 were mainly sourced from Upper Cretaceous plutons of both oceanic (e.g. Bonga) and continental affinity (Magangué Arc, *Silva et al., 2016*; Antioquia Batholith), and from the Permo-Triassic igneous-metamorphic terranes in the LMV and northern CC. Our paleo-tectonic reconstructions show that after a considerable (~1077 km) northwestward displacement of the Caribbean oceanic terranes in Late Cretaceous times, such terranes including San Jacinto, had almost reached their current position, thus supporting our provenance considerations.

These data also support a forearc basin setting in which both the oceanic and continental affinity, Upper Cretaceous magmatic arcs were being eroded and providing sediment for the marine basin to the northwest. Though evidence of Paleocene to early Eocene magmatism has not been yet found in the LMV and SJFB, it is likely that plutons of such ages exist, considering that Paleocene to early Eocene magmatism has been documented in surrounding areas such as the northern CC (Paleocene Sonsón Batholith, *Bayona et al., 2012*; *Bustamante et al., 2017*), the SNSM and the Guajira peninsula to the north (*Cardona et al., 2014*). If the SNSM and the northern CC were connected, as interpreted by *Montes et al. (2010*) and *Mora et al. (2017a*), and if both the northern CC and the southern SNSM were being uplifted in the late Paleocene (*Restrepo et al., 2009*; *Villagómez et al., 2011b*), then the most likely sources for the sediments of Sequence 2 were the ancient northern CC and southern SNSM, located to the E and SE of the SJFB in early Eocene times. Furthermore, the presence of Permo-Triassic, lower Paleozoic and Meso to Neo-Proterozoic detrital zircon ages (**Figure 4.5**b), in addition to a group of Cretaceous zircons with initial εHF values <0, provide strong lines of evidence in favor of a sediment that was sourced from older continental basement blocks. Although these older sources may well derive from the core of the CC and SNSM also, it is also possible that these could be derived from farther-removed sources of the Eastern and Central Cordilleras and the Putumayo basement. A far-traveled component may have also contributed re-worked Cretaceous and/or Paleogene zircons (e.g. *Horton et al., 2010*; *Nie et*

al., 2012) to the SJFB, but the Hf systematics of most zircons dated here and their resemblance to proximal basement sources, indicate that re-working of far-traveled Cretaceous and Paleocene sources are unlikely to represent a major component (**Figure 4.5** and **Figure 4.6**).
Moreover, paleo-geographic reconstructions of northern South America (e.g. *Hoorn et al., 2010*) do not support a connection between SJFB and LMV with old continental basement blocks such as the Eastern Cordillera or the Putumayo basement. This fact restricts the sediment source areas to the Central Cordillera, which was probably connected to the SNSM as suggested by *Mora et al. (2017a),* and to the Western Cordillera.

4.5.5 Eocene onset of flat subduction

The notorious lower to middle Eocene angular unconformity that marks the top of Sequence 2 (San Cayetano) is the most important evidence of the final episode of activity of the Romeral Fault System and of a major shortening event in northern Colombia (**Figure 4.7** to **Figure 4.11**). This event also marks the end and fossilization of the San Jacinto forearc basin and the birth of a new basin of middle Eocene to Recent age (Lower Magdalena).

Several researchers have related this regional angular unconformity to the accretion of the San Jacinto terrane from the south, along the RFS (*Duque-Caro, 1979*; *Cediel et al., 2003*). An equally dramatic angular unconformity produced by a middle Eocene tectonic episode has been recognized in Colombia for many years (e.g. *Hubach, 1957*; *Forero, 1974*; *Duque-Caro, 1980*; *Villamil, 1999*; *Bayona et al., 2013*) and it has also been identified in reflection seismic data in surrounding basins such as the Cesar-Ranchería (*Mora and García, 2006*) and the Middle Magdalena Valley basin (MMV, *Gomez et al., 2005*). The Santa Marta-Bucaramanga Fault System, which is considered the northeastern boundary of the LMV against the Cesar-Ranchería basin, also experienced a middle Eocene tectonic episode as revealed by reflection seismic data (*Mora and García, 2006*).

Using apatite (U-Th)/He thermochronology, *Restrepo et al. (2009*) and *Villagómez et al. (2011b*) identified middle Eocene exhumation pulses in the northern CC (Antioqueño Plateau) and in the southern SNSM. However, while *Restrepo et al. (2009*) related the middle Eocene exhumation of the northern CC to a change in the rate of convergence between Nazca (Farallon) and South America, *Villagómez et al. (2011b*) relate it to underthrusting of the Caribbean plate beneath northern South America. Paleo-tectonic reconstructions (*Ross and Scotese, 1988*; *Müller et al., 1999; Pindell and Kennan, 2009*; *Kroehler et al., 2011*; *Boschman et al. 2014*; *Matthews et al. 2016*) show that between 56 and 45 Ma there was a major readjustment in the configuration of the South American, Caribbean and North American plates (**Figure 4.15**). The model by *Boschman et al. (2014),* in which there is a notorious decrease in both velocity and obliquity at ~ 48 Ma, correlates better with the identified lower to middle Eocene regional unconformity and with a regional shortening event, in agreement with the proposed major change in convergence velocity and obliquity between the Caribbean and South American plates (**Figure 4.16**). Though the model by *Matthews et al. (2016*) also shows a minor decrease in convergence velocity after 48 Ma, obliquity decreased earlier, at ~ 58 Ma. Hence, correlations with the middle Eocene unconformity and the proposed major tectonic readjustment are not as clear as with the model by *Boschman et al., (2014*).

Furthermore, the cessation of magmatism in northern Colombia would also be related to this plate tectonic readjustment, which probably took place between 56 and 45 Ma. Previous studies in the Guajira peninsula (Parashi intrusive, *Cardona et al., 2014*), in the SNSM (Santa Marta batholith, *Mejía et al., 2008*) and in the northern Central Cordillera (*ANH, 2011*) concluded that subduction-related magmatism in northwestern Colombia occurred only until early middle Eocene times (50-45 Ma, *Bayona et al., 2012*). Post-Eocene magmatism has been documented only in the central and southern Colombian Andes, where it is related to the subduction of the Nazca (Farallón) plate under western South America. It is then possible that arc magmatism ended due to an early to middle Eocene plate-tectonic readjustment, consisting of a reduction in both convergence velocity

and obliquity, and its expression in the stratigraphic record would be the lower to middle Eocene unconformity.

The lack of arc volcanism has been related to flat subduction of thickened and buoyant slabs (*Gutscher et al., 2000*; *Ramos and Folguera, 2009*; *Syracuse et al., 2016*; *Manea et al., 2017*). Flat-slab subduction of thick oceanic crust results in surface uplift and exhumation of forearc basin strata, and also inhibits subduction-related magmatism adjacent to the forearc basin (*Ridgway et al., 2012).* This seems to be the case of northwestern Colombia where the thick oceanic Caribbean plateau is currently being subducted under the South American plate, in an area where there has been no magmatism since early to middle Eocene times. Taking into account the present-day lithospheric and mantle geometry, as interpreted in **Figure 4.12**, we calculated that the onset of subduction of the Caribbean plate occurred in early to middle Eocene times, 56 to 43 Ma ago (**Table 4.2**). Interestingly, this calculated time of onset of subduction of the Caribbean plateau coincides with the time of plate tectonic readjustment between the Caribbean and the Americas (**Figure 4.16**), and with the estimated age of the lower to middle Eocene unconformity in the San Jacinto fold belt (planktonic foram zones P.9 to P.10, 50.4 to 45.8 Ma) and the time of cessation of magmatism in northern Colombia (50-45 Ma; *Bayona et al., 2012*). Though these calculations are very sensitive to slab angles, lengths and convergence rates, the slab length measurements by *Van Benthem et al. (2013*) are quite similar (900 km) and hence are the obtained ages of plateau subduction (**Table 4.2**). *Boschman et al. (2014*) also estimated 850 km of subduction beneath Colombia since 50 Ma from their tectonic reconstructions. According to this, the onset of the low-angle subduction of the Caribbean plateau would have occurred in early to middle Eocene times, and it was also then when the rough geodynamic configuration that we have today in the northwestern corner of South America was formed. It is thus probable that the middle Eocene uplift pulses of the CC and SNSM (*Restrepo et al., 2009*; *Villagómez et al., 2011b*) which produced unroofing on the order of 2 km in the northern CC and the widespread deposition of coarse-grained molasses in northern Colombia, are also related to the inception of flat subduction.

To summarize (**Figure 4.16**), a major lower to middle Eocene plate-tectonic readjustment, consisting of a notorious decrease in both convergence velocity and obliquity in lower to middle Eocene times, seems to be the most likely cause of: 1) the onset of flat-slab subduction in northwestern Colombia, 2) the cessation of magmatism in northern Colombia in the middle Eocene, 3) a major shortening event with the exhumation and partial erosion of the Upper Cretaceous to lower Eocene San Jacinto forearc basin, 4) the end of the tectonic activity of major Cretaceous fault systems such as Romeral and Palestina, and 5) the later onset of right-lateral strike-slip displacement along the newly formed Oca-El Pilar fault system (*Müller et al., 1999*; *Pindell and Kennan, 2009; Boschman et al., 2014*). The imprint of such tectonic readjustment in the stratigraphic record of the San Jacinto fold belt is the lower to middle Eocene unconformity, though the upper Eocene unconformity could also be related.

The previous interpretation implies that the onset of flat subduction, which we correlate with the cessation of arc magmatism, occurred at lower to middle Eocene times, when convergence slowed down and became more orthogonal. Though more perpendicular convergence could tend to favor subduction with arc magmatism, several studies suggest that convergence obliquity is not among the controlling parameters of flat subduction. According to *Espurt et al. (2008*), two main causes have been proposed to explain the formation of flat subduction zones in South America: 1) the fast movement of South America towards the trench in the hot spot reference frame, and 2) the subduction of buoyant anomalies such as oceanic plateaus. Both conditions are occurring in NW Colombia, thus supporting the proposed flat-slab subduction.

4.5.6 Middle to late Eocene renewed forearc sedimentation

After the lower to middle Eocene plate tectonic readjustment and the onset of flat subduction, the San Jacinto area experienced renewed forearc extension, subsidence and sedimentation which comprised coarse-grained clastics and shallow marine carbonates of Sequences 3 and 4 (Chengue and San Jacinto). In middle Eocene times, the RFS and the northern Palestina Fault System both

became inactive as seen in the cross-sections in **Figure 4.7**. Reflection seismic data (**Figure 4.10** and **Figure 4.11**) shows that the deposits of Sequence 3 and 4 are affected by SE-NW-trending faults which have similar orientation as those related to Sequence 2 (San Cayetano), and therefore they would be older inherited features which were reactivated. Terrigenous rocks were classified as lithic arkoses to litharenites and were related to the dissected arc, transitional arc and lithic recycled orogen provenance terranes of *Dickinson (1985*).

Our U-Pb geochronology and Hf isotope geochemistry results show the same Late Cretaceous and Permo-Triassic peaks as seen in samples from the sequence below (San Cayetano, **Figure 4.5**). Additionally, there seems to be a reduction in Proterozoic and Paleozoic provenance for these samples, suggesting less erosion of distant old massifs related and more erosion of younger basement massifs, though recycling of zircons is also a possibility. Considering that the SJFB had already been accreted by late Eocene times, the predominance of Upper Cretaceous and Permo-Triassic terranes suggests that sediment supply was mostly coming from the northern CC and SNSM in the SE and NE.

4.5.7 The middle to late Eocene unconformity

The contact between Sequences 3 and 4 (Chengue and San Jacinto) is also an unconformity of middle to late Eocene age (35-40 Ma) which has been recognized in the SJFB (*Duque-Caro, 1984*; *1991*; *Guzman, 2007*) as the expression of a third shortening phase, related to the plate tectonic readjustment and to the onset of flat slab subduction. *Van der Lelij et al (2016*) suggested that the Santa Marta-Bucaramanga fault was active at ~40 Ma, that rapid exhumation at that time is well documented along the western margin of South America and that such widespread contractional phase could be related to an episode of accelerated convergence of ~15 cm/yr, between the South American margin and the Farallón plate. However, much more data and studies are required to understand the significance of this unconformity and its possible relationship with major plate tectonic processes.

4.5.8 Late Eocene to Oligocene

Sequence 4 (San Jacinto) was possibly also deposited in a shallow subduction forearc setting, in late Eocene to early Oligocene times. It comprises shallow marine carbonate facies in the central and southern SJFB and siliciclastic deposits (fan deltas) in the central-eastern part. As shown by seismic data, these deposits are affected by the same family of SE-NW-trending extensional faults that affects Sequences 2 and 3.

Cardona et al. (2012) stated that the conglomerates deposited after the middle Eocene tectonism contain less igneous and metamorphic rock fragments and more sedimentary rock fragments, quartz and stable heavy minerals compared to the pre-middle Eocene conglomerates of Sequence 2, suggesting a depletion of the more proximal volcanic sources. Petrographic analyses (*Ecopetrol/ICP, 2014*) revealed that the origin of siliciclastic samples of this sequence is related to transitional to quartzose recycled orogens, with few samples related to a magmatic arc. Though such data suggest less supply from magmatic arc sources, our new U-Pb geochronology and Hf isotope geochemistry results reveal that the upper Eocene to lower Oligocene sediments in the SamanEst-1 well were mainly sourced from Upper Cretaceous (Coniacian-Maastrichtian) plutons with a Hf isotopic composition very close to that of the Bonga pluton (*Mora et al., 2017a*). The apparent contradiction between petrography analyses suggesting recycled orogen provenance versus geochronology suggesting magmatic arc provenance, could also be related to zircon recycling from older sedimentary units. However, the secondary magmatic arc signature from both petrography and geochronology still suggests mixed source areas for the northern SJFB such as the present-day Magangué-Cicuco high and the northern CC, located towards the SSE (**Figure 4.3**).

Figure 4.16 very clearly shows that the Caribbean-NW South America convergent margin became relatively stable since Oligocene times, exhibiting low convergence velocities and

obliquities. We relate this to the evolution of the margin from a highly oblique convergent margin, possibly exhibiting subduction erosion (*Clift and Vannucchi, 2004*) in Late Cretaceous to Eocene times, to a more orthogonal convergent margin, exhibiting subduction accretion since early Miocene times, when the accretionary prism probably started forming.

4.6 Conclusions

In this study we have linked the Late Cretaceous to Eocene tectono-stratigraphy of the San Jacinto fold belt of NW Colombia with the plate tectonic evolution of northwestern South America, which experienced Caribbean plateau collision and flat subduction. Using a regional geology and geophysics database, we were able to relate the deposition of four unconformity-bounded forearc basin sequences to specific collision/subduction stages and to relate their bounding unconformities to major tectonic episodes. The Upper Cretaceous Cansona sequence (Sequence 1) was deposited in a marine forearc environment in which a "normal" thickness Caribbean plate was being subducted beneath northwestern South America, producing contemporaneous magmatism in the present-day northern Central Cordillera and Lower Magdalena Valley basin. Coeval strike-slip faulting by the Romeral wrench fault system accommodated right-lateral displacement due to strongly oblique convergence. In latest Cretaceous to early Paleocene times, the Caribbean oceanic plateau collided with South America causing a major shortening event and marking a change to a turbiditic marine sedimentation with abundant terrestrial input, that characterizes the upper Paleocene to lower Eocene San Cayetano sequence (Sequence 2). This sequence was also deposited in a forearc setting with an active volcanic arc that probably represents the final melting stage of the previously subducted "normal" thickness Caribbean slab. A lower to middle Eocene angular unconformity at the top of the San Cayetano sequence, a second major shortening event, the termination of the activity of the Romeral Fault system and the cessation of arc magmatism are interpreted to indicate the onset of low-angle subduction of the thick and buoyant Caribbean oceanic plateau beneath South America, which occurred between 56 and 43 Ma. Onset of low-angle subduction was probably caused by a major change in plate convergence angle and velocity, as suggested by paleo-tectonic reconstructions. As low-angle subduction was gradually established, coarse-grained clastics and carbonates of the Chengue sequence (Sequence 3) were deposited in the forearc of a newly formed subduction complex. A middle to late Eocene unconformity also related to a contractional event, separates the Chengue from the San Jacinto sequence (Sequence 4), which comprises similar types of terrigenous and calcareous deposits. Detrital zircon U-Pb geochronology and Hf-isotope geochemistry suggest that the upper Paleocene to upper Eocene San Cayetano and Chengue/San Jacinto Sequences were mostly sourced from Upper Cretaceous oceanic and continental-affinity magmatic arcs and from Permo-Triassic igneous-metamorphic basement blocks. Low-angle subduction of the Caribbean plateau has continued to the present and appears to be the main cause of the amagmatic post-Eocene deposition. Our interpreted plate-tectonic configuration of northern Colombia implies the existence of a tear or STEP fault in the Caribbean plate, located towards the western end of the Oca-San Sebastián-El Pilar fault system.

5 Controls on forearc basin formation and evolution: Insights from Oligocene to Recent tectono-stratigraphy of the Lower Magdalena Valley basin of northwest Colombia

This chapter is a reformatted version of a paper in internal revision. The supplementary material has been placed in *Appendix C*.

Citation: Mora, J.A., Oncken, O., Le Breton, E., Mora, A.R., Veloza, G., Velez, V. and De Freitas, M., (in preparation). Controls on forearc basin formation and evolution: Insights from Oligocene to Recent tectono-stratigraphy of the Lower Magdalena Valley basin of northwest Colombia. It was submitted to Marine and Petroleum Geology.

Abstract

Mechanisms of forearc basin formation and evolution remain poorly understood at a global scale, though recent studies emphasize the dominant role of sediment flux at the trench on basin evolution. The convergent margin of northwest Colombia, where South America and the Caribbean have been interacting since Late Cretaceous times and where the San Jacinto and Lower Magdalena Valley forearc basins are located, offers a unique opportunity to study such mechanisms. A recent study in San Jacinto linked Upper Cretaceous to Eocene forearc sequences with changes in subduction parameters. By contrast, formation of the Lower Magdalena amagmatic forearc basin occurred in a stable setting from the Oligocene to the present, characterized by the slow and nearly orthogonal, low-angle subduction of the Caribbean plateau. We use a regional database to reconstruct the subsidence, extension, sedimentation and paleo-geographic history of the Lower Magdalena forearc basin, and to propose possible mechanisms controlling its evolution, in the absence of major changes in plate kinematics and in a flat-slab subduction setting. We show that after the collapse of a pre-Oligocene magmatic arc, late Oligocene to early Miocene fault-controlled subsidence allowed initial basin fill at relatively low sedimentation rates. Extensional reactivation of inherited, pre-Oligocene basement faults was crucial for the tectonic segmentation of the basin with the formation of its two depocenters (Plato and San Jorge). Oligocene to early Miocene uplift of Andean terranes made possible the connection of the Lower and Middle Magdalena valleys, and the formation of the important Colombian drainage system (Magdalena River system). The proto-Magdalena river in the north and the proto-Cauca river in the south both started delivering high volumes of sediments in middle Miocene times, as fault-controlled subsidence was gradually replaced by sagging due to increased sedimentary load. Such increase in sedimentation delivered great volumes of sediments to the trench, causing the formation of an accretionary prism farther west of San Jacinto. This probably weakened the plate interface and caused underplating, with the development of forearc highs in the San Jacinto area. A stronger backstop under the Lower Magdalena explains shortening in the forearc high and accretionary wedge areas to the W, while the Lower Magdalena remained essentially unaffected. Tectonic segmentation of the basin with the formation its two depocenters (Plato and San Jorge), was due to the influence of inherited basement structures and to flat-slab subduction processes. Our results highlight the fundamental role of sediment flux, of the inherited basement structure and of flat-slab subduction on the evolution of forearc basins such as the Lower Magdalena.

Keywords: Forearc basin, flat-slab subduction, tectono-stratigraphy, Lower Magdalena, Caribbean, subsidence.

5.1 Introduction

The privileged location of forearc basins makes them suitable for providing unique insights into subduction zone dynamics. These basins typically develop along continental margins and island arcs where oceanic plates are subducting beneath the overriding crust (*Noda, 2016*). While initial concepts of forearc basins were first developed in the 70s (*Dickinson, 1973, 1974*; *Karig, 1974*; *Seely et al., 1974*; *Karig and Sharman, 1975*), *Ridgway et al. (2012*) discussed the modification of forearc basins by flat-slab subduction and concluded that flat-slab subduction processes substantially modified the tectonic configuration of the upper plate, producing sedimentary basins that do not easily fit into the standard magmatic arc-forearc basin-accretionary prism template. *Noda (2016*) considered that initial concepts of forearc basins were basically related to growth of accretionary prisms, though these basins also form along tectonically erosive margins. Accordingly, *Noda (2016*) proposed a new classification scheme for forearc basins from the viewpoints of material transfer between the two plates (accretionary or non-accretionary) and the long-term strain field in the basin (compressional or extensional).

Previous research shows that mechanisms of forearc basin formation remain poorly understood, including subsidence mechanisms (*Fuller et al., 2006*; *Noda, 2016*). *Ingersoll (1988, 2012*) stated that the factors controlling forearc geometry include 1) the initial setting, 2) sediment thickness on subducting plate, 3) rate of sediment supply to trench, 4) rate of sediment supply to forearc area, 5) rate and orientation of subduction, and 6) time since initiation of subduction. According to *Dickinson and Seely (1979*), a prime factor governing forearc evolution is the quantity of sediment delivered to the forearc region, and large-scale lateral accretion can occur only if there are large quantities of trench-fill, abyssal-plain and/or slope sediments. *Noda (2016*) states that an increase or decrease of the sediment flux may change the type, geometry and deformation style of the forearc basin. Furthermore, the same author also concludes that changes of the sediment flux and configuration of the subducting plate (i.e. direction, dip, velocity and roughness) can affect the condition of accretion or erosion in the outer wedge, as well as the style of deposition in the forearc basin. Therefore, it is clear from previous studies that sediment flux plays a fundamental role on forearc basin evolution.

The Oligocene to Recent, Lower Magdalena Valley basin (LMV) of northwestern Colombia is located in an area where the Caribbean and South American plates, as well as the Chocó-Panamá block, have been interacting since the Cretaceous (**Figure 5.1**). The LMV was previously classified as a forearc basin (*Mantilla et al., 2009*; *Bernal et al., 2015a*) in spite of lacking an active magmatic arc. The San Jacinto fold belt, located to the W of the LMV and adjacent to it, has also been considered an older (Cretaceous to Eocene) forearc basin (*Duque-Caro, 1979*; *1991*) which was later inverted and deformed. *Mora et al. (2017b*) reconstructed the formation and evolution of San Jacinto and linked Upper Cretaceous to Eocene forearc sequences with major changes in subduction parameters, such as plate convergence velocity and obliquity. The origin and evolution of the LMV have been recently related to flat-slab subduction of the Caribbean oceanic plateau beneath South America, since Oligocene times (*Mora et al., 2017b*).

In this study, we used a regional reflection-seismic and well database to reconstruct the sedimentary infill and tectono-stratigraphic evolution of the LMV, including estimates of subsidence (total vs tectonic) and extension, and timing of kinematic regimes and shortening/extension events. Through paleo-tectonic reconstructions, we studied the subduction parameters (convergence velocity and obliquity) since Oligocene times and compared the plate tectonic evolution with the tectono-stratigraphic basin history. Our results show that the formation and evolution of the LMV were controlled by other mechanisms, apart from changes in tectonic plate convergence. The objective of this contribution is therefore to propose mechanisms that possibly controlled the evolution of the Lower Magdalena forearc basin. Our results suggest a linkage between a dramatic increase in sediment supply to the LMV at ~17 Ma, the connection between the Middle and Lower Magdalena valleys and the formation of the proto-Magdalena River drainage system. Such a connection was possible due to the Oligocene to early Miocene uplift of

Andean terranes, as suggested by previous studies (*Hoorn et al., 2010*; *Caballero et al., 2013a*; *Reyes-Harker et al., 2015*; *Anderson et al., 2016*). The topographic growth of the Colombian Eastern Cordillera, the Santander massif and the Perijá Ridge forced the isolation of the Magdalena, Orinoco and Amazon drainage systems and provided huge amounts of sediments into these river systems (*Caballero et al., 2013a*; *Anderson et al., 2016*). We will also discuss the fundamental role of increased sediment supply to forearc and trench areas on the evolution of the LMV, and the influence of inherited basement structures on tectonic segmentation and the formation of its two depocenters.

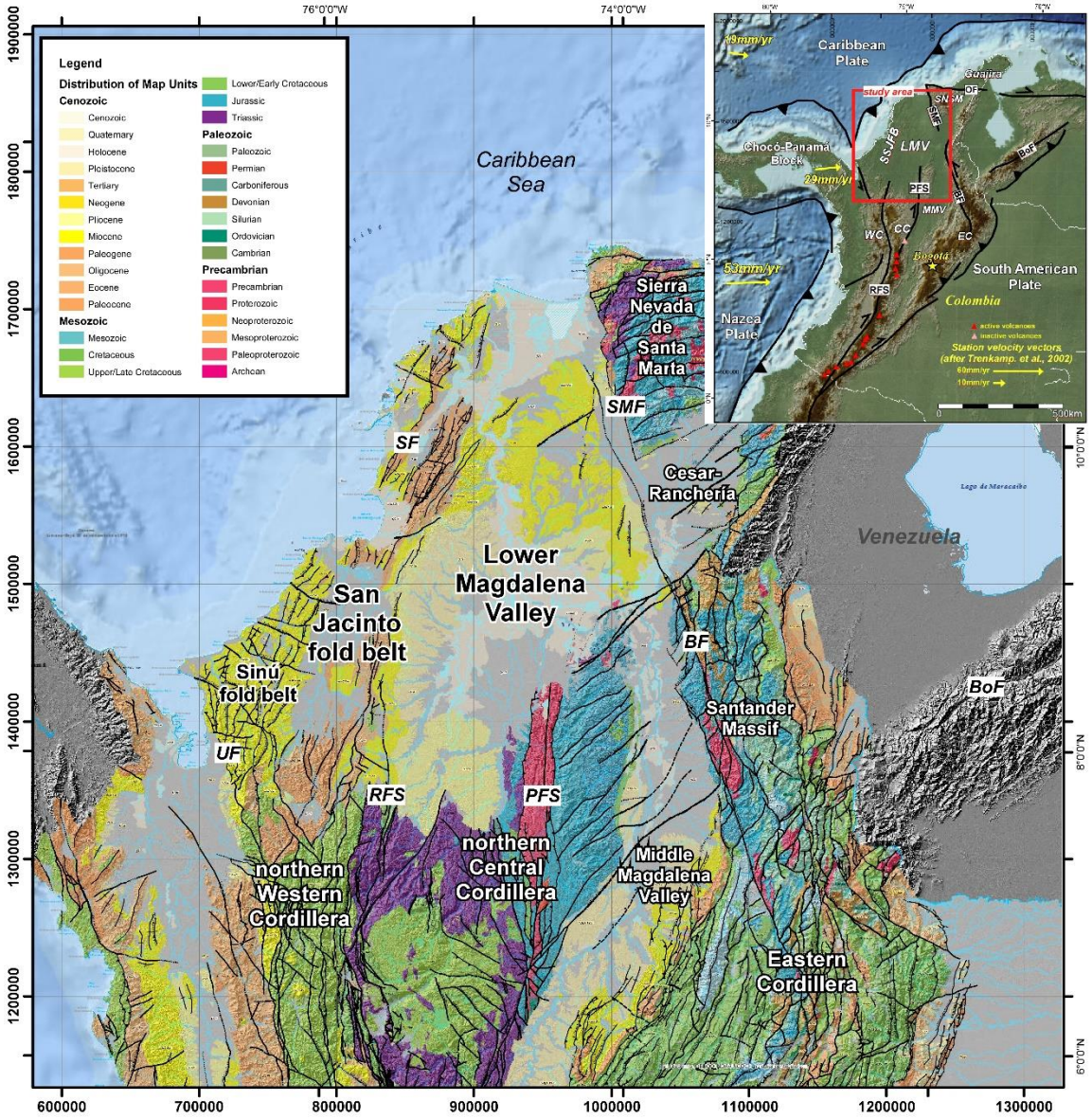

Figure 5.1. Geological map of the Lower Magdalena and San Jacinto fold belt, highlighting major structural and morphologic features. RFS: Romeral Fault System; PFS: Palestina Fault System; SF: Sinu Fault; BF: Bucaramanga Fault; SMF: Santa Marta Fault; OF: Oca Fault; UF: Uramita Fault; BoF: Bocono Fault. Geology after *Gomez et al. (2015*). Inset, tectonic map of northwestern South America with topography and bathymetry, showing the location of the Lower Magdalena Valley basin (LMV), the Sinú-San Jacinto fold belt (SSJFB), and the active volcanoes. Present-day tectonic plate motions are shown in yellow (after *Trenkamp et al., 2002*). WC: Western Cordillera; CC: Central Cordillera; EC: Eastern Cordillera; RFS: Romeral Fault System; PFS: Palestina Fault System; BF: Bucaramanga Fault; SMF: Santa Marta Fault; OF: Oca Fault; BoF: Bocono Fault.

5.2 Geological Framework

The LMV of northwestern Colombia is located in an area in which the Caribbean oceanic plate, including the Chocó-Panamá block, and the South American continental plate have been interacting throughout the Cenozoic (**Figure 5.1**). It has long been long recognized from GPS data (e.g. *Müller et al., 1999*; *Trenkamp et al., 2002*) that NW South America and the Caribbean have been converging in a nearly orthogonal fashion since Oligocene times, and that they continue to do so today (*Symithe et al., 2015*). Furthermore, recent geophysical studies (*Mantilla et al., 2009*; *Bernal et al., 2015a, b*) have provided new and more robust evidence mainly from gravity modeling and seismic tomography, supporting a flat-subduction. According to this and in spite of lacking a magmatic arc, the basin has been interpreted as making part of a subduction complex (*Mantilla et al., 2009)* which includes an accretionary prism (Sinú) and a forearc high (San Jacinto) to the W.

The LMV is a lozenge-shaped basin, covering an area of 42,000 km^2 and located between two major basement terranes, the northern Central Cordillera (CC) in the S and SE and the Sierra Nevada de Santa Marta (SNSM) in the NE (**Figure 5.1**). The Santa Marta left-lateral, strike-slip fault system is separating the northeastern part of the basin from the SNSM, while the northern extension of the Romeral Fault System (RFS) is separating the Lower Magdalena from the San Jacinto fold belt (SJFB) to the west. Pre-Oligocene sedimentary units are exposed in the SJFB, which has been considered the northward extension of the Western Cordillera of Colombia (*Barrero et al., 1969*; *Duque-Caro, 1979*; *Cediel et al., 2003*) and has been related to an oceanic-type basement. The RFS, which is also considered to continue to the north to form the western boundary of the LMV, appears to be separating the oceanic to transitional basement under the belt from the felsic continental basement of the South American crust which floors the LMV in the east (*Duque-Caro, 1979, Flinch, 2003*; *Mora et al., 2017a*). In the SJFB, located west of the RFS, there are Upper Cretaceous to Eocene sedimentary units that are not preserved in the LMV to the east (*Duque-Caro, 1979; 1984*; *Mora et al., 2017b*). By contrast, Oligocene to Recent units that have been mostly eroded in the SJFB, are well preserved in the LMV and will be the focus of the tectono-stratigraphic analysis performed in this study (**Figure 5.2**).

5.2.1 The Basement of the LMV

The basement under the LMV is considered to be the extension of the basement terranes that crop out in the northern CC and therefore consists of a core of Permo-Triassic metamorphic and igneous rocks, which were intruded by Upper Cretaceous granitoids (*Montes et al., 2010*; *Mora et al., 2017a*). However, the existence of an oceanic affinity terrane in the basement of the western LMV was recently proposed, based on Hf isotope geochemistry of an Upper Cretaceous pluton (Bonga pluton, *Mora et al., 2017a*). In terms of structural fabrics, the basement of the LMV comprises extensional faults with two predominant orientations, a main SE-NW trend in the southwestern half of the basin and a secondary SW-NE trend in the northeastern part (*Mora et al., 2017a*). Those structures were formed by several mechanisms including the Romeral and Palestina strike-slip movement, Jurassic rifting and Late Cretaceous to Eocene forearc extension due to oblique convergence (*Mora et al., 2017a*). The extensional reactivation of the pre-existing basement fabric was crucial for the subsidence and sedimentation history of the LMV basin.

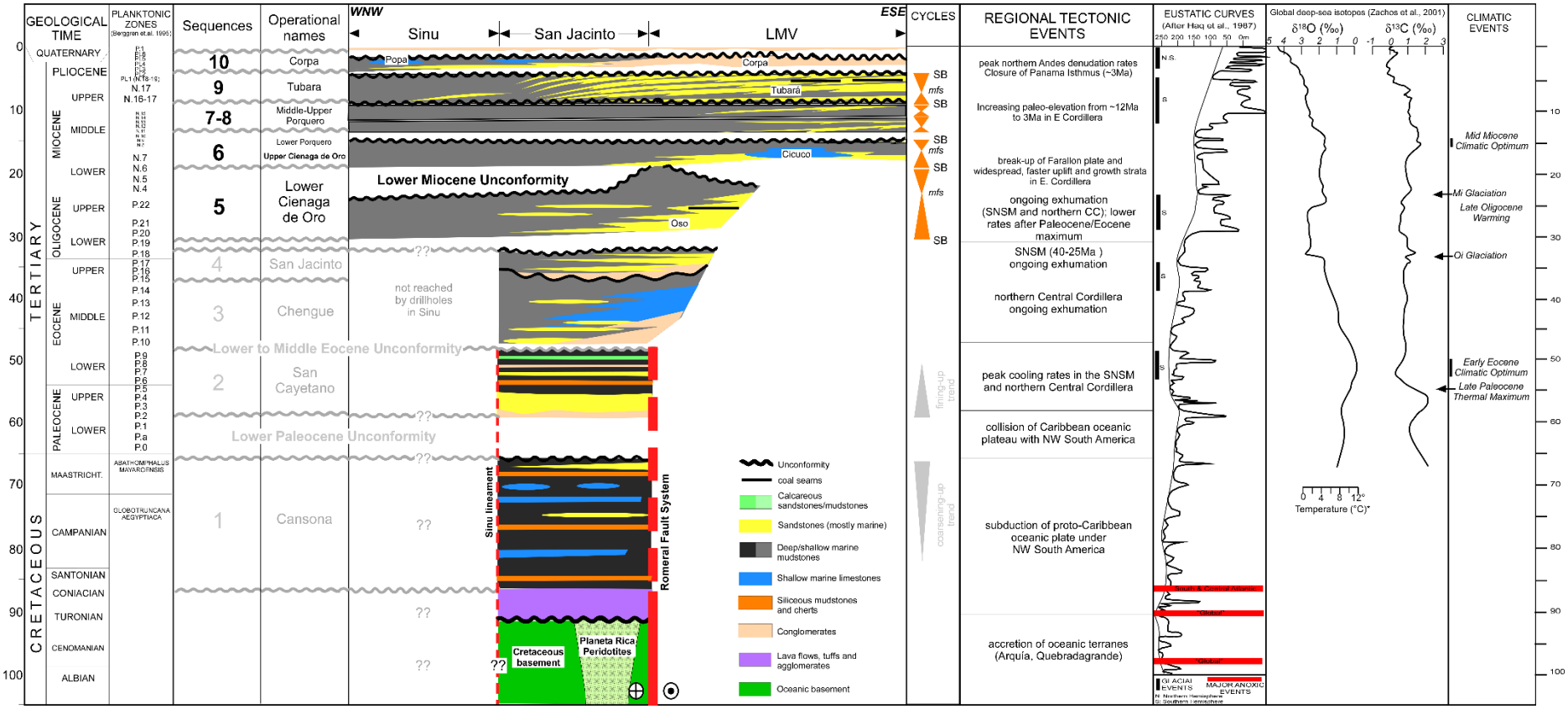

Figure 5.2. WNW-ESE-trending chronostratigraphic chart of the Sinú, San Jacinto and Lower Magdalena areas, based on different sources (*Hocol, 1993*; *ICP, 2000*; *Guzman, 2007*) and adjusted with our recent analyses of well and outcrop samples. Biostratigraphy is based on numerous papers and industry reports by *Duque-Caro (1979, 1984*, *1991*, *2000, 2001*, *2011a to 2014*), tectonic events are after *Villagómez et al. (2011a,b*), *Parra et al. (2012*), *Saylor et al. (2012*), *Mora et al. (2013a*), *Caballero et al. (2013a, b*), *Mora et al. (2015*), *De La Parra et al. (2015*), while the eustatic curves are from *Haq et al. (1987*) and the climatic events from *Zachos et al. (2001*).

5.2.2 Upper Cretaceous to Lower Oligocene units in the SJFB

The SJFB records the existence of a Late Cretaceous to Early Eocene forearc basin, which was inverted in early to middle Eocene times and was then covered and sealed by middle Eocene to lower Oligocene clastics (**Figure 5.2** and *Mora et al., 2017b*). These authors divided the sedimentary succession in the SJFB into four tectono-stratigraphic sequences, bounded by regional unconformities, which are related to major tectonic events. The two oldest Upper Cretaceous to lower Eocene sequences (Sequence 1, Cansona and Sequence 2, San Cayetano) are preserved mainly to the west of the RFS, while the younger middle Eocene to lower Oligocene sequences (3 and 4, Chengue and San Jacinto) sealed the RFS as they extended farther to the east, into the western LMV.

5.2.3 Upper Oligocene to Recent units in the LMV

The Oligocene to Recent stratigraphic succession in the basin has been mostly studied in drill holes and outcrops located in the western part, towards the SJFB (**Figure 5.1**). It comprises a mainly fine-grained, marine succession in which several unconformities have been identified, allowing its separation into different stratigraphic sequences (**Figure 5.2**). According to *Montes et al. (2010*), the succession is made up, from bottom to top of longitudinal bars, laterally adjacent to delta plain deposits, sheltered bays or lagoons, near a muddy delta mouth, and tidal flats and tidal channel deposits. The stratigraphy of the area has been studied previously by several researchers (*Duque-Caro, 1972; 1979; 1984*; 1991; *Duque et al., 1996*; *ICP, 2000*; *Guzman et al., 2004*; *Guzman, 2007*: *Bermudez et al., 2016*), but the abundance of lithostratigraphic names has hampered a better understanding of the stratigraphic evolution of the area. For that reason, in this study we based our tectono-stratigraphic framework on the available biostratigraphic data, tied to the reflection-seismic and drillhole data. We follow the sequence numbering proposed by *Mora et al. (2017b*) and also propose correlations of our sequences with the most widely used lithostratigraphic and operational names (**Figure 5.2**).

5.3 Methodology

5.3.1 Construction of the tectono-stratigraphic framework and paleogeographic maps

We used a regional database provided by Hocol S.A. for the construction of the tectono-stratigraphic framework of the LMV (**Figure 5.3**), and followed the typical oil and gas industry workflow for seismic interpretation and mapping. The main interpreted horizons are the top of the acoustic basement, the top of the upper Oligocene, the lower Miocene unconformity, the near top of the N.7 planktonic foraminifera zone (lower part of Sequence 6), the upper Miocene unconformity, the middle Pliocene unconformity, corresponding to the base of Sequence 10 (**Figure 5.4**) and an intra-Sequence 10 reflector which doesn't appear in the area of the B-1 well. The integration of seismic and well data with the published outcrop studies from the eastern SJFB allowed the construction of paleogeographic maps for selected time windows. We integrated the U-Pb geochronology data from *Montes et al. (2015*) to further constrain the Oligocene to Middle Miocene paleogeography of the area. Structural mapping was complemented by the detailed analysis of growth strata in order to define the timing of the activity of the major faults and thus, to define the Oligocene to Recent kinematic history for the basin.

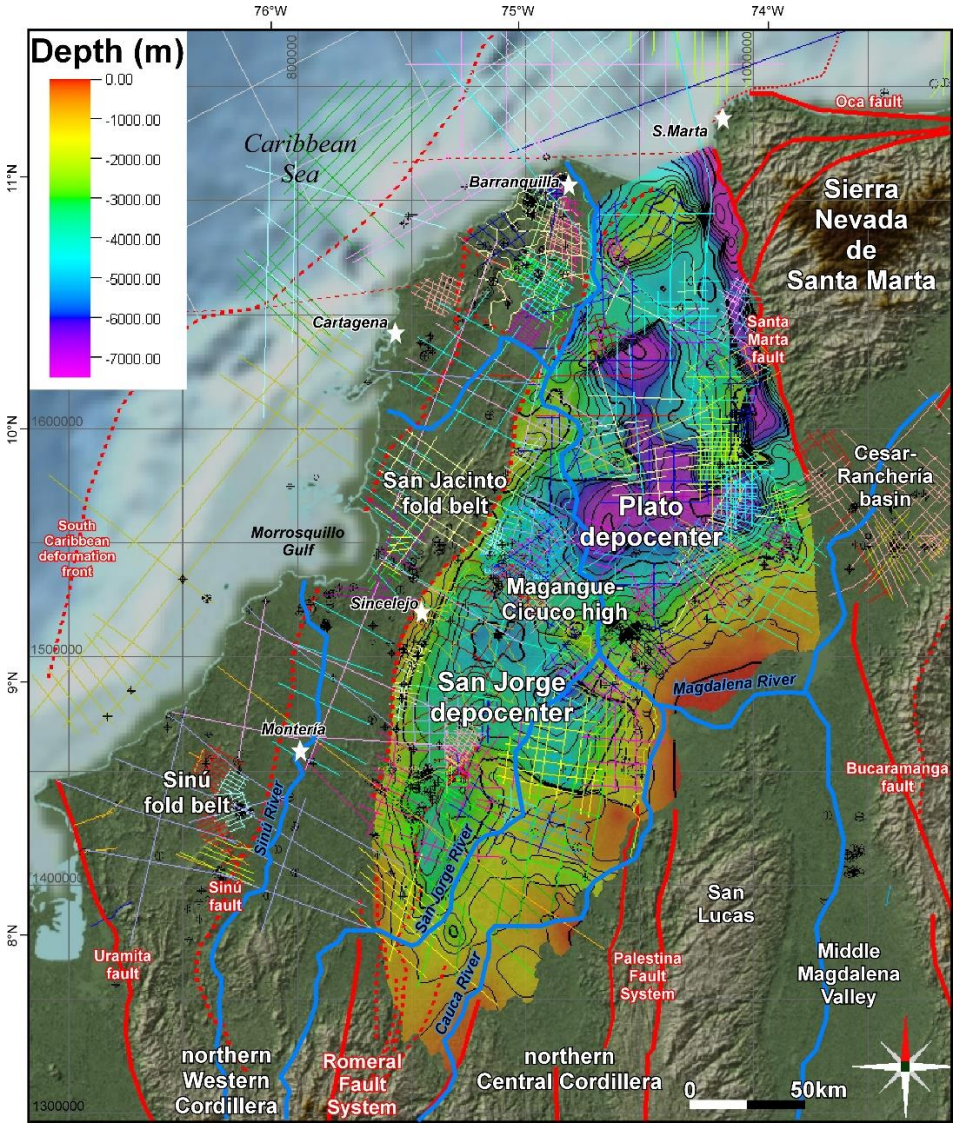

Figure 5.3. Reflection seismic and well database used for this study, provided by Hocol S.A. Colors of seismic lines represent different seismic surveys. Topography and main drainages are also shown, as well as the structural map in depth of the basement under the LMV (after *Mora et al. 2017a*).

5.3.2 Subsidence history, extension and shortening in the LMV

We carried out geohistory and subsidence analyses (*Watts and Ryan, 1976*; *Steckler and Watts, 1978*; *Sclater and Christie, 1980*; *Allen and Allen, 2005*) using available well data, and constructed a regional structural cross section along the LMV, perpendicular to the main structural fabric, in order to obtain extension estimates. We also calculated the crustal thickness without sedimentary fill, as an alternative approach to calculate the amount of extension of the crust beneath the LMV. Tectonic plate convergence velocities and obliquities since the Oligocene (**Figure 5.5**) were measured for correlation with subsidence patterns, sedimentation rates and the main regional Andean tectonic events. We also used burial history charts from well data to study and illustrate the different subsidence and uplift (shortening) episodes in the LMV (**Figure C 1**).

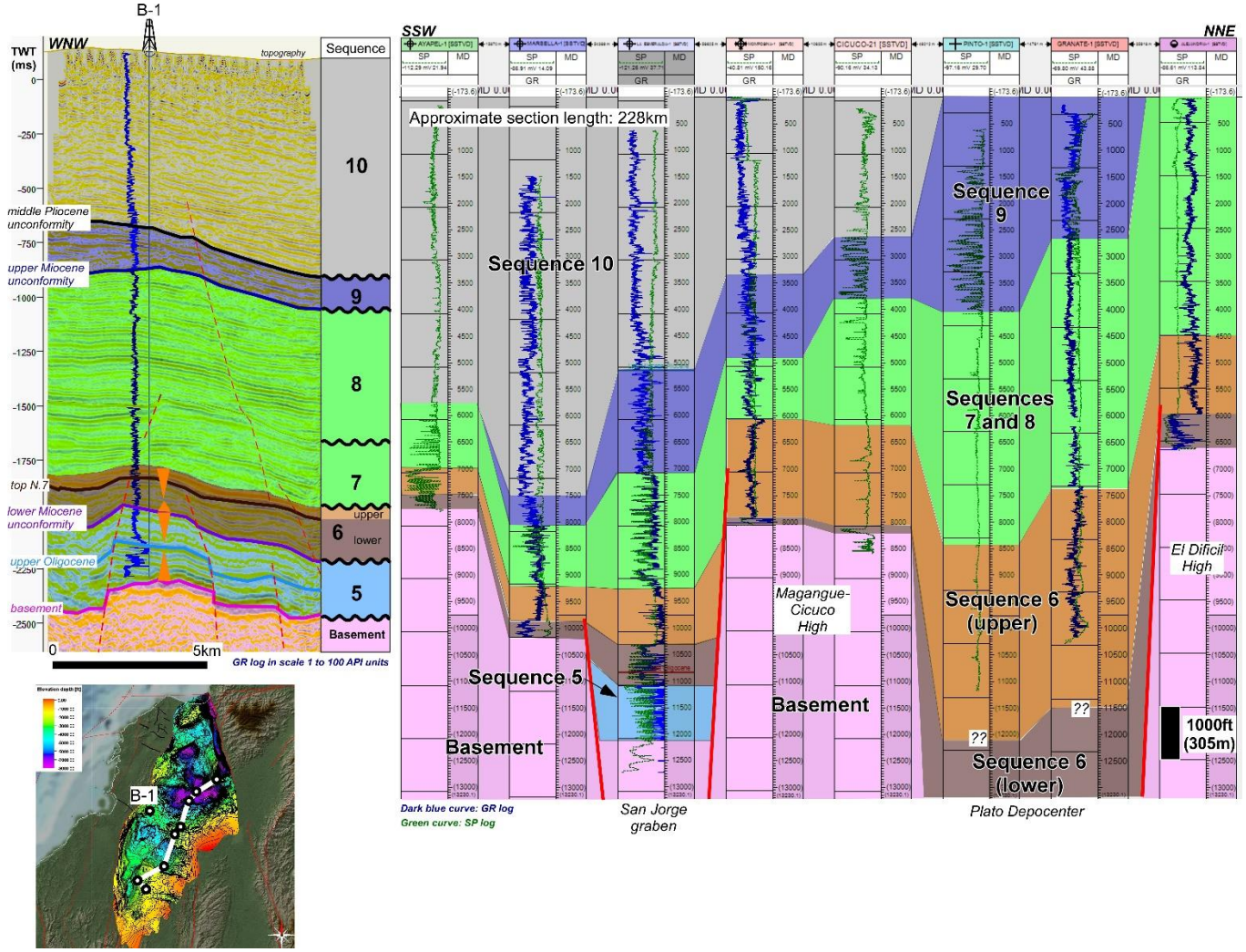

Figure 5.4. Example of a well-seismic tie (left) and a regional, NNE-SSW-trending well correlation (right) in the LMV. The left panel shows the tie of the B-1 well with the closest seismic line, displaying the interpreted horizons and the main stratigraphic sequences; the regional well correlation in the right panel shows the electrical facies of the studied sequences and the thickness variations. Main faults are shown as red lines.

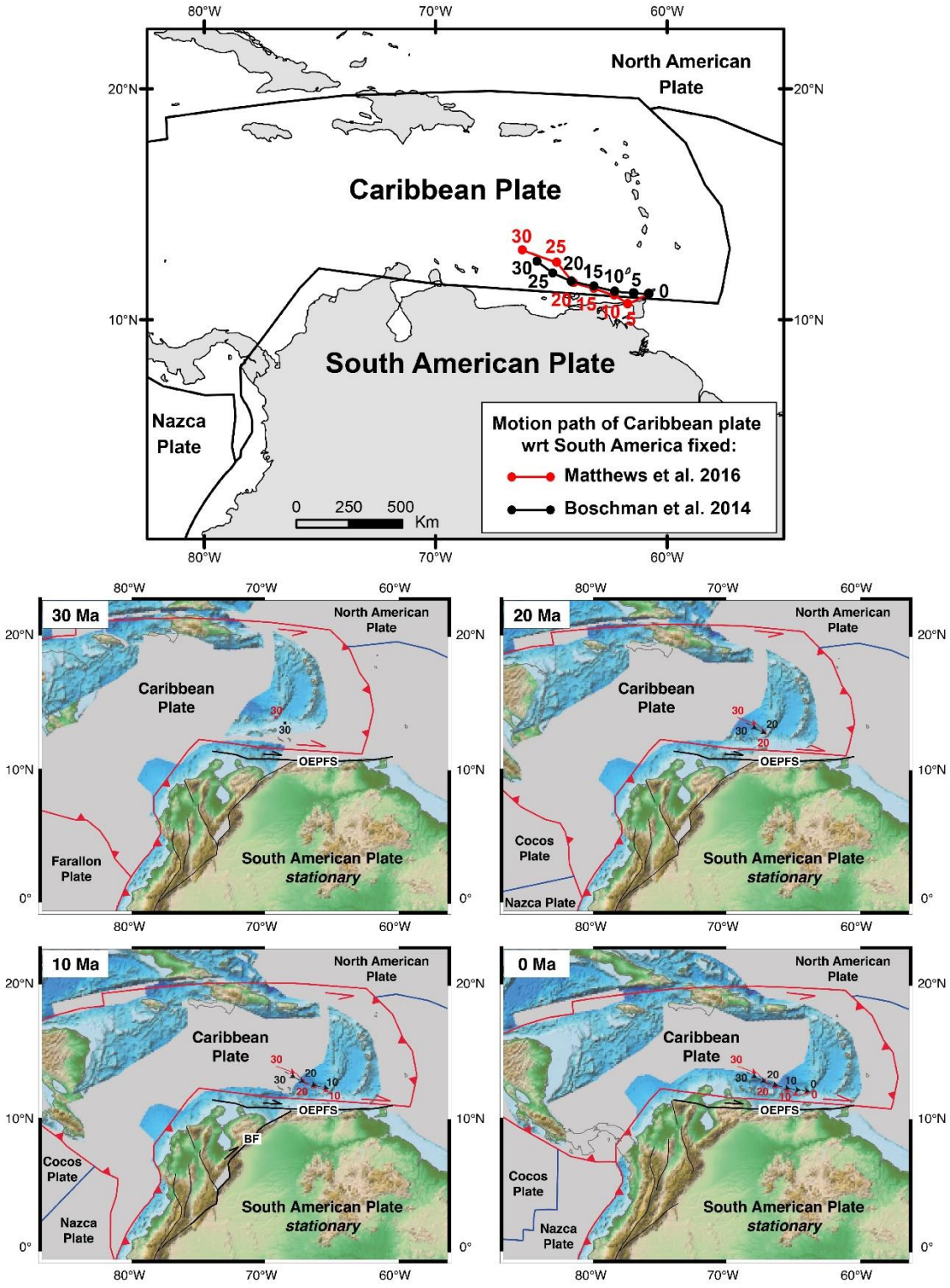

Figure 5.5. Paleo-tectonic reconstructions at 30, 20, 10 and 0 Ma, illustrating the displacement of the Caribbean plate relative to fixed South America. The displacement vectors of the Caribbean plate relative to South America are shown in red arrows according to the model of *Matthews et al. (2016*, GPlates database) and in black dashed arrows according to *Boschman et al. (2014*). The plate boundaries (spreading ridges in blue, subduction and transform zones in red) and continent polygons are from *Matthews et al. (2016*). The main fault zones of NW South America are labelled and drawn in thick black lines when active. This reconstruction incorporates the "escape" of the northern Andes block along the Bocono Fault (BF) in both models. The overall displacement of the Caribbean plate relative to a stationary South American plate since Oligocene times is relatively stable and does not show major changes in convergence velocity nor in obliquity. See the text for further discussion. OEPFS:Oca-El Pilar-SanSebastian Fault system.

Sequence	Lithostratigraphic and operational names	Planktonic foram zones (Berggren et al., 1995; Blow, 1969)	Age	Structural and thickness maps	Description	Kinematics	Subsidence and sedimentation
10	Corpa (Sincelejo,Betulia, Popa)	Pl.3 to Pl.6?	upper Pliocene to lower Pleistocene	Two main packages preserved in the southern LMV, the lower one is a SSW-NNE-trending elliptic depocenter and the upper one is a round depocenter on top of the San Jorge graben; total thickness close to 3 km.	In the southern LMV, corresponds to fluvio-deltaic, low-angle clinoforms prograding from S to N (paleo-Cauca deposits); in the NW SJFB, carbonates are preserved (Popa Fm.).	After Corpa deposition, NNW-SSE and SW-NE-trending extensional faults in Plato are inverted and older units are intensely eroded; onlap of the upper Corpa to the W indicates onset of recent uplift of the San Jacinto fold belt (~1.7 Ma?)	Subsidence due to sagging, much higher subsidence in San Jorge; high sedimentation rates (~500 m/Ma)
unconformity			*middle Pliocene*				
9	Tubara (Cerrito, Zambrano)	N.17 (M.14) to Pl.2	upper Miocene to lower Pliocene	Overfilled the Plato depocenter and was highly eroded, first in the south and later in the north, where preserved thicknesses are >2 km (Plato);	Sigmoidal, shelf margin clinoforms represent increased progradation to the NNW, of continental to shallow marine deposits of the proto-Magdalena river in the north (Plato)	After Tubara deposition, NW-SE and SW-NE-trending extensional faults in San Jorge are inverted and older units are partially eroded	Subsidence due to sagging, higher subsidence in Plato until depocenter is overfilled; low sedimentation rates (<150 m/Ma, due to partial erosion)
unconformity		*absence of N.15 to N.16 (M.8 to M.9)*	*middle to upper Miocene*				
7 and 8	Middle-Upper Porquero (Mandatu, Hibacharo, Perdices, Jesus del Monte)	N.12 to N.16 (M.9-M.13)	middle to upper Miocene	Highly variable thickness due to variable preservation/erosion	Mostly fine-grained, thick deposits preserved mainly in depocenters	Less fault control, Algarrobo strike-slip fault and El Dificil fault active; local paleo-highs in San Jacinto (NW-SE contraction)	Subsidence due to sagging but minor fault control, higher subsidence in Plato; low sedimentation rates (<150 m/Ma, due to local, partial erosion)
unconformity		*absence of N.11 to N.12 (M.8 to M.9)*	*Middle Miocene*				
6	Upper Cienaga de Oro and Lower Porquero (Alférez)	N.7 to N.11 (M.4-M.8)	lower to middle Miocene	More widespread deposition focused also in topographic lows; average thickness is 400-600 m (1200-2000 ft)	Lower thin part is transgressive and onlaps the basement to the SE, while thicker upper part is progradational; Low areas were filled with clastic marine deposits while paleohighs were covered by carbonates	Active WNW-ESE-trending (Mojana, Sucre, Apure South) and SW-NE-trending (Pivijay, Pijiño, El Dificil South) extensional faults	Fault-controlled subsidence which tends to decrease with time; much higher sedimentation rates (60 to > 300 m/Ma)
unconformity		*absence of N.4 to N.6 (M.1 to M.3)*	*lower Miocene*				
5	Lower Cienaga de Oro (Carmen)	P.22 to N.6 (M.3)	lower Oligocene to lower Miocene	Gradually filled paleo-topographic basement lows from WNW to ESE; found at >3.5 km in San Jorge graben and at >5 km in Plato; thickest in the W towards the SJFB where >1.5 km are preserved in local depocenters	Lower part shows an onlap pattern to the SE; interpreted as a retrogradational, transgressive package with a fining and deepening upwards pattern; transition from basal sandy, shallow marine facies to muddy, deeper marine facies. Upper muddy part has been mostly eroded	Active WNW-ESE-trending (Mojana, Sucre, Apure South) and SW-NE-trending (Pivijay, Pijiño, El Dificil South) extensional faults	Fault-controlled subsidence, low sedimentation rates (<60 m/Ma) but would be higher due to erosion of upper part of the sequence

Table 5.1. Main characteristics of the studied Oligocene to Quaternary tectono-stratigraphic sequences in the LMV. More information, detailed descriptions and sources of biostratigraphic, petrographic and sedimentologic reports are found in *Text C1*.

5.4 Results

5.4.1 Stratigraphic and Structural Framework of the Lower Magdalena Valley basin

The pre-existing basement architecture played a crucial role in the Oligocene to Recent sedimentary evolution of the LMV, therefore we build on the previous analyses and maps of *Mora et al. (2017a, b*, presented here in Chapters *4* and *5*) to study the structural and stratigraphic evolution of the basin. Based on regional reflection-seismic and well data, six major Oligocene to Recent tectono-stratigraphic sequences, separated by major regional unconformities (depositional sequences sensu *Catuneanu et al., 2009*), were identified and defined in the LMV (**Figure 5.2**). Numbering of the sequences starts from 5, considering that pre-Oligocene Sequences 1 to 4 were previously studied by *Mora et al. (2017b*) in the SJFB. The main characteristics of the studied sequences are summarized in **Table 5.1** and a detailed description of each sequence is found in *Text C1*.

5.4.1.1 Sequence 5 (Oligocene to lower Miocene)

We interpret the Oligocene to lower Miocene deposits as a transgressive, 2nd-order sequence, which filled from NW to SE the lowest paleo-topographic areas formed by the basement of the LMV (**Figure 5.6** and **Figure 5.7**, **Table 5.1**). Based on studies of planktonic foraminifera in wells and outcrops, this sequence which is called "Lower Ciénaga de Oro", has been associated to the planktonic zones P.20 to N.6 (M.3), equivalent to an early Oligocene to early Miocene age. Seismic data shows that the Oligocene to lower Miocene deposits gradually filled the proto-San Jorge and Plato depocenters from the W and NW and that the main structural basement features, such as the Sucre, Mojana and Pivijay extensional faults, were active (**Figure 5.6** to **Figure 5.8**). The best preserved, lower part of the sequence is interpreted as a retrogradational, transgressive package which records the advance of marine sedimentation from NW to SE and was deposited initially in shallow marine environments, which gradually changed to deeper marine and more anoxic environments.

5.4.1.2 Sequence 6 (Lower to middle Miocene)

This sequence was deposited after a regional early Miocene unconformity and records a major change in sedimentation in the basin, related to an increase in sediment supply. Biostratigraphic analyses indicate that it is a 3rd-order sequence of lower to middle Miocene age (Burdigalian to Serravalian, zones N.7/M.4 to N.11/M.8) (**Figure 5.6** to **Figure 5.8**, **Table 5.1**). Deposition of this sequence extends farther to the E and SE and begins with retrogradational, shallow marine clastics and carbonates which then change to progradational deltaic deposits (**Figure 5.9**). The two main families of extensional fault were active since late Oligocene times gradually decreased their activity through time. North of the Magangué-Cicuco high, this sequence is thicker and comprises deep-water, clastic deposits (mud to gravel-rich deposits, *Richards, 2001*) with the presence of an impressive submarine canyon which has been related to the proto-Magdalena drainage (*ICP, 2000*; *Bernal et al., 2015c*).

5.4.1.3 Sequences 7 and 8 (Middle to Upper Miocene)

Two tectonic events, one in the late Miocene and the other one in the middle Pliocene are responsible for the partial erosion of the middle to upper Miocene sequences in the southern and southwestern LMV. These sequences are also the result of abundant sediment supply from the E and SE, they continue to evidence high sedimentation rates and to display a progradational pattern

to the NW. These sequences represent 3rd-order cycles of middle to upper Miocene age (Serravallian-Tortonian) and are also limited by regional unconformities (*Duque-Caro, 1979*; *Hocol, 1993*; *Duque-Caro et al., 1996*; *ICP, 2000*; *Guzman, 2007*). The sequences, called "Middle and Upper Porquero", exhibit mainly fine-grained facies with progradational stacking patterns, which are best preserved in the depocenters where erosion was less intense.

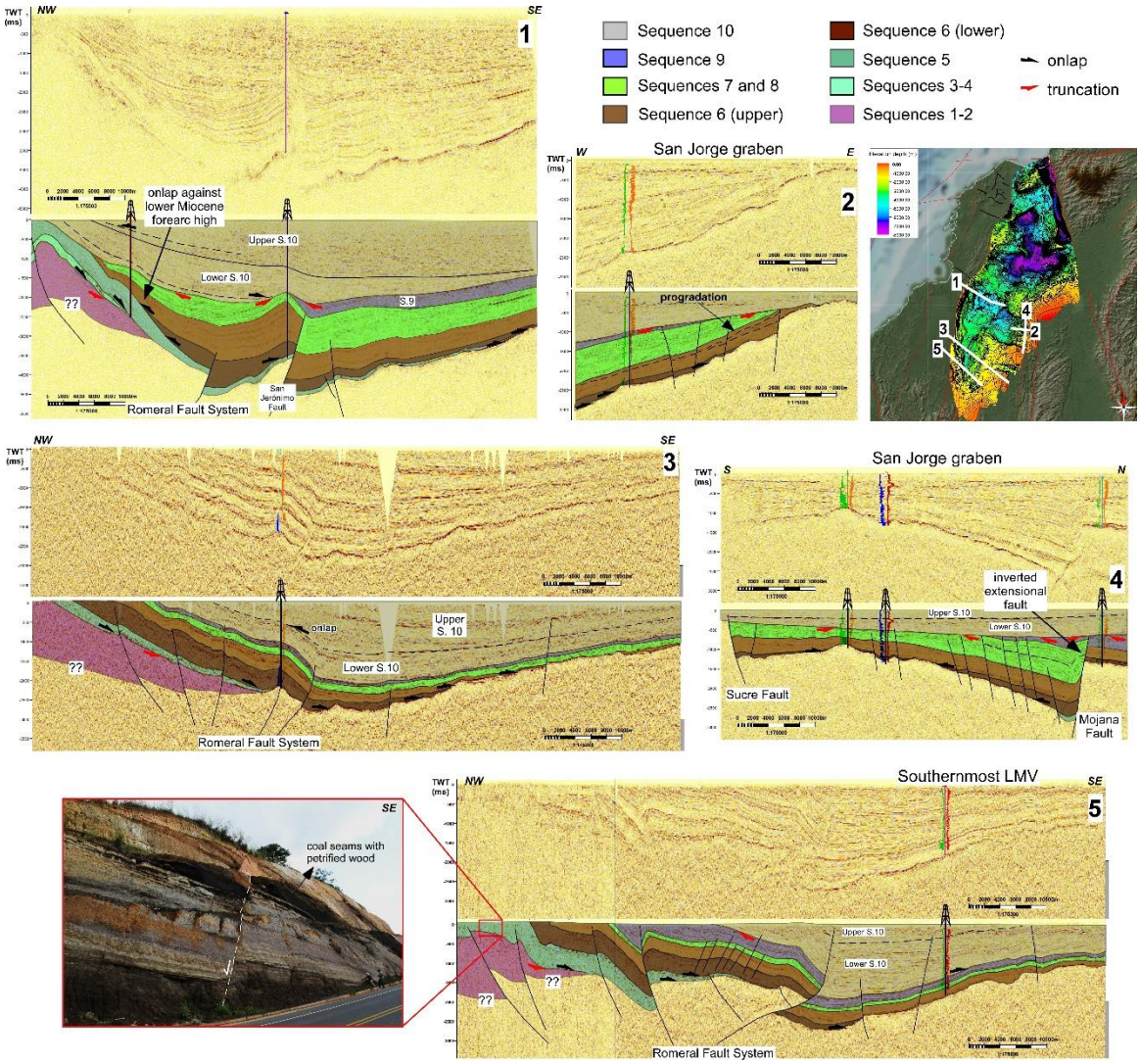

Figure 5.6. Selected seismic sections from the southern LMV, showing the well ties and the seismic stratigraphic characteristics, depositional patterns and thicknesses of the Oligocene to Quaternary sequences. The onlapping pattern to the SE of the Oligocene to Middle Miocene sequences (sections 1, 3 and 5) and the fault-controlled deposition of the same sequences in the San Jorge graben (section 4) are illustrated. Evidence of a lower Miocene paleohigh is depicted in Section 1, with the interpreted onlap to the NW of sequences 6 to 8, while Section 2 displays the progradation of sequences 7 and 8 in the San Jorge graben. Section 3 also shows the onlap to the NW of the upper part of Sequence 10, indicative of the uplift of the SJFB. A photo of an outcrop of deltaic, coal-bearing strata of Sequence 5, affected by recent extensional faulting and located in the southernmost LMV, is also shown.

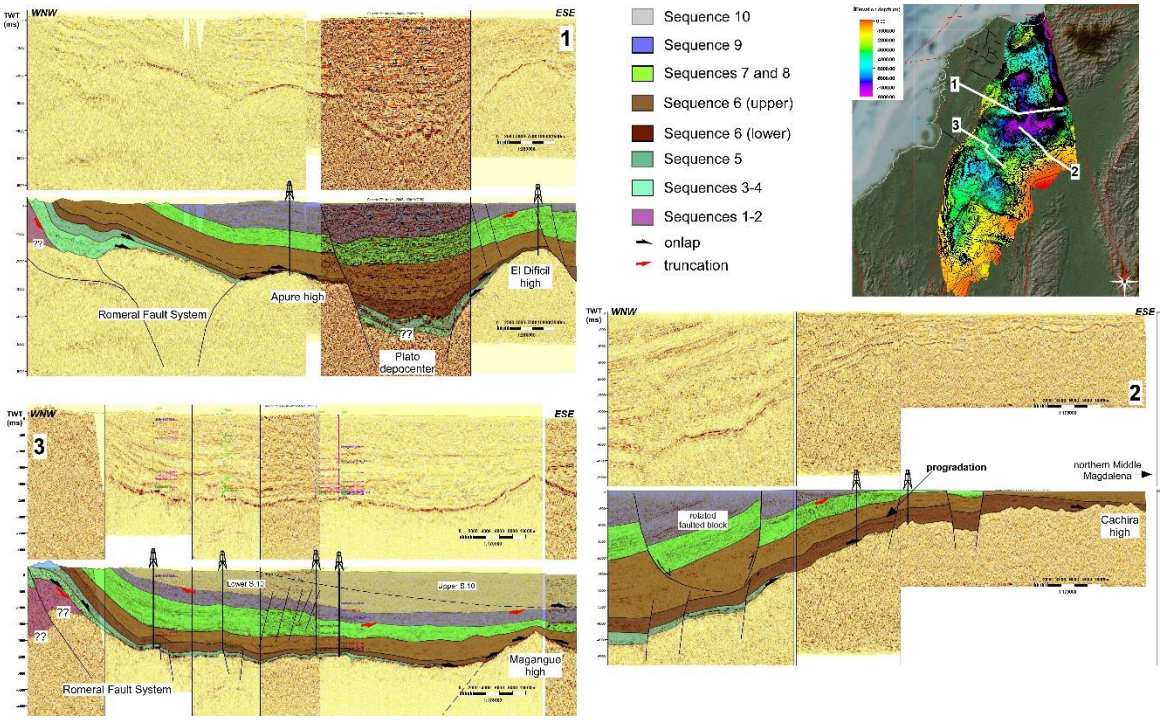

Figure 5.7. Selected seismic sections from the Magangué-Cicuco high (section 3) and northern LMV (Plato depocenter), showing the well ties and the seismic stratigraphic characteristics, depositional patterns and thicknesses of the Oligocene to Quaternary sequences. The onlapping pattern to the SE and against basement highs (e.g. Apure, El Dificil and Magangue) is illustrated.

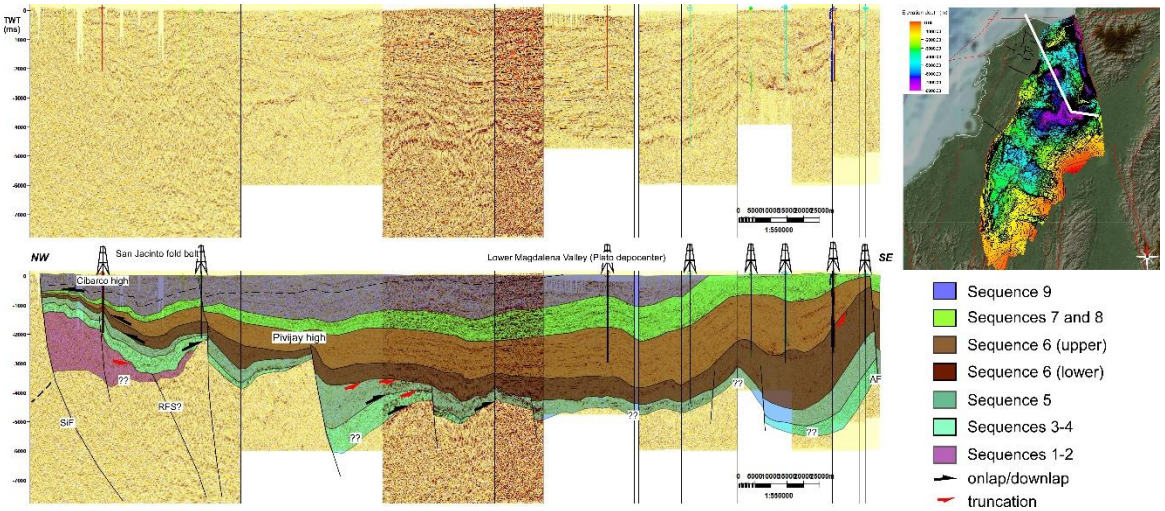

Figure 5.8. Regional seismic section from the northern LMV (Plato depocenter), showing the well ties and the seismic stratigraphic characteristics, depositional patterns and thicknesses of the Oligocene to Quaternary sequences. Evidences of a Miocene paleohigh are the onlapping and downlapping patterns of low-angle clinoforms to the NW, in the area of the Cibarco high (buried San Jacinto fold belt). In the SE, the oldest sequences have not been drilled, so interpretation is based on seismic data, which has a poor image at deep levels. RFS: possible Romeral Fault System; SiF: Sinú Fault; AF: Algarrobo fault.

5.4.1.4 Sequence 9 (Upper Miocene to lower Pliocene-Tubará)

This 3rd-order sequence of upper Miocene to lower Pliocene age (zones N.17/M.14 to Pl.2 zones, Tortonian to Zanclean) represents the accelerated migration towards the NNW of shelf-edge clinoforms of the paleo-Magdalena river, which almost completely filled the Plato depocenter and reached the approximate position of the present-day coastline in early Pliocene times (**Figure 5.8** and **Figure 5.10**, **Table 5.1**). Reflection-seismic data shows that this sequence, which is better preserved in the Plato depocenter, is composed of low-angle (0.3-0.6°) and wide (100-200 km) sigmoidal clinoforms which advanced from SSE to NNW, representing the gradual advance of the proto-Magdalena river.

5.4.1.5 Sequence 10 (Upper Pliocene to Pleistocene)

This sequence, which has been very poorly studied and comprises several higher order sequences, represents renewed subsidence in the southern LMV, focused in the San Jorge graben where the thickest deposits occur (**Figure 5.6**). It is well preserved in the southern LMV, south of the Magangué-Cicuco high, where it is called "Corpa", while in the north deposition appears to have been much thinner and the sedimentary record was eroded due to Pleistocene to recent deformation (**Figure 5.10** and **Figure 5.11**, **Table 5.1**). Taking into account the unconformities above the Tubará upper Miocene to lower Pliocene sequence, and below the upper Pleistocene to recent deposits, we infer here a late Pliocene to early Pleistocene age for this sequence, spanning from 3 to 1.3 Ma (3^{rd}-order cycle). We divided this sequence into two seismic packages (see *Text C1*). The area where the thickest deposits are preserved coincides with the structurally deepest area, which continues to subside today (**Figure C 2**a). The expression of the Corpa Sequence in reflection-seismic data consists of low-angle clinoforms broadly prograding from South to North, which appear to represent the deposits of the paleo-Cauca drainage system, including fluvial channels, lakes and swamps (**Figure 5.11** to **Figure 5.12**). The internal seismic-stratigraphic architecture of the Corpa Sequence reveals the time when the SJFB started to be uplifted, which appears to be close to the boundary between the Pliocene and Pleistocene (section 3, **Figure 5.6**).

5.4.2 Oligocene to Recent paleo-geography and kinematics of the LMV

In this section, we present the results of the integration and analysis of all our seismic, well and outcrop data, which are the basis for proposing an Oligocene to Recent kinematic and paleo-geographic evolution of the LMV. We have represented such evolution both in map view (**Figure 5.9** to **Figure 5.11**) and in cross-section view (**Figure 5.16** and **Figure 5.17**). In **Figure 5.9** to **Figure 5.11**, detrital zircon U-Pb geochronology from *Montes et al. (2015)* is also plotted (purple circles with their respective histograms), in order to show the influence of Permo-Triassic and older basement sources (black bars in histograms), Cretaceous sources in the Western and Central Cordilleras (green bars in histograms) and Eocene to Miocene sources (yellow and orange bars).

Seismic and well data shows that the LMV basin was initially filled by Oligocene, shallow-marine deposits of Sequence 5, which filled the paleo-topographic lows, as the sea transgressed from NW to SE (**Figure 5.9**a). Fault-controlled subsidence observed in the seismic indicates that there was an extensional reactivation of pre-existing basement faults with different trends, with the NE-SW being the most important. Detrital zircon geochronology shows that a fluvial system was draining Cretaceous and older terranes in the SW (Central and Western Cordilleras). In the north, supply from Cretaceous terranes is not observed, though a connection with the Cesar-Ranchería basin (CR) has been suggested (*Mora and García, 2003).*

After an early Miocene unconformity, basal deposits of Sequence 6 covered wider areas to the E, and correspond to shallow-marine clastic deposits in low areas and calcareous deposits in high areas (**Figure 5.9**b). Fault controlled subsidence continued, indicating similar extensional regime and trends as in the Oligocene, greatly influenced by the basement fabric. At least two

important forearc highs (Betulia and Cibarco, **Figure 5.9**b) are documented towards the western LMV, based on seismic onlap patterns (section 1 in **Figure 5.6** and **Figure 5.8**). The upper part of the sequence starts displaying progradational patterns, which together with the occurrence of Cretaceous detrital zircons in the eastern San Jorge depocenter, suggest the onset of drainages from the S or SE. This suggests a possible connection with the Middle Magdalena valley basin (MMV), though according to *Caballero et al., (2013b*) and *Horton et al. (2015*), the MMV was an intramontane closed basin.

In middle Miocene times (**Figure 5.10**a), seismic and well data shows that deposition became strongly progradational to the NW and N, and that there was a dramatic increase in sediment supply. Connection between the LMV and MMV is more probable, and correlates well with thick progradational packages filling the San Jorge depocenter in the south, and turbiditic and gravity-driven deposits filling the deep part of the Plato depocenter in the north. Forearc highs in the W are better developed, while fault-controlled subsidence and sedimentation is more localized and less important.

In late Miocene to early Pliocene times (Sequence 9), the proto-Magdalena shelf clinoforms rapidly prograde to the NW and fill the Plato depocenter until they reach the current coastline, while the proto-Cauca and proto-San Jorge deposits also fill the southern LMV (**Figure 5.10**b). Fault-controlled subsidence ceased in the Plato depocenter, while the San Jorge graben and the forearc highs experienced Pliocene, NE-SW and ESE-WNW-trending contraction and the main extensional faults are inverted (**Figure 5.10**b). Upper Pliocene deposits of Sequence 10 are poorly preserved in Plato, while they are well preserved in the San Jorge area, which is actively subsiding due to sagging (**Figure 5.11**a). In the Pleistocene, the Plato area and the forearc highs are uplifted, while the San Jorge area continues to subside and accumulates thick fluvio-deltaic deposits in a round basin (**Figure 5.11**b). The San Jacinto fold belt is tilted to the SE, due to thrusting in the accretionary prism farther west. A digital elevation model from the study area (**Figure C 2**a) shows that today, the northern LMV (Plato) and the San Jacinto fold belt are positive relief areas, while the southern LMV (San Jorge) continues subsiding due to sagging. These patterns suggest that ESE-WNW-trending contraction and NNE-SSW-trending extension have been active since late Pliocene times, in agreement with the displacement vector of the Caribbean plate relative to fixed South America (**Figure 5.1**, **Figure 5.11**b, **Figure C 3**).

Thickness analyses of each sequence allowed us to study the development and migration of depocenters since late Oligocene times (**Figure C 2**b). The detailed depocenter evolution and the possible reasons for depocenter migration are discussed in forthcoming sections.

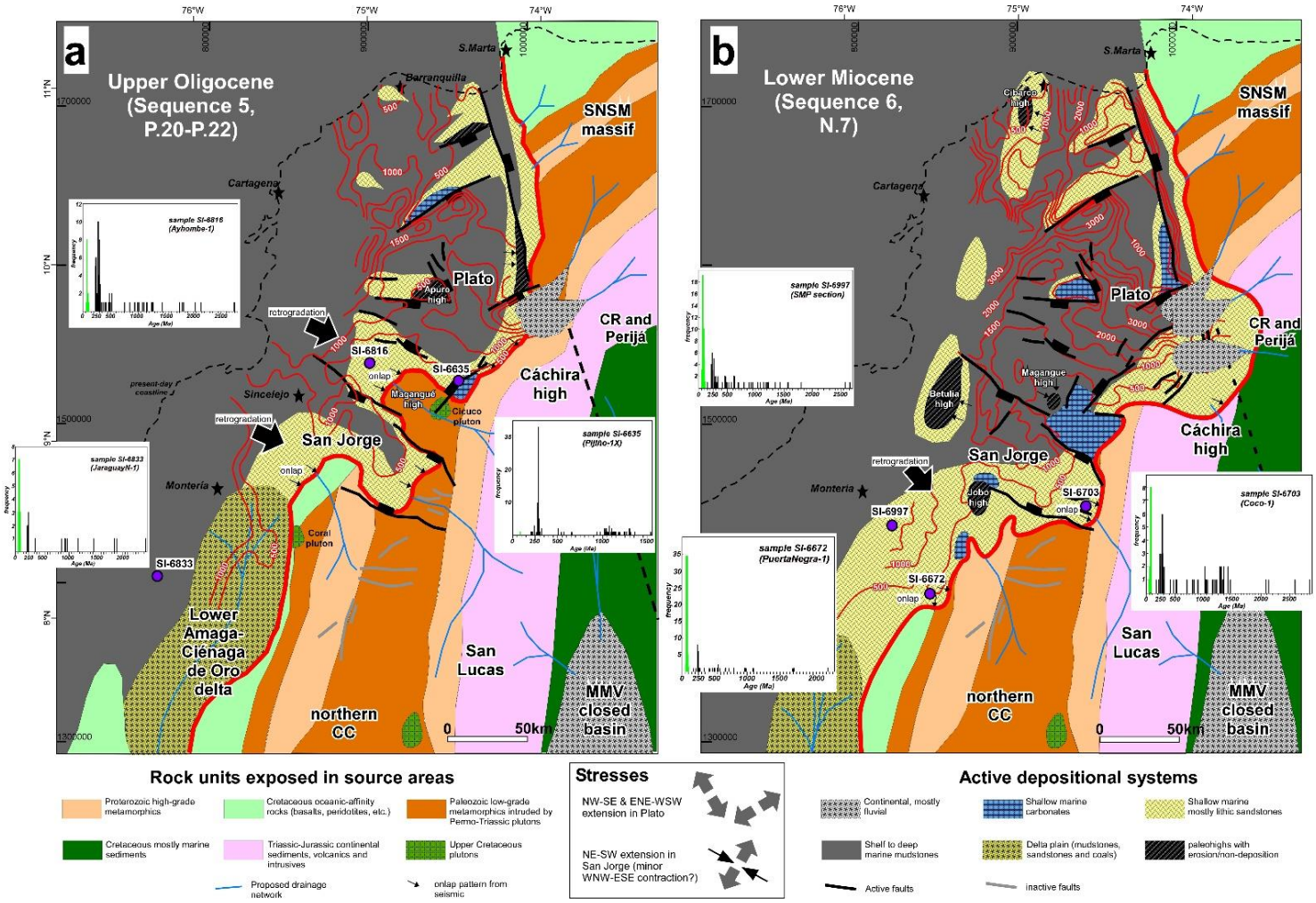

Figure 5.9. Interpreted late Oligocene (a) and early Miocene (b) paleogeography, based on seismic interpretation and well data, showing interpreted source areas (based on *Mora et al. 2017a* and others), active sedimentation areas and proposed paleo-drainages in blue; thin red contours are thicknesses in meters of each sequence and the thick red contour represents the interpreted limit of deposition of each sequence. Main stresses according to interpreted active faults are also depicted. The development of local paleohighs (e.g. Betulia and Cibarco) in the present-day SJFB, as interpreted from seismic data, is also shown. CR: Cesar Ranchería; SNSM: Sierra Nevada de Santa Marta; CC: Central Cordillera.

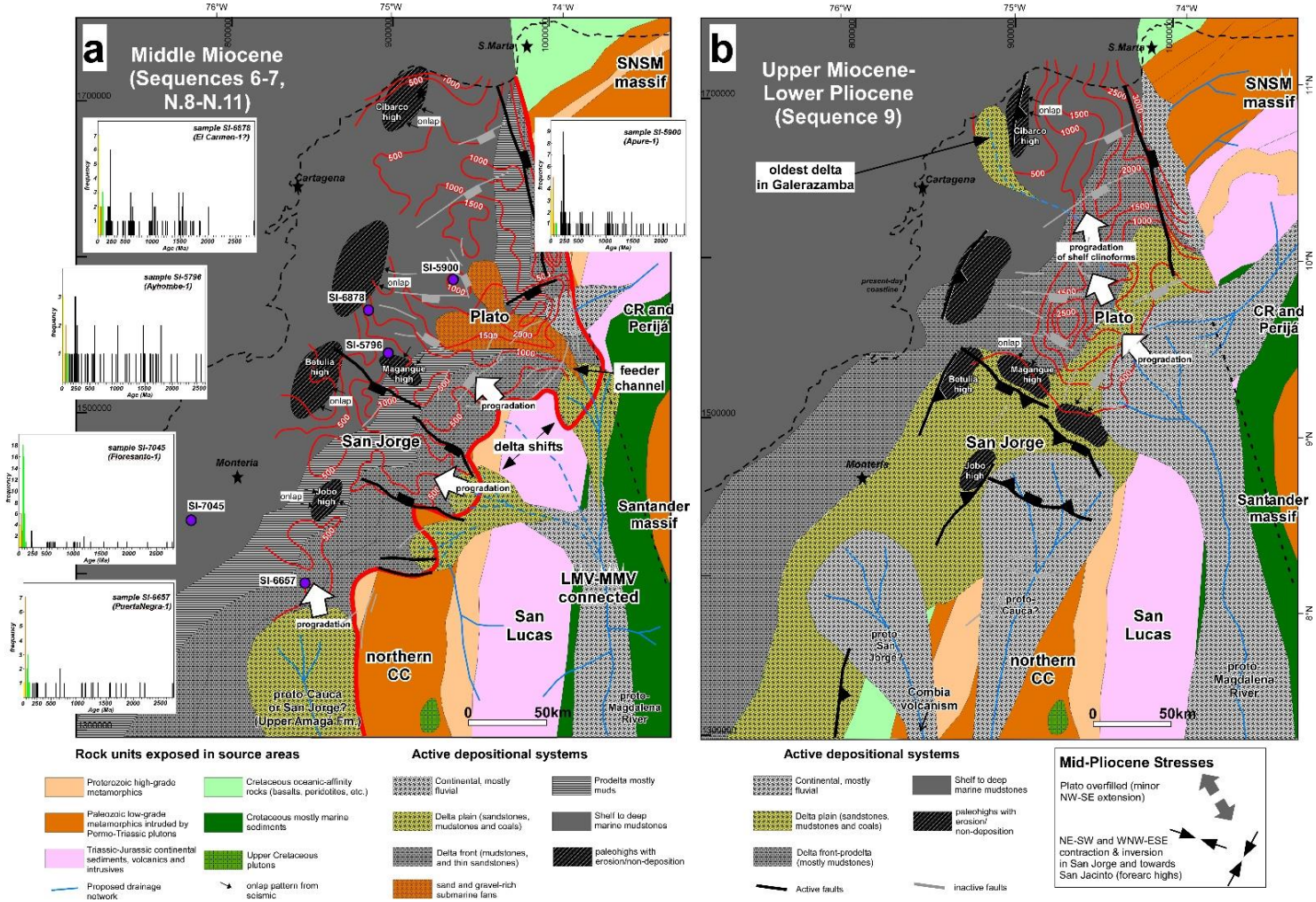

Figure 5.10. Interpreted middle Miocene (a) and late Miocene to early Pliocene (b) paleogeography, based on seismic interpretation and well data, showing interpreted source areas (based on *Mora et al. 2017a* and others), active sedimentation areas and interpreted paleo-drainages in blue. Thin red contours are thicknesses in meters of each sequence and the thick red contour represents the interpreted limit of deposition of each sequence. Middle Pliocene stresses according to interpreted active faults are depicted. The development of paleohighs, as interpreted from seismic data, is also shown. CR: Cesar Ranchería; MMV: Middle Magdalena Valley basin.

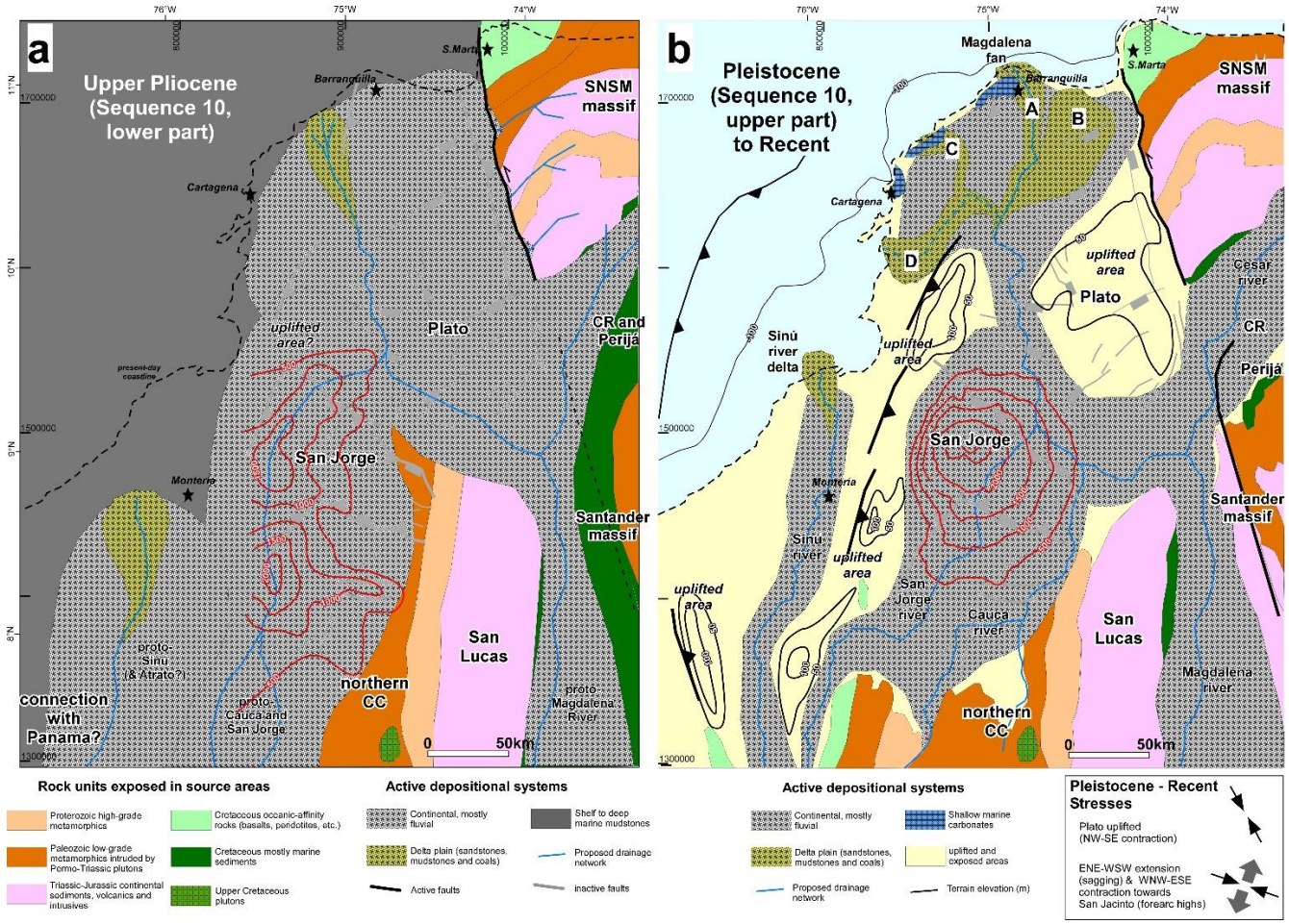

Figure 5.11. Interpreted late Pliocene (a) and Pleistocene (b) paleogeography, based on seismic interpretation and well data, showing interpreted source areas (based on *Mora et al. 2017a* and others), active sedimentation areas and interpreted paleo-drainages in blue; thin red contours are thicknesses in meters of each sequence. In late Pliocene times, when the Magdalena river system reached the present-day coastline, the Plato depocenter was already overfilled, while sedimentation continued in the western San Jorge depocenter, which continued subsiding. In the Pleistocene, while the Magdalena river delta shifted its position, uplift of the San Jacinto fold belt and of the Plato depocenter created a round depocenter, which continues to subside today (Figure 5.11a). Letters A to D represent positions of the Magdalena deltas (from *Romero-Otero, 2015*), with A representing the current position. CR: Cesar Ranchería. Main Pleistocene to Recent stresses are also depicted.

5.4.3 SSW-NNE cross-section structure of the LMV

The LMV basement structure has been described in detail by *Mora et al. (2017a*), who subdivided the structural fabric into four main, extensional fault families and proposed tectonic mechanisms to explain their origin. The two main families, trending ESE-WNW and ENE-WSW are responsible for most of the extension in the LMV, and they consist of nearly vertical extensional faults, which exhibit small heaves. Seismic-stratigraphic analyses show that deposition of the late Oligocene to early Miocene sequences (Ciénaga de Oro and Lower Porquero) had fault control, and that after the middle Miocene, deposition was mainly due to sagging, giving rise to the classic Steer's Head model of basin geometry (*Miall, 2000*). This is evident from the seismic data and from the regional cross-section (**Figure 5.12**), where the majority of the extensional faults are displacing the upper Oligocene to middle Miocene sequences, with related thickness changes across the major faults. This style is very clear in the San Jorge graben of the southern LMV, which shows an asymmetric shape with thicker syntectonic deposits in the northern half of the graben, indicating that the northern Mojana fault had more extensional displacement than the Sucre fault in the south (**Figure 5.6**, section 4). By contrast, the late Miocene to Pleistocene sequences filled broader depocenters in a uniform way, with only minor and localized fault displacements. The latest subsidence episode, which appears to continue active, is related to sagging of the San Jorge graben that allowed the deposition of the very thick Pliocene to Pleistocene sequences (Sequence 10, Corpa). The faults that exhibit the biggest heaves are related to the Santa Marta-Algarrobo fault system, which displays a listric style with mostly Neogene syntectonic strata and important fault-block rotation (**Figure 5.12**).

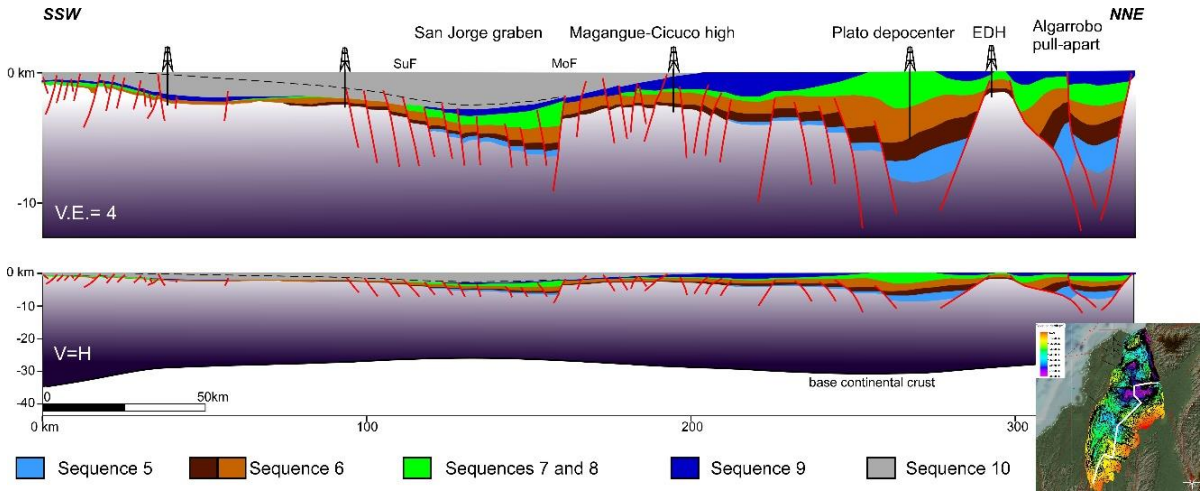

Figure 5.12. Regional structural cross-section in depth (kilometers), in two different scales to show the stratigraphic relationships, thicknesses and preservation of the studied Oligocene to Quaternary sequences. The lower section (scale 1:1), also shows the base of the continental crust, based on data by *Poveda et al. (2015*) and *Bernal et al. 2015a*. EDH: El Dificil High; MoF: Mojana Fault; SuF: Sucre Fault. Dashed line in Sequence 10 represents clinoform progradation to the north.

5.4.4 Sedimentation Rates and Subsidence in the LMV and San Jacinto fold belt

Thicknesses and ages from 32 wells drilled in the LMV and SJFB were compiled to calculate sedimentation rates and to carry out subsidence analyses of those provinces. Due to poor preservation of Oligocene to Recent deposits in the SJFB, analyses of sedimentation and subsidence rates there are less reliable. In the LMV, where the succession is much more preserved, our analyses

indicate that after the Early Miocene unconformity there was a dramatic increase in sedimentation and subsidence rates (upper panels in **Figure 5.13** and **Figure C 1**). Sedimentation rates of the upper Oligocene to lower Miocene sequence (5) were lower than 60 m/Ma, though this number could be higher considering erosion of the upper part of the sequence (planktonic zones N.4/M.1 to N.6/M.3). By contrast, Sequence 6, deposited after the early Miocene unconformity, exhibits much higher sedimentation rates, generally above 60 m/Ma and locally exceeding 300 m/Ma, in some areas such as the Plato Depocenter. Sequences 7 to 9 appear to display lower sedimentation rates, generally less than 150 m/Ma, but considering the erosion experienced by these sequences, they probably also exhibited sedimentation rates higher than 200 m/Ma. Sequence 10 (Corpa), which is well preserved in the southern LMV, displays very high sedimentation rates with an average of 530 m/Ma, exhibiting highest values in the Magangué-Cicuco high and in the western San Jorge depocenter. Our calculated sedimentation rates are in agreement with previous calculations by Molina (1978; in *ICP, 2000*).

Our estimates of corrected total and tectonic subsidence show important variations depending on the geographic location (**Figure 5.13**). The highest subsidence estimates were obtained in the southern Plato depocenter with 4.8 km of total subsidence and 2.1 km of tectonic subsidence. In the San Jorge graben, 3.7 km of total subsidence and 1.8 km of tectonic subsidence were calculated. In spite of erosion of the Latest Miocene to Recent strata in the SJFB, the estimated total subsidence is close to 3 km and the tectonic subsidence around 1.5 km.

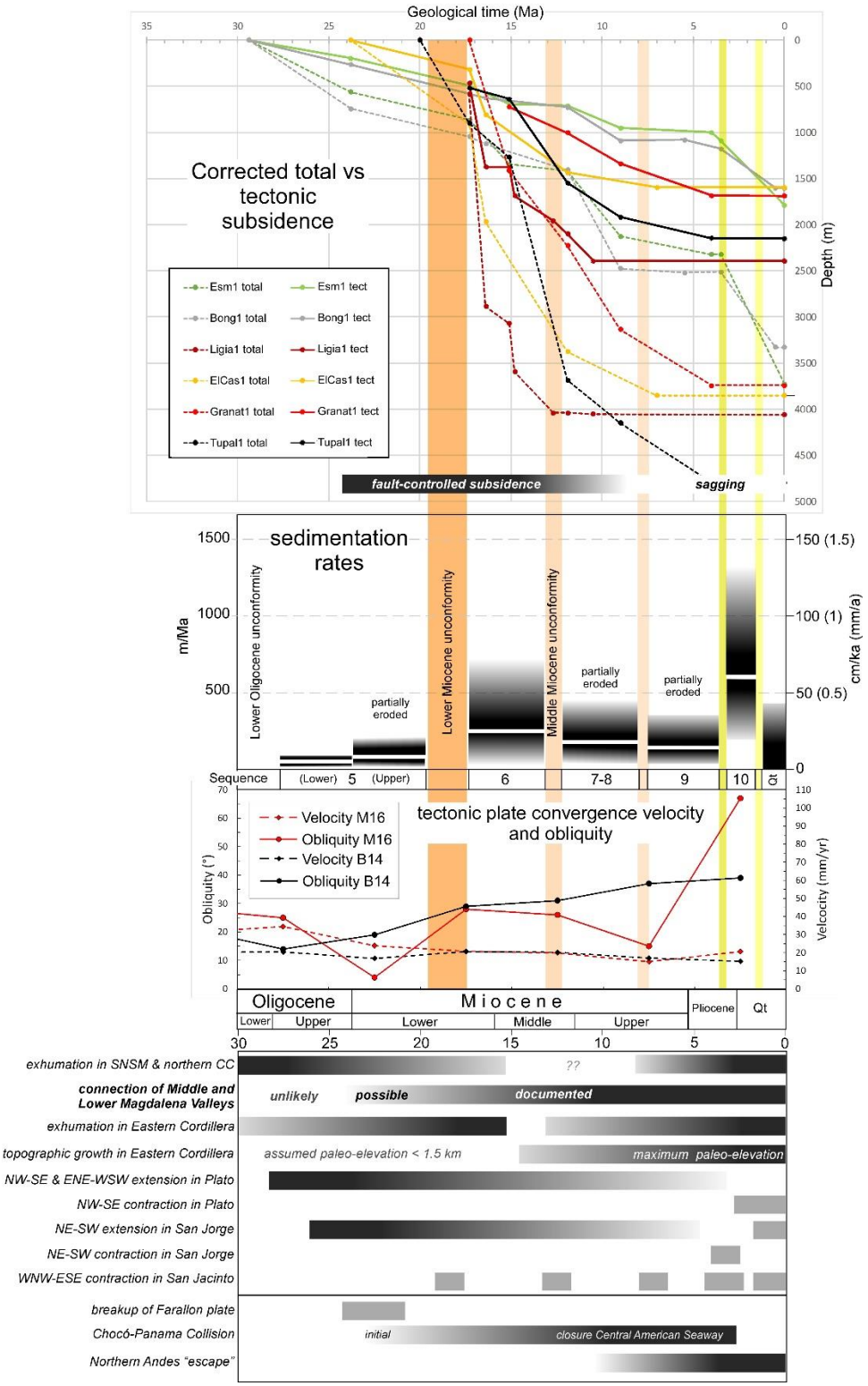

Figure 5.13. Integration of the subsidence (total vs tectonic), sedimentation rate and Oligocene to present day, tectonic plate convergence velocity and obliquity, compared with major tectonic events and tectono-stratigraphic unconformities. Tectonic (continuous lines) and total (dashed lines) subsidence plots of representative wells in the LMV and San Jacinto are displayed in the upper panel, and sedimentation rates in the central panel. The third panel from top to bottom exhibits the changes in plate convergence velocity and obliquity with time, for two different paleo-tectonic models (*Boschman et al. 2014* in black, B14; *Matthews et al. 2016* in red, M16), compared with the Oligocene to Quaternary tectono-stratigraphic sequences and unconformities (vertical bars of orange to yellow shades) and major tectonic events (black to grey horizontal bars in the lower panel). We calculated velocities and obliquities in time-steps of 5 Ma, hence the points in the convergence velocity and obliquity graph represent the middle of each time interval.

5.4.5 Extension in the LMV

In this study, we followed three different approaches in order to obtain well-supported extension estimates for the lithosphere and crust beneath the LMV. The first approach was to do a simple line-length calculation using a NNE-SSW-trending, depth-converted structural cross-section (**Figure 5.12**), which we built in the Move software of Midland Valley. The second approach was a backstripping technique assuming an Airy isostasy model and using sediment thickness data from the drill holes, in order to construct the total vs tectonic subsidence curves and to obtain the stretching factor (β factor, *McKenzie, 1978*; **Figure 5.14**). The third approach was to compile crustal thickness and Moho depth data from NW Colombia (e.g. *Poveda et al., 2015*; *Bernal et al. 2015a*) and use our basin floor (basement) depth map to obtain the crustal thickness beneath the LMV, after removing the sedimentary infill (**Figure 5.15**).

At this point, we must highlight the advantages and limitations of each of the methods we used to calculate extension in the LMV. The line-length measurement using the depth-converted structural cross-section, constructed from reflection-seismic data, is the method that involves more uncertainty for several reasons. First of all, due to the resolution of the seismic data, extension caused by sub-seismic features is not taken into account. In second place, analysis along a 2-D section assumes plane strain, therefore neither oblique nor ductile deformation are taken into account. Furthermore, this approach assumes correct geometric representations of structural geometries, and final calculations are affected by depth conversion. For these reasons, the line-length balancing method considerably underestimates the obtained amounts of extension.

The prototype uniform stretching model of *McKenzie (1978*) involves assumptions such as uniform stretching with depth, instantaneous extension, stretching by pure shear and the operation of Airy isostasy throughout, among others. However, observations in regions of continental extension suggested re-examination of the assumptions in the uniform stretching model, and modifications to the prototype model were proposed (*Allen and Allen, 2005*). Therefore, it is clear that by using the simple uniform stretching model of *McKenzie (1978*) we are making assumptions that have been re-examined and that do not involve a wide number of additional variables. Furthermore, the uniform stretching model does not provide clues to understanding the dynamics of continental stretching.

Although dynamic modeling is beyond the reach of this study, our estimates obtained by using the crustal thickness measurements and the basement depth maps are our best approximations for extension calculations, because they allow areal and volumetric balancing and they are independent of the limitations of the other two methods (line length and uniform stretching). In spite of having a very detailed basement map, an important limitation of this method is that the crustal thickness map is very generalized because it was obtained from data of only five stations for receiver function approach (*Poveda et al., 2015*) and three cross-sections for the gravity modeling (*Bernal et al., 2015a*). There are also inherited uncertainties from each of these methods, which according to *Poveda et al. (2015*), would be in the order of 9 km in the Moho depth estimation, and 3 to 8% in thickness estimations. For the modeling of the gravity transects by *Bernal et al. (2015a*), the best-possible match between the calculated and observed gravity anomalies was obtained after varying the densities and geometries of pre-defined layers, but still some errors (2.27 to 4.38 km) are reported for such modeling.

According to the tectonic subsidence curves from wells located in the SJFB and in most of the LMV (except for the deep Plato depocenter), there is 10-50% of extension related to β values between 1.1 and 2, while in the deep parts of the Plato depocenter, β values range from 2 to 4 (> 50% of extension, **Figure 5.14**). The simple line-length calculation in the Move software showed that the basement of the LMV has been extended 41 km, which is equivalent to 12.1% of extension (**Figure 5.12**). Nevertheless, the Algarrobo listric fault system accounts for 7.1% of the total extension, while the rest of the LMV including the Plato and San Jorge depocenters, experienced only 14 km of extension, equivalent to only 5%. Concerning the crustal thickness and Moho depth data, *Poveda et al. (2015*) used a receiver functions technique to obtain crustal thicknesses ranging from 26 km in the Montería area, to 50 km in the southeastern boundary of the basin against the northern Central Cordillera. *Bernal et al. (2015a*) reported Moho depths from gravity modelling

which range from 24 km in the north of the LMV to 36 km in the south (**Figure 5.15**a). As shown by *Mora et al. (2017a*), the basement beneath the LMV reaches depths of 8 km in the Plato depocenter and 6 to 7 km in the San Jorge graben (**Figure 5.15**b). Removal of the sedimentary fill suggests that the crust is thinnest in the northwestern part of the basin where the sedimentary infill is very thick and where *Bernal et al. (2015a*) report crustal thicknesses close to 24 km (**Figure 5.15**c). A thin crust was also measured in the western San Jorge depocenter (~20 km), based on the data by *Poveda et al. (2015*), who also measured the highest thicknesses in the northern SJFB (37 km).

Crustal thickness calculations in northern Colombia (*Poveda et al., 2012*) suggest that the continental crustal thickness in relatively undeformed areas such as the Middle Magdalena Valley basin ranges from 40 to 45 km. Therefore, if we assume an initial crustal thickness in the LMV area of 40 km, the maximum extension would be more than 50% (β=2) in the northwestern Plato depocenter and around 50% in the Montería-San Jorge graben area, while in the rest of the basin, extension would range between 12 and 32% (β from 1.13 and 1.45). This means that the LMV experienced high extension in the two depocenters (Plato and San Jorge) and low extension in the rest of the basin. However, if a higher initial crustal thickness is assumed (45 km or more), extension would have been much bigger. **Table 5.2** summarizes our extension estimates using the three different approaches previously described and the previous extension calculations by *Montes et al. (2010*).

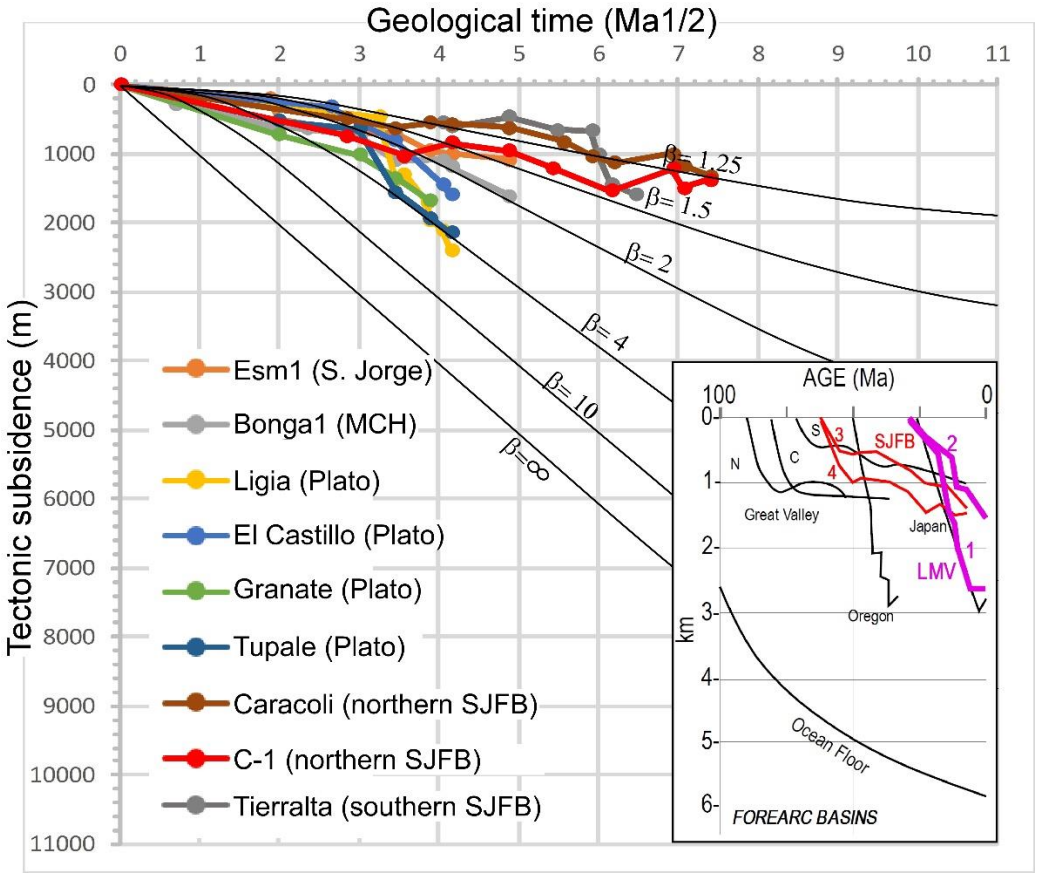

Figure 5.14. Tectonic subsidence data plotted against the square root of the geological time, in order to have an idea of the β-factor (*McKenzie, 1978*) and the extension in the LMV. In most of the study area, β values range from 1.2 to 1.5, except for the Plato depocenter where they can be > 2 (> than 50% extension). Inset shows a comparison of our tectonic subsidence curves for the LMV and SJFB with data from other forearc basins compiled by *Angevine et al. (1990*), showing a good correlation with some basins. 1. Northern LMV (Plato); 2. Southern LMV (San Jorge); 3. Southern San Jacinto; 4. Northern San Jacinto. MCH: Magangue-Cicuco high.

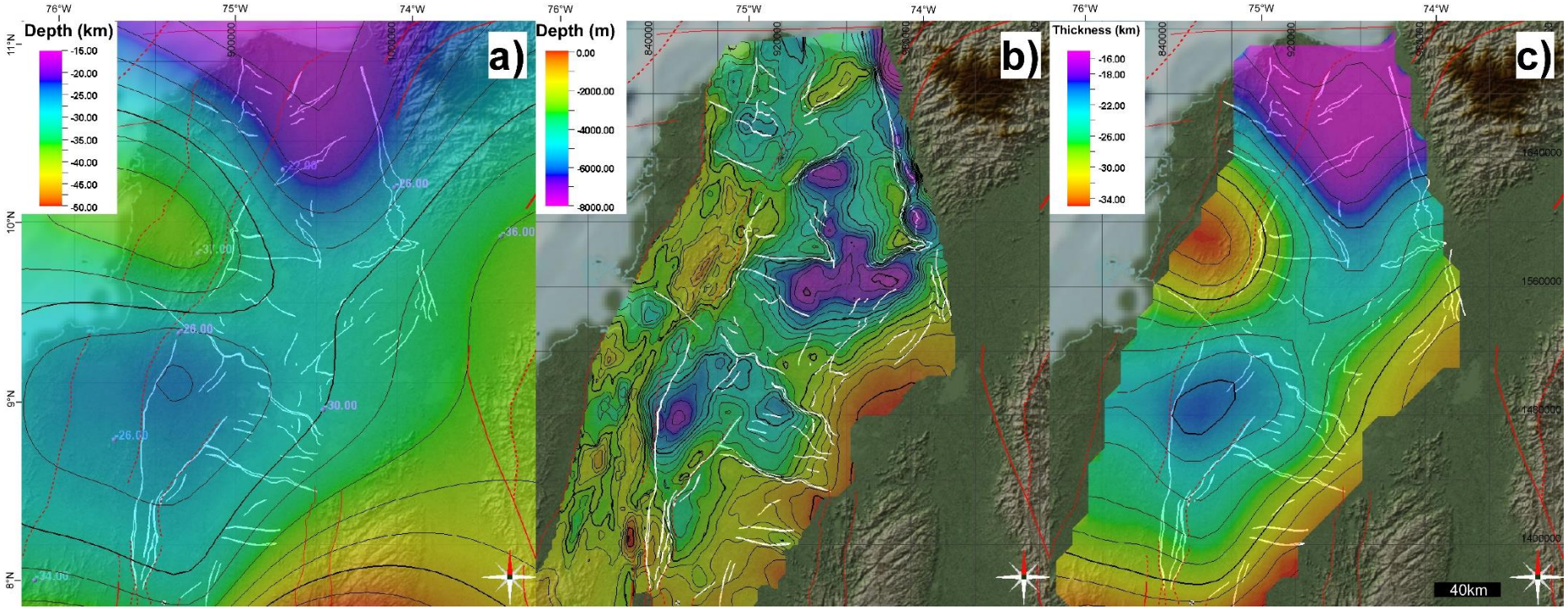

Figure 5.15. Maps used to calculate extension in the LMV and SJFB. a) Depth map of the Moho discontinuity, representing the crustal thickness, based on *Poveda et al. (2015*) and *Bernal et al. (2015a*), showing that the crust thickness ranges from 22 km in the northern LMV to >30 km in the central and SW San Jacinto. Stations with measured values are depicted in lavender (values obtained from *Bernal et al. 2015a* where extrapolated as points from their regional gravity sections). b) Basement map in depth (km) of the LMV, based on *Mora et al. 2017a*). c) Crustal thickness map without sedimentary infill, obtained by subtracting the basement map in (b) from the crustal map in (a). It must be noted that the thinner crust (<20 km) in the NW of the LMV, where no thickness data is available, resulted from mapping extrapolation.

	Extension calculations in LMV (β and %)	Comments
Tectonic subsidence curves	1.1 to 2 (10-50%)	β=2 to 4 (50-75%) in deep Plato depocenter
Line-length in cross-section	12.1%	Algarrobo Ft. accounts for 7%
Crustal thickness measurements	1.13 to 1.45 (12-32%*)	β=2 (50%) in Montería area*
Montes et al., 2010	1.5 to 2 (33-50%)	NE-SW extension between 86 and 115km

**assuming initial crustal thickness of 40km*

Table 5.2. Compilation of extension calculations in previous (*Montes et al. 2010*) and this study, according to the different methods that were used. Further explanation in the text.

5.5 Discussion

According to paleo-tectonic reconstructions (*Müller et al., 1999*; *Pindell and Kennan, 2009*; *Boschman et al., 2014; Matthews et al., 2016; Mora et al., 2017b*), the plate-tectonic setting of northwestern Colombia since the Oligocene has been characterized by a slow (~2 cm/yr) and nearly orthogonal convergence and subduction of the Caribbean oceanic plate beneath the South American plate (**Figure 5.5**). The formation and Oligocene to Recent evolution of the LMV has therefore been influenced by the interaction with the Caribbean oceanic plateau, which has been considered as a flat-slab subduction (*Bernal et al., 2015a*; *Mora et al., 2017a, b*). Hence, the stratigraphic succession in the LMV must have recorded any major changes in the convergence and subduction regime. However, the last 30 Ma were characterized by low convergence obliquities and relatively low velocities, which do not appear to show abrupt changes in their trend (**Figure 5.13**), making difficult to correlate reported tectonic events such as subsidence or uplift pulses with regional plate tectonic events. In spite of the relative stability of the Oligocene to Recent convergence between the Caribbean plate and NW South America, our results indicate a close relationship between the lower Miocene unconformity, the increase in subsidence and sedimentation in the LMV and the uplift of the Eastern Cordillera and related mountain ranges. Such an uplift resulted in the formation of the Magdalena fluvial system, when the eastern LMV was connected to the Middle Magdalena valley. Our results also highlight the influence of inherited basement structures on tectonic segmentation of the LMV, with the development and evolution of the two main depocenters. In this section, we start by discussing the possible causes of the formation of the LMV, then the basin and depocenter evolution, subsidence history and trends, and finally we propose possible mechanisms that controlled the basin evolution, in the absence of major variations in the Oligocene to Recent plate-tectonic regime.

5.5.1 Origin of the Lower Magdalena Valley basin

The best-supported and more widely accepted hypothesis for the plate tectonic setting of NW Colombia in Late Cretaceous times, relates to the subduction of the "normal" thickness oceanic Caribbean plate and later of the Caribbean plateau beneath South America (*Mantilla et al., 2009*; *Bernal et al., 2015a, b*; *Mora et al., 2017b*). *Mora et al. (2017a*) and *Silva et al. (2016)* recently proposed the existence of a subduction-related, Upper Cretaceous magmatic arc that forms the basement underneath the LMV. Though no evidence has yet been found of Paleocene to Eocene arc magmatism under the LMV, there are reports of Paleocene to lower Eocene magmatic arc rocks in the northern CC and SNSM (*Bayona et al., 2012*; *ANH, 2011*a; *Bustamante et al., 2017*), suggesting that there was a continuous, Upper Cretaceous to lower Eocene magmatic arc, extending between those areas. *Dickinson (1995*) attributed forearc subsidence to several factors, one of them

being the cooling and thermal subsidence of the arc massif. *Noda (2016*) proposed a general model of forearc basin evolution and argues that during the infant stage of subduction, the forearc may be extensional until the sinking plate retreats the hinge to obtain a sufficient downdip motion, and that such extension possibly leads to fault controlled subsidence in the overriding crust. According to the aforementioned, we consider that the formation of the LMV is related to the cooling and thermal subsidence of the Cretaceous to lower Eocene, intra-continental magmatic arc of NW Colombia, and to the fault-controlled subsidence at the initial subduction stages. Cooling caused the extensional reactivation of the main pre-Oligocene basement features such as the Mojana and Sucre faults that limit the San Jorge graben, and the Pivijay, Apure, Pijiño and other faults of the Plato depocenter. Extensional reactivation of inherited basement structures was crucial for the tectonic segmentation of the LMV, with the formation and development of its two basin depocenters (Plato and San Jorge). However, it is also possible that initial subsidence could have been caused by crustal thinning due to possible Cretaceous to Eocene subduction erosion (*Clift and Vannucchi, 2004*), as suggested by *Mora et al. (2017a, b*).

5.5.2 Oligocene to Recent forearc basin evolution

Our results show that fault-controlled subsidence took place in the LMV from Oligocene to middle Miocene times, spanning for 15- 19 Ma, and that it was replaced by sagging which lasted for ~14 Ma. An increase in sedimentation at ~ 17 Ma, after an early Miocene regional unconformity, would have influenced the change of fault-controlled subsidence to sagging, thus implying that sedimentary loading became the main subsidence mechanism since middle Miocene times. The increased sediment supply also strongly influenced the plate interface, by lubricating the subduction channel, thus affecting the transmission of stresses to the upper plate and producing underplating. Crustal thickening by tectonic underplating of subducted materials has been proposed as a cause of uplift in forearc coastal terranes such as the Chile forearc (e.g. *Glodny et al., 2005*; *Clift and Hartley, 2007*). In the LMV, underplating has been proposed based on deep seismic imaging by Mora et al. (2017a, **Figure A 1**), and in this study we have identified Miocene to Recent paleo-highs in seismic sections in the current SJFB (e.g. section 1 in **Figure 5.6** and Cibarco high in **Figure 5.17**), which would represent forearc highs. Therefore, uplift in the forearc as seen in the western LMV and current San Jacinto fold belt, may be related to tectonic underplating. The occurrence of a deformed outer high to the W (San Jacinto fold belt) and an undeformed forearc basin behind it, to the E (LMV), is explained if the continental basement beneath the LMV acted as a static backstop (**Figure 5.18**), with geologically reasonable contrasts in mechanical properties compared to the sediments just trenchward of it (*Byrne et al., 1993; Mantilla et al., 2009*).

In late Oligocene times, low-angle subduction was ongoing when the pre-Oligocene magmatic arc subsided and the LMV experienced SE-NW and NE-SW-trending extension and fault-controlled subsidence, with the formation of the two basin depocenters. The Oligocene basin was far from being overfilled, hence it was probably an underfilled, mostly sloped, forearc basin (sensu *Dickinson, 1995*), or an accretionary extensional forearc basin (*sensu Noda, 2016*).

The early Miocene unconformity seems to mark an important change in sedimentation in the LMV, as shown by our results. This unconformity partly overlaps in age with plate tectonic events such as the breakup of the Farallón plate and the initial collision episode of the Chocó-Panamá block, though there is no concrete evidence to support a direct correlation. However, such tectonic events could have exerted some influence in the uplift of Andean terranes, which started shaping the drainage systems in northern Colombia (*Hoorn et al., 2010*; *Caballero et al., 2013a*; *Reyes-Harker et al., 2015*; *Anderson et al., 2016*). The early Miocene increase in subsidence coincides with faster exhumation rates in surrounding areas such as the Santander Massif (*Mora et al., 2015*; *Van der Lelij et al., 2016)* and the Santa Marta Massif (*Villagomez et al., 2011b*). Further south, in the Eastern Cordillera, *Parra et al., (2010*) and *De la Parra et al. (2015*) in the Eastern foothills and *Caballero et al. (2013a*) in the Western foothills, documented a clear correlation between increasing subsidence rates and faster thrust-induced denudation rates by about 20 Ma.

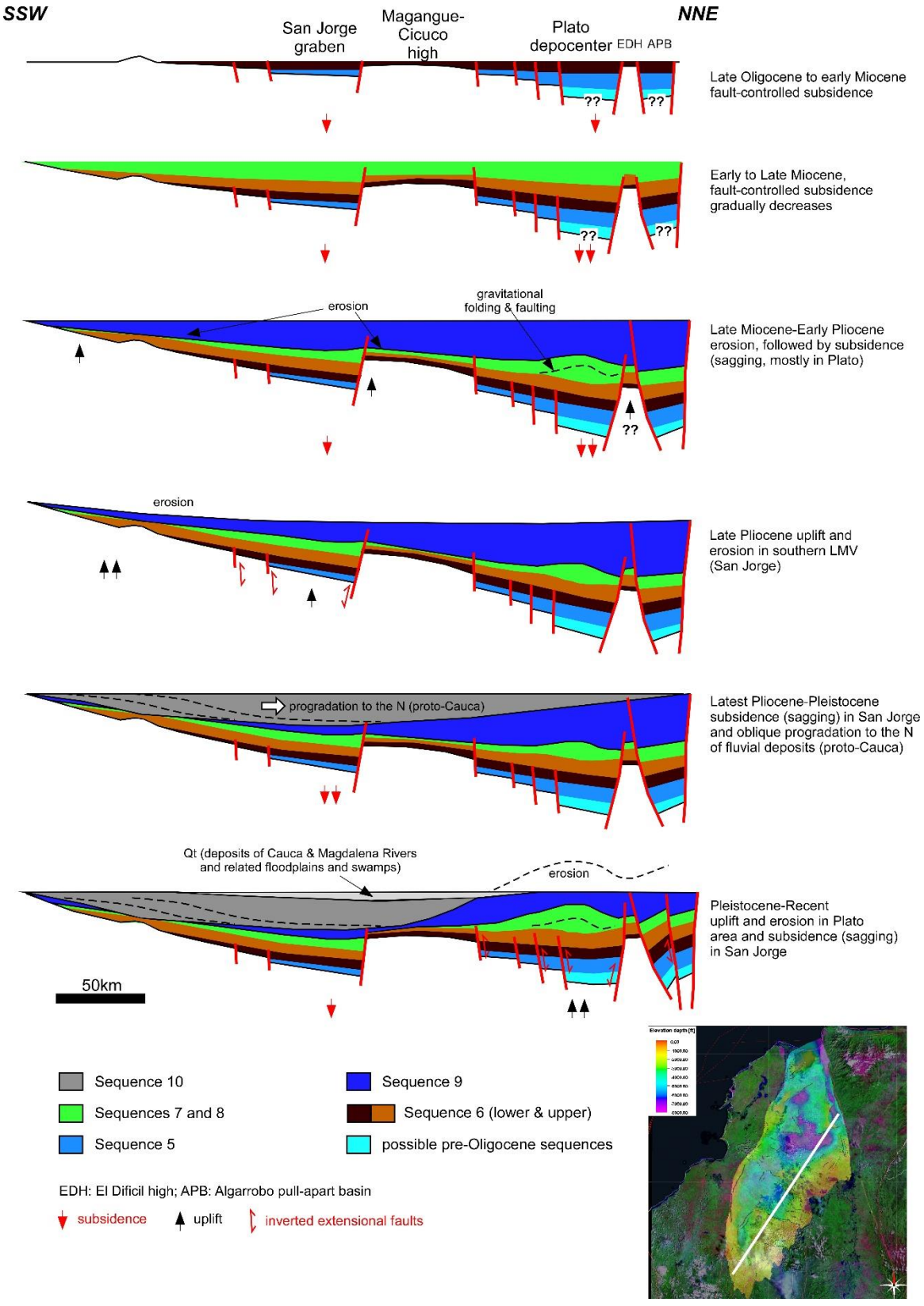

Figure 5.16. Simplified, Oligocene to Recent evolution of the LMV, as shown in a NNE-SSW-trending regional section. Oligocene to middle Miocene fault-controlled subsidence which affected Sequences 5 to 7, was replaced by sagging during deposition of Sequences 8 to 10. After the middle Miocene, the two depocenters (Plato and San Jorge) started to experience different subsidence and uplift phases.

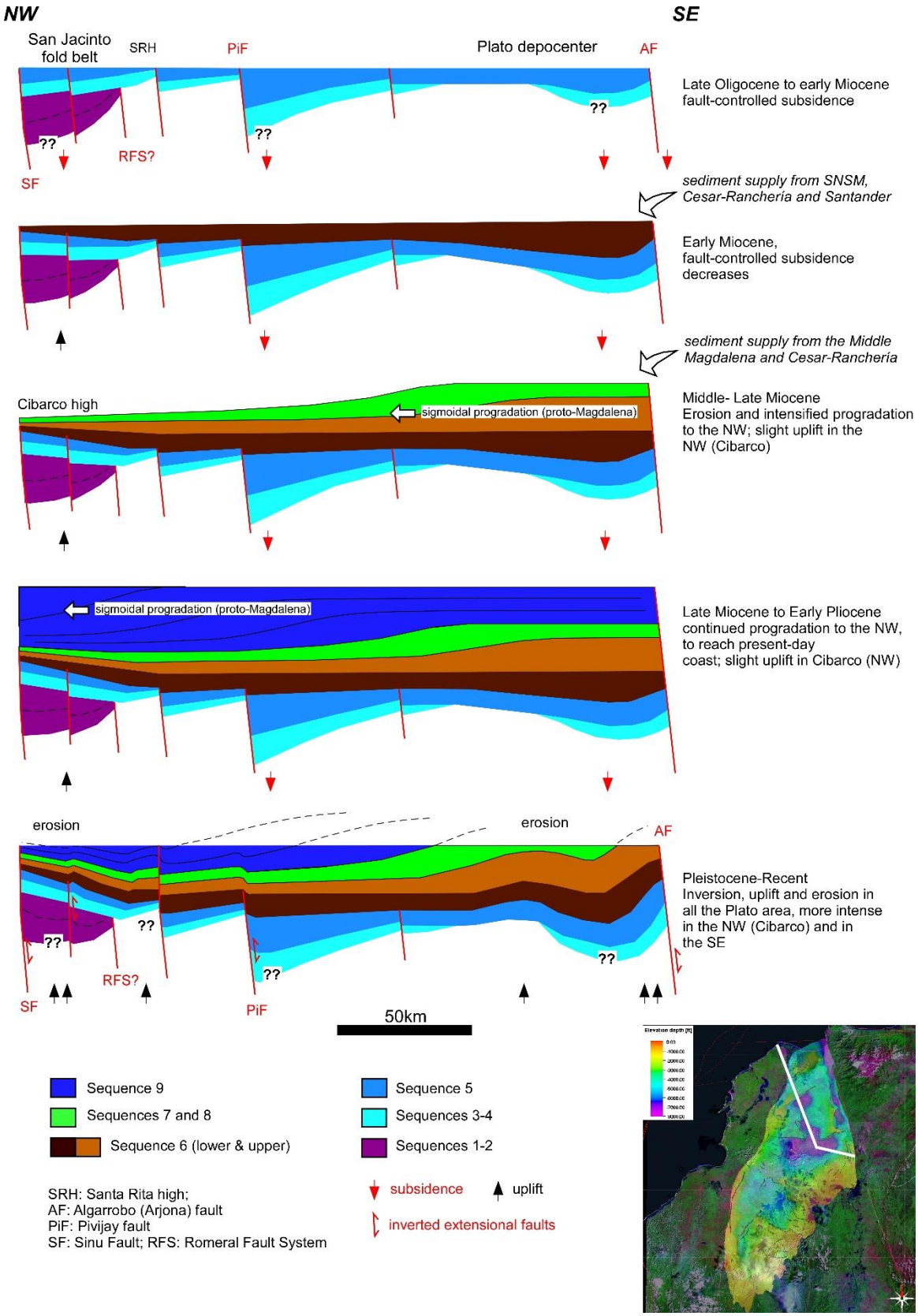

Figure 5.17. Simplified, Oligocene to Recent evolution of the LMV, as shown in a SE-NW-trending regional section. After Eocene to Middle Miocene fault-controlled extension, connection with the Middle Magdalena caused sigmoidal progradation to the NW of Sequences 7 to 9 in the Plato depocenter, until it became overfilled. Pleistocene to Recent shortening was responsible for the inversion of previous extensional faults and intense erosion towards the area of the Algarrobo fault (AF).

After the unconformity, there was a change in both sedimentation style and amount of sedimentary supply to the basin. The upper part of Sequence 6 (lower to middle Miocene) starts exhibiting progradation of deltaic clinoforms to the NW, indicating connections with important drainage systems, which supplied enormous amounts of sediments from the SE and S. At the same time, there was more development of forearc highs in the San Jacinto area, suggesting increasing sediment supply to the trench and continued underplating. The basin was still underfilled and mostly extensional, but it was possibly changing from sloped to ridged (sensu *Dickinson, 1995*), due to the occurrence of mainly submerged paleohighs (**Figure 5.18**). Fault controlled subsidence and NE-SW and SE-NW-trending extension continued active in the LMV.

Deposition in the LMV was quite stable from middle to late Miocene times (Sequences 7 and 8), but highly influenced by a well-established connection with the proto-Magdalena and Cauca drainage systems, which delivered abundant, mostly distal, fine-grained sediments to the basin. Therefore, the subduction channel was continuously lubricated by sediments delivered to the trench, while underplating and subsequent uplift in forearc high areas continued. An extensional regime prevailed in the LMV, though fault-controlled subsidence decreased with time and was gradually replaced by sagging.

A second important change in sedimentation occurred after the late Miocene unconformity, when upper Miocene to lower Pliocene Sequence 9 was deposited and partial erosion of Sequence 7 and 8 took place in the southern LMV. *Wijninga et al. (1996*), *Mora et al. (2008*), *Hoorn et al. (2010*) and *Mora et al. (2010b*) documented that the main phase of topographic growth in the Colombian Eastern Cordillera occurred between the late Miocene (~15 Ma) and Plio-Pleistocene (~3 Ma) while denudation rates were the fastest (*Mora et al., 2008*; *Caballero et al., 2013b*) and deformation rates reached the Cenozoic peaks (>8 mm/year, *Mora et al. 2013a*). Therefore, uplift in the eastern Cordillera and surrounding areas was increasingly more important for the shaping of the drainage systems, which delivered important amounts of sediments to the basin. From middle Miocene to Pliocene times, the morphology of the basin evolved from an underfilled, marine, sloped to ridged basin, to an overfilled, terraced to shelved, shallow marine forearc basin, with the occurrence of SSW-NNE-trending, submerged or locally emergent paleo-highs (**Figure 5.18**).

An important shortening event that affected the LMV, evident from seismic data, occurred shortly after the deposition of Sequence 9 (**Figure 5.10**b), in middle Pliocene times (~3.6 Ma, **Figure 5.13**). Erosion of older sequences, mainly 7 to 9, occurred in areas such as the Magangué-Cicuco high and southern LMV, while normal faults such as those bounding the San Jorge graben were slightly inverted. Such inversion was related to NE-SW-trending contraction, though SE-NW-trending contraction also occurred in the forearc highs (San Jacinto). This shortening event did not affect the overlying Plio-Pleistocene Sequence 10, as evidenced from the seismic data. Good examples of structures inverted by this tectonic event are shown in sections 1, 3 and 5 of **Figure 5.6**.

After the middle Pliocene shortening event, the subsidence and uplift patterns in the basin depocenters changed, and the north (Plato) was uplifted while the south (San Jorge) started rapidly subsiding by sagging (**Figure 5.13**, **Figure 5.16**). The deposition of transitional to continental Sequence 10 was influenced by the late Pliocene to Pleistocene peak deformation rates in the northern Andes (*Mora et al., 2008* and *Caballero et al., 2013a*), related to the final collision of Panamá and to the closure of the Central American Seaway (*O´Dea et al., 2016*). Since the northern LMV (Plato) became a positive relief area, offshore areas such as the Magdalena fan and the trench continued to receive huge amounts of sediment from the Magdalena River, and from the Sinú River farther south (**Figure 5.11**).

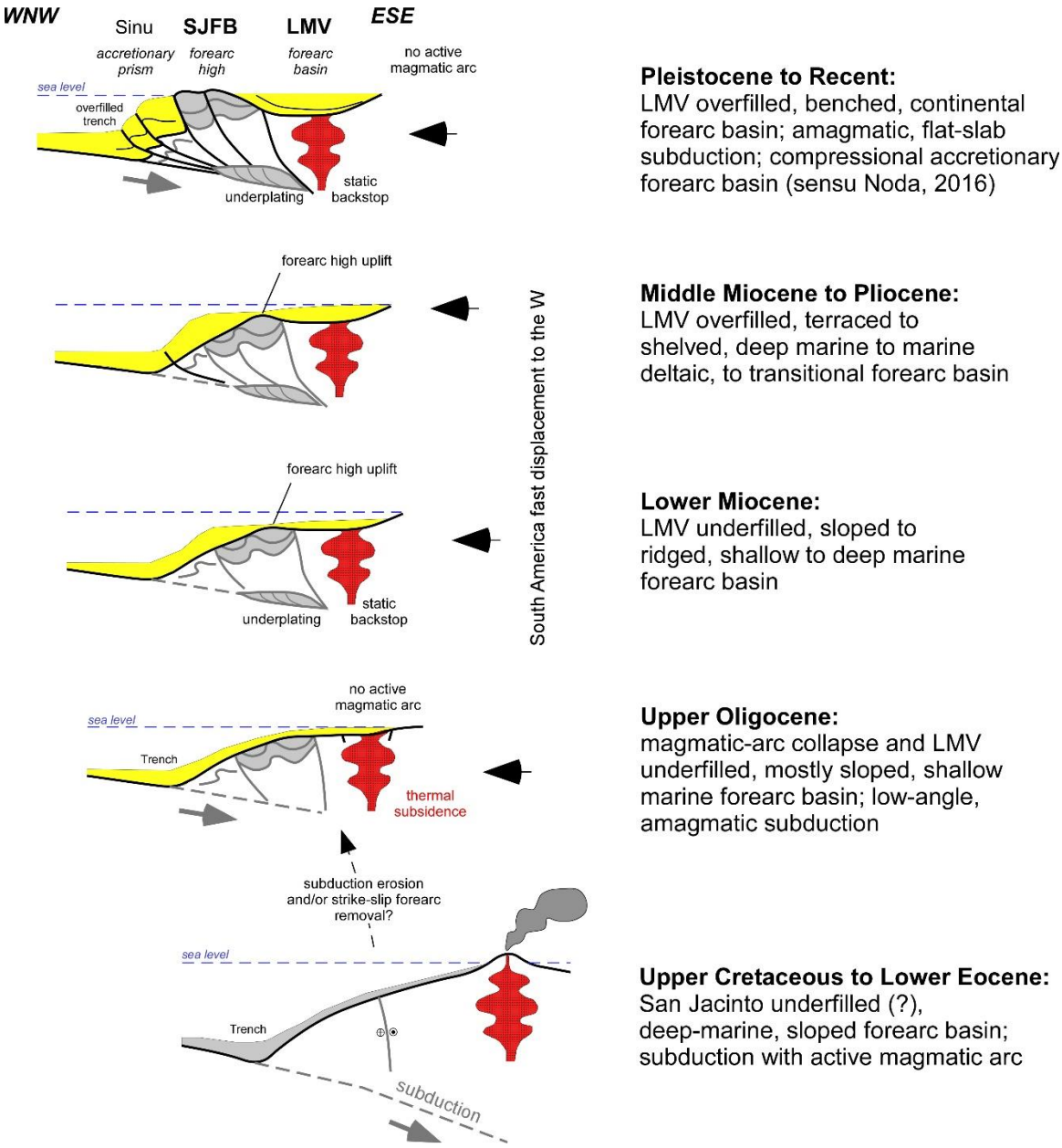

Figure 5.18. Interpreted evolution of the morphology of the LMV and San Jacinto from an Upper Cretaceous to Eocene underfilled, sloped forearc basin (sensu *Dickinson, 1995*) with an active magmatic arc, to the current amagmatic and overfilled, benched continental forearc basin. Increased Miocene sediment flux, the inherited basement structure and a flat-slab subduction were the main controls on Oligocene to Recent forearc basin evolution, as discussed in the text.

The San Jorge depocenter of the southern LMV continued sagging as fluvio-deltaic deposits of the proto-Cauca and San Jorge Rivers filled the lowest areas. In Pleistocene times (~1.7 Ma) the San Jacinto fold belt was tilted to the SE due to deep, northwest-verging thrusting occurring in the accretionary prism farther west (**Figure 5.6** to **Figure 5.8**). This tilting caused only subtle reactivation and localized inversion of structures within the Romeral Fault System. The uplift of the San Jacinto fold belt resulted in a more continuous forearc high, which would be the surface expression of continued underplating processes, driven by the high sediment supply to the trench. The development of a relatively continuous forearc high in San Jacinto was fundamental for the formation of the Sinú River valley, which became an additional and important source of sediments to the Morrosquillo Gulf offshore area. At the same time, it isolated the Cauca and San Jorge rivers and connected them to the Magdalena River in the north. Such processes produced the present-day

morphology of the basin, which can be described as an overfilled, benched, continental forearc basin (sensu *Dickinson, 1995*; **Figure 5.18**).

5.5.3 Tectonic segmentation and depocenter evolution in the LMV

Since middle Eocene times, the San Jacinto fold belt and the LMV became part of the same forearc basin, which deepened to the W, towards the trench area, as the accretionary prism started to develop. Upper Oligocene and Miocene depocenters were more developed in the north (Plato, **Figure C 2**b), and they migrated landward to the E, probably due to the development of forearc highs. In Pliocene times, after the north became overfilled, the southern depocenter (San Jorge) started becoming more important and it migrated landward (to the E). While the landward migration of depocenters is a distinctive feature of compressional accretionary forearc basins (sensu *Noda, 2016*), the depocenter shifting from north to south indicates tectonic segmentation into differentially subsiding zones, as seen in several forearc basins such as the Great Valley of California (*Angevine et al., 1990*; *Xie and Heller, 2009*; inset in **Figure 5.14**). Forearc basin segmentation has also been related to continental forearc basins formed in flat-slab subduction settings (*Ridgway et al., 2012*), where marked along-strike changes in basin configuration were related to insertion of wide fragments of thick crust. Other causes of forearc basin tectonic segmentation include bathymetric changes in the underlying subducted slab that isostatically impact the overlying plate (*Kobayashi, 1995*), and collision of crustal fragments in the subduction zone (*Clift and MacLeod, 1999*).

Our results suggest that the pre-Oligocene basement fabric in the LMV, which is different beneath each depocenter (*Mora et al., 2017a* and **Figure C 3**), was probably the main cause of the tectonic segmentation of the basin. The Oligocene extensional reactivation of inherited basement faults allowed the formation of the two depocenters, while later fault reactivations controlled the response of each depocenter to the regional stress regimes. For instance, the NE-SW-trending contraction that we document in the southern LMV after the deposition of Sequence 9 (**Figure 5.10**b) is perpendicular to the SE-NW contraction trend, which is directly related to the convergence vector of the Caribbean relative to South America (**Figure C 3**). Therefore, two possible tectonic events could be related to the NE-SW-trending contraction observed in the southern LMV (**Figure 5.13**). The first one could be the escape of the northwestern Andean block, which occurred after 11 Ma along the East Andean front fault zone in Colombia and the Boconó fault system in Venezuela, as implemented in the paleotectonic model of *Matthews et al., (2016;* **Figure 5.5**). The second one would be the collision stages of the Chocó-Panamá block with northern South America, occurring in late Miocene to Pliocene times (*Montes et al., 2015*; *O'Dea et al., 2016*), which could have also caused the selective reactivation of the basement faults in the LMV (**Figure 5.13**).

5.5.4 LMV Subsidence history and trends

Global studies of basin subsidence history (*Xie and Heller, 2009*) concluded that subsidence curves from forearc basins, as a group, have a diverse range of shapes, indicating that a variety of factors may contribute to basin subsidence. According to *Dickinson (1995*), there are four subsidence mechanisms in forearc basins: negative buoyancy of the descending slab, loading by the subduction (accretionary) complex, sediment or volcanic loading and thermal subsidence of the arc massif. Our results suggests that in the LMV, thermal subsidence of the arc and crustal thinning were more important initially (late Oligocene to middle Miocene), and then they were replaced by sedimentary loading as the main subsidence mechanism in the basin during the late Miocene to Recent. Flexural compensation due to sediment loading could have also occurred in the LMV, though it depends on the strength of the lithosphere (*Allen and Allen, 2005*).

Our subsidence curves (**Figure 5.13**) and burial history charts (**Figure C 1**) show that the most dramatic change in subsidence occurred after the early Miocene unconformity, between 17.3 and 12.7 Ma, when there was a notorious increase in subsidence with the deposition of Sequence

6. Initial subsidence of the oldest, Oligocene to lower Miocene, Sequences 5 and 6 was fault-controlled. Early to late Miocene subsidence related to Sequences 6 to 8 was much higher and reached values of 2.5 km in the axis of the Plato depocenter. It thus appears that as fault-controlled subsidence decreased, sediment supply increased and rapidly loaded the basin depocenters, causing subsidence by sagging. In late Miocene times (10-7 Ma), subsidence was interrupted by an uplift and erosion episode whose expression is the late Miocene unconformity (**Figure C 1**). After the late Miocene tectonic episode, subsidence re-started and was also higher in the Plato depocenter, where greatest thicknesses of the Tubará Sequence were preserved. Tubará subsidence was then abruptly interrupted by the middle Pliocene tectonic episode (**Figure C 1**) which caused intense erosion in the Magangué-Cicuco high and southern LMV. The final, well-documented subsidence episode in the LMV occurred in the south, where more than 2 km of mainly continental sediments of Sequence 10 (Corpa) were deposited in a sag basin.

Comparison with subsidence curves from other forearc basins in the world shows a fair match (*Angevine et al., 1990*, inset in **Figure 5.14**). Data from the few wells in the northern SJFB show that the area experienced lower but constant subsidence rates compared to the LMV, and the SJFB curves show a similar trend to other forerarc basins in the world. The data from the deep Plato depocenter in the northern LMV (steep pink curve in the inset of **Figure 5.14**) matches very well the trend of the Japan forearc basin reported by *Angevine et al. (1990*), while the data from other shallower areas in the LMV shows a less steep curve related to the lower amount of tectonic subsidence. The marked differences in subsidence rates and trends between the SJFB and LMV in Oligocene to Recent times show that while the main depocenters in the LMV were rapidly subsiding, the SJFB experienced much less subsidence, possibly due to the development of forearc highs. The high sedimentation rates in the LMV, especially in the Miocene, suggest that there was an important influence of sediment load in the total basin subsidence. Tectonic segmentation within both the LMV and the SJFB is also evident from the subsidence curves (inset in **Figure 5.14**).

5.5.5 Proposed mechanisms controlling LMV evolution

Our results and analyses allow us to conclude that the LMV is an amagmatic and tectonically segmented forearc basin. Among all the mechanisms controlling the evolution of forearc basins, we consider based on our results, that three mechanisms strongly controlled the evolution of the LMV. Such mechanisms are: sediment flux due to uplift and drainage evolution in hinterland areas, pre-existing basement fabric and configuration of the subducting plate.

Our reconstruction of the extension, subsidence, sedimentation and paleogeographic history suggests that sediment flux in the LMV was an important mechanism in controlling basin evolution because, 1) it supplied sediment to the trench and as a consequence, triggered underplating and uplift in forearc high areas, 2) it rapidly filled the basin, providing sedimentary loads which kept the depocenters subsiding, as fault-controlled subsidence became less effective, and 3) it defined the basin geometry and type. Due to the sediment flux, the LMV evolved from an underfilled, sloped, marine forearc basin to an overfilled, benched, terrestrial forearc basin (sensu *Dickinson, 1995*, **Figure 5.18**). Considering the classification by *Noda (2016*), the whole margin evolved from an extensional non-accretionary-type to a compressional accretionary-type forearc basin, and such evolution was strongly controlled by changes in sediment flux.

However, we consider that the pre-existing basement structural fabric underneath the LMV was also crucial for the formation and evolution of the LMV. Tectonic segmentation of the LMV with the formation of its two depocenters was possible due to the differential reactivation of the inherited, basement fault families identified under the Plato depocenter in the north and the San Jorge depocenter in the south (*Mora et al., 2017a*; **Figure C 3**). Such segmentation probably influenced the development of the proto-Magdalena and Cauca drainage systems and would therefore be the cause of the variations we see in terms of sedimentary thicknesses and facies from one depocenter to the other.

Concerning the configuration of the subducting plate, we have shown using paleo-tectonic models that tectonic plate kinematics and configuration were stable throughout the evolution of the

LMV (**Figure 5.5**). However, such evolution was probably influenced by the low-angle subduction of an irregular Caribbean oceanic plateau, which would have caused the along-strike tectonic segmentation and stratigraphic variations observed in the LMV, as observed in other similar basins (*Ridgway et al., 2012*). Moreover, though we relate uplift in the forearc highs with high sediment supply to the trench and underplating, it is possible that flat-slab subduction also influenced exhumation in forearc high areas and produced regional and local unconformities, as proposed by *Ridgway et al. (2012*). Flat-slab subduction would also be responsible for the lack of a magmatic arc in the LMV, a condition that would otherwise have formed a completely different forearc basin.

5.5.6 Implications for hydrocarbon potential

Because of their low geothermal gradients and the absence of good reservoir and source rock facies, forearc basins are not considered especially attractive targets for hydrocarbon exploration (*Dickinson and Seely, 1979*; *Brooks, 1990*; *Dickinson, 1995*; *Ridgway et al., 2012*). However, the LMV is an important hydrocarbon province in northern Colombia, where production is obtained from upper Oligocene to lower Miocene clastic and carbonate reservoirs of Sequences 5 and 6, accounting for ~7% of Colombia's gas production (*De Freitas et al., 2013*). We consider that due to its very particular history and characteristics, some of the obstacles for the development of petroleum systems in the LMV were partly overcome. In first place, tectonic segmentation allowed significant extension and high sediment flux to be focused in the two basin depocenters. A relatively continuous, high sediment supply from hinterland areas, taking place during ~15 Ma, allowed favorable conditions for hydrocarbon generation in a forearc setting. In spite of not very high geothermal gradients, the high sediment flux and rapid burial in a relatively short time, made possible the entrance of source rocks into the hydrocarbon generation window, as will be shown in *Chapter 6*. Tectonic segmentation allowed a complex sedimentary facies distribution, resulting in different source and reservoir qualities in each of the depocenters. Most gas and light oil fields in the LMV are located in basement highs around the northern Plato depocenter, where upper Oligocene to lower Miocene shallow marine clastic and calcareous reservoirs were deposited, while source rocks were rapidly buried to depths in excess of 3.5 km (12000 feet) in the central Plato depocenter. In the south (San Jorge), where fewer gas fields exist, conditions for hydrocarbon generation were not as favorable as in the north (*Chapter 6*), due to more intense shortening and erosion episodes (**Figure C 1**) and to the development of different quality source and reservoir rocks. Nevertheless, further research is required to assess the remaining hydrocarbon potential of the LMV, and of the forearc high areas to the W, in the San Jacinto fold belt, which also appears as an important exploration frontier in NW Colombia.

5.6 Conclusions

The formation of the Lower Magdalena amagmatic, forearc basin occurred in a stable setting from the Oligocene to the present, characterized by the slow and nearly orthogonal, low-angle subduction of the Caribbean plateau. In this work, we used a regional database to reconstruct the subsidence, extension, sedimentation and paleo-geographic history of the Lower Magdalena forearc basin, and to propose possible mechanisms controlling basin evolution, in the absence of major changes in plate kinematics and in a flat-slab subduction setting. Six Oligocene to Recent tectono-stratigraphic sequences were identified, comprising a general shallowing-upwards and progradational succession. We show that after the collapse of a pre-Oligocene magmatic arc, late Oligocene to early Miocene fault-controlled subsidence allowed initial basin fill at relatively low sedimentation rates. Extensional reactivation of inherited, pre-Oligocene basement faults was crucial for the tectonic segmentation of the basin with the formation of its two depocenters (Plato and San Jorge). Oligocene to early Miocene uplift of Andean terranes made possible the connection of the Lower and Middle Magdalena valleys, and the formation of the most important Colombian drainage system (Magdalena River system). The proto-Magdalena river in the north and the proto-Cauca river in the south both started delivering high amounts of sediment in middle Miocene times, as

fault controlled subsidence was gradually replaced by sagging, due to increased sedimentary load. Such an increase in sedimentation delivered huge amounts of sediments to the trench, causing the formation of an accretionary prism farther west of San Jacinto. This probably weakened the plate interface and caused underplating, with the development of forearc highs in the San Jacinto area. Inherited basement structures and flat-slab subduction of an irregular Caribbean plateau would be related to the along-strike basin segmentation and to the formation of two main depocenters (Plato and San Jorge), each one with particular subsidence and uplift histories and hydrocarbon potential. A stronger backstop under the Lower Magdalena explains shortening in the forearc high and accretionary wedge areas to the W, while the Lower Magdalena remained essentially unaffected. Our results highlight the fundamental roles of sediment flux, of inherited basement structure and of flat-slab subduction on the evolution of forearc basins such as the Lower Magdalena.

6 A Three-Dimensional Insight into the Lower Magdalena Valley Forearc Basin of NW Colombia: Implications for Thermal History and Petroleum Systems

This chapter is a reformatted version of a paper in internal revision. Supplementary figures have been placed in *Appendix D*.

Citation: Mora, J.A., Ondrak, R., Gonzalez, R., Oncken, O., Kinoshita, E., Serna, L., Zamora, W., Velez, V. and De Freitas, M., (in preparation). A Three-dimensional insight into the Lower Magdalena Valley forearc basin of NW Colombia: Implications for thermal history and petroleum systems. To be submitted to the AAPG Bulletin (American Association of Petroleum Geologists).

Abstract

A three-dimensional model of the Lower Magdalena Valley basin of NW Colombia was built from seismic and well data and used to reconstruct the thermal and maturation history of the basin. We reconstructed the stratal architecture of the basin, implemented within the model episodes of uplift and erosion, and constructed a geothermal gradient map, which was used to construct heat flow maps for 3-D modeling. Model results indicate that the onset of hydrocarbon generation occurred at ~15 Ma (middle Miocene) for upper Oligocene to lower Miocene hydrocarbon source rocks in the northern part of the basin (Plato depocenter), while younger lower Miocene sources started generating at ~ 9 Ma (middle-late Miocene). Maturation was influenced by sedimentation at very high rates of thick, deep marine to deltaic, Oligocene to upper Miocene sequences. Late Miocene generation was interrupted by shortening and uplift events at Pliocene (4-3 Ma) and Pleistocene times, though it appears to be ongoing in main depocenters. Low to fair source rock quality appears to be compensated by high thicknesses of the Oligocene to lower Miocene sources, which would still be generating below 3350 m (11,000 ft) in the main pod of active source rock in the northern Lower Magdalena (Plato depocenter). By contrast, the effects of shortening pulses and low heat flow would have inhibited maturation of Oligocene to lower Miocene source rocks in the San Jorge graben of the southern Lower Magdalena, suggesting the need of additional hydrocarbon sources to explain the dry gas occurrences in that part of the basin. Proposed additional sources are pre-Oligocene units preserved in the western San Jorge depocenter and biogenic generation.

Keywords: Lower Magdalena Valley basin, basin modelling, thermal and maturation history, petroleum systems, Colombia

6.1 Introduction

Forearc basins are commonly considered to have a low hydrocarbon potential due to poor reservoir facies development and low geothermal gradients (*Dickinson and Seely, 1979*; *Brooks, 1990*; *Ridgway et al., 2012*). However, there are examples of prolific forearc basins such as the Cook Inlet in Alaska and the Talara basin of Perú (*Dickinson and Seely, 1978*; *Janssen et al., 2012*). The Lower Magdalena Valley basin (LMV) of northwestern onshore Colombia (**Figure 6.1**) has been recently classified as a forearc basin (*Mantilla et al., 2009*; *Bernal et al., 2015b*; *Mora et al., 2017b*), in spite of the absence of an active magmatic arc. Precisely due to the lack of arc magmatism, the origin and evolution of the LMV have been recently related to flat-slab subduction of the Caribbean oceanic plateau beneath South America since Oligocene times (*Mora et al., 2017b*). The LMV is

considered a poorly explored basin that holds a moderate amount of hydrocarbon reserves, accounting for ~7% of Colombia's gas production (*De Freitas et al., 2013*). However, we consider that there might be significant underestimated potential, considering the poor understanding of the basin evolution and petroleum systems. Most of the previous regional studies were focused on the construction of a tectono-stratigraphic framework, paleo-geographic reconstructions and on the characterization of source, reservoir and sealing rocks (*Aleman, 1983*; *Beroiz et al., 1986*; *Hocol, 1993; ESRI-ILEX, 1995*; *ICP, 2000*; *Bernal et al., 2015b*; *Chapter 5* of this thesis). Other studies have dealt with the definition of petroleum systems based on geochemical analyses of rocks, fluids and gases (*Petrobras/Ecopetrol, 1996; ICP, 2000*; *Rangel et al., 2003*; *ANH, 2011b*). However, very few studies (e.g. *He, 2000*) have attempted an integration of the existing information into a three-dimensional model of the basin. The objective of this contribution is to present the results of an integrated, three-dimensional basin modelling of the LMV, which incorporates the plate tectonic and basin evolution, as well as the tectono-stratigraphic framework recently proposed by *Mora et al. (2017 a, b*) and in *Chapter 5* of this thesis, and to discuss implications on the petroleum systems.

The LMV has been a commercially-productive hydrocarbon province since the discovery of the El Difícil oil field in 1942. With the later discovery in the southern LMV (San Jorge depocenter) of the Jobo-Tablón field in 1946 and of the Cicuco field (1956) in the Magangué-Cicuco basement high (**Figure 6.1**), the basin became an important mainly gas-producing province. The most recent gas discoveries were Guepajé-Ayhombe (1992), La Creciente (2006) and Bonga-Mamey (2011) in the western Magangué-Cicuco high, and the Nelson (2012) and Clarinete (2015) dry gas discoveries in the western San Jorge depocenter. Source rocks are considered to be Oligocene to Miocene shallow marine to deltaic mudstones with mostly type-III kerogen (*ICP; 2000*), which would have generated hydrocarbons in the two main basin depocenters, the Plato depocenter in the north and the San Jorge depocenter in the south (**Figure 6.1**). Light oil and gas condensate is produced in basements highs surrounding the Plato depocenter to the east (e.g. Cicuco and El Dificil), while wet gas is produced in the western Magangué-Cicuco high (e.g. Bonga-Mamey, La Creciente), and dry gas is produced in the western San Jorge depocenter (e.g. Jobo-Tablón, Nelson and Clarinete). The most important uncertainties in terms of generation relate to the heat flow (present-day and past) and to source rock kinetics, though erosion also has a large uncertainty. Therefore, several scenarios of heat flow, kinetics and erosion were tested and the results will be discussed.

6.2 Geological Framework

The LMV and San Jacinto fold-belt (SJFB) of northwestern Colombia are located in an area in which the Caribbean oceanic plate, including the Chocó -Panamá block, and the South American continental plate have been interacting throughout the Cenozoic (inset in **Figure 6.1**). Though there has been some debate about the existence of a flat-subduction of the Caribbean under South America, beneath the Lower Magdalena Valley, recent geophysical studies (*Mantilla, 2007*; *Mantilla et al., 2009*; *Bernal et al., 2015a*; *Mora et al., 2017b*) have provided new and more robust evidence supporting a flat-subduction. The basin is then part of a subduction complex which includes an accretionary prism (Sinú) and forearc high (San Jacinto) to the W, and an inactive magmatic arc (northern Central Cordillera) to the E and SE (**Figure 6.1**). Flat subduction that apparently started in late Eocene to early Oligocene times (*Mora et al., 2017b*), could have caused slab refrigeration (*Dumitru, 1990*; *Dumitru et al., 1991*; *Stevens- Goddard and Carrapa, 2017*), which would have contributed to decrease the temperature and heat flow in the whole subduction complex.

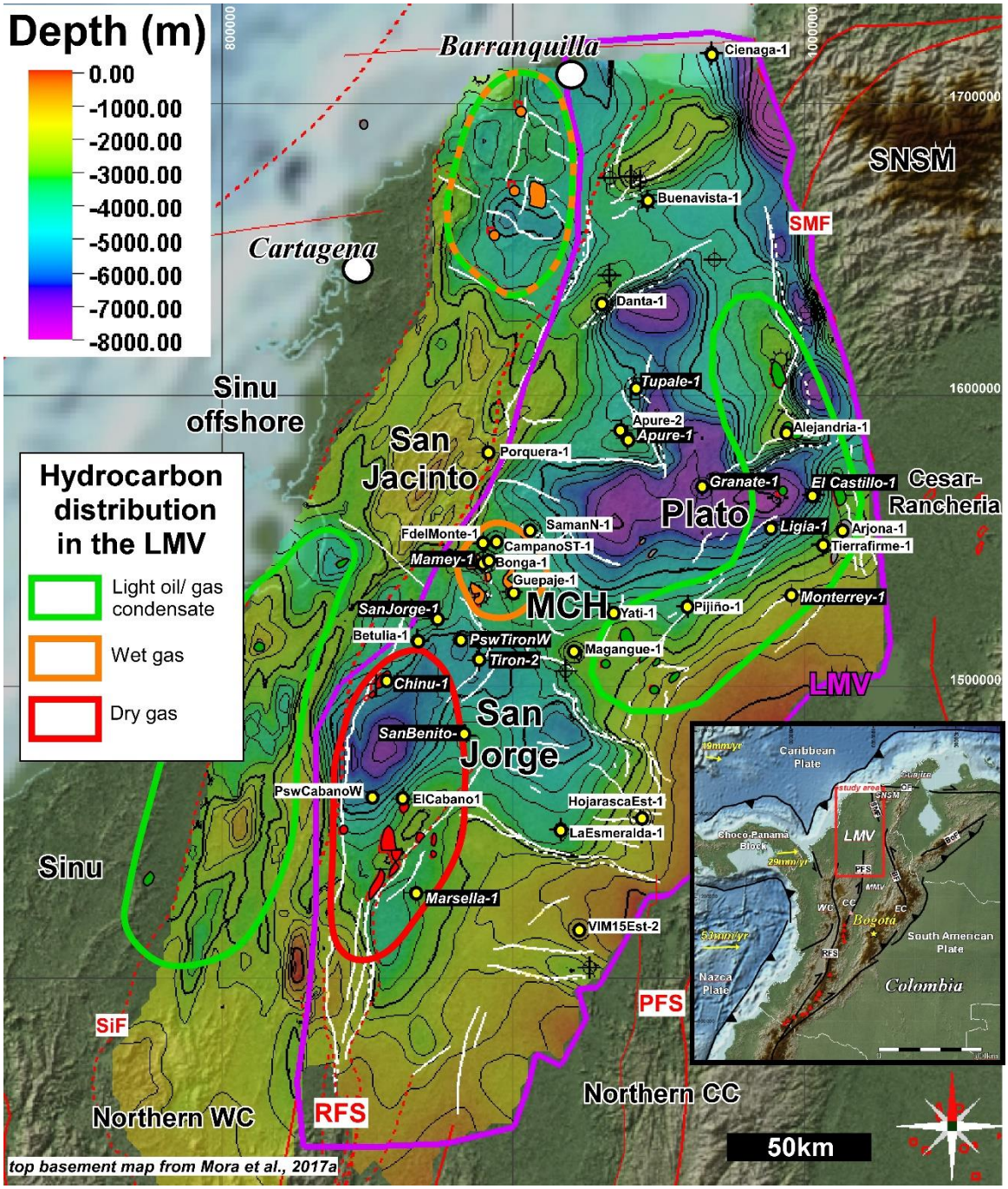

Figure 6.1. Location of the 3-D model, database and distribution of hydrocarbons in the Lower Magdalena Valley basin, showing the basement structure and the main structural provinces within the basin. The pink contour is the limit of the LMV and of the 3-D model; distinction between dry gas, wet gas and light oil/condensate accumulations (red, orange and green contours respectively with the corresponding fields depicted), was based on the relationship between produced oil condensate vs gas (bbls/MMscf). Calibration wells are shown in black labels with text in italics. LMV: Lower Magdalena Valley basin; MCH: Magangue-Cicuco high; RFS: Romeral Fault System; PFS: Palestina Fault System; SMF: San Marta Fault; SiF: Sinú Fault; SNSM: Sierra Nevada de Santa Marta; WC: Western Cordillera; CC: Central Cordillera. Inset, tectonic map of northwestern South America with topography and bathymetry, showing the location of the Lower Magdalena Valley basin (LMV), the Sinú-San Jacinto fold belt (SSJFB), and the active volcanoes. Present-day tectonic plate motions are shown in yellow (after *Trenkamp et al., 2002*). WC: Western Cordillera; CC: Central Cordillera; EC: Eastern Cordillera; RFS: Romeral Fault System; PFS: Palestina Fault System; BF: Bucaramanga Fault; SMF: Santa Marta Fault; OF: Oca Fault; BoF: Bocono Fault.

The LMV is a lozenge-shaped basin, covering an area of 42,000 km^2, located between two major basement terranes, the northern Central Cordillera (CC) in the S and SE and the Sierra Nevada de

Santa Marta (SNSM) in the NE (**Figure 6.1**). The Santa Marta left-lateral strike-slip fault is separating the northeastern part of the basin from the SNSM, while the northern extension of the Romeral Fault System (RFS) is separating the Lower Magdalena from the SJFB to the west. Pre-Oligocene sedimentary units are exposed in the SJFB, which is considered the northward extension of the Western Cordillera of Colombia (*Barrero et al., 1969*; *Duque-Caro, 1979*; *Cediel et al., 2003*) and is related to an oceanic-type basement. The RFS, which is also considered to continue from the south to form the western boundary of the LMV, appears to be separating the oceanic to transitional basement under the belt from the felsic continental basement of the South American crust which floors the LMV in the east (*Duque-Caro, 1979*, *Flinch, 2003*; *Mora et al., 2017a*). *Mora et al. (2017a*) recently proposed the presence of oceanic affinity terranes in the basement of the western LMV, suggesting that the complexity of the RFS described farther south in maps and outcrops between the Central and Western Cordilleras, continues to the north. In fact, the northern extension of the RFS is also an important tectonostratigraphic feature as shown by the different stratigraphic successions which are preserved on both sides of the fault system (**Figure 6.2**). In the SJFB, located east of the RFS, there are Upper Cretaceous to Eocene sedimentary units which are not preserved in the LMV to the east (*Duque-Caro, 1979*; *Mora et al., 2017b*). By contrast, Oligocene to Recent units, which have been mostly eroded in the SJFB, are very well preserved in the LMV.

6.2.1 The Basement of the LMV

The basement under the LMV is considered to be the extension the basement terranes, which outcrop in the northern CC and therefore consists of a core of Permo-Triassic metamorphic and igneous rocks, which were intruded by Upper Cretaceous granitoids *(Silva et al., 2016*; *Mora et al., 2017a*). However, the existence of an oceanic affinity terrane in the basement of the western LMV was recently proposed, based on Hafnium isotope geochemistry of an Upper Cretaceous pluton (Bonga pluton, *Mora et al., 2017a*). In terms of basement fabrics, the basement of the LMV comprises extensional faults with two predominant orientations, a main SE-NW trend in the western half of the basin and a secondary SW-NE trend in the northeastern part (*Mora et al., 2017a*; **Figure 6.1**). Such structural grain was formed by several mechanisms including the Romeral and Palestina strike-slip movement, Jurassic rifting and Late Cretaceous to Eocene forearc extension due to oblique convergence (*Mora et al., 2017a*). The extensional reactivation of the pre-existing basement fabric was crucial for the subsidence and sedimentation history of the LMV basin.

6.2.2 Upper Cretaceous to Lower Oligocene sequences in the SJFB

The SJFB records the existence of a Late Cretaceous to Early Eocene forearc basin which was inverted and fossilized in Early to Middle Eocene times and was then covered by Middle Eocene to Lower Oligocene clastics (*Mora et al., 2017b*). *Mora et al. (2017b*) divided the sedimentary succession in the SJFB into four tectono-stratigraphic sequences, bounded by regional unconformities which relate to major tectonic events (**Figure 6.2**). The two older Upper Cretaceous to Lower Eocene sequences (Sequence 1- Cansona and 2- San Cayetano) are preserved mainly to the west of the RFS, while the younger Middle Eocene to Lower Oligocene sequences (3- Chengue and 4- San Jacinto), fossilized and sealed the RFS as they extended farther to the east, into the western LMV.

6.2.3 Upper Oligocene to Recent units in the LMV

The Oligocene to Recent units in the LMV were subdivided into six sequences according to my proposal in Chapter 5, and here we will follow such subdivision and sequence numbering (**Figure 6.2**). Structural maps in depth of the main stratigraphic surfaces are depicted in **Figure 6.3**.

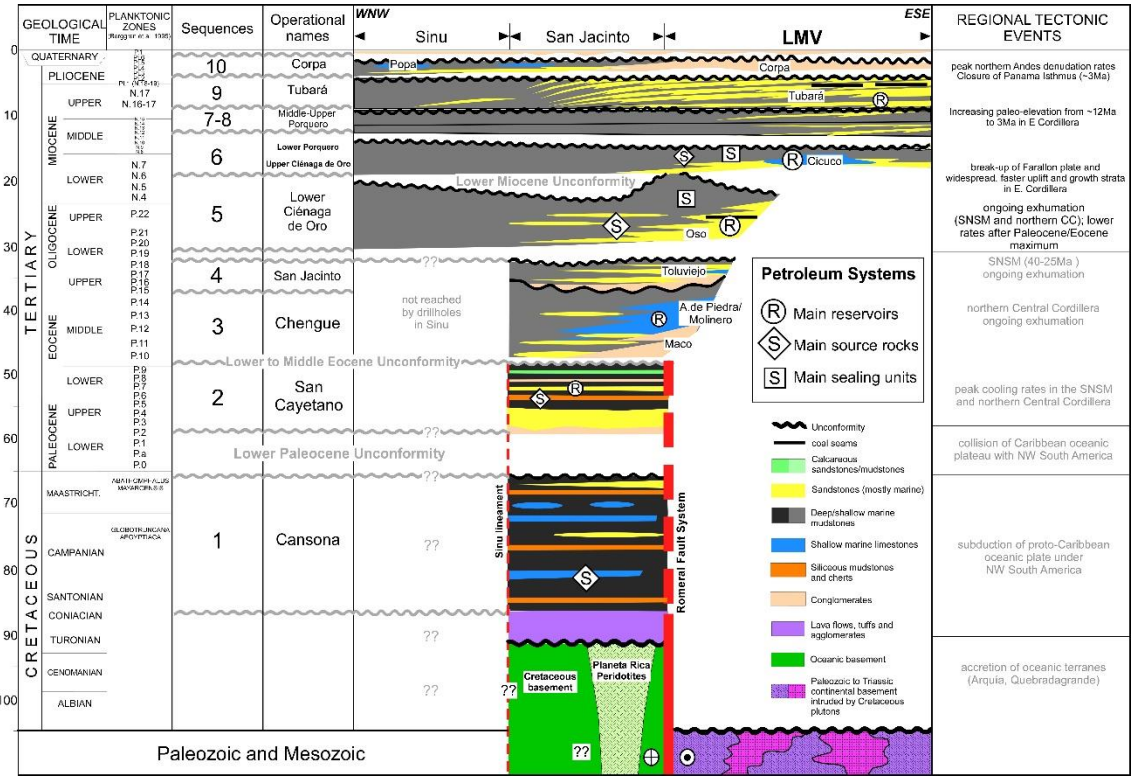

Figure 6.2. Stratigraphic column of the LMV, San Jacinto and Sinú fold belts, based on different sources (e.g. *Hocol, 1993*; *ICP, 2000*; *Guzman, 2007*; *Mora et al. 2017b* and *Chapter 5*). Biostratigraphy is based on numerous papers and industry reports by *Duque-Caro (1979, 1984, 1991, 2000, 2001)*, and tectonic events are after *Villagómez et al. (2011a, b)*, *Parra et al. (2012)*, *Saylor et al. (2012)*, *Mora et al. (2013a)*, *Caballero et al. (2013a, b)*, *Mora et al. (2015)*, *De La Parra et al. (2015)*.

6.2.3.1 Sequence 5: Upper Oligocene to lowermost Miocene

Though Eocene deposits could exist at the base of the some depocenters of the LMV, the oldest and clearly identified sedimentary deposits correspond to the Oligocene to early Miocene Sequence 5 (see *Chapter 5*, **Figure 6.2**), equivalent in outcrops to the El Carmen Formation (*Duque-Caro, 1972; Duque et al., 1996*; *ICP, 2000*; *Guzman et al., 2004*; *Guzman, 2007*). This unit crops out in the eastern flank of the SJFB where it has been described as a dark grey mudstone succession with abundant planktonic foraminifera and local development of sandy layers towards the base (Oso and Nepomuceno sandstone members, *Duque-Caro et al, 1996*; *Guzman, 2007*). Well data from the western LMV show that the sequence is transgressive and was deposited in shallow marine environments (details *Chapter 5*). The age of this unit has been constrained by planktonic foraminiferal zonations (*Blow, 1969*; *Duque-Caro et al., 1996*) and includes the zones P.18 to N.6, comprising the Oligocene to Lower Miocene (Burdigalian). The sequence exhibits the highest thicknesses in the western part of the LMV, towards the San Jacinto fold belt, where more than 1.5 km would be preserved in local depocenters (**Figure 6.4**). This sequence is informally called Lower Cienaga de Oro (*Hocol, 1993*; *ICP, 2000*).

6.2.3.2 Sequence 6. Lower to middle Miocene

The lower to middle Miocene sedimentary sequence (Sequence 6, according to *Chapter 5*), has been well studied in several outcrops of the northeastern SJFB such as the Carmen-Zambrano stratigraphic section, where biostratigraphic zonations based on planktonic foraminifera were made (*Petters and Sarmiento, 1956*; *DePorta, 1962*; *Stone, 1968*; *Duque et al., 1996*; *Guzman et al., 2004*; *Guzman, 2007*). It consists of mudstones with local development of sandstones and limestones (Barcelona Member), which were deposited in wave-dominated delta and prodelta environments (*Guzman, 2007*). The unit has been related to the planktonic zones N.7 to N.10 (Burdigalian to Serravallian, *Duque-Caro et al., 1996*; *Guzman, 2007*), and it is commonly limited at the base by a regional Early Miocene (Burdigalian) unconformity. Thickness maps from well and seismic data show that average thickness of the sequence is 400-600 m (1200-2000 ft) and that it is thickest in the eastern Plato depocenter where more than 2.5 km (>8000 ft) of Lower to Middle Miocene deposits are preserved (**Figure 6.4**). This sequence is informally called Upper Ciénaga de Oro (*Hocol, 1993*; *ICP, 2000*).

6.2.3.3 Sequences 7 and 8: Middle to upper Miocene

The middle to Late Miocene succession (Sequences 7 and 8, Chapter 5) has been studied in the Carmen-Zambrano and other stratigraphic sections and has been called Hibácharo, (Upper) Porquero and Mandatú Formation (upper unit of the Rancho Group, Guzman, 2007). The Mandatú Formation in the Carmen-Zambrano area displays a deepening-upward pattern, grading from tidal mud-dominated delta-front deposits to deeper mudstone deposits with slump structures (*Guzman, 2007*). This succession has been related to the planktonic foram zones N.11 to N.15 (Serravallian to Tortonian, *Duque-Caro et al., 1996*; *Guzman, 2007*) and is also limited at the bottom by a middle Miocene (Serravallian) unconformity. These sequences are informally called Middle and Upper Porquero (*Hocol, 1993*; *ICP, 2000*).

6.2.3.4 Sequence 9: Upper Miocene to lower Pliocene (Tubará)

A regional late Miocene unconformity separates the late Miocene fine-grained, deltaic units from a coarser-grained succession, which receives different names according to its locality (Zambrano, Cerrito and Tubará; *Duque-Caro et al., 1996*; *Guzman, 2007*) and which corresponds to Sequence 9 according to Chapter 5 (**Figure 6.2**). The interpreted depositional environment for this succession is much more proximal and consists of transitional to continental deposits which have been related to the N.17 to PL.2 planktonic foram zones, spanning from the late Miocene (Tortonian) to the early Pliocene (*Duque-Caro et al., 1996*; *Guzman, 2007*). In this work we will use the name "Tubará" for this succession, which displays the northwestward migration of shelf margin clinoforms in the Plato depocenter.

6.2.3.5 Sequence 10: Upper Pliocene to Pleistocene (Corpa)

The youngest sedimentary package that will be studied in this work, comprises continental to transitional, mostly coarse-grained, late Pliocene to Pleistocene deposits, which as usual, receive different names according to the locality and facies (Sincelejo, Betulia, Corpa and Popa, *Duque-Caro et al., 1996*; *Guzman, 2007*). While the names "Sincelejo" and "Corpa" refer to coarse-grained fluvial to transitional deposits, flood-plain and lacustrine deposits have been called "Betulia", and shallow-marine limestones which outcrop in the northernmost SJFB have been called "Popa" (*Duque-Caro et al., 1996*; *Guzman, 2007*). In this work we will call "Corpa" this late Pliocene to Pleistocene thick succession, which is mostly preserved in the southern LMV, and which corresponds to Sequence 10 according to the proposal in *Chapter 5* of this thesis.

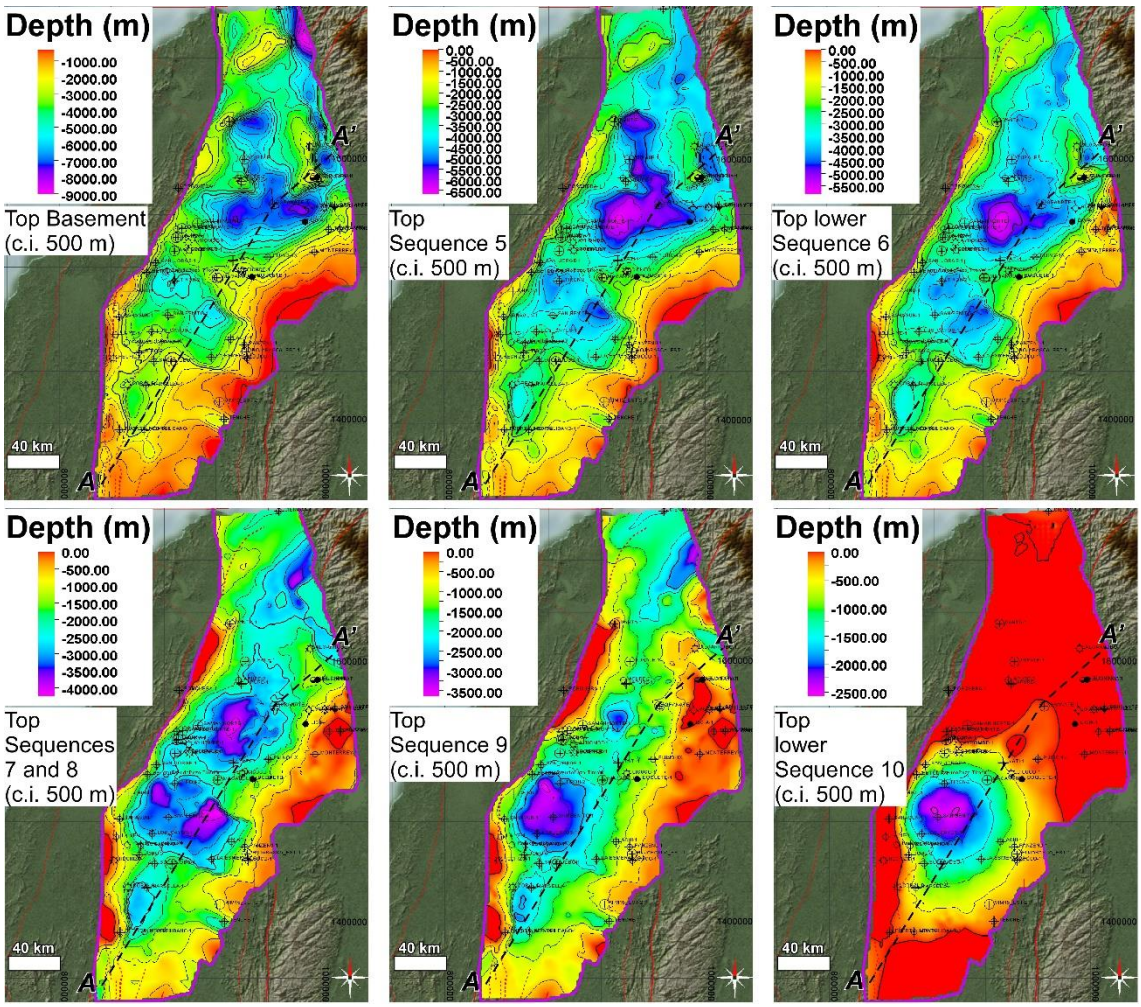

Figure 6.3. Maps of tops of the main tectono-stratigraphic sequences implemented into the PetroMod 3-D model. The top basement map merges with the Eocene unconformity in the western LMV. AA' indicates location of the transect shown in **Figure 6.6**.

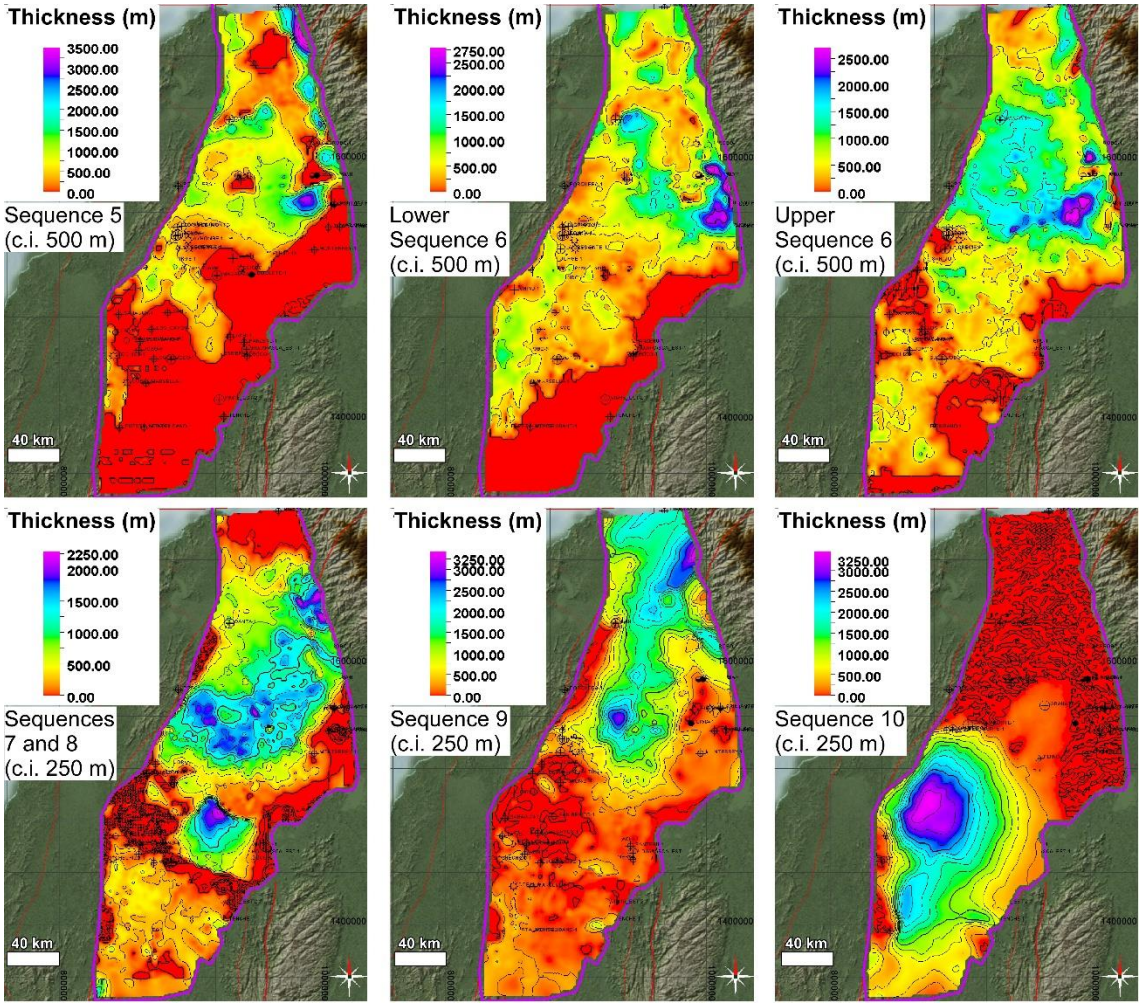

Figure 6.4. Thickness maps of the main tectono-stratigraphic sequences in the model area, as implemented into the program PetroMod.

6.2.4 Sedimentary petrology and provenance

The sedimentary infill of the LMV comprises an overall coarsening- and shallowing-upwards succession, typical of forearc basins, which display more distal marine facies towards the W and NW. However, tectonic segmentation of the basin in two main depocenters (**Figure 6.1**), possibly related to flat subduction (*Chapter 5*), caused that both depocenters had a different subsidence and uplift history, as well as different facies distribution. Due to its marine, fine-grained nature, the sequence has fairly good microfossil content, especially planktonic foraminifera which have allowed the identification of foram zones as those proposed by *Petters and Sarmiento (1956*) and *Blow (1969*), for the biostratigraphic dating of the succession and initial paleo-bathymetric interpretations (*Duque-Caro, 1979; 1984; 1991*). Hence, micro-paleontological planktonic foram zonations have been relevant for performing seismic ties with the wells and for the proper identification and interpretation of the depositional sequences in the reflection seismic data. The coarse-grained fractions which are more preserved in the E and SE and towards the base of the stratigraphic sequences, comprise litharenites, sublitharenites and lithic and feldspathic arkoses and quartzarenites, with the development of carbonates on some basement paleohighs. However, most of the basin infill comprises fine-grained, terrigenous and also calcareous claystones and siltstones. Sediment source areas have been located in the E, SE, NE and S, and correspond to the unroofing

of basement and sedimentary units which are reported in the Eastern, Central and Western Cordilleras towards the SE and S, and of the Sierra Nevada de Santa Marta (SNSM) and Perijá massifs towards the E and NE. Sediments in the eastern and southeastern portions of the basin exhibit a higher influence of Permo-Triassic and older basement rocks with continental affinity of the Central and Eastern Cordilleras, while sediments in the western and southwestern portions display more influence of Cretaceous allochtonous terranes with oceanic affinity of the Western Cordillera (see *Chapter 5*).

6.2.5 Structural geology and basin geometry

The San Jacinto fold belt and the Lower Magdalena Valley were both formed in a forearc setting which resulted from the interaction between the Caribbean oceanic plateau with the northwestern corner of the South American continental plate (*Duque-Caro, 1979*; *Mantilla et al., 2009*, *Bernal et al., 2015a*, *Mora et al., 2017 a,b*). Following the early Eocene tectonism, the area of the Romeral Fault System (RFS) collapsed and allowed the deposition mostly to the west of the fault system, of the Middle Eocene to Lower Oligocene Chengue and San Jacinto sequences, between 45 and 30 Ma. The Oligocene collapse of the Upper Cretaceous to Eocene magmatic arc to the east of the RFS allowed the deposition of marine Upper Oligocene to Recent sequences in both the LMV and the San Jacinto fold belt. Oligocene to Recent sedimentation was focused in two main depocenters within the LMV, separated by a SE-NW-trending basement high, called the Magangué-Cicuco High. The deeper Plato depocenter is located in the northern half of the basin, which the San Jorge depocenter, which is a SE-NW-trending graben, is located in the southern half. While flat subduction has been suggested as a cause of the observed along-strike variations in structure and stratigraphy, the high sediment supply, especially after early Miocene times, provided the sedimentary load, which kept subsidence ongoing, and also allowed the burial of potential source rocks into oil-window depths (*Chapter 5*).

For 3D-modeling purposes we consider here four regional Oligocene to Recent unconformities, which are related to uplift and erosion events: Earliest Miocene, late Miocene, middle Pliocene and Pleistocene to Recent (*Chapter 5*, **Figure 6.2**). The earliest Miocene unconformity spans from 23 to 17.3 Ma and separates the Sequence 5 from Sequence 6. Reflection-seismic data showed the existence of localized upper Oligocene to lower Miocene paleo-highs in the western LMV, close to the boundary of the San Jacinto fold belt, where these sequences are thinner or can even be absent. During the deposition of Sequences 6 to 8 in middle to late Miocene times, subsidence was much higher in the northern Plato depocenter compared to the southern San Jorge depocenter (*Chapter 5*). In late Miocene times, the southern and central LMV were uplifted and large parts of the Lower to Middle Miocene succession were eroded, especially in the Magangué-Cicuco high. The late Miocene unconformity, spanning from 12.7 to 11.9 Ma and separating the Upper Porquero and the Tubará Sequences, is related to this uplift pulse. After 11.9 Ma, subsidence restarts in the Plato depocenter, allowing the deposition of thick fluvio-deltaic sediments of the Late Miocene-Early Pliocene Tubará Sequence. The southern LMV is uplifted again in middle Pliocene times, causing the erosion of important thicknesses of underlying sequences, especially the Tubará sequence. The expression of this uplift phase is the impressive, angular, Middle Pliocene unconformity, spanning from 3.6 to 3.1 Ma, separating the Tubará from the Corpa Sequences. While the LMV has remained an extensional area to the present-day, Pleistocene (~1.7 Ma) contraction and inversion deformed the San Jacinto area and created the west-verging San Jacinto fold belt. However, a digital-elevation model of the LMV shows that today there is active subsidence in the San Jorge graben while the Plato depocenter has been slightly uplifted and is a subtle positive feature (*Chapter 5*).

6.3 Conceptual geological model

We used a regional database provided by Hocol S.A. for the construction of the 3D model presented here, including most of the reflection-seismic and drill hole data in the basin and surrounding areas. In this study we have integrated previous interpretations and maps of the acoustic basement presented by *Mora et al. (2017a*), as well as those of Oligocene to Recent stratigraphic sequences studied in *Chapter 5*. We also integrated information from several geological mapping and sampling reports which have been carried recently along the fold belt (*Guzman et al., 2004*; *B&G, 2006*; *Guzman, 2007*; *ATG-ANH, 2009*; *Ecopetrol/ICP, 2014*).

6.3.1 Tectono-stratigraphic model

To construct the tectono-stratigraphic model, we carried out regional seismic interpretation and mapping in two-way-time (TWT) of the main sequences described by in *Chapter 5* in Schlumberger's Petrel v.2013 software. The following sequences were interpreted and mapped: 1) near top of the basement, equivalent to the west to the middle Eocene unconformity; 2) near top upper Oligocene (top P.20 to P.22 planktonic foram zones); 3) Lower Miocene (top N.7 zone); 4) Middle Miocene (top N.8 to N.11 foram zones); 5) Upper Miocene unconformity, equivalent to the base of the Sequence 9 (Tubara); 6) Middle Pliocene unconformity, equivalent to the base of the Sequence 10 (Corpa); 7) Lower Pleistocene, equivalent to the top of the lower part of Sequence 10; 8) Topography, equivalent to the top of Sequences 9, 10 and recent deposits. For thermal modeling, we depth-converted the maps obtained in Petrel and exported them as surface maps to Schlumberger´s PetroMod v. 2011.1.1 software, and lithologies as indicated by facies distribution were assigned.

Thickness and depth maps show similar trends and values as those presented in previous studies (e.g. *ICP, 2000*), though the database we used is more complete (**Figure 6.3** and **Figure 6.4**). Based on regional seismic interpretations, integrated with well and outcrop data, we built erosion maps which were implemented in the 3-D model (**Figure 6.5**). The basin infill is thickest in the southeastern Plato depocenter where in spite of the lack of deep well data, our seismic interpretations suggest that the basement is found at ~ 8 km (~24,000 ft). In the deepest San Jorge depocenter of the southern LMV, the basement would be found at ~6.5 km (~21,000 ft). The oldest sequence (upper Oligocene to lower Miocene Sequence 5) is thickest towards the San Jacinto fold belt to the W (~1.5 km = ~ 5,200 ft), though high thicknesses may also be preserved in the deep Plato depocenter (see *Chapter 5*). Lower to middle Miocene deposits (Sequence 6) are thickest in the eastern Plato depocenter where at least ~3.6 km (~12,000 ft) would be preserved, considering that the base of the sequence has not been reached by any well. High thicknesses of the middle to upper Miocene sediments of Sequences 7 and 8 were also deposited especially in the northern LMV (Plato), though important thicknesses were eroded in some areas such as the Magangué-Cicuco high (**Figure 6.5**). Consequently, more than 2 km (6,500 ft) of sediments corresponding to Sequence 9 are preserved in the Plato depocenter. After Sequence 9 filled the northern part of the basin, important thicknesses of this sequence were eroded in middle Pliocene times (**Figure 6.5**). In late Pliocene to Pleistocene times, more than 3 km (10,000 ft) of fluvio-deltaic to lacustrine deposits of the proto-Cauca river, corresponding to Sequence 10, were unconformably deposited and are mostly preserved in the southern LMV (San Jorge depocenter, see *Chapter 5*).

6.3.2 Erosion events

Four main erosion events were identified in the study area. The oldest one, of early Miocene age, appears to be the less important in terms of eroded thicknesses (**Figure 6.5**). A second, late Miocene tectonic event, corresponding to the base of Sequence 9 (Tubará), was responsible for the erosion of important thicknesses of Sequences 7 and 8 especially in the Magangué-Cicuco high. The third

erosion event corresponds to the base of Sequence 10 (Corpa) and accounts for the erosion of Early Miocene shortening caused the erosion of the upper, fine-grained portion of Sequence 5 in most of the basin. A middle Pliocene event accounted for the erosion of most of Sequence 9 in the southern LMV, where only a thin basal part of this sequence is preserved. The fourth, Pleistocene to Recent shortening event was responsible for the uplift of the northern LMV (Plato) and for the final tilting and contraction in the San Jacinto fold belt towards the W, causing the intense erosion of most of the Oligocene to recent units.

According to the identified erosion events, we used the Petrel software to construct erosion maps that were exported and added to the PetroMod 3D model. Using seismic, outcrop and well data, we calculated the possible original depositional stratigraphic thickness of each sequence and constructed the respective original thickness maps. We also constructed maps of the preserved thickness of each sequence. Finally, we obtained approximated eroded thickness maps from the difference between the previously constructed thickness maps (original vs preserved). Though the LMV has remained relatively undeformed, we showed in *Chapter 5* that uplift pulses accounted for the erosion of considerable parts of the stratigraphic defined sequences. Therefore, our erosion estimates are an approximation and can imply an important error, which will affect the modeling results. Of all the erosion events, the early Miocene unconformity implies the least erosion, being related to the removal of 50 to 120 m of section of Sequence 5 in the western and northwestern LMV (**Figure 6.5**a). In the southeastern LMV and in the eastern Maganagué-Cicuco High, 500 to 1000 m of section corresponding to Sequences 7 and 8 of the Porquero unit has been removed by the late Miocene erosional event (**Figure 6.5**b). The middle Pliocene erosive event would have removed more than 1 km of sediments of Sequence 9 (Tubará) in the southern LMV while the Pliocene to Recent shortening event was more intense in the northeastern LMV, where 700 – 1000 m of section mostly corresponding to Sequences 8 to 10 were removed.

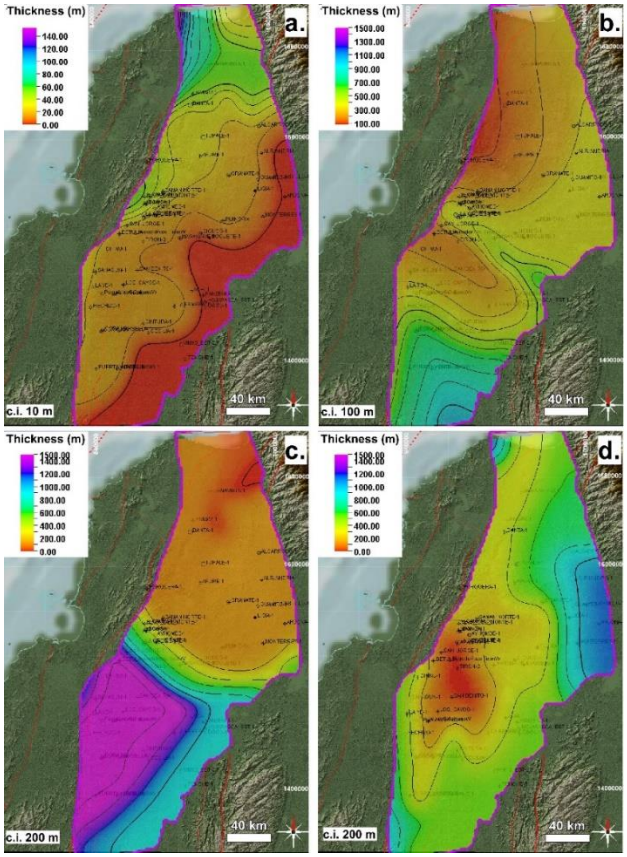

Figure 6.5. Erosion maps implemented in the 3-D model. a). Erosion related to the lower Miocene unconformity; b) erosion related to the upper Miocene unconformity; c) erosion related to the Pliocene unconformity and d) erosion related to Pleistocene to recent uplift and erosion.

6.3.3 Facies and lithology distribution

Based on previous regional facies maps and paleogeographic reconstructions (*ICP, 2000*; *Chapter 5),* we interpret that Sequence 5 was a shallow-marine, transgressive sequence which onlapped the basement from W to E, filling paleo-topographic lows. Its lower part of upper Oligocene age, comprises reservoir facies while its upper part is fine-grained and comprises organic-rich mudstones. These mudstones of Sequence 5 are considered to be important source rock intervals in the basin. Lower to Middle Miocene Sequence 6 was deposited in wider areas farther to the E and also has a lower, transgressive clastic and carbonate portion which also has reservoir facies. Its upper portion exhibits a progradational pattern from E to W and displays deltaic facies, which are both reservoir and source rocks. Lower to middle Miocene deposits reflect the connection of the LMV with the northern Middle Magdalena Valley basin (MMV), and the formation of the Magdalena River system, which started to discharge huge amounts of sediments in the eastern LMV. Middle to Upper Miocene Sequences 7 and 8 consist of mostly fine-grained, deltaic to deep marine deposits which continue prograding to the WNW and are mainly sealing and overburden units. Upper Miocene to Lower Pliocene Sequence 9 displays coarser-grained delta plain deposits, which represent the overfilling of the northern LMV (Plato, *Bernal et al., 2015b*; *Chapter 5*) by the proto-Magdalena river. Upper Pliocene to Pleistocene deposits of Sequence 10 (Corpa), which are mostly preserved in the southern LMV (San Jorge) are fluvio-deltaic and prograde from S to N, representing a thick overburden in the San Jorge depocenter. These deposits correspond to the advance to the north of the proto-Cauca river, which filled the southern part of the LMV (*Chapter 5*). **Figure 6.6** shows the proposed facies distribution both in cross section view and an example of a facies map of the lower half of Sequence 5.

According to the previously described facies types and distribution, and taking into account previously constructed paleogeographic maps for each sequence (*Chapter 5*), we defined 30 facies types, each one with an assigned lithology. Petroleum system elements (source rock, reservoir, seal, etc.) were assigned to the respective facies. For the source rock facies, TOC (Total organic carbon) and HI (hydrogen index) maps were included, based on the regional compilation of geochemical data. A summary of the ages, horizons, depth maps, erosion maps, layers, facies maps and petroleum system elements implemented in the 3D model is shown in **Table 6.1**.

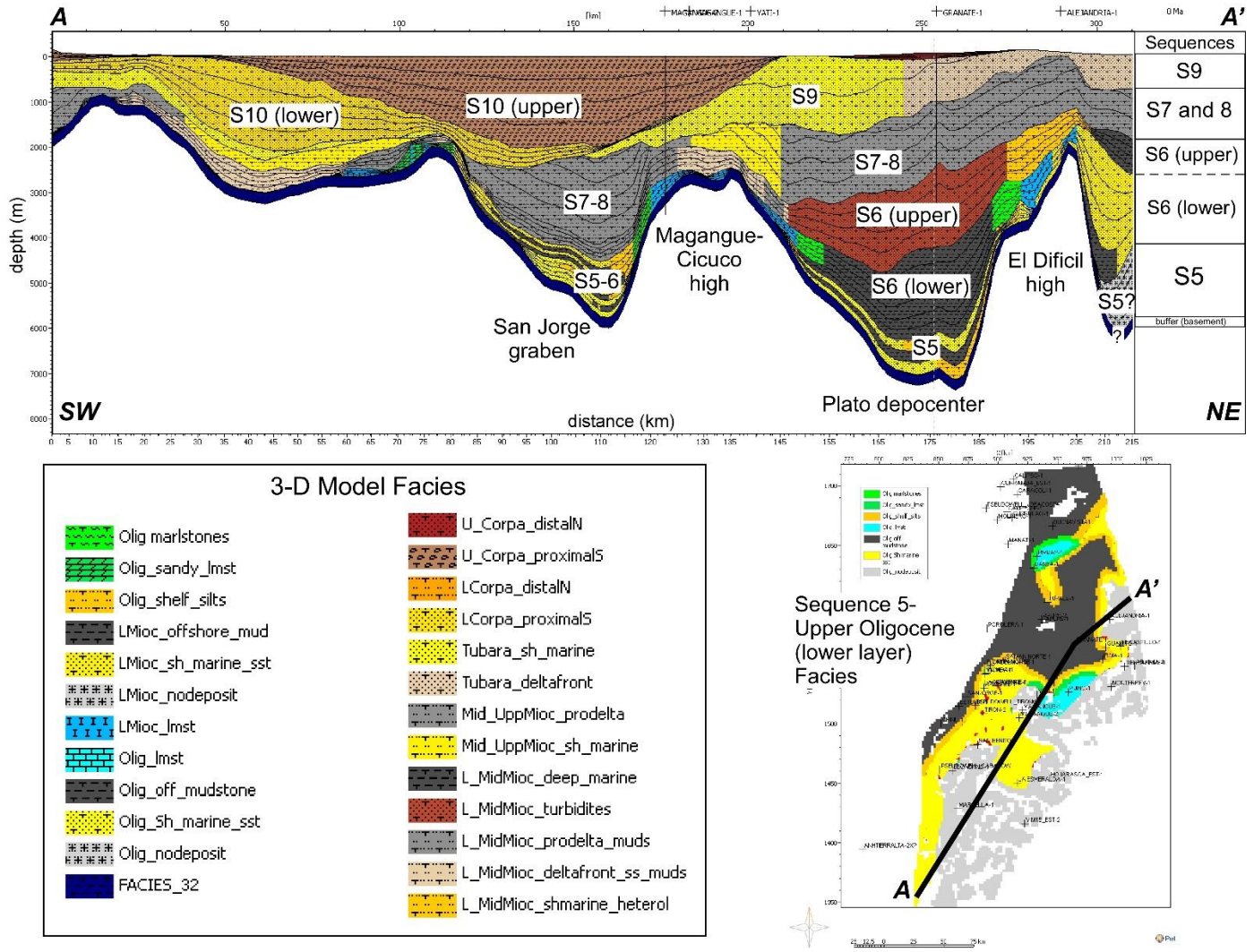

Figure 6.6. Northeast-southwest transect through the PetroMod 3-D model of the LMV, showing the implemented tectono-stratigraphic sequences and facies. The facies map of the upper Oligocene, Sequence 5 (lower part) with the location of the transect is also depicted.

Age (Ma)	Horizon	Depth Map	Erosion Map	Layer	Event Type	Facies Map	Petroleum System Elements
0.00	*Erosion_23_Top*			*Recent erosion*	*Erosion*		
0.80	**Top UpperSequence 10 UpperCorpa**	**Topography_DEM**	**Pleistocene_Recent_Erosion**	**Sequence 10 UpperCorpa**	**Deposition**	**UpperCorpa_Facies**	Overburden
1.02	Sequence 10 UpperCorpa_1	Sequence 10 UpperCorpa_1		Sequence 10 UpperCorpa_1	Deposition	UpperCorpa_Facies_Split_1	Overburden
1.25	Sequence 10 UpperCorpa_2	Sequence 10 UpperCorpa_2		Sequence 10 UpperCorpa_2	Deposition	UpperCorpa_Facies_Split_2	Overburden
1.48	Sequence 10 UpperCorpa_3	Sequence 10 UpperCorpa_3		Sequence 10 UpperCorpa_3	Deposition	UpperCorpa_Facies_Split_3	Overburden
1.70	**Top LowerSequence 10 LowerCorpa**	**IntraSequence 10 LowerCorpa**		**Sequence 10 LowerCorpa**	**Deposition**	**LowerCorpa_Facies**	Overburden
2.05	Sequence 10 LowerCorpa_1	Sequence 10 LowerCorpa_1		Sequence 10 LowerCorpa_1	Deposition	LowerCorpa_Facies_Split_1	Overburden
2.40	Sequence 10 LowerCorpa_2	Sequence 10 LowerCorpa_2		Sequence 10 LowerCorpa_2	Deposition	LowerCorpa_Facies_Split_2	Overburden
2.75	Sequence 10 LowerCorpa_3	Sequence 10 LowerCorpa_3		Sequence 10 LowerCorpa_3	Deposition	LowerCorpa_Facies_Split_3	Overburden
3.10	*Erosion_21_Top*			*MidPliocene_lowerCorpaUnconf*	*Erosion*		
3.58	**Base Sequence10_Corpa_Unconformity**	**BaseSequence10_Corpa**	**Erosion base Seq10_Corpa**	**Sequence 9 Tubara**	**Deposition**	**Tubara_Facies**	Overburden
4.43	Sequence 9 Tubara_1	Sequence 9 Tubara_1		Sequence 9 Tubara_1	Deposition	Tubara_Facies_Split_1	Overburden
5.29	Sequence 9 Tubara_2	Sequence 9 Tubara_2		Sequence 9 Tubara_2	Deposition	Tubara_Facies_Split_2	Overburden
6.14	Sequence 9 Tubara_3	Sequence 9 Tubara_3		Sequence 9 Tubara_3	Deposition	Tubara_Facies_Split_3	Overburden
7.00	*Erosion_19_Top*			*UpperMiocene unconformity*	*Erosion*		
8.00	**Base Sequence9 Tubara Unconformity**	**Base Sequence9 Tubara**	**Erosion base Seq9_Tubara**	**Sequence 7 and 8**	**Deposition**	**Mid_UppMioc_UppPorquero_Facies**	Seal and overburden
8.78	Sequence 7 and 8 _1	Sequence 7 and 8 _1		Sequence 7 and 8_1	Deposition	Mid_UppMioc_UppPorquero_Facies_Split_1	Seal and overburden
9.56	Sequence 7 and 8 _2	Sequence 7 and 8 _2		Sequence 7 and 8_2	Deposition	Mid_UppMioc_UppPorquero_Facies_Split_2	Seal and overburden
10.34	Sequence 7 and 8_3	Sequence 7 and 8_3		Sequence 7 and 8_3	Deposition	Mid_UppMioc_UppPorquero_Facies_Split_3	Seal and overburden
11.12	Sequence 7 and 8 _4	Sequence 7 and 8 _4		Sequence 7 and 8_4	Deposition	Mid_UppMioc_UppPorquero_Facies_Split_4	Seal and overburden
11.90	*Hiatus_17_Top*			*MiddleMioc unconf*	*Hiatus*		
12.70	**Top UpperSequence 6 LowerPorquero**	**Top UpperSequence 6 LowerPorquero**		**Sequence 6 upper part**	**Deposition**	**L_MidMioc_Facies**	Seal
13.62	Sequence 6 upper part_1	Sequence 6 upper part_1		Sequence 6 upper part_1	Deposition	L_MidMioc_Facies_Split_1	Seal
14.55	Sequence 6 upper part _2	Sequence 6 upper part _2		Sequence 6 upper part_2	Deposition	L_MidMioc_Facies_Split_2	Seal
15.47	Sequence 6 upper part _3	Sequence 6 upper part _3		Sequence 6 upper part_3	Deposition	L_MidMioc_Facies_Split_3	Seal
16.40	**Top LowerSequence 6 UpperCienagadeOro**	**Top LowerSequence 6 UpperCienagadeOro**		**Sequence 6 Lower part**	**Deposition**	**LMiocene_Facies**	Source rock
16.62	Sequence 6 Lower_1	Sequence 6 Lower_1		Sequence 6 Lower part_1	Deposition	LMiocene_Facies_Split_1	Reservoir rock
16.85	Sequence 6 Lower_2	Sequence 6 Lower_2		Sequence 6 Lower part_2	Deposition	LMiocene_Facies_Split_2	Source rock
17.07	Sequence 6 Lower_3	Sequence 6 Lower_3		Sequence 6 Lower part_3	Deposition	LMiocene_Facies_Split_3	Reservoir rock
17.30	*Erosion_15_Top*			*LowerMiocene_Unconf*	*Erosion*		
23.80	**Top Sequence 5 LowerCienagadeOro**	**Top Sequence 5 LowerCienagadeOro**	**Erosion_base Seq6**	**Sequence 5**	**Deposition**	**Oligocene_Facies**	Seal
25.04	Sequence 5_1	Sequence 5_1		Sequence 5_1	Deposition	Oligocene_Facies_Split_1	Source rock
26.28	Sequence 5_2	Sequence 5_2		Sequence 5_2	Deposition	Oligocene_Facies_Split_2	Reservoir rock
27.52	Sequence 5_3	Sequence 5_3		Sequence 5_3	Deposition	Oligocene_Facies_Split_3	Source rock
28.76	Sequence 5_4	Sequence 5_4		Sequence 5_4	Deposition	Oligocene_Facies_Split_4	Reservoir rock
30.00	**Basement_Unconformity**	**Basement_Unconformity**		**Buffer layer**		**basement**	
31.00	Buffer layer at base of model	Buffer at base					

Table 6.1. Ages, horizons, maps and petroleum system elements and events implemented in our 3-D model of the Lower Magdalena Valley basin.

6.3.4 Geothermal gradient

The modeled area of the LMV overlies a thinned continental crust with thicknesses ranging from 20 to 40 km (*Poveda et al., 2015*; *Bernal et al., 2015a*), and appears to be in a thermal subsidence stage in the San Jorge graben, while to the north (Plato) it is currently being uplifted (see *Chapter 5*). Geothermal gradient and heat-flow data in the LMV and SJFB are scarce, restricted to industry reports (e.g. *ICP, 2000*; *He, 2000*) and to the geothermal gradient map of Colombia (*Ingeominas/ANH, 2008*). For that reason we compiled the bottom-hole temperatures (BHT's) from Hocol's drill hole database, consisting of 205 wells, and constructed a geothermal gradient map the LMV and SJFB (**Figure 6.7**a) by assuming an actual, average surface temperature of 30°C (86°F). Considering that most of the data consists of single BHT measurements, a 10% correction was applied to account for the cooling effect of the drilling mud in the temperatures (**Figure D 1**a). However, we also had access to temperature data from a couple of well tests, which has the advantage of not being affected by the cooling effect of the drilling mud. Comparison of the data from the tests, which were performed at stratigraphic intervals relatively close to the basement, with the BHT data did not show a large difference (2-5°C; 3.6 – 9°F), an indication that the 10% correction we applied is reasonable. In the LMV, most of the wells reached the basement, hence the measured bottom-hole temperatures in this basin represent the near top of the basement. In other areas such as the SJFB, where the basement has not been reached by any wells, the measured bottom-hole temperatures correspond to different stratigraphic intervals, mostly within pre-Oligocene units.

Our geothermal gradient map shows that the different tectonic provinces in and around the study area have different temperature trends (**Figure 6.7**a and **Figure D 1**a). The coldest province is the Sinú-offshore area, west of the Sinú lineament, where a thick succession of young, Miocene to recent poorly-consolidated sediments is preserved and low gradients < 14°C /km (7.7°F/1000 ft) were obtained. The southern LMV (San Jorge depocenter), the western Magangué-Cicuco high and the southern SJFB are also cold (geothermal gradients < 20° C/ km, 11°F/1000 ft), while the northern LMV (Plato), most of the SJFB and the southern Sinú fold belt are warmer and exhibit gradients between 20 and 30 °C/km (11 to 16.5°F/1000 ft). These values are in agreement with the map of geothermal gradients of Colombia (*Ingeominas/ANH, 2008*), while our obtained average geothermal gradient of 19.6°C/km is in agreement with previous studies (e.g. *ICP, 2000*), which reported a gradient of 20°C/km (11° F/1000 ft).

6.3.5 Upper boundary conditions

We used our regional well and outcrop database to constrain the paleo-water depths (PWDs) for each of the sequences implemented in the model. Regional paleo-water depth maps were constructed in Petrel and exported to PetroMod. The overall succession in the LMV exhibits a general shallowing- and coarsening-upwards trend, starting with shallow-marine, upper Oligocene deposits towards the base of Sequence 5, passing to deltaic and deep marine deposits from the upper Sequence 5 to Sequence 8, and then changing to fluvio-deltaic (Sequence 9) and mostly fluvial deposits of Sequence 10. Therefore, paleo-water depths range from shelf depths (100-200 m) towards the base of Sequence 5, to delta front, prodelta and even turbiditic deposits (200-1,500 m) in Sequences 6 to 8, and then to shallower depths related to deltaic and fluvial deposits (30-200 m) in Sequence 9 and 10.

Oligocene to Pleistocene sediment-water interface temperatures (SWITs) were modeled in accordance to *Wygrala (1989*) considering the current latitude of the study area in northern South America. A present-day surface temperature of 30°C (86°F) has been assumed for the northwestern Colombian Caribbean lowlands, based on statistical, historical climate and temperature reports.

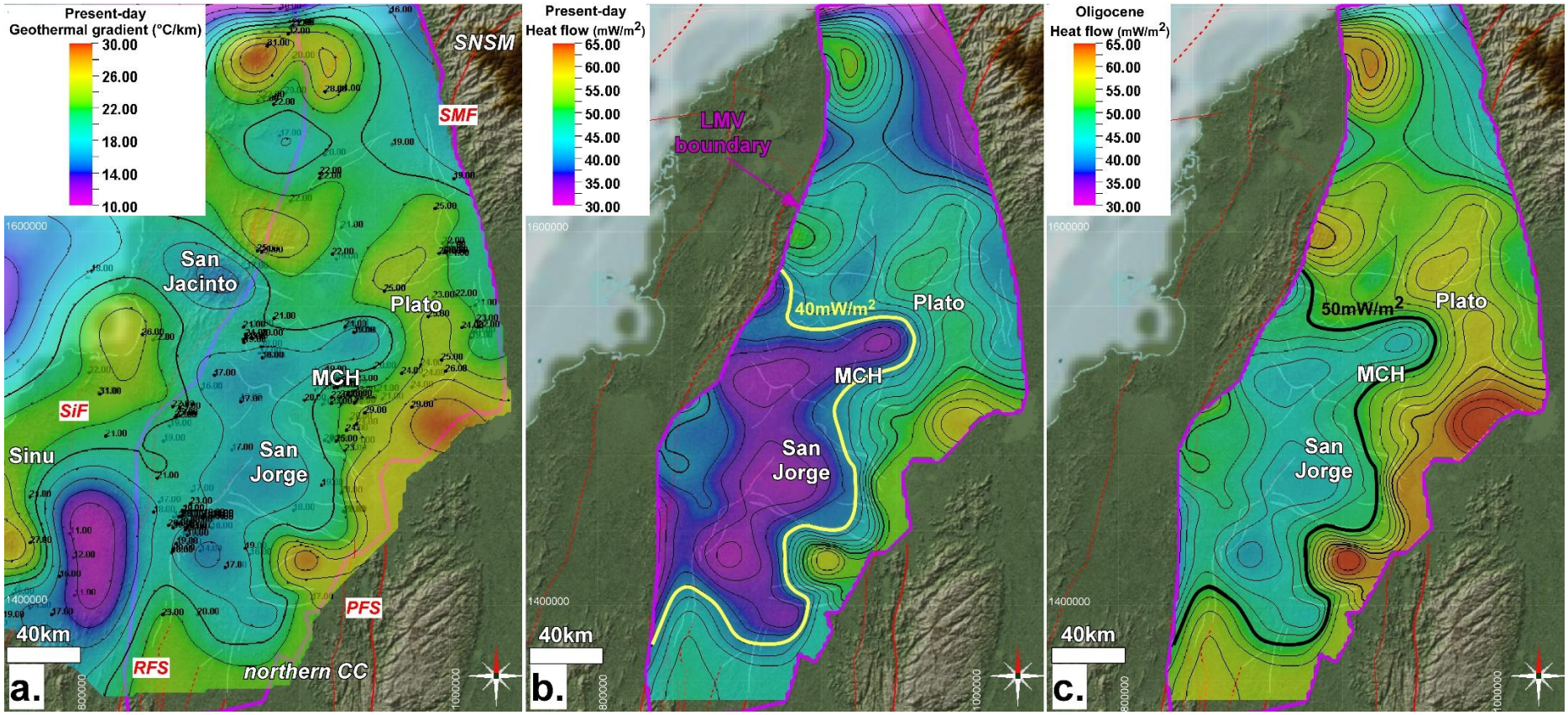

Figure 6.7. a). Present-day geothermal gradient map of the LMV, San Jacinto and Sinú fold belts, obtained from BHT and well test data. b). Present-day average heat flow map of the LMV, obtained from the geothermal gradient map, using an average thermal conductivity value of 2 W/m/K; such value was selected considering that the succession in the LMV is mostly fine-grained. c). Oligocene heat flow map assuming a minor decrease in heat flow since 35 Ma (average difference of ~10 mW/m^2). MCH: Magangue-Cicuco high; RFS. Romeral Fault System; PFS: Palestina Fault System; SMF: Santa Marta Fault; SiF: Sinu Fault.

6.3.6 Lower boundary conditions: basal heat flow

Concerning the basal heat flow data, we followed two different approaches to construct present-day heat flow maps of the study area that will be used for modelling purposes. The first approach was to use the heat flow values from the calibration of the 1D-models that we built in the LMV and SJFB, using the wells with vitrinite reflectance, Tmax or other temperature or maturity measurements. The heat flow values which gave the best match between the modeled curves and the measured temperature and maturity values were used to make preliminary, regional heat flow maps of the LMV and SJFB. These maps provided the first idea of heat flow values and trends in the study area. The second approach was to use the fundamental relation for conductive heat transport given by Fourier's Law, which states that the heat flow is directly proportional to the temperature gradient and takes the mathematical form

$$Q = -K(dT/dz) \quad (6.1)$$

where K is the coefficient of thermal conductivity, T is the temperature at a given point in the medium and z is the coordinate in the direction of the temperature variation (*Allen and Allen, 2005).* Considering the absence of thermal conductivity laboratory measurement of rocks in the basin, we assumed a range of thermal conductivity values according to the dominant lithologies in the study area (claystones and siltstones), and we produced three different maps which represent three different present-day, basal (near basement) heat flow scenarios: a low heat-flow map which was obtained by using a thermal conductivity value of 1.2 Wm^{-1} K^{-1}, a mean heat-flow map was obtained with a thermal conductivity value of 2 Wm^{-1} K^{-1} and a high heat flow map was obtained by using a thermal conductivity value of 2.8 Wm^{-1} K^{-1}(see **Figure D 2**). The map obtained with the thermal conductivity value of 2 Wm^{-1} K^{-1} yielded the current basal heat flow values which were closest to previously obtained values by *He (2000*), and to the calibrations of the 1-D models. Therefore, our present-day basal heat flow maps follow the same trends of the geothermal gradient map and have values which are comparable to previous studies and to calibration data.

Forearc basins unrelated to arc magmatism exhibit low heat flows (20-45 mW/m^2) and hence fall in the category of hypothermal (cooler than normal) basins (*Allen and Allen, 2005*). This seems to be the case of the LMV and SJFB where heat flows can be low (30-40 mW/m^2) in the southern SJFB, according to temperature data from recent stratigraphic wells drilled by the ANH (National Hydrocarbons Agency). Nevertheless, heat flow can also be higher in other areas such as the central and northern SJFB and eastern Plato depocenter in the northern LMV (40-58 mW/m^2, **Figure 6.7**b). The SJFB exhibits a high heat flow trend which is roughly parallel to the trend of the fold belt, suggesting a relationship with its stratigraphic and structural configuration, which is markedly different compared to that of the LMV, as shown by *Mora et al. (2017b*). The low heat flow values in the southern SJFB may be related to the presence of nearby outcrops of peridotites and basalts which produce almost no radiogenic heat (*Allen and Allen, 2005*). The basement under the LMV seems to display a more uniform configuration, yet the gradients and basal heat flow trends are quite different from the SW to NE. Considering that granitic rocks produce large amounts of radiogenic heat (*Allen and Allen, 2005*), it would be expected that the LMV would exhibit higher heat flow values considering the reports of granitoid plutons in several areas (*Mora et al., 2017a*). However, the occurrence of granitic plutons in cold areas such as the SW (San Jorge depocenter) and the western Magangué-Cicuco high, where sedimentary infill is much thinner, suggests that there is not much influence of possible heat conduction from the basement. Heat flow variation caused by in-situ heat generation by radioactive decay is expected to be much more prominent that the effects from the underlying crust. Change in radioactive heat production should occur in the SE-NW direction from one facies belt to the other, yet the gradient and heat flow maps do not show a clear change in that direction. Variations observed in modern basal heat flow are thus more likely to represent influences of the local hydrodynamic regime, which would be more related to the sedimentary infill of the basin.

Mora et al. (2017b, Chapter 5) proposed that there has been amagmatic, flat subduction of the Caribbean plateau beneath NW Colombia since middle Eocene times. This would imply in first place that the flat subduction of the cold Caribbean plateau would have been responsible for possible slab refrigeration (*Dumitru, 1990*; *Dumitru et al., 1991*), lowering the temperature above the flat slab zone since the Oligocene, and in second place, that the thermal and heat-flow regime remained fairly constant since the basin started to be filled in late Oligocene times. We also converted the vitrinite reflectance values to paleo-temperatures, using the EASY%Ro model of vitrinite maturation of *Sweeney and Burnham (1990*), and assuming a heating rate of 1°C/Ma. With this procedure, we obtained a difference of ~8°C between the Oligocene-lower Miocene paleo-temperature gradients and the present day gradients. Based on all the aforementioned, we implemented in our 3-D model basal heat flow maps for the Oligocene, which are 10°C hotter than the present-day, basal heat flow map (**Figure 6.7**c).

We also tested different basal heat flow scenarios for calibration purposes (**Figure 6.8**), three with variable heat flows with time and one with a constant heat flow. In the first mean or average scenario, we ran the simulation using the previously described, mean present-day and Oligocene heat flow maps. Two other variable heat flow scenarios included present-day and Oligocene maps which had either 10% higher and lower heat flows than the average maps. For the fourth scenario, we assumed a constant heat flow of 40mW/m^2 from the Oligocene to the present. The modelled curves according to each scenario were then plotted in the vitrinite reflectance and temperature extractions which will be described in the next sections. It must be taken into account that the variation in heat flow between the northern and southern LMV, as depicted in **Figure 6.8**, is due to the fact that the maps we used were built from geothermal gradients, therefore they show a variation in basal heat flow according to the location (e.g. higher basal heat flow in the north).

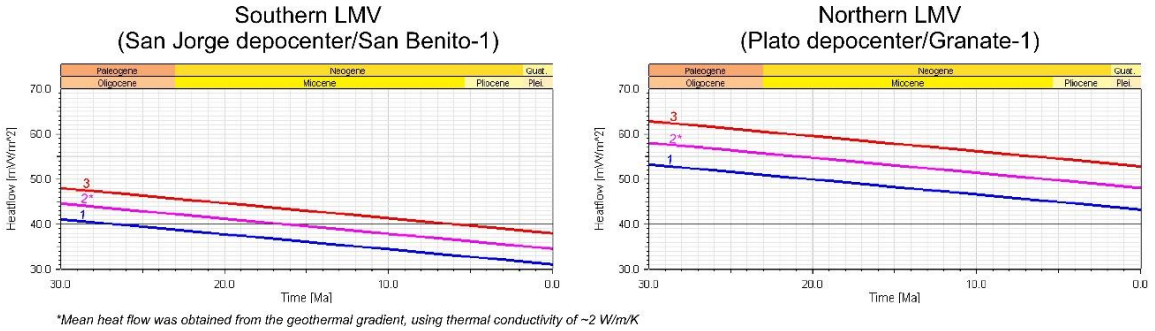

Figure 6.8. Basal heat flow scenarios implemented and tested in the 3-D model. The pink curve (2) is the average or mean heat flow scenario obtained by using the geothermal gradient and a thermal conductivity value of 2 W/m/K. The blue curve (1) is the low heat flow scenario corresponding to the average heat flow minus 10%, and the red curve (3) is the high heat flow scenario corresponding to the average heat flow plus 10%. The graph in the left corresponds to the location of the San Benito-1 well in the southern LMV while the graph in the right corresponds to the location of the Granate-1 well in the northern LMV. The difference in heat flows from north to south shows that the assumed present-day, basal heat flow varies according to the location in the basin.

6.3.7 Calibration data: vitrinite reflectance

Vitrinite reflectance and temperature data from several wells were available from Hocol's database for model calibration (**Figure D 1**b). The most complete calibration data is available in the Magangué-Cicuco high and the northern LMV (Plato depocenter), while only scarce calibration data is available in the southern LMV (San Jorge depocenter). A detailed revision of the available geochemical data in the study area showed that its quality is not very good and that it must be taken with care. In first place, geochemical analyses were done in very different laboratories, for such reason some of the data is inconsistent or anomalous. Additionally, much of the data is old and

comes from wells drilled more than 30 years ago. Concerning vitrinite reflectance, several wells showed anomalous linear trends with depth, (e.g. Tupale-1, **Figure 6.9** and **Figure D 1**b) and some even had inverted trends. Furthermore, samples at shallow depths tend to display very high vitrinite reflectance, suggesting the occurrence of reworked material in the younger sequences. According to all the aforementioned, we discarded wells with anomalous geochemical and temperature data, and used the most reliable ones for calibration (**Figure 6.9** to **Figure 6.13**

Model predictions of vitrinite reflectance after *Sweeney and Burnham (1990*) are in accordance with measured values in most of the wells (**Figure 6.9**). Vitrinite reflectance trends of wells indicate moderate increases in maturity with depth, reaching vitrinite reflectance values of 0.6 % between 3,048 and 3,658 m (10,000 and 12,000 ft) in the Plato depocenter, corresponding to Sequences 5 and 6 (upper Oligocene to lower Miocene). By contrast, in the San Jorge depocenter the lower sequences (5 and 6) exhibit low maturities with vitrinite reflectance values below 0.6%. Towards the upper part of most of the vitrinite reflectance profiles, younger sequences (6 to 9) show anomalously high maturities, suggesting that there would be some reworking of organic matter.

We performed 1-D extractions from the 3-D model and displayed burial history diagrams that show subsidence and uplift history at a certain location, which could be a well or a pseudowell. Such diagrams are very useful to analyze the evolution of temperature and maturity through time (**Figure 6.10**). Vitrinite reflectance predictions indicate that Oligocene and older sediments in the central Plato depocenter have been thermally mature (> 0.6% Ro) since early Miocene times. In the southern LMV (San Jorge depocenter), most of the wells such as La Esmeralda-1, remain immature and have not entered the oil window. Only a pseudowell in the deepest part of the depocenter to the W (Pseudowell-TironW), would show maturities indicative of an incipient entrance to the oil window, especially in Pleistocene times (**Figure 6.10**).

Concerning erosion, though some bends in the 1-D curves could relate to some of the Miocene unconformities, the most complete vitrinite reflectance profiles come from wells drilled in the Plato depocenter, where there was less influence of regional shortening and uplift events. In the areas where there was more deformation and uplift, the lack of systematic vitrinite reflectance data hampers the identification of possible unconformities or other changes in the normal trends.

Model results for vitrinite reflectance at selected intervals within the sequences with highest generating potential (upper Oligocene to lower Miocene Sequences 5 and 6), show that maturity, as indicated by vitrinite reflectance is highest in the northern LMV (Plato depocenter), where reflectance values of 2% and higher were obtained (**Figure 6.11**). Maturity in the southern LMV (San Jorge depocenters) is much lower with the highest vitrinite reflectance values around 0.6% occurring in the deepest reaches in the northwestern part of the depocenter.

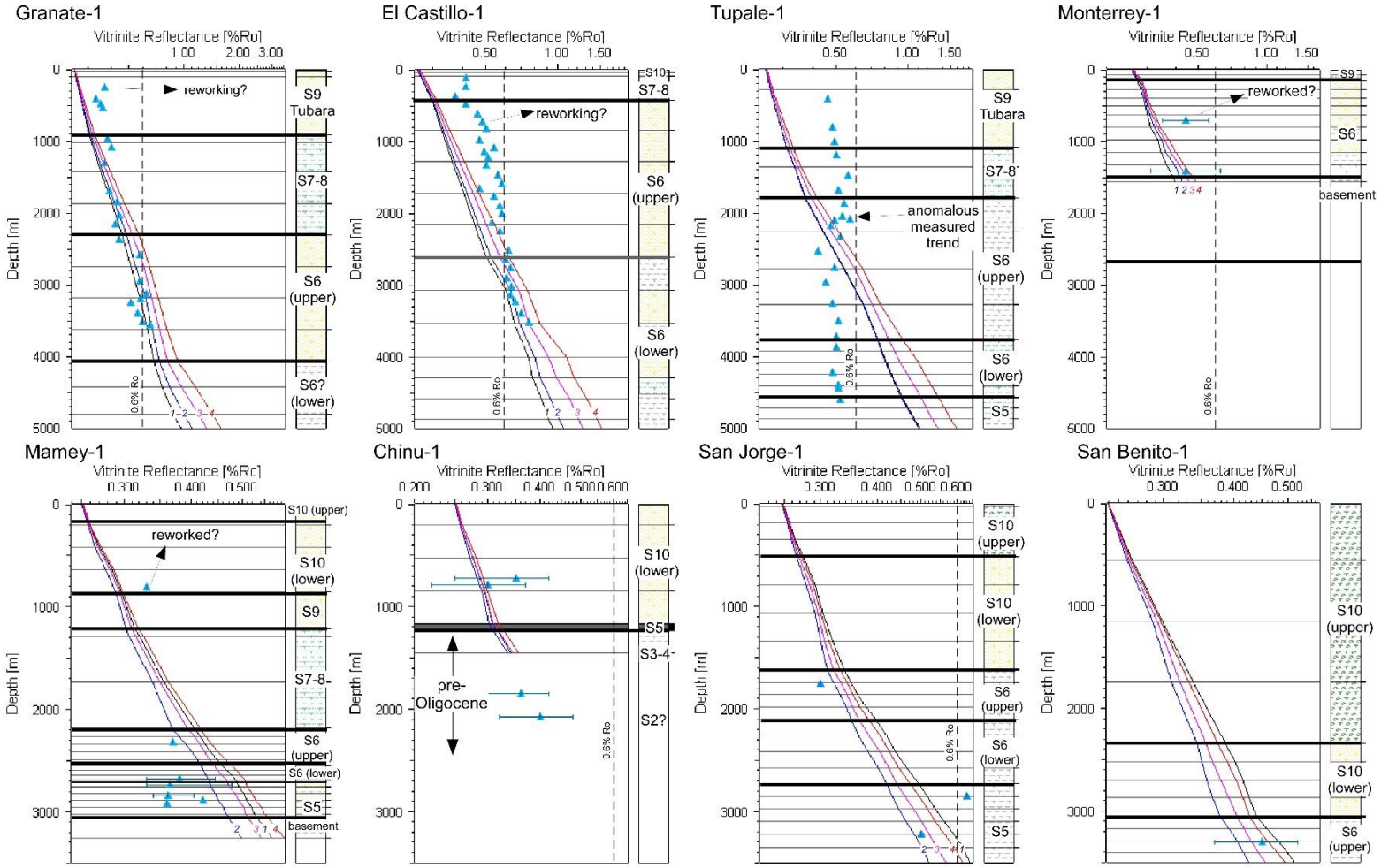

Figure 6.9. One-dimensional model extractions at selected well locations showing modeled (curves) and measured (triangles) vitrinite reflectance data from wells. Each curve corresponds to a different heat flow scenario: the pink curve (3) is the average or mean basal heat flow from the Oligocene to Recent, obtained from the geothermal values by using a thermal conductivity value of 2 W/m/K; the dark blue curve (2) is the mean Oligocene to Recent, basal heat flow minus a 10% while the red curve (4) is the mean heat flow plus a 10%; the black curve (1) corresponds to a constant heat flow of 40 mW/m^2 from the Oligocene to Recent. Compare vitrinite reflectances of the wells in the upper part, located in the northern LMV (Plato), with wells in the lower part, located in the southern LMV (San Jorge).

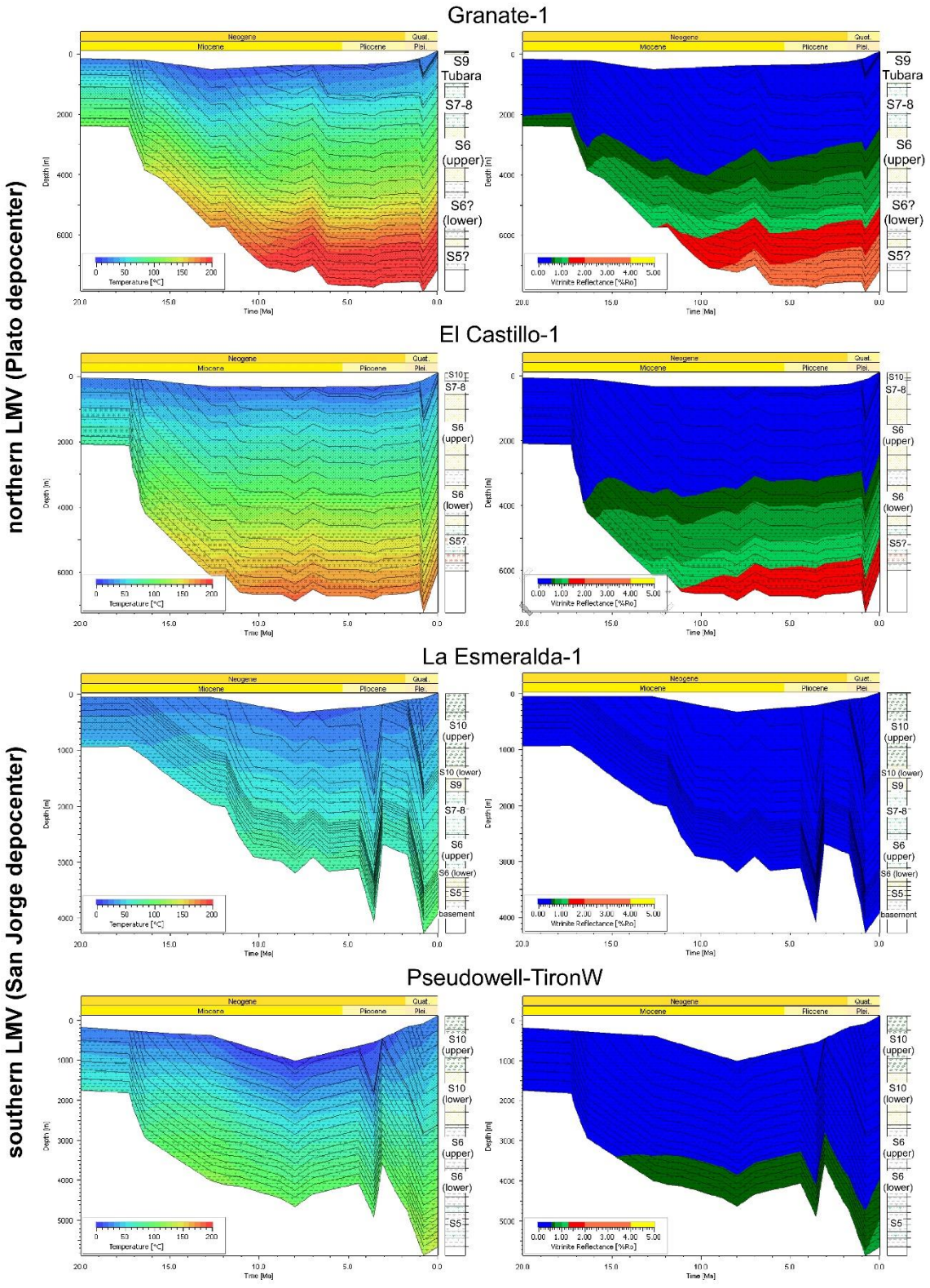

Figure 6.10. One-dimensional histories extracted from the model at three well locations for temperature (left) and vitrinite reflectance (right). There is a marked contrast in histories between the north (Plato) and the south (San Jorge).

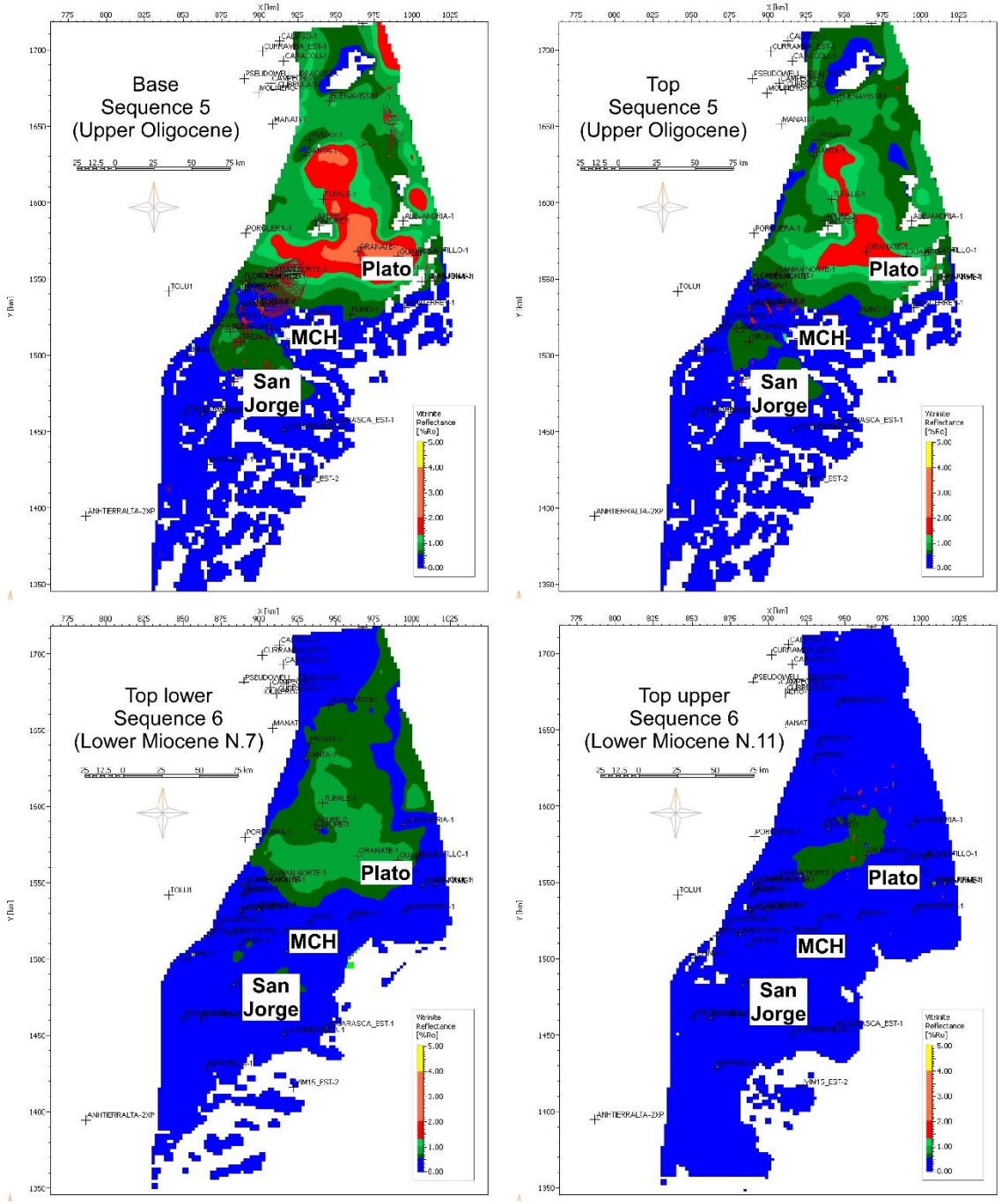

Figure 6.11. Model results for vitrinite reflectance in percent at tops of the two main source rock levels (upper Oligocene sequence 5 and lower Miocene, lower sequence 6). Modelled flow paths and hydrocarbon accumulations are also plotted, showing a good match with the real accumulations.

6.3.8 Temperature

Present-day temperature trends are quite similar to the maturity trends indicated by the vitrinite reflectance (**Figure 6.11** and **Figure 6.12**), showing that the highest temperatures predicted by the 3-D model occur in the Plato depocenter of the northern LMV. At the San Jorge depocenter in the southern part of the basin, predicted temperatures do not exceed 150°C (302° F). Predicted temperature gradients are low in all the LMV (**Figure 6.13**), though they are higher in the north

(Plato, >20°C/km), and lower in the south (<20°C/km). In spite of the few temperature data for calibration, the modelled temperatures show a normal increase in temperature gradients with depth. The continuous deposition and subsidence in the Plato depocenter as shown in the 1-D temperature histories (**Figure 6.10**), contrasts with the San Jorge depocenter in the south, where the effects of Pliocene uplift and erosion decreased the temperature of the sediments and inhibited an earlier and faster maturation.

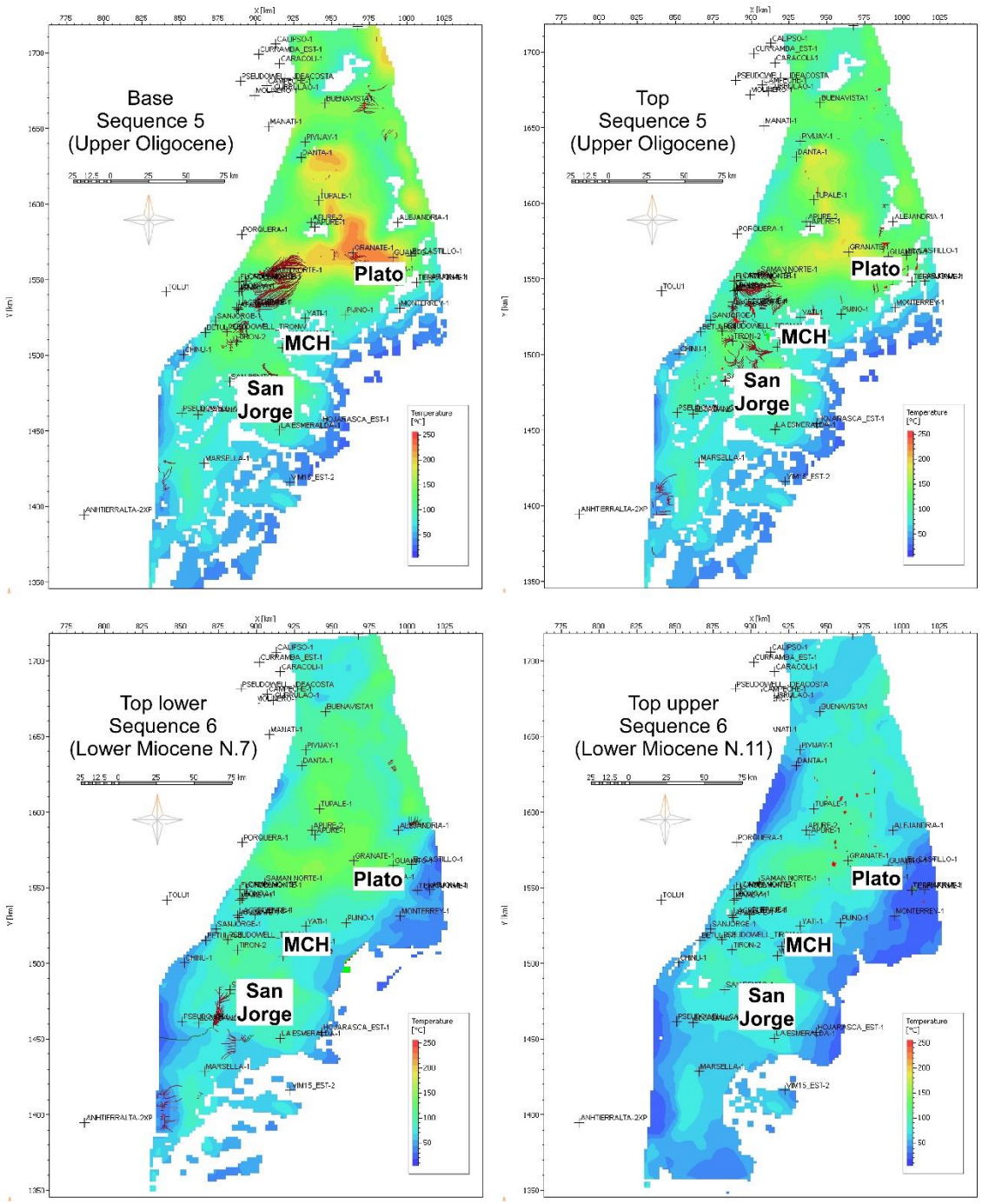

Figure 6.12. Model results for temperature in °C at the tops of the two main source rock levels (upper Oligocene sequence 5 and lower Miocene, lower sequence 6).

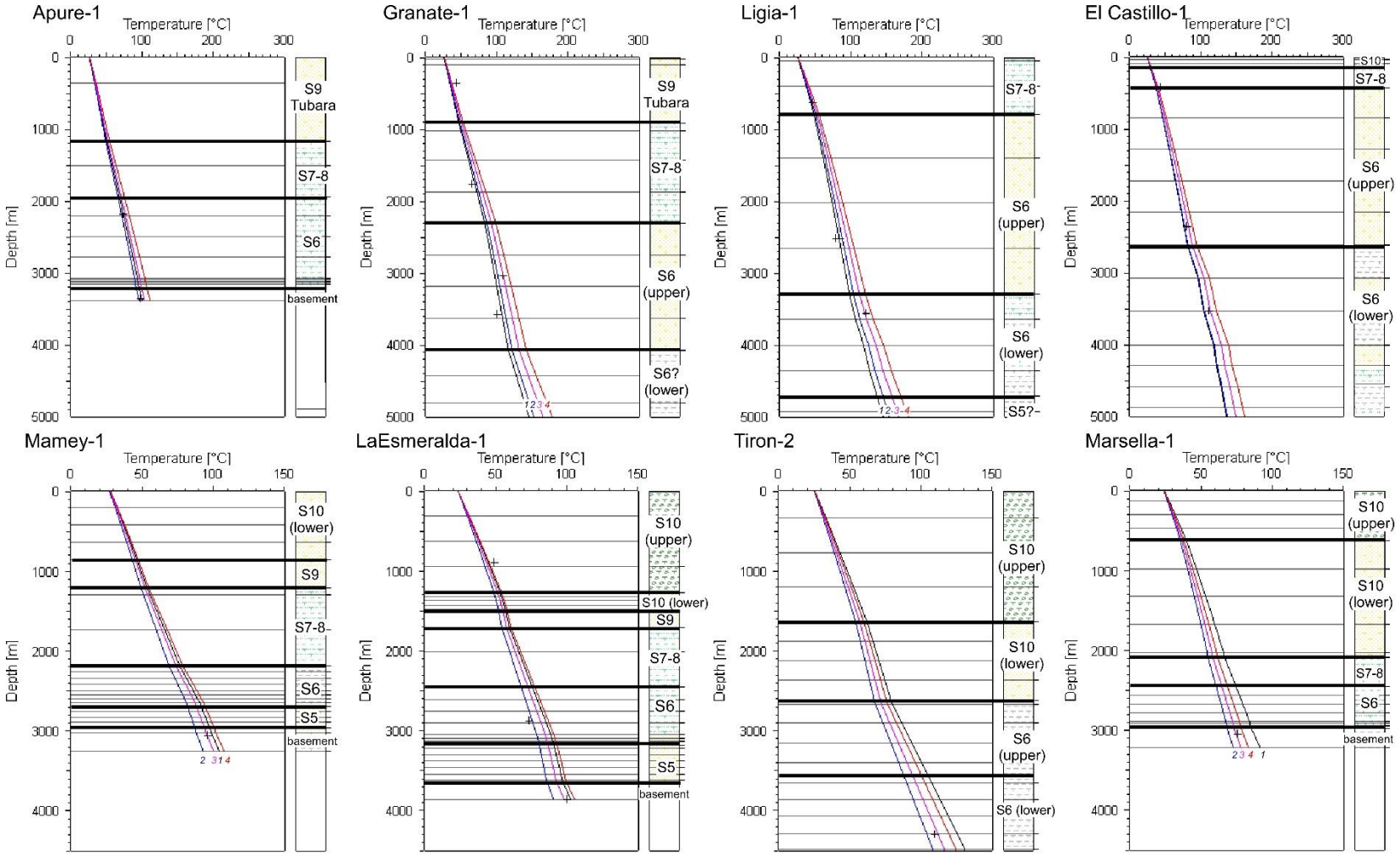

Figure 6.13. One-dimensional extractions at selected well locations showing modeled (curves) and measured (crosses) temperature data from wells. Each curve corresponds to a different heat flow scenario: the pink curve (3) is the average or mean basal heat flow from the Oligocene to Recent, obtained from the geothermal values by using a thermal conductivity value of 2 W/m/K; the dark blue curve (2) is the mean Oligocene to Recent, basal heat flow minus a 10% while the red curve (4) is the mean heat flow plus a 10%; the black curve (1) corresponds to a constant heat flow of 40 mW/m^2 from the Oligocene to Recent.

6.4 Results: Transformation Ratios

Based on the thermal maturation model, transformation ratios were calculated mostly using published type III kinetics of *Burnham and Sweeney (1989*) and *Sweeney and Burnham (1990*), though several runs were made using other type III kinetics (*Behar et al., 1997* for the Mahakam delta and *Pepper and Corvi, 1995*), as well as type II kinetics of *Sweeney and Burnham (1990*). Previous studies have shown that type III kerogen is dominant in Tertiary shallow marine to deltaic deposits of the LMV (*ICP, 2000*; *Vargas and Mantilla, 2006*). Our revision of source rock characteristics shows that upper Oligocene to lower Miocene, organic-rich rocks in Sequences 5 and 6 have better characteristics in the north (Plato depocenter), where they have higher hydrogen indexes (30-250 mgHC/gTOC) and could contain some type II kerogen, while in the south (San Jorge depocenter), hydrogen indexes are lower (30-100 mgHC/gTOC) and there is only type III kerogen. Results after using all the previously mentioned type III kinetics show that almost complete transformation has occurred at the base of Sequence 5 (upper Oligocene) in the deepest parts of the Plato depocenter of the northern LMV (**Figure 6.14**), though there was complete transformation in more areas of the depocenter by using the kinetics of *Behar et al. (1997*). Transformation ratios decrease in lower Miocene sediments and only minor transformation occurred in middle Miocene sediments. Using type II kinetics of *Sweeney and Burnham (1990*) resulted in complete transformation of organic matter in almost the entire Plato depocenter and in higher transformation ratios in the lower part of Sequence 6. The upper part of Sequence 6 (lower to middle Miocene) was not transformed at all.

In the San Jorge depocenter of the southern LMV, results indicate that there is no transformation of both Sequences 5 and 6 with all the type III kinetics, while using type II kinetics causes only minor transformation in the western part of the depocenter (**Figure 6.14**). According to our results, significant transformation would only occur in a high heat flow scenario, which is not supported by the temperature and maturity data, and in a type II kinetics scenario, which is not the case of the source rocks in the LMV. Therefore, it appears that the gas accumulations existing in the southern LMV are not explained by thermogenic generation from Oligocene to Miocene source rocks, in a pod located in the western San Jorge depocenter, as it has been previously suggested.

The 3-D models we built have a grid spacing of 2 km x 2 km, contain 565,068 elements, 14 lithologies, 30 facies and 31 layers. In spite of the thick layering and a not very fine grid, we obtained fairly good results in terms of modeled hydrocarbon accumulations versus the real fields in the LMV. Our model predicts mostly gas accumulations in Sequence 5 reservoirs, located in high areas surrounding the Plato depocenter of the northern LMV, with fewer accumulations in Sequence 6 reservoirs. Some of the predicted accumulations coincide with important existing wet gas fields (e.g. Bonga and La Creciente to the W of the Plato depocenter). In the south, the model predicts much less gas accumulations, some of which are in agreement with the few gas fields that occur in that area. Though we consider that the modeled fields have a fair correlation with the real fields, it is also evident that further refinement of the model is needed to obtain a better match between modelled and real fields. Such refinement refers for example to the implementation of the main faults, which were not implemented in this model. Further activities that would enrich the models are the usage of source rock specific kinetics obtained in the laboratory as well as of biogenic kinetics.

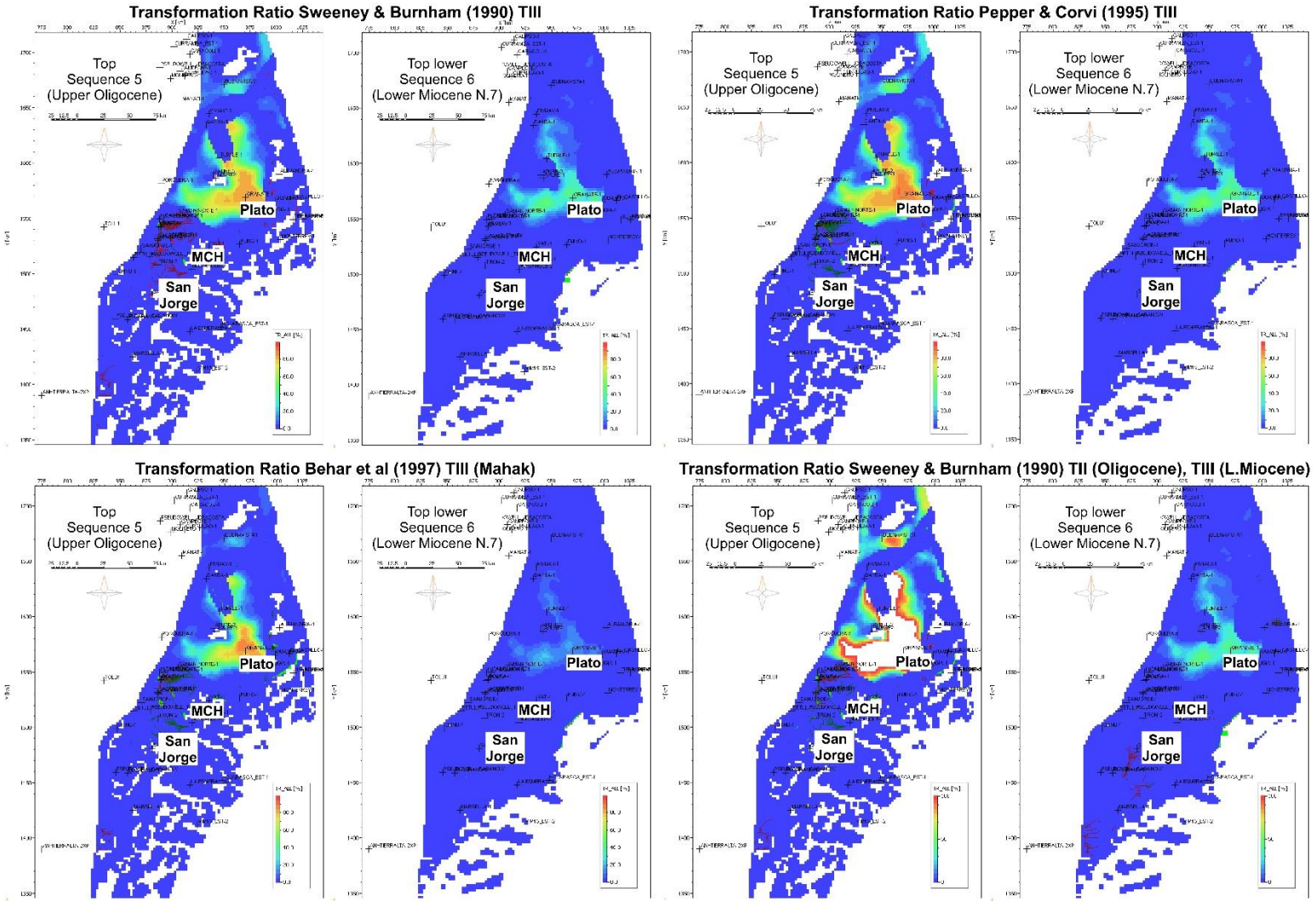

Figure 6.14. Transformation ratios predicted by the model applying type II and III kinetics of *Sweeney and Burnham (1990*), *Behar et al. (1997*) and *Pepper and Corvi (1995*).

Transformation ratios plotted against time (**Figure 6.15**) indicate that in a large part of the Plato depocenter (Granate-1 well), most of the transformation of organic material in upper Oligocene sediments (continuous lines in **Figure 6.15**) has already occurred during the middle Miocene (15-10 Ma), regardless of the kinetics applied. However, the earliest and fastest transformation occurred when the type II kinetics of *Sweeney and Burnham (1990*) were applied (red curve), and the latest and slowest with the type III kinetics of *Behar et al (1997*, green curve). Fastest transformation of the sediments towards the base of Sequence 5, related to type III kinetics, occurred with the models by *Pepper and Corvi (1995*) and *Sweeney and Burnham (1990*).

Concerning the lower Miocene sediments at Plato (dashed lines in Granate-1 graph in **Figure 6.15**), the onset of transformation of organic matter occurs later, at ~9 Ma and it is faster when type II kinetics of *Sweeney and Burnham (1990*) are applied. The fastest transformation related to type III kinetics occurs with the models of *Pepper and Corvi (1995*) and *Sweeney and Burnham (1990*). In the southern LMV (Tiron-2 and pseudowell TironW in **Figure 6.15**), only insignificant and very recent transformation occurs, regardless of the kinetics applied and including type II kinetics of *Sweeney and Burnham (1990*).

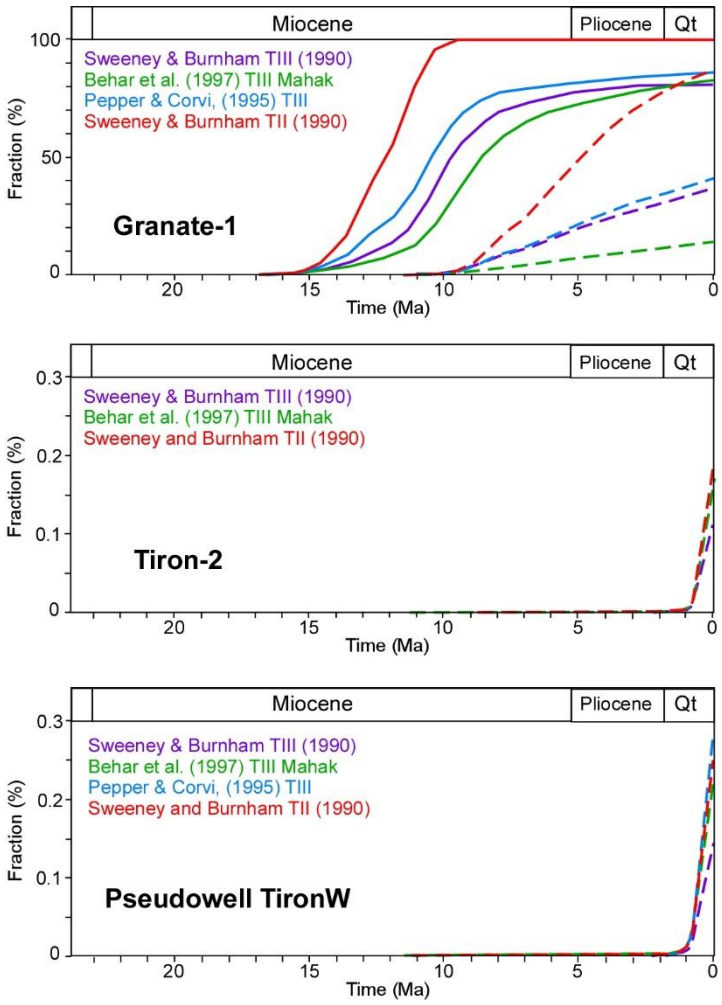

Figure 6.15. Transformation ratios at the base of the upper Oligocene Sequence 5 and at the top of the lower Miocene, lower Sequence 6 at several well locations applying type III kinetics of *Sweeney and Burnham (1990*), *Behar et al., (1997*) and *Pepper and Corvi (1995*); type II kinetics were also applied to see their effect on transformation ratios in the basin. Continuous lines are upper Oligocene sources and dashed lines are lower Miocene sources. Note the marked contrast between the north (Granate-1) and the south (Tiron-2 and TironW), where transformation was insignificant.

6.5 Discussion

6.5.1 Hydrocarbon to source rock correlations

According to *Magoon and Dow (1994*), a petroleum system encompasses a pod of active source rock and all related oil and gas and includes all the essential elements and processes needed for oil and gas accumulations to exist. It has a stratigraphic, geographic and temporal extent and its name combines the names of the source rock and the major reservoir rock, also expressing the level of certainty. *Magoon and Dow (1994*) thus proposed that if the petroleum system is considered known, its name is followed by an exclamation mark (!); if it is considered hypothetical, it is followed by a point (.) and if it is considered speculative its name is followed by a question mark (?). In the LMV, available geochemical studies (*Petrobras/ECP, 1996*; *ICP, 2000*; *Rangel et al., 2017*) have indicated that there is essentially one oil family related to shallow marine, Tertiary rocks, which displays a good correlation with the upper Oligocene to lower Miocene source rocks of Sequences 5 and 6 (informally called "Ciénaga de Oro" Formation, *ICP, 2000*). Such oil to source rock correlation is best supported in the Plato depocenter of the northern LMV, where more data from oils and source rocks is available, and where several hypothetical petroleum systems have been proposed (e.g. Ciénaga de Oro (.) and Porquero - Ciénaga de Oro (.); Vargas and Mantilla, 2006). In the southern LMV, the main hydrocarbon accumulations consist of dry gas which according to the only available isotopic analyses (*Beroiz et al., 1986*), has a mixed biogenic and thermogenic origin. Biomarker data from hydrocarbons in the southern LMV do not correlate with any oil from the northern LMV (Plato), and it has been previously suggested that generation in the south occurred in the deepest part of the San Jorge depocenter. However, in addition to the lack of data in the south, this area has not been previously modeled in detail.

6.5.2 Implications of 3-D modeling results on Petroleum Systems in the LMV

6.5.2.1 Northern LMV (Plato depocenter)

The 3-D model of the Lower Magdalena Valley basin presented herein provides additional constraints for sites of potentially active hydrocarbon generation. Modeling results indicate that upper Oligocene to lower Miocene deposits are mature in the northern part of the basin (Plato depocenter) and immature in the southern part (San Jorge), due to different source rock qualities, burial histories and heat flows. For that reason, 1-D and 2-D extractions from the 3-D model show that the oil window is found at shallower depths in the north (Plato), where modelled temperatures and maturities indicate that the early oil window is located between ~3,300 and 4,000 m (~11,000 and 13,000 ft, **Figure 6.16**). The oil window at Plato would cover an area of 4,213 km^2 (1,042,000 acres). In the southern LMV, temperature and maturity data indicate that only sediments buried deeper than ~4,500 m (~15,000 ft) in the western San Jorge depocenter, would be in the early oil window (**Figure 6.16**). A third pod of active source rock would also exist in the deepest part of the Algarrobo pull-apart basin, where only middle Miocene sediments have been drilled by exploratory wells, but where older Tertiary sediments of sequence 6 and 5 would be preserved. The absence of oil and gas seeps in the area of influence of the Santa Marta fault, which forms the northeastern limit of the Algarrobo pull-apart basin appears to be a point against possible generation in this area. This could be related to the coarse-grained, clastic facies of Oligocene to lower Miocene units that have been recently reported in the Aracataca basin (*Piraquive, 2016*; *Piraquive et al., 2017*). However, the lack of temperature and maturity data hampers a better definition of this possible pod of active source rock.

The results of our 3-D model allow us to characterize in much more detail than in previous studies the petroleum systems in the LMV, following the definition of *Magoon and Dow (1994*). The Plato depocenter is the area of the LMV in which more well data are available, where more oil and gas fields are located and where the best hydrocarbon to source rock correlations have been obtained. Therefore, this study confirms the previously proposed petroleum systems in the northern LMV (Ciénaga de Oro (.) by *Vargas and Mantilla, 2006*; Ciénaga de Oro (!) and Porquero-Ciénaga de Oro (!) by *ANH (2011b*). However, considering that our tectono-stratigraphic framework is different from the one used by *Vargas and Mantilla (2006*) and *ANH (2011b*), we would propose at least three known petroleum systems in the Plato depocenter and surroundings: A petroleum system that only includes Sequence 5, which would be called Lower Ciénaga de Oro-Lower Ciénaga de Oro (!); a system with source rocks in Sequence 5 and reservoirs in Sequence 6, called Lower Ciénaga de Oro- Upper Ciénaga de Oro (!); and a system only including Sequence 6 which would be called Upper Ciénaga de Oro (!), **Figure 6.17**a).

6.5.2.2 Southern LMV (San Jorge depocenter)

The oil-source rock correlations, the distribution of hydrocarbons in the basin and the results of our 3-D modeling all suggest that the Plato depocenter is not related to the dry gas accumulations in the western San Jorge depocenter. Hence, we propose that different petroleum systems are responsible for such accumulations. Proprietary industry reports have suggested that an equivalent hypothetical petroleum system, called Ciénaga de Oro (.), exists in the San Jorge depocenter, and that it would be responsible for the dry gas accumulations existing there. We do not discard that such hypothetical system is partly responsible for the dry gas accumulations in the south petroleum system (**Figure 6.17**b). However, the results of our 3-D model have shown that the area has been extremely cold and that potential source rocks are immature, even in the deepest part of the depocenter. This means that neither a pod of active source rock nor migration pathways have been properly defined for the southern LMV. Therefore, our results suggest the necessity of having other additional sources for hydrocarbon generation in the southern LMV.

One possible source would be bacterial activity in the early stages of diagenesis, which would have generated biogenic gas (*Waples, 1981*). This is in agreement with the few isotopic studies that have been performed in the area (*Beroiz et al., 1986*), which conclude that the gases in the Jobo-Tablon area in the western San Jorge depocenter have isotopic values between biogenic and thermogenic compositions. Nevertheless, it is more likely that such biogenic generation would relate to gas accumulations at shallow levels, such as those reported in younger sequences (e.g. 7 to 9, Porquero to Tubará). However, preliminary tests with biogenic kinetics suggest that such processes are more important in the south (San Jorge) while thermogenic processes are more important in the north (Plato), though further studies and modeling are needed to confirm this.

A second source relates to the recent proposal by *Mora et al. (2017a, b*) who interpret pre-Oligocene sequences preserved beneath the western San Jorge depocenter, west of the San Jerónimo fault. Several wells in that area have drilled a succession that was initially interpreted as the basement, and have found sediments that correlate in age and lithology with the Upper Cretaceous to Eocene sequences that outcrop in the San Jacinto fold belt to the west (Sequence 1 to 4 of *Mora et al., 2017b*). In San Jacinto, Sequence 1 (Upper Cretaceous Cansona) contains organic-rich mudstones and shales of deep marine origin and with type II kerogen, while Sequence 2 (upper Paleocene to lower Eocene San Cayetano) contains marine mudstones with type III kerogen (*ICP, 2000*). The absence of wet gas or light oil accumulations in the south suggests that probable source rocks are type III, hence from all the pre-Oligocene potential source rocks, it is more likely that the source rocks in Sequence 2 (San Cayetano) would have contributed to the generation of dry gas in the south of the LMV. According to this, we propose a new, hypothetical petroleum system in the western part of the San Jorge depocenter (**Figure 6.17**c), called San Cayetano- Upper Ciénaga de Oro (?). Nevertheless, much more geochemical studies of source rocks and hydrocarbons are required in this area to solve the existing uncertainties.

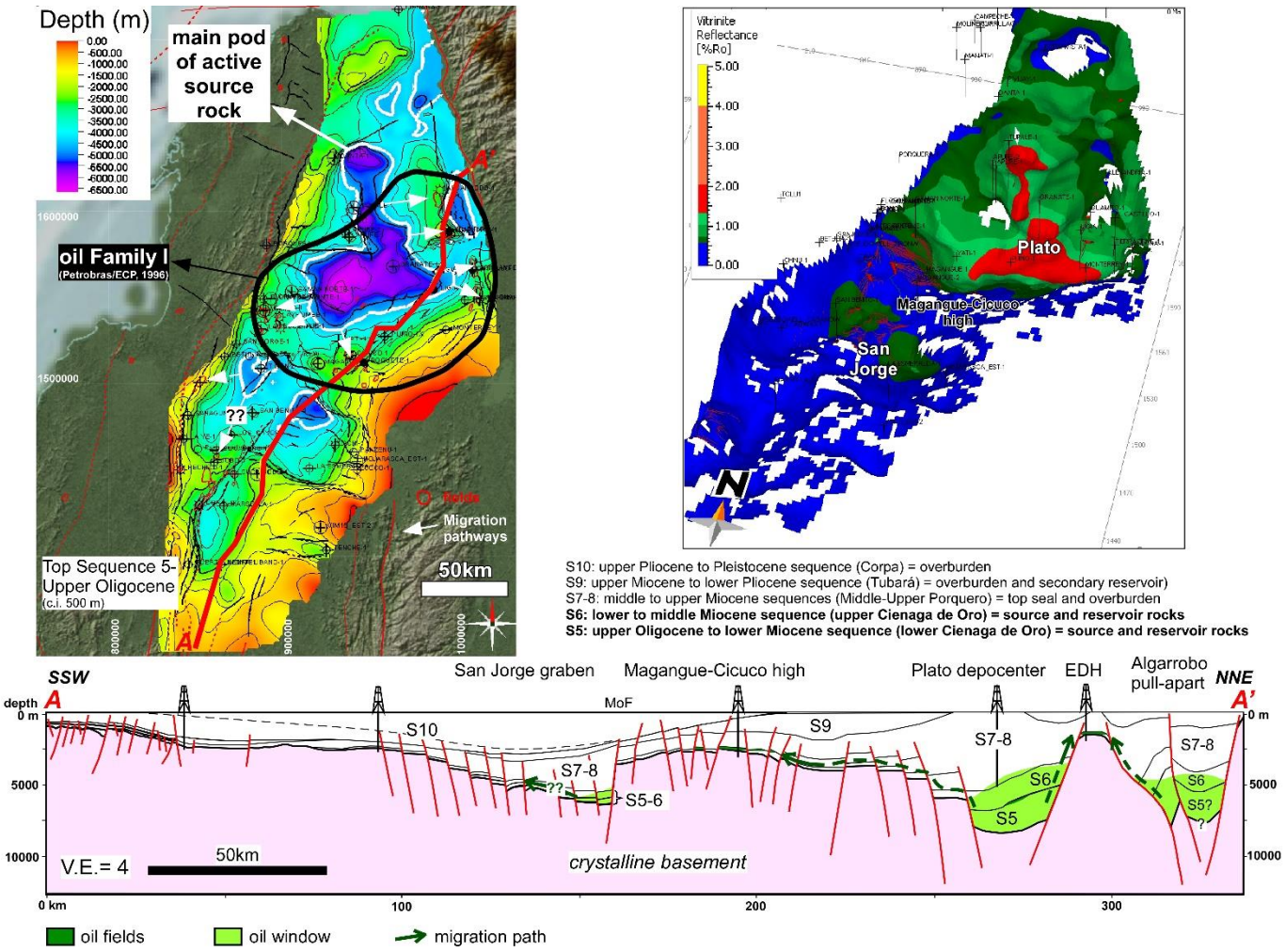

Figure 6.16. Northeast-southwest cross section, map view and 3-D image of the LMV showing the pods of active source rock (white contours in the map and green infill in the cross section), migration pathways (arrows) and petroleum system elements in the basin. In the 3-D image, modelled flow paths and hydrocarbon accumulations at the top of the Oligocene Sequence 5 are plotted, showing a good match with real accumulations. In the north (Plato), known petroleum systems in Sequence 5 and 6 are proposed, in agreement with previous studies; in the south, pods of active source rock and migration pathways have not been well defined, hence speculative and hypothetical petroleum systems are proposed.

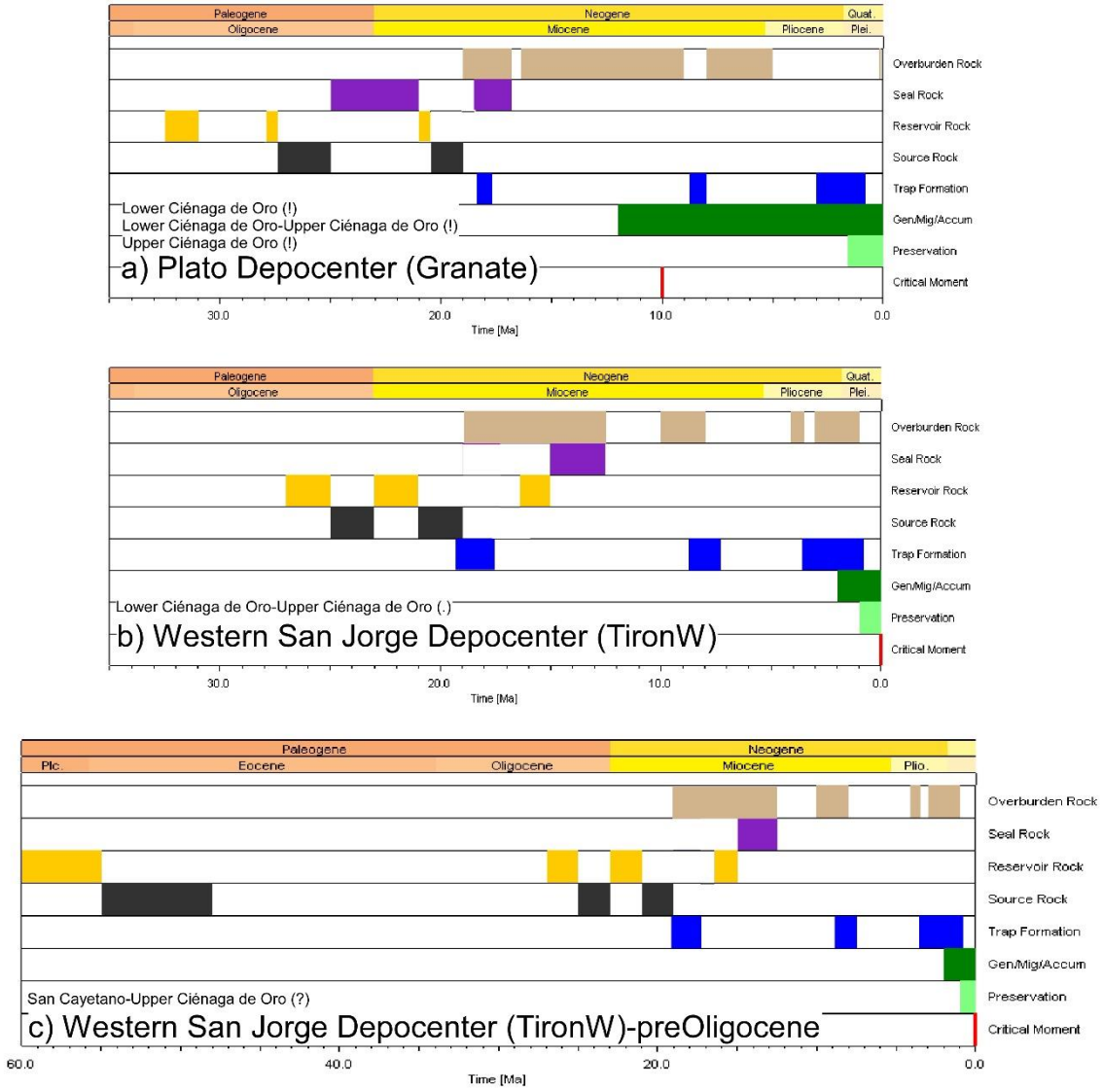

Figure 6.17. Events charts proposed for the LMV in this study for the two basin depocenters (Plato in the north and Western San Jorge in the south). In the south (charts b and c), the critical moment is the present-day considering the results of our model, which considers that insignificant transformation of organic matter occurs, when Oligocene to lower Miocene thermogenic generation is assumed.

6.5.3 Influence of basin evolution on LMV Petroleum Systems

The LMV is a forearc basin which has been tectonically segmented into two depocenters, due to inherited basement structures and to flat-slab subduction processes, producing a particular structural configuration and stratigraphic and facies distribution (see *Chapter 5*). We have seen in this chapter that there are important differences in terms of heat flow and source rock quality between both depocenters of the LMV. Such differences allowed us to propose that there are different petroleum systems in each depocenter and it is clear that each depocenter has a different hydrocarbon potential. Checking out the location of the present-day oil and gas fields and the type of produced hydrocarbons (**Figure 6.1**), the differences between the northern depocenter (Plato) where most of

the fields are located, and the southern depocenter are evident. Therefore, our results are suggesting a direct relationship between basin evolution and hydrocarbons systems.

Thermal history in forearc basins is also very particular and remains poorly understood. As pointed out in *Chapter 5*, a Miocene to Recent high sediment supply has also contributed to partially overcome some of the major obstacles for the development of petroleum systems. Our 3-D modeling study in the LMV has provided important information about the thermal and maturation history of the basin and is the basis for future studies to quantitatively assess light oil and gas generation from organic-rich Oligocene to Miocene or older source rocks. Unfortunately, most of the wells are old, data is limited and its quality in some cases is not very good. Hence, we recommend the acquisition of different types of data such as systematic vitrinite reflectance and other geochemical data, temperature data including more well test data, thermal conductivity and kinetic lab analyses, as well as oil and gas isotopic analyses. The uncertainty regarding the possible pre-Oligocene pod of active source rock in the western San Jorge depocenter requires further analyses and drilling as deep as possible into that sequence. Further data acquisition and analyses will make possible the assessment the most relevant variables, heat flow and kinetics, and to obtain more accurate basin models which will provide a valuable aid for hydrocarbon exploration in the LMV.

6.6 Conclusions

A three-dimensional model of the Lower Magdalena Valley basin of NW Colombia was built from seismic and well data, and used to reconstruct the thermal and maturation history of the basin. We reconstructed the stratal architecture of the basin, implemented within the model episodes of uplift and erosion, and constructed a geothermal gradient map of the basin, which was the main input for the construction of heat flow maps for 3-D modeling. Calculated geothermal gradients were higher in the northern LMV (Plato) and lower in the south, and the obtained average geothermal gradient for the basin is low (19.6 °C/km; 11°F/ 1000ft). Obtained heat flows lie within the range reported globally for forearc basins unrelated to arc magmatism and indicate that the basin is hypothermal. Geochemical data indicate that better quality source rocks occur in the northern LMV (Plato). Model results indicate that the onset of generation occurred at ~15 Ma (middle Miocene) for upper Oligocene to lower Miocene source rocks in the northern part of the basin (Plato depocenter), while lower Miocene sources started generating at ~ 10 Ma (middle-late Miocene). Maturation was influenced by sedimentation at very high rates of thick, deep marine to deltaic, Oligocene to upper Miocene sequences. Late Miocene generation was interrupted by shortening and uplift events at Pliocene (4-3 Ma) and Pleistocene times, though it appears to be ongoing in main depocenters. Poor to fair source rock quality (low TOCs and HIs, type III to II kerogen) appears to be compensated by high thicknesses of the Oligocene to lower Miocene sources, which would still be generating below 3350m (11,000 ft) in the main pod of active source rock (Plato depocenter). By contrast, the effects of shortening pulses and low heat flow would have inhibited maturation of Oligocene to lower Miocene source rocks in the San Jorge graben of the southern Lower Magdalena, suggesting the need of additional hydrocarbon sources to explain the dry gas occurrences in that part of the basin. Possible explanations are generation through bacterial activity at early stages of diagenesis (biogenic gas) or a pre-Oligocene pod of active source rock in the western San Jorge depocenter. Basin segmentation due to inherited basement structure and to flat-slab subduction, led to the deposition of different source rocks, caused different subsidence and uplift histories as well as different thermal regimes in the northern and southern LMV depocenters. Therefore, we are directly relating basin formation and evolution to the hydrocarbon distribution and prospectivity in this basin.

7 Conclusion and Outlook

In this thesis, I examined the plate tectonic, structural and stratigraphic evolution of the Lower Magdalena Valley basin and San Jacinto fold belt of Northwest Colombia, through the integration and interpretation of different kinds of geological and geophysical data such as reflection seismic, air gravity and magnetics, seismicity, basement and detrital zircon geochronology, Hf-isotope geochemistry, biostratigraphy, sequence stratigraphy and tectono-stratigraphy. The results of such examination were used as the main input for the three-dimensional basin and petroleum systems modelling that I carried out in the LMV and for preliminary 1-D and 2-D models in the SJFB, aiming to improve our understanding on the petroleum systems in those areas.

The motivation for this project, as stated in *Chapter 1*, was to try to fill the gap that exists in the current understanding of the Cretaceous to Recent plate tectonic and basin formation and evolution in NW Colombia, in order to provide solid foundations for hydrocarbon exploration activities in the Lower Magdalena Valley basin and San Jacinto fold belt. In the first chapter I wrote several questions which I try to answer in this thesis, aiming to obtain a better understanding of the formation and evolution of the LMV and SJFB, as well as of the petroleum systems they hold. In this section I will provide the answers to these questions referring to each of the related chapters of my thesis.

1. *What is the structure and age of the basement underneath such basins? How, when, and in which tectonic setting was it formed?*

Through detailed interpretations of reflection seismic data and new U-Pb and Hf isotope geochemistry in zircon (*Chapter 3*), I was able to confirm that the basement of the Lower Magdalena Valley basin is the northward continuation of the basement terranes of the northern Central Cordillera, thus that the Lower Magdalena experienced a similar pre-Tertiary tectonic history as the latter. My detailed seismic mapping revealed that the basement structure of the Lower Magdalena is much more complex than previously considered and that it comprises two regions of different fault trends, a western region with a dominant ESE-WNW-trending fault family and a northeastern region with a NE-SW-trending family. The most important structural features in the Lower Magdalena are the Plato and San Jorge depocenters, which are separated by the Magangué-Cicuco basement high. Estimated basement depths in these depocenters range from more than 24 thousand feet (>7 km) in Plato and more than 17 thousand feet (>5 km) in San Jorge. New geochronological data prove the extension into the Lower Magdalena Valley basin not only of a Permo-Triassic terrane (232-300 Ma, Tahamí-Panzenú), but also of the Upper Cretaceous (75-89 Ma) magmatic arc of the northern Central Cordillera, confirming the along-strike continuity to the north of the arc which includes the Antioquia and Sabanalarga plutons. Hf isotopic analyses from the Bonga Upper Cretaceous pluton suggest that the preceding melts were mantle-derived and possibly intruded young crust with oceanic affinity, which I interpret as the northern continuation of the Lower Cretaceous Quebradagrande Complex underneath the westernmost segment of the LMV. Therefore I propose that in Late Cretaceous times (Santonian-Maastrichtian), a “normal” thickness Caribbean plate was being subducted under the South American plate, producing a magmatic arc represented by the Bonga pluton which intruded a dominantly oceanic terrane. The NE-SW trend of basement faults in the northeastern Lower Magdalena is probably inherited from the Jurassic rifting event which is responsible for the conspicuous fabric of surrounding terranes outcropping to the east of the Palestina Fault system, while the ESE-WNW trend in the western Lower Magdalena is inherited from a Late Cretaceous to Eocene, extension and dextral strike-slip episode, which has been recognized in the western Andean forearc from Ecuador to Colombia.

2. *How was the paleo-tectonic evolution of NW Colombia and how did it influence the formation and evolution of the SJFB and LMV?*

Through the integration of detailed tectono-stratigraphic analyses and paleo-tectonic reconstructions, I was able to link the kinematic and convergence history of the Caribbean and South American plates with the formation and infill of the LMV and SJFB. Therefore I directly connected the interpreted paleo-tectonic evolution of NW Colombia to the formation and evolution of the LMV and SJFB.

In *Chapter 4*, I linked the Late Cretaceous to Eocene tectono-stratigraphy of the San Jacinto fold belt of NW Colombia with the plate tectonic evolution of northwestern South America, which experienced Caribbean plateau collision and flat subduction. Using a regional geology and geophysics database, I was able to relate the deposition of four unconformity-bounded forearc basin sequences to specific collision/subduction stages and to relate their bounding unconformities to major tectonic episodes. The oldest Upper Cretaceous sequence (Sequence 1-Cansona) was deposited in a marine forearc environment in which a "normal" thickness Caribbean plate was being subducted beneath northwestern South America, producing contemporaneous magmatism in the present-day northern Central Cordillera and Lower Magdalena Valley basin. Coeval strike slip faulting by the Romeral wrench fault system accommodated right-lateral displacement due to strongly oblique convergence. In latest Cretaceous to early Paleocene times, the Caribbean oceanic plateau collided with South America causing a major shortening event and marking a change to a turbiditic marine sedimentation with abundant terrestrial input, that characterizes the upper Paleocene to lower Eocene San Cayetano sequence (Sequence 2). This sequence was also deposited in a forearc setting with an active volcanic arc that probably represents the final melting stage of the previously subducted "normal" thickness Caribbean slab. A lower to middle Eocene angular unconformity at the top of the San Cayetano sequence, a second major shortening event, the termination of the activity of the Romeral Fault system and the cessation of arc magmatism are interpreted to indicate the onset of low-angle subduction of the thick and buoyant Caribbean oceanic plateau beneath South America, which occurred between 56 and 43 Ma. Onset of low-angle subduction was probably caused by a major change in plate convergence angle and velocity, as suggested by paleo-tectonic reconstructions. Low-angle subduction of the Caribbean plateau has continued to the present and appears to be the main cause of the amagmatic, post-Eocene deposition.

In *Chapter 5*, I used my regional database to reconstruct the subsidence, extension, sedimentation and paleo-geographic history of the Oligocene to Recent Lower Magdalena forearc basin, and to propose possible mechanisms controlling basin evolution, in the absence of major changes in plate kinematics and in a flat-slab subduction setting. I showed that after the collapse of a pre-Oligocene magmatic arc (Bonga), late Oligocene to early Miocene fault-controlled subsidence allowed initial basin fill at relatively low sedimentation rates. Extensional reactivation of inherited, pre-Oligocene basement faults was crucial for the tectonic segmentation of the basin and the formation of its two depocenters (Plato and San Jorge). Oligocene to early Miocene uplift of Andean terranes made possible the connection of the Lower and Middle Magdalena valleys, and the formation of the most important Colombian drainage system (Magdalena River system). The proto-Magdalena river in the north and the proto-Cauca river in the south both started delivering enormous amounts of sediment in middle Miocene times, as fault controlled subsidence was gradually replaced by sagging, due to increased sedimentary load. Such dramatic increase in sedimentation delivered huge amounts of sediments to the trench, causing the formation of an accretionary prism farther west of San Jacinto. This probably weakened the plate interface and caused underplating, with the development of forearc highs in the San Jacinto area. A stronger backstop under the Lower Magdalena would explain shortening in the forearc high and accretionary wedge areas to the W, while the Lower Magdalena remained essentially unaffected. These results highlight the fundamental role of sediment flux, of the inherited basement structure and of flat-slab subduction on the evolution of forearc basins such as the Lower Magdalena.

3. *What is the configuration of the convergent margin between the Caribbean and South American plates in NW Colombia?*

I integrated different types of geological and geophysical data such as reflection-seismic, potential methods, seismicity, seismic tomography, well and outcrop data to propose a three-dimensional model of the geometry of the convergent margin of northwest Colombia. I support previous proposals of a flat-slab subduction of the Caribbean plateau beneath NW South America, which according to my interpretation appears to form different slab segments with different subduction angles, steepening towards the ESE. In *Chapter 4* I mapped the subducting slab in order to propose a three-dimensional geometry of the convergent margin. I thus propose the existence of a tear or STEP fault (subduction transform edge propagator, *Govers and Wortel, 2005*) toward the western end of the Oca-El Pilar-San Sebastián fault system. The Caribbean plateau is therefore being torn into two major slab segments, a steeper slab to the south, imaged by a Wadati-Benioff zone and by seismic tomography, and a shallow to flat slab to the north, which corresponds to the Caribbean oceanic floor offshore northern Colombia and Venezuela.

4. *What kind of basins are the SJFB and LMV and which were the mechanisms that controlled their formation and evolution?*

In *Chapter 4* I showed that the Cretaceous to Eocene units preserved in the San Jacinto fold belt were deposited in a forearc setting with an active magmatic arc, due to the oblique convergence of the Caribbean and "normal" thickness oceanic plate and the South American plate. Proposed basin formation mechanisms are oblique convergence caused arc-parallel extension and clockwise block rotation due to dextral strike-slip, as reported in similar forearc basins in Ecuador. After a major plate readjustment in early to middle Eocene times, convergence becomes more orthogonal and low-angle subduction shuts off the magmatism. In *Chapter 5* I proposed that sedimentation began in Oligocene times due to the thermal collapse of the pre-existing magmatic arc, which caused the older faults to extensionally reactivate. Oligocene to Recent sedimentary infill of the the LMV occurred in the absence of major changes in terms of convergence velocity and obliquity, therefore controls on basin evolution are more related to hinterland areas where uplift and denudation of Andean terranes caused a dramatic increase in sediment supply in early to middle Miocene times. Hence, I propose that the initial fault-controlled subsidence possibly driven by crustal cooling was replaced by sedimentary loading in middle to late Miocene times. Sediment supply was also responsible for underplating and uplift in the forearc high in the current San Jacinto fold belt. However, low-angle subduction was also fundamental for the basin evolution because it precluded the formation of a magmatic arc and possibly also influenced the segmentation of the basin with its two depocenters. The different basement fabrics described in *Chapter 3* also influenced the way the basin was deformed according to the regional stress field. According to the aforementioned, the LMV is an amagmatic forearc basin which was tectonically segmented due to inherited basement structures and to flat-slab subduction processes, and which was strongly controlled by sediment supply.

5. *What are the implications of the plate tectonic and basin evolution of the LMV and SJFB on hydrocarbon systems?*

I proposed in *Chapter 5* that the LMV is an amagmatic, tectonically segmented forearc basin formed in a low-angle subduction setting, conditions that probably led to an overall decrease in regional heat flow (slab refrigeration?). In *Chapter 6* I further discussed the general conception about the low hydrocarbon potential of forearc basins due to low heat flows and poor quality reservoirs. However, after my basin analysis, I consider that while the relatively low heat flow does not favor

hydrocarbon generation and migration, the high sediment supply which allowed the rapid deposition of thousands of meters of poor to fair quality, organic-rich source rocks in the depocenters of the LMV partly compensated for such low heat flows. This is demonstrated not only by the hydrocarbon production in the basin, but also by the 3-D modeling I carried out. High sediment supply overfilled the Plato depocenter in the north and allowed source rocks to enter the oil window since middle Miocene times.

Basin segmentation due to basement inherited structures and flat-slab subduction, influenced the deposition of different source rocks, the different subsidence and uplift histories as well as the different thermal regimes in the northern and southern LMV depocenters. Therefore, I have been able to directly relate the proposed basin formation and evolution to the hydrocarbon distribution and prospectivity. In *Chapter 6* I showed that such segmentation was crucial for hydrocarbon systems because it provided more favorable conditions for hydrocarbon generation and entrapment in the northern depocenter (Plato), compared to the southern depocenter (San Jorge). I showed that the subsidence and uplift histories in each depocenter were different, especially after late Miocene times and that in the north, not only the heat flows are higher, but also the source rocks have a higher quality. Hence, the present-day location of most of the hydrocarbon fields around the northern Plato depocenter is due to the particular basin evolution and infill of this segmented and amagmatic forearc basin. Results of my 3-D modelling also show that in the south the basin evolution and infill was not so favorable for hydrocarbon generation. However, there are still issues to be solved in that area, such as the fact that the existing hydrocarbon accumulations are not explained by thermogenic generation from Oligocene to lower Miocene source rocks.

Finally, in the San Jacinto fold belt, thermal maturity data (e.g. *GEMS, 2017*) and preliminary modelling results support my interpretation in the sense that the area behaved as a forearc high from Miocene to Recent times. For such reason the source rocks are mostly immature and they probably were never deeply buried, a conclusion that appears to be not very favorable for hydrocarbon prospectivity but that requires much further studies. Nevertheless, the results of this thesis provide new insights into the controls and influence of plate tectonics and basin evolution on petroleum systems.

Recommendations and the way forward

After finishing this study, I have become more aware of the fact that though I think I obtained very interesting and useful results, my thesis is just the starting point for future studies in several different geoscientific fields in my study area.

In the area of plate tectonics and geodynamics, I am surprised of the scarcity of data available in NW Colombia, compared to the neighbouring countries (Venezuela and Ecuador). Therefore, I recommend several activities in order to obtain a good image of the deeper parts of the crust and upper mantle, such as deep penetration, wide angle, reflection seismic acquisition, gravity modelling, seismic tomography and seismological and GPS data acquisition and analysis. Though my study area is relatively aseismic, it should be possible to obtain more focal mechanism solutions, especially from the San Jacinto fold belt. A complex but very interesting area is the south of the LMV and SJFB, where the Caribbean and Nazca plates are interacting in some way which we still do not understand, hence future research could focus in those areas. An important aspect to highlight is that more than 5 million people live in the area of influence of this convergent margin, which has not been properly characterized in terms of seismicity and physical properties of the subduction interface. Therefore, earthquake hazard studies in the northwestern Colombia convergent margin are also highly recommended and needed.

Good quality, conventional reflection seismic acquisition is also required in the SJFB, where the coverage is not very dense, imaging is very poor and there is high structural and stratigraphic complexity. The scale of the stratigraphic sequences I defined (mostly 2nd –order) is too regional, hence we need more detailed surface geology and well studies, with multiple rock analyses, such as different biostratigraphy tools (combination of forams, palynology, nannofossils, etc.), geochronology, thermochronology, paleomagnetism and others which will help to reconstruct in more detail the deposition of pre-Oligocene sequences in San Jacinto. It is evident that there are hydrocarbon systems working in the area, but more seismic, more wells and more field geology campaigns are required for a better assessment of the hydrocarbon potential of this frontier area. Construction and restoration of balanced cross sections for 2-D modelling of petroleum system are also necessary to properly reconstruct the thermal and maturation history of the fold belt.

Though there is much more data and less geological complexity in the LMV, we need to produce more refined basin and hydrocarbon system multidimensional models to better understand the hydrocarbon systems and potential, especially in the southern LMV. I recommend doing lab analyses such as source rock kinetics, thermal conductivities and obtaining more temperature and heat flow measurements from well tests in order to produce more refined 3-D models which will provide quantitative resource assessment. Isotopic and biomarker analyses of hydrocarbons to do more oil to source rock correlations are also necessary especially for the southern part of the LMV.

Appendix A

Supplementary figures for *Chapter 3* (*Mora et al., 2017a*):

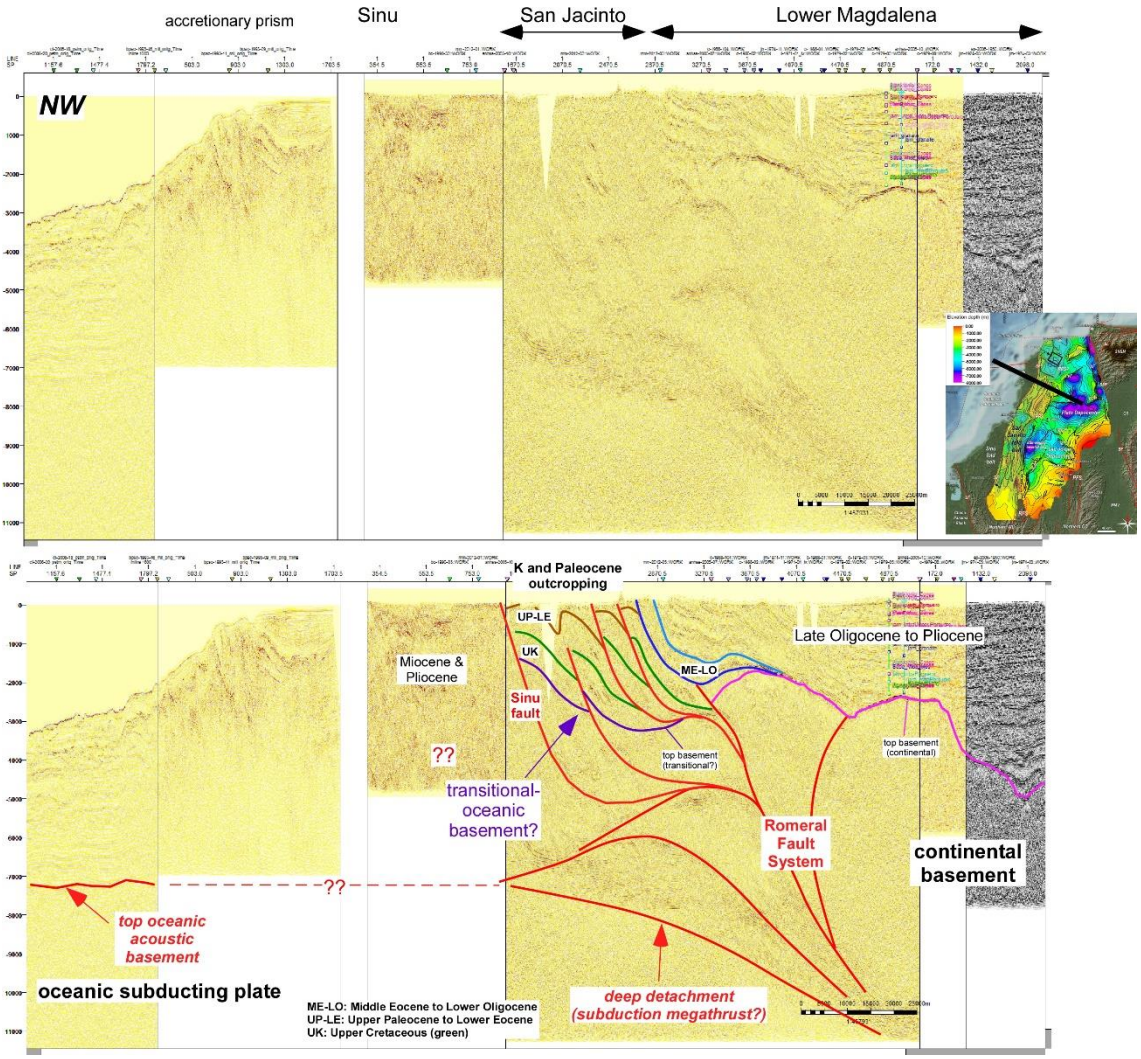

Figure A 1. Uninterpreted and interpreted regional reflection-seismic cross-section showing the possible deep structure under the Lower Magdalena Valley basin and San Jacinto fold belt expression. A deep, SE-dipping detachment has been interpreted as the subduction megathrust which we have correlated and mapped with the oceanic acoustic basement in offshore areas. We also show the structural style of the San Jacinto belt and the interpretation which was done to obtain the basement map shown in **Figure 3.4**.

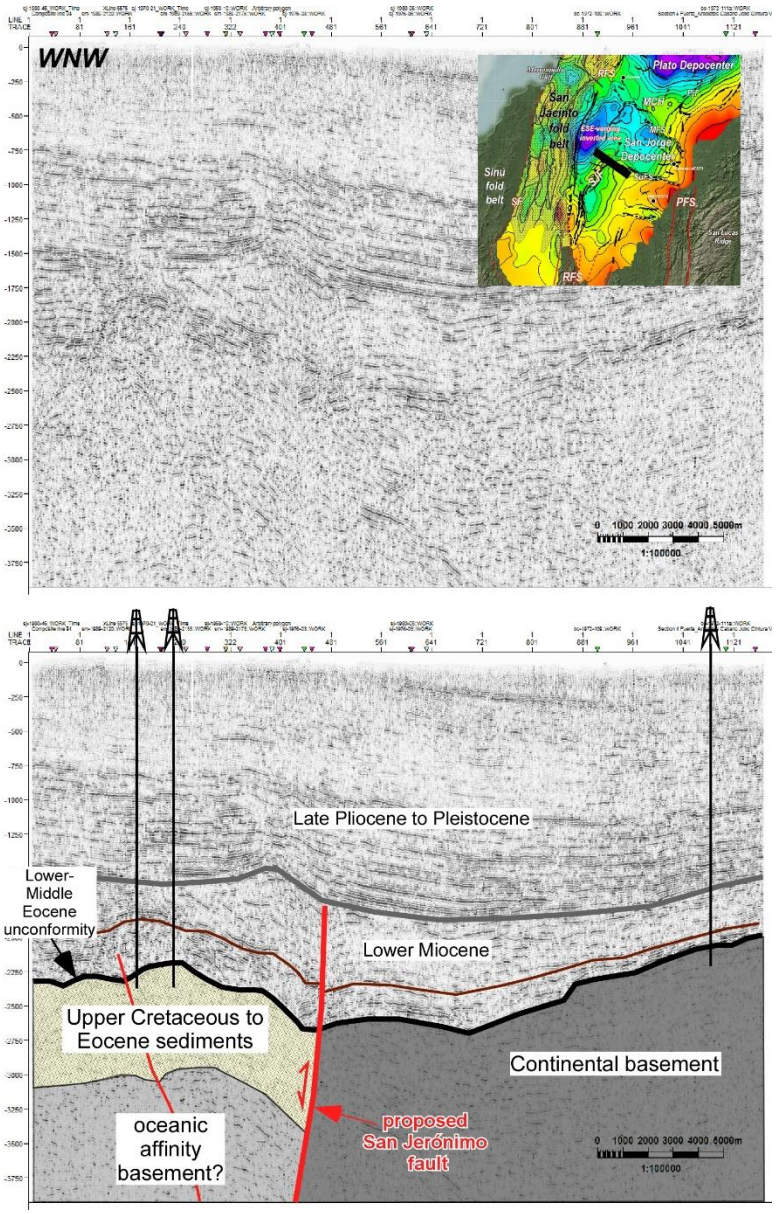

Figure A 2. Uninterpreted and interpreted, reflection-seismic line in the Jobo-Tablón area, showing the expression of an eastern, east-verging splay of the Romeral Fault System which we interpret here as the northern continuation of the San Jerónimo Fault.

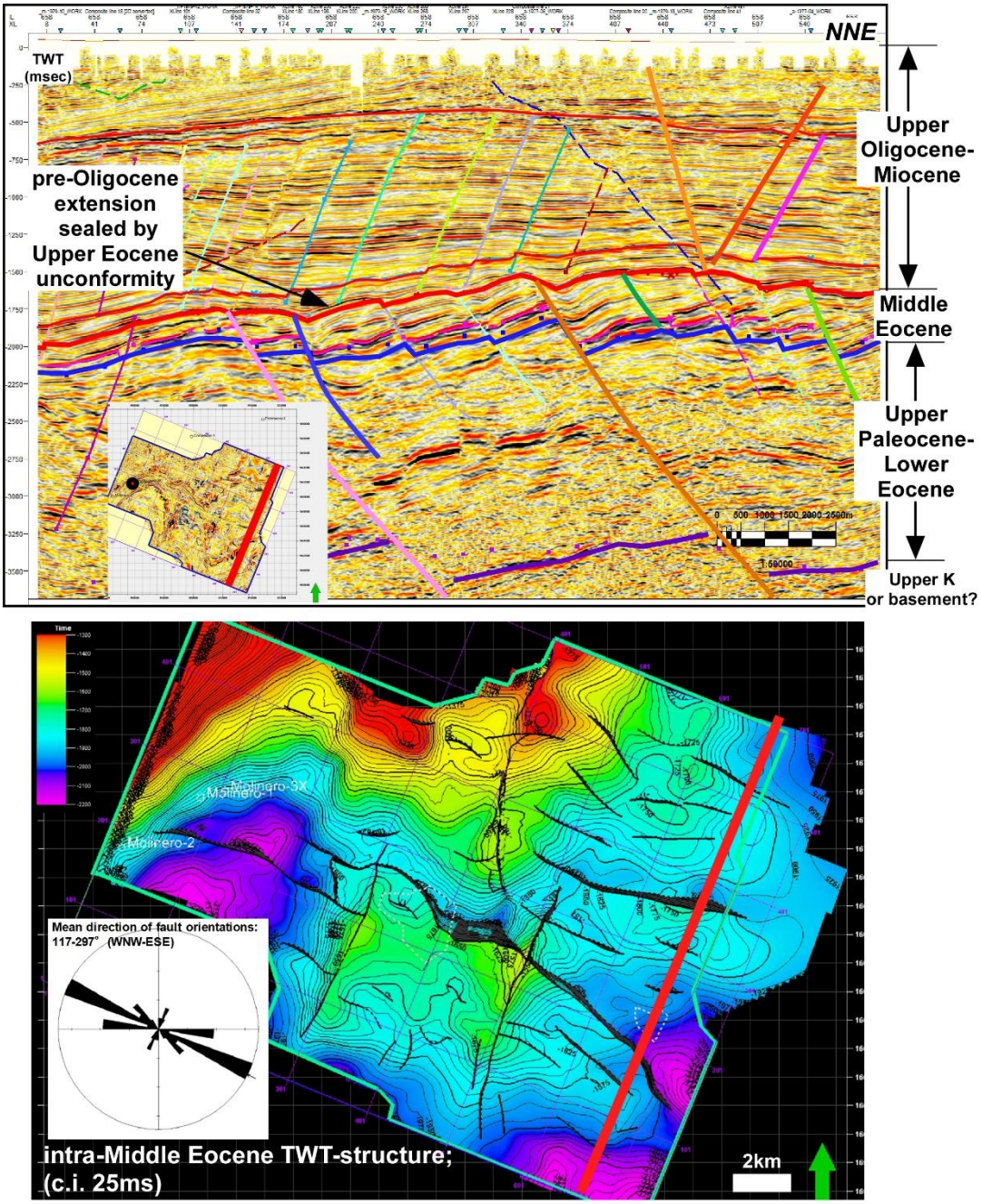

Figure A 3. Seismic-reflection line from a 3D-survey in the northern San Jacinto fold belt (see location in **Figure 3.2**, **Figure 3.4** and **Figure 3.8**), showing the extensional structural style of the pre-Oligocene sequences in that part of the fold belt (modified from *Mora et al., 2013*).

Appendix B

Supplementary material for *Chapter 4* (*Mora et al., 2017b*):

Introduction

The supplementary information provided here as additional text, includes detailed descriptions of the studied pre-Oligocene tectono-stratigraphic sequences in the San Jacinto fold belt of NW Colombia (Text B1), the methodology followed to carry out the U-Pb geochronology and Hf Isotope geochemistry (Text B2), and the procedure followed to construct the map and cross-section of the subducted Caribbean oceanic slab segments beneath NW South America, including relevant regional cross-sections (Figure B1). We also include as supplementary figures the uninterpreted reflection-seismic sections (Figures B2 to B5), which correspond to **Figure 4.8** to **Figure 4.11** in the main text.

Text B1. Detailed description of tectono-stratigraphic sequences

Sequence 1 (Cansona-Upper Cretaceous)

The oldest sequence is of Upper Cretaceous age and comprises the bituminous shales, cherts and limestones of the Cansona unit (*Duque-Caro, 1979*; *Guzman et al., 2004*; *Guzman, 2007*). While a Coniacian age has been reported for the lower part, based on ammonites studied by *Etayo-Serna et al. (1969)*, a Campanian-Maastrichtian age has been proposed for the upper part, based on planktonic foraminiphera, nannoplankton and palynomorphs (*Aleman, 1983*, *Guzman et al., 2007*; *ATG-ANH, 2009*; *Dueñas and Gómez, 2013*). Given that it spans for more than 10 Ma, it can be classified as a 2nd-order cycle (*Vail et al., 1977*), which would correspond to a high rank/low frequency cycle in the hierarchy pyramid of *Catuneanu et al. (2009*). Facies and thickness information of this sequence comes from several stratigraphic sections (*Duque-Caro, 1979*, *Guzman et al., 2004*, *ATG-ANH, 2009*). Biostratigraphic data compiled by *Duque-Caro (2000, 2001*) and *Guzman (2007*) show an absence of lower Paleocene planktonic foraminiferal zones (P.0 to P.2) in the SJFB, indicating the existence of a regional unconformity which marks the upper limit of this sequence (**Figure 4.4**). This unconformity would be related to the "Calima orogeny" proposed by *Barrero (1979*), based on observations in the Colombian Western Cordillera. Considering that its base is just exposed in one stratigraphic section (Cacao creek, *Aleman, 1983*, *ICP, 2000*), the measured thicknesses are incomplete and highly variable, though in the most complete section (Cacao) the measured thickness is approximately 762 m.

Very few petrographic analyses have been carried out to the rocks of this Upper Cretaceous Sequence. According to *Ecopetrol/ICP (2014*), the sandstones of this sequence range from lithic arkoses towards the base to litharenites towards the top, with a predominance of metamorphic and sedimentary lithics. Geochemical data from different sources (*Beroiz et al., 1986*; *ESRI/ILEX, 1995*; *Petrobras/Ecopetrol, 1996*; *Niño, 2005*; *Sánchez and Permanyer, 2006* and *Osorno and Rangel, 2015)* shows that the organic-rich facies of the Upper Cretaceous Cansona sequence have high quantities of organic matter (Total Organic Content TOC > 1%) which is formed mainly by type II kerogen (*Tissot et al., 1974*; *Peters and Cassa, 1994*), in the form of amorphous organic matter with much less content of vitrinite, dinoflagellates, algae, and other components. These rocks were deposited in moderately deep marine settings with reduced terrigenous supply (*Niño, 2005*; *Juliao-Lemus et al., 2016*). The fine-grained middle and upper parts of Sequence 1 (Cansona), may be correlated with Upper Cretaceous units in the northeastern Western Cordillera such as the Pendersico Formation (*Alvarez and Gonzalez, 1978*; *Diaz-Cañas, 2015*).

Sequence 2 (San Cayetano-upper Paleocene to lower Eocene)

Sequence 2 has received several names (Arroyo Seco, Luruaco) but in this work, it comprises the San Cayetano unit which has been dated as upper Paleocene to lower Eocene (planktonic foraminiferal zones P.3 to P.9, *Duque-Caro, 2000; 2001; 2011a, b, c; 2012b, 2013b*) and according to its duration, it also corresponds to a 2nd-order cycle (*Vail et al., 1977*) or to a high rank/low frequency cycle (*Catuneanu et al., 2009*). The late Paleocene was characterized by a high global sea level (eustatic curves in **Figure 4.2**, *Haq et al., 1987*), which could have influenced the onset and extension of San Cayetano sedimentation. A late Paleocene

thermal maximum and an early Eocene climatic optimum (*Zachos et al., 2001*, **Figure 4.2**) would have also influenced sedimentation of this sequence. While very few samples have yielded an upper Paleocene age (zones P.3 to P.5), in most of the outcrops and wells the basal section of the unit is not exposed or was not drilled. In stratigraphic sections (e.g. San Cayetano section, northern San Jacinto anticlinoria), more than 1600 m were measured (*ICP, 2000*). In the northernmost SJFB, old and recent wells have drilled a monotonous silty section of upper Paleocene to lower Eocene age, with thicknesses of more than 2000 m. The top of the San Cayetano sequence has been considered a regional unconformity of middle Eocene age which has been reported in surface geology studies and a few poor-quality reflection seismic sections. Biostratigraphic data show that there's a big hiatus in the center of the SJFB, where the lower Eocene is missing, while to the north the section is more complete and the contact with the overlying sequence appears to be a disconformity (**Figure 4.4**).

Well and outcrop data show that this sequence exhibits an overall fining-upward trend, with higher contents of sandy and conglomeratic lithologies in its lower half and higher contents of muddy lithologies towards the top. However, there are notorious facies variations from south to north that appear to define three areas with markedly different lithologies and facies, apparently controlled by structural features (**Figure 4.4**). Conglomerates and sandstones are dominant in the central part of the SJFB, while in the south the conglomeratic facies are subordinate. Towards the north, there's a notorious facies change which appears to be related to a SE-NW-trending structural feature, which has been called in geological maps the "El Dique Fault" (EDF, **Figure 4.1** and **Figure 4.4**; *Gomez et al., 2007*). The conglomerates and sandstones which occur in the central SJFB were deposited in fan deltas (*Guzman, 2007*), while the sandstones in the Luruaco area have been related to turbidites (*Geosearch, 2006* and **Figure 4.10**).

Petrographic analyses from outcrops in the northern SJFB show that Sequence 2 (San Cayetano) consists of litharenites with fragments of plutonic (granites), volcanic porphyritic, metamorphic (quartzites and schists) and sedimentary rocks (cherts and mudstones; *Llinás, 2012*). In the C-1 well, also located in the northern SJFB, dominant rock types are very fine to fine-grained litharenites, sublitharenites, subarkoses and arkoses. Lithics are mainly vulcanites, cherts, quartzites and other metamorphites, micrites, mudstones and few plutonites (*Petroscopía S.A., 2013*).

Geochemical studies (*Beroiz et al., 1986*; *Hocol, 1993*; *ESRI/ILEX, 1995*; *Niño, 2005*; *GEMS Ltda., 2007, 2014*) show a notorious change in the organic-rich facies of this sequence compared to the Upper Cretaceous Cansona sequence. While organic content is much lower (TOC<2%), the organic matter is formed mainly by vitrinite and in much less proportion by amorphous organic matter, liptinite and inertinite (*Niño, 2005*). This composition evidences a very clear input of higher land plants characteristic of a type III kerogen. Paleocene to Eocene sedimentary units equivalent to Sequence 2 are not well preserved in the northern Western Cordillera due to uplift and erosion, hence it is very difficult to make a comparison with that area.

Sequence 3 (Chengue-middle to upper Eocene)

Sequence 3 corresponds to the Chengue Group, defined by the P.10 to P.14 planktonic foraminiferal zones of middle to late Eocene age (*Duque-Caro, 2000; 2001; 2011a, b, c; 2012b, 2013b*); it spans for nearly 10 Ma, hence it also corresponds to a 2nd-order or high rank/low frequency cycle (*Vail et al., 1977*; *Catuneanu et al., 2009*; **Figure 4.2**). Biostratigraphic data indicates that the unconformity between Sequences 2 (San Cayetano) and 3 (Chengue) corresponds to the P.9 to P.10 zones of *Duque-Caro (2000, 2001, 2011 a, b, c*), implying a time interval of 46 to 51 Ma which includes the limit between the lower and middle Eocene. This sequence has been eroded in the southern part of the SJFB and is more preserved in the northern part (**Figure 4.4**). The sequence displays notorious facies and thickness changes from south to north, and the El Dique fault also seemed to exert some influence on sedimentation and facies distribution. While south of the fault there is a predominance of conglomeratic facies (Maco and Pendales units), north of the fault red algae carbonates are locally developed in the Arroyo de Piedra area (**Figure 4.4**).

Carbonates of Sequence 3 were sampled from outcrops in the northern SJFB (Arroyo de Piedra limestones) and studied in thin section. They consist of packstones/biomicrites to grainstones/biosparites with red algae fragments and structures (ooid, oncoliths and rodoliths), and fragments of benthic foraminifera and echinoderms. These carbonates were also described in a core from a well located in the northern SJFB (M-3X), in which seven shoaling-up high-frequency cycles or parasequences (*Van Wagoner et al.,1990*) were identified, and the interpreted environment was a shallow (<30m water depth), moderately high energy carbonate platform (*Cross, 2014*). Outcrop and well samples from the northern SJFB were also selected for detailed petrographic and C-, O- and Sr isotope stratigraphic analyses (*Ares, 2014*), in an attempt to obtain a better dating of the Eocene carbonates. Though preliminary conclusions from isotope chemostratigraphy suggested a good correlation in age between the carbonates in the northern SJFB (Arroyo de Piedra) and those in the central and southern SJFB (Toluviejo, *Ares, 2014*), in this study we consider that such a conclusion is

not well supported because the standard curve of the $^{87}Sr/^{86}Sr$ ratio for the Eocene is very flat (*McArthur et al., 2001*), making very difficult to obtain an accurate dating of Eocene carbonate samples. According to *Faure and Mensing (2005*), the most favorable conditions for dating marine carbonate rocks exist for samples of post-Eocene age (i.e. 40-0 Ma), because in this time interval, the $^{87}Sr/^{86}Sr$ ratio of seawater increase steadily from 0.70775 to 0.70918. Furthermore, the obtained Sr isotopic values were anomalously high and thus the obtained ages were too young, approaching the age of the southern carbonates (Toluviejo). Also in the north, the most abundant microfacies were algae-rich and benthic foraminiferal grainstones and packstones in which the most abundant foraminifera assemblage comprised Orbitoides (Discocyclina) and Nummulites, and the carbonates were interpreted as deposited in a shallow marine carbonate platform (*Ares, 2014*). However, recent detailed sedimentological studies of Oligocene to Miocene carbonates in northwestern offshore Venezuela suggest that deposition of carbonates with red algae and large benthic foraminifera is also possible in deeper marine settings such as distally steepened ramps, related to oligophotic (poor light) carbonate production (*Pomar et al., 2015*). Therefore, more detailed studies have to be carried out not only to define more precisely the depositional environments but also to obtain more reliable depositional ages of the Cenozoic carbonates in northwestern South America.

The siliciclastic units of Sequence 3 were also studied in outcrop and thin section. The unit known as Maco conglomerate consists of polymictic conglomerates and calcareous, feldspathic litharenites in which the most abundant lithics are black chert fragments, followed by quartzarenites and minor metamorphic and igneous plutonic and volcanic rocks (*Llinás, 2012*). The thickness of Sequence 3 is highly variable and ranges from 150 m (490 ft) in paleohighs to more than 1000 m (>3200 ft) in low areas. *Parra and Rincón (2014*) recently studied foraminiferal assemblages in two stratigraphic sections in the northern SJFB and proposed an early to Middle Eocene age and deposition in shelf neritic to possible bathyal environments for the Chengue unit.

Sequence 4 (San Jacinto-upper Eocene to lower Oligocene)

Sequence 4 comprises the siliciclastic San Jacinto unit and calcareous Toluviejo unit (**Figure 4.2** and **Figure 4.4**). According to biostratigraphic studies (*Duque-Caro, 1979*; *Guzman, 2007*) it is defined by the P.15 to P.20 planktonic foraminiferal zones of upper Eocene to lower Oligocene age (*Duque-Caro, 2000, 2001, 2011a, b, c; 2012b; 2013a, b*), and therefore it is also a 2nd -order or high rank/low frequency cycle (*Vail et al, 1977*; *Catuneanu et al., 2009*). The average thickness of Sequence 4 is 342 meters, though it is highly variable along depositional strike. This sequence was recently drilled by two stratigraphic wells, the SamanEst-1 and the T-2XP (**Figure 4.3** and **Figure 4.4**). In the SamanEst-1, almost one thousand meters of interbedded mudstones, sandstones and conglomerates were found and the succession was dated as upper Eocene to lower Oligocene (zones P.15 to P.20, *Duque-Caro, 2013a*). The basal succession drilled by the well was made of polymictic conglomerates with abundant igneous, metamorphic and sedimentary lithics. In the T-2XP well in the southern SJFB, Sequence 4 displays both carbonate facies of the Toluviejo unit and clastic sandy facies of the San Jacinto unit (**Figure 4.4**). In other areas (e.g. Chalán), the Toluviejo unit has been described as a succession of calcareous sandstones and conglomerates, classified as quartzarenites to litharenites with sedimentary and igneous lithics, and packstones and grainstones of red algae and large benthic forams (Lepidocyclines).

In thin section, the San Jacinto unit of Sequence 4 exhibits an increase in quartz content and a decrease in feldspar and lithic content, compared to the samples of the older sequences, and most samples were classified as sublitharenites and subarkoses, with minor arkoses to litharenites (*Ecopetrol/ICP, 2014*). Geochemical studies of Sequences 3 and 4 (Chengue and San Jacinto) show that mudstones facies can have poor to very good organic matter contents (TOC commonly <3%; *Hocol, 1993*; *ESRI/ILEX, 1995*; *Niño, 2005*; *GEMS Ltda., 2014*), in the form of vitrinite and amorphous matter and with minor proportions of liptinite and inertinite. This evidences an important input of higher land plants characteristic of a type III kerogen for these sequences.

Text B2. Methodology for Detrital zircon U-Pb Geochronology and Hf Isotope Geochemistry

Zircons were separated from cores and cuttings using standard gravimetric and magnetic techniques. Prior to crushing, all samples were soaked in a strong organic solvent and thoroughly rinsed with water in order to remove any external contamination to the cores and cuttings caused by residual drilling mud. In the case of cuttings, samples were sieved with a 1 mm mesh and only the larger and similarly-looking rock fragments retained by the mesh were processed for zircon separations to minimize potential contamination by cavings. Zircon crystals were randomly mounted in epoxy resin and polished to expose an internal surface prior to laser ablation – inductively coupled plasma – mass spectrometry (LA-ICP-MS) measurements. Alongside each sample, fragments of the Sri Lanka (SL2) natural zircon crystal (564 Ma; *Gehrels et al. 2008*) were

mounted for use as the U-Pb primary reference material, and fragments of Mud Tank ($^{176}Hf/^{177}Hf$= 0.282507; *Woodhead and Hergt, 2005*), FC-1 ($^{176}Hf/^{177}Hf$ = 0.282183; *Fisher et al., 2014*) and R-33 ($^{176}Hf/^{177}Hf$ = 0.282764; *Fisher et al., 2014*) were used as reference material for Hf isotopic compositions.

Analytical procedures for the U-Pb and Yb-Lu-Hf isotopic measurements followed the methods described in *Cecil et al. (2011*); all analyses were conducted in a Nu Plasma multicollector-ICP-MS instrument coupled to a Photon Machines Analyte-G2 laser ablation system using static collection mode at the Arizona LaserChron Center, University of Arizona. In brief, for U-Pb geochronology, isotopes ^{238}U, ^{232}Th, ^{208}Pb, ^{207}Pb and ^{206}Pb were measured simultaneously in faraday collectors whereas ^{204}(Pb+Hg) and ^{202}Hg were measured in discrete-dynode ion-multipliers. Instrumental inter-element and isotopic fractionations affecting the measured $^{206}Pb/^{238}U$ and $^{207}Pb/^{206}Pb$ compositions were corrected by a standard-sample bracketing approach using the Sri Lanka reference crystal, which was measured once or twice every five unknowns, and normalizing all data with respect to its known ID-TIMS values (*Gehrels et al. 2008*). For Yb-Lu-Hf measurements, all masses from 171 to 180 were measured simultaneously on ten faraday cups equipped with 3 x 1011 Ω resistors. Hafnium mass fractionation was corrected by normalizing the data using an exponential law relative to a $^{179}Hf/^{177}Hf$ value of 0.7325 (*Patchett and Tatsumoto, 1981).* Ytterbium mass fractionation was corrected using a $^{173}Yb/^{171}Yb$ value of 1.129197 (*Vervoort et al. 2004)* and a session-specific $^{176}Yb/^{173}Yb$ bias correction factor derived from the measurement of high-Yb natural and synthetic zircon crystals (see *Ibanez-Mejia et al. 2015* for details). All $^{176}Hf/^{177}Hf$ compositions reported here are relative to a Mud Tank value of 0.282507 (see *Fisher et al. 2014*); this reference crystal was analyzed once or twice every ~15 unknowns during our session. Additionally, the reference crystals FC-1 and R-33 were also analyzed in repeated occasions throughout the session to monitor the accuracy of the Hf mass-bias and Yb interference corrections. These crystals are particularly well suited for the latter, owing to their relatively high HREE concentrations with respect to other widely available reference zircons and the average composition of natural crystals. We obtained mean values of 0.282167 ± 58 (2 S.D., n= 56, MSWD= 1.5) and 0.282725 ± 62 (2 S.D., n= 78, MSWD= 0.7) for FC-1 and R-33, respectively, which are accurate with respect to their reference solution-MC-ICP-MS values within quoted uncertainties.

Text B3. Construction of the cross-section (**Figure 4.12**) and depth map (**Figure 4.13**) of the subducted oceanic slab beneath NW South America

For the analysis of the subduction configuration under the SJFB and LMV, we first plotted the seismicity data from the Colombian Geological Service in a cross-section, which is nearly parallel to the convergence vector of the Caribbean plate, as measured by *Trenkamp et al. (2002*) in the San Andrés Island (**Figure 4.12**). Based on our regional reflection seismic interpretations and using stacking processing velocities, we then constructed a depth map of the near top of the subducting oceanic plate that connects with the subduction megathrust under the SJFB and LMV (**Figure 4.9**). Finally, we mapped the near top of the intermediate-depth seismicity data associated to the Bucaramanga slab of *Pennington (1981*) and merged it with reflection seismic depth map of the shallowest and flattest slab, obtaining a good approximation to the geometry and depth of the subducted oceanic plate beneath northwestern Colombia (**Figure 4.13**). It must be noted that the earthquakes were not relocated using standard seismological procedures; however, considering that the error is relatively small (<10km), our plots serve the purpose of showing the broad geometry and configuration of the subduction zone in NW Colombia.

As seen in the cross-section (**Figure 4.12**), seismicity increases and deepens to the E and SE, towards the Perijá Ridge, where we have a well-defined area of intermediate-depth seismicity, which represents the along strike projection to the north of the Bucaramanga intermediate seismicity nest (*Zarifi et al., 2007*). We plotted in the cross-section the near top of the oceanic subducting plate as interpreted from seismic reflection data (thick black line) and assumed a crustal thickness of ~15km based on previous estimates (*Bernal et al., 2015a*). We also plotted the near top of the intermediate-depth seismicity data (dashed black line) corresponding to the Bucaramanga slab of *Pennington (1981*), which was recently redefined by *Syracuse et al. (2016*) and called by them "Caribbean" segment. The deepest and steepest slab segment to the ESE is a projection of the slab imaged by *Bezada et al. (2010*) under the Mérida Andes, using P-wave tomography.

According to the map and cross section, the oceanic plate appears to be subducted under San Jacinto and the Lower Magdalena at a very low angle, in agreement with recent studies in the area (*Bernal et al., 2015a*; *Mora et al., 2017a*). There is a good correlation of our shallow top of the subducted oceanic slab with the intermediate-depth seismicity data farther to the east, suggesting the existence of a bend in the slab, approximately coinciding with the Palestina Fault System at the surface (**Figure 4.12** and **Figure 4.13**). East of this bend, intermediate-depth seismicity is imaging the Caribbean flat-slab of *Syracuse et al. (2016*). The depth map of the top of the subducted oceanic slab (**Figure 4.13**) also shows the notorious change in slab dip

between the flattest segment below the SJFB and LMV and the intermediate-depth segment below the northern Central and Eastern Cordilleras, the Perija Ridge and the Sierra de Santa Marta (SNSM). The interpretation of reflection seismic data from northernmost Colombia, including offshore areas, shows also that the subducted slab changes its strike direction from SSW-NNE to almost W-E and that change coincides with the trace of the Oca Fault (OF), which is the western segment of the Oca-San Sebastián-El Pilar right-lateral wrench system.

In WNW-ESE cross-section (**Figure 4.12**), the subducted Caribbean plate can thus be subdivided into three slab segments of different dip and separated by kinks or bends: a northwestern shallow and very flat slab segment, a central intermediate-depth and flat slab segment and a southeastern deep and very steep slab segment imaged by *Bezada et al. (2010*). However, available data is not enough to properly image the transition from the intermediate-depth to the steep deepest slab segments, which instead of a sharp kink could be a smoother and curved transition, as depicted in **Figure 4.12**. According to our interpretations in the cross-section, the northwestern flat slab segment currently underneath the SJFB and LMV is dipping at 8.2° to the ESE and has a length of 278 to 308 km from the trench to the area of the Palestina Fault system, where it reaches depths between 45 and 50 km. The central flat slab segment (Caribbean slab of *Syracuse et al., 2016*), is dipping 25° to the ESE and has a length of 341 to 371 km until it reaches depths between 180 and 200 km below the Mérida Andes. The southeastern slab segment, projected from the image by *Bezada et al. (2010*), would be dipping to the SE at an angle of 79° and extending down for 401 to 431 km to reach depths of nearly 600 km. Based on these measurements, the total length of the Caribbean subducted slab beneath northern Colombia and western Venezuela would range from 1020 to 1110 km. *Van Benthem et al. (2013*) measured around 900 km of the Caribbean slab length from their tomographic images, which is not very different from our value, though they lack the detail of the two shallow flat slab segments that we have.

Supplementary Figures for *Chapter 4* (*Mora et al., 2017b*):

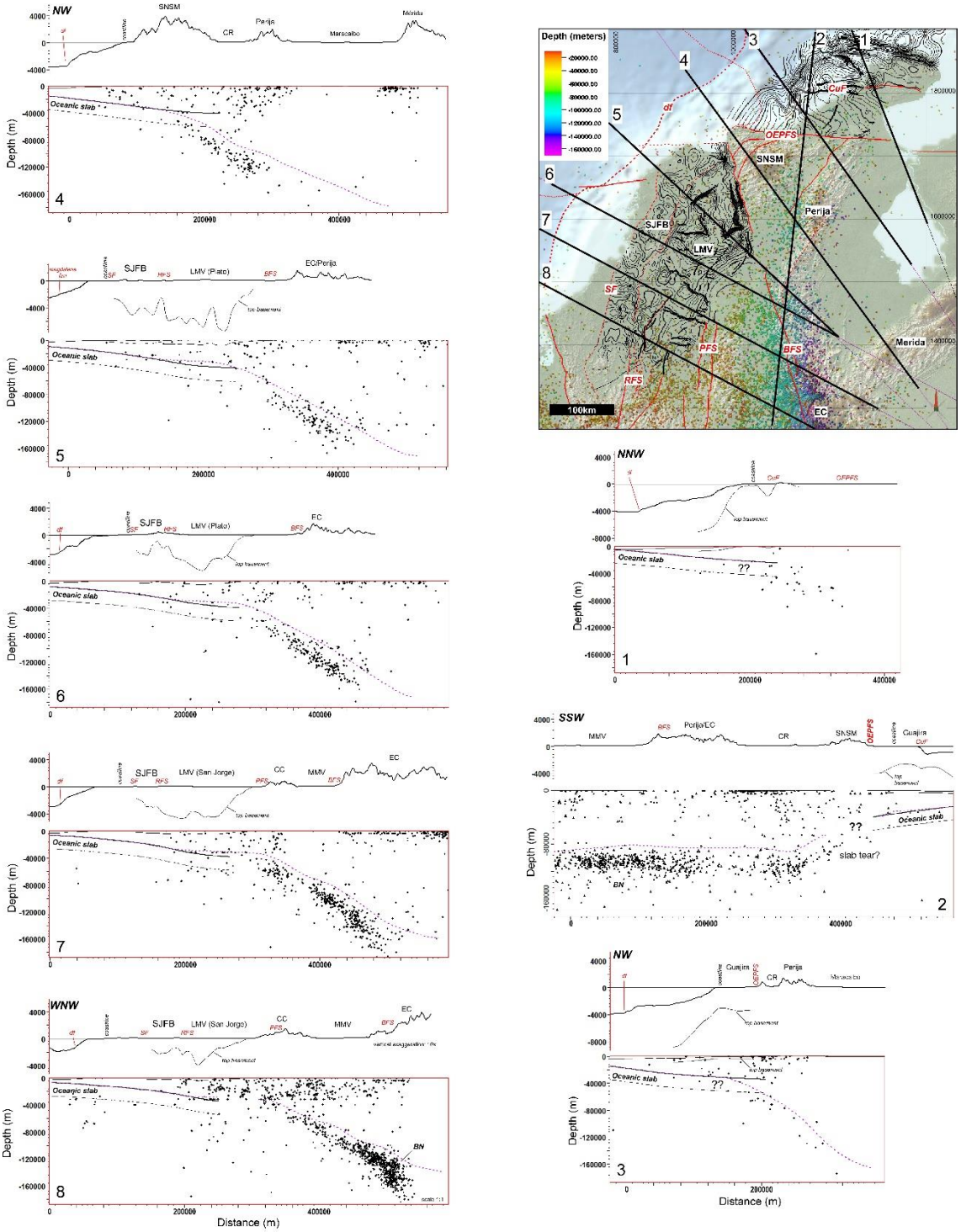

CuF: Cuisa Fault; OEPFS: Oca-El Pilar Fault System; BFS: Bucaramanga Fault System; PFS: Palestina Fault System; RFS: Romeral Fault System; SF: Sinu Fault; SNSM: Sierra Nevada de Santa Marta; LMV: Lower Magdalena Valley; SJFB: San Jacinto Fold Belt; CC: Central Cordillera; CR: Cesar-Rancheria basin; EC: Eastern Cordillera; MMV: Middle Magdalena Valley basin; df: deformation front of the accretionary prism.

Figure B 1. Regional cross-sections showing the configuration of the subducted Caribbean oceanic plate, as interpreted from reflection-seismic mapping for the shallow part and intermediate-depth seismicity for the deep part.

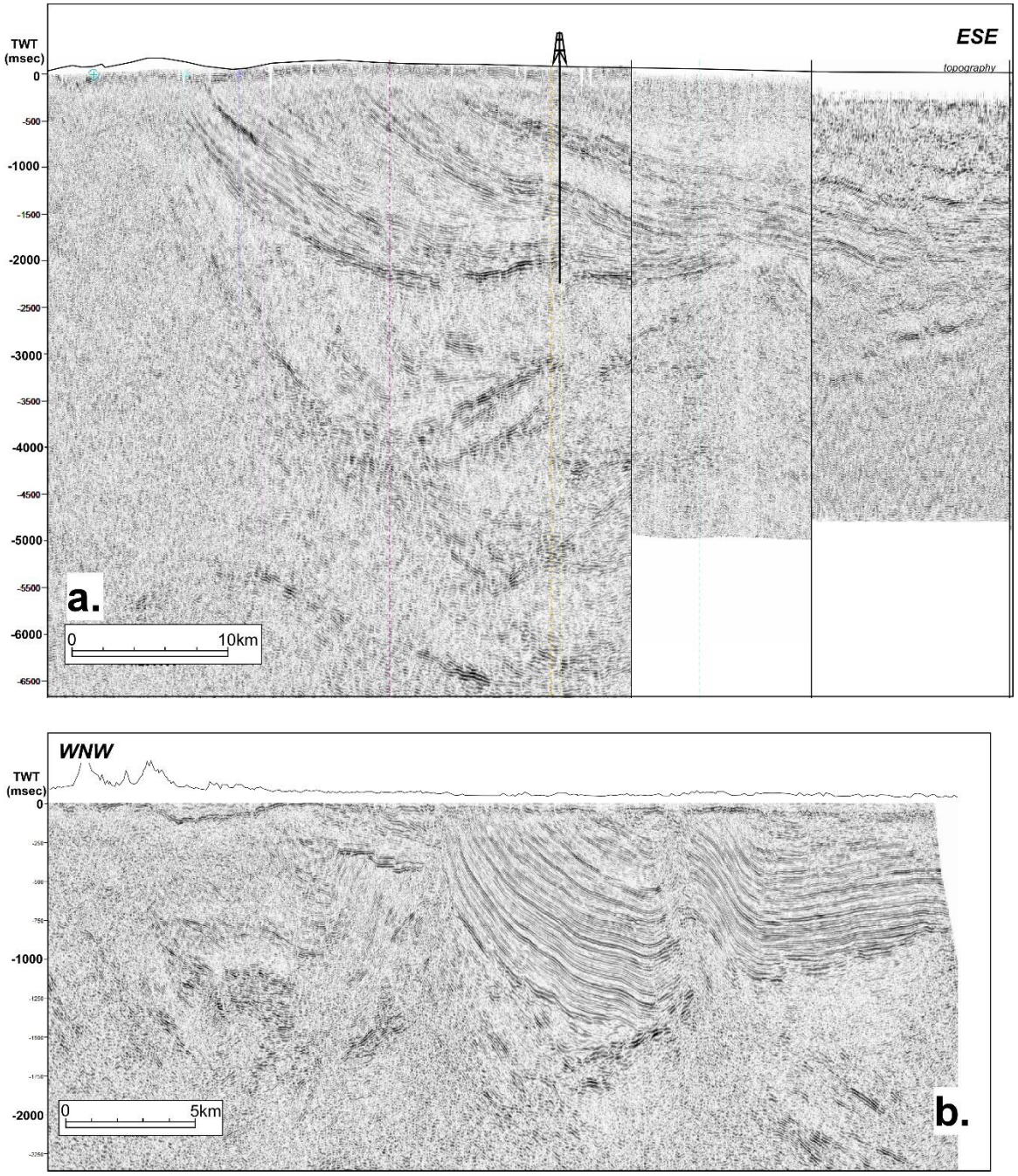

Figure B 2. These are the same two seismic lines presented as **Figure 4.8**a and b, without interpretation.

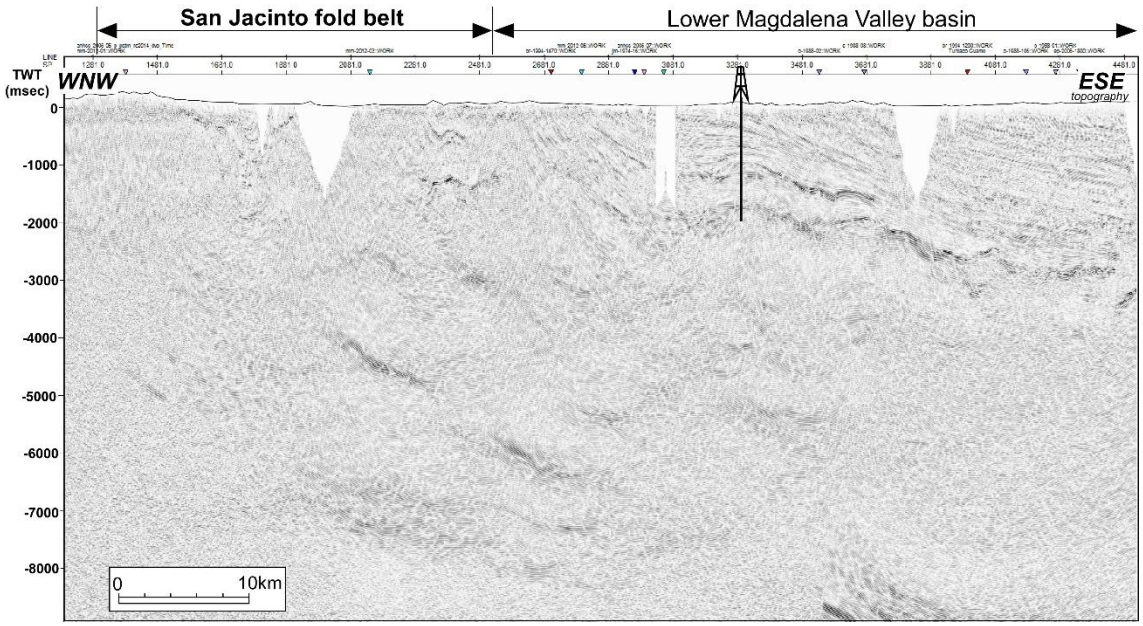

Figure B 3. This is the same seismic line presented as **Figure 4.9**, without interpretation.

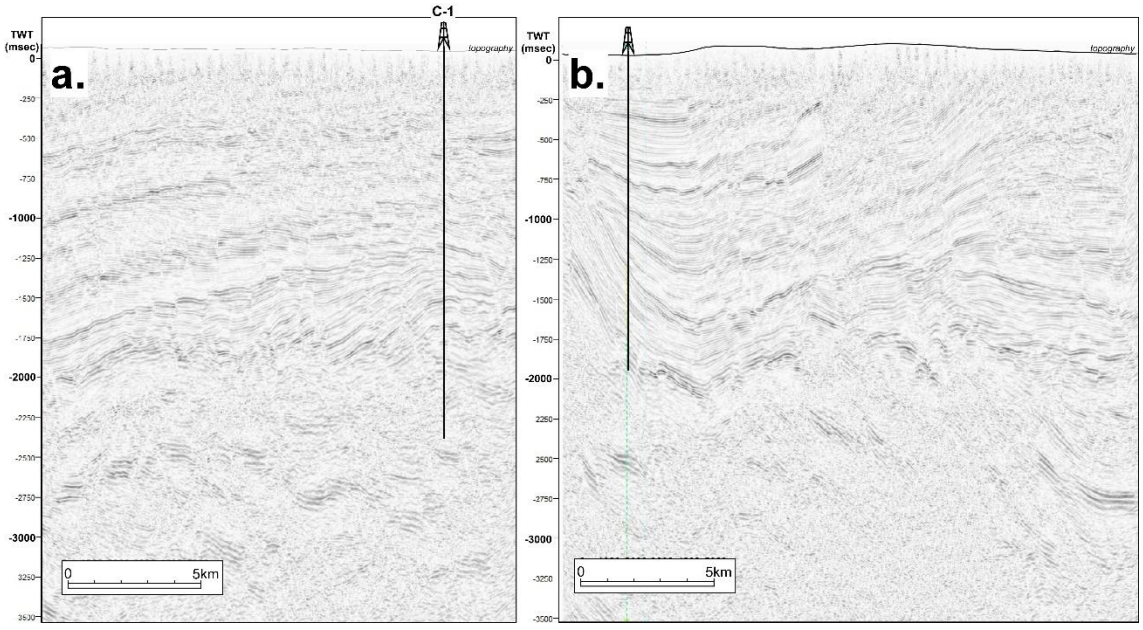

Figure B 4. These are the same two seismic lines presented as **Figure 4.10**a and b, without interpretation. Line orientations are not shown due to confidentiality reasons.

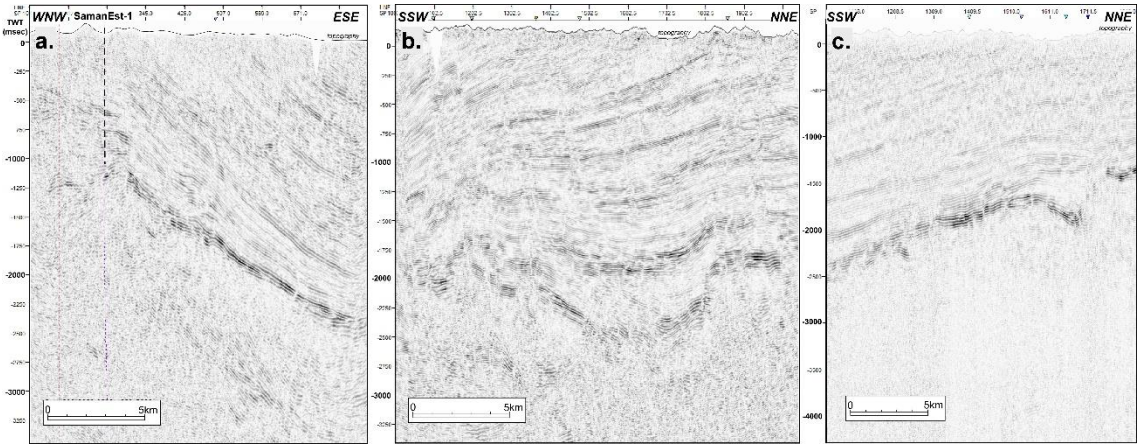

Figure B 5. These are the same three seismic lines presented as **Figure 4.11**a to c, without interpretation.

Appendix C

Supplementary text and figures for *Chapter 5*:

TextC1.

Construction of the Tectono-stratigraphic framework in the LMV

We interpreted in two-way-time (TWT) more than 25,000 km of 2D and more than 2000 km^2 of 3D-reflection-seismic data, all of which were tied to most of the 150 wells that have been drilled in the basin. In this study we have integrated previous interpretations and maps of the acoustic basement presented by *Mora et al. (2017a*), as well as those of pre-Oligocene stratigraphic sequences mostly preserved in the SJFB and studied by *Mora et al. (2017b*). We have based our interpretations in the biostratigraphic data and charts that *Duque-Caro (1979, 1984, 1991, 2000, 2001, 2010, 2013, 2014*) has constructed for the LMV and SJFB (

Figure 5.2), based on previous planktonic foraminiferal zonations (*Petters and Sarmiento, 1956*; *Blow, 1969*).
We interpreted in TWT the main sequences and unconformities in the LMV and adjacent areas using Schlumberger's Petrel seismic interpretation package, provided by Hocol S.A. These horizons were mapped in TWT and depth-converted using all the well data to create pseudo-velocity maps of all the basin. Seismic-stratigraphic analyses were carried out in order to define stratal stacking patterns, terminations and contacts (*Catuneanu et al., 2009*). Well data (electrical logs, cores and reports) was also incorporated to the seismic-stratigraphic analysis in order to define depositional environments and facies and to characterize each seismic-stratigraphic sequence in more detail.

Subsidence history and extension in the LMV

For the geohistory and subsidence analyses (*Allen and Allen, 2005*) we used data from 32 representative wells located in different parts of the basin, including the San Jacinto fold belt. After compilation of stratigraphic tops and thicknesses and plotting the observed (uncorrected) subsidence for each well, we integrated porosity data from the wells to estimate decompacted depths and assumed depositional water depths for each unit, based on biostratigraphy and facies analyses of electrical logs, cores and cuttings. To calculate the tectonic subsidence we integrated density data from the wells and other sources.
We constructed a regional, NNE-SSW-trending, structural cross-section along the LMV, perpendicular to the main structural fabric, in order to calculate the amount of extension that the basin has experienced and for comparison with our calculations of extension from the basin subsidence analyses. The 338 km-long section was constructed in the Petrel software, using our 2D-seismic database and it was then exported to the Move software (Midland Valley) provided by Hocol S.A. and by the GFZ. The cross-section was depth-converted using velocity data from drill holes and the interpretation of the main sequences was performed in depth. With the interpreted depth-converted section, we calculated the extension using the simple line-length tools available in the Move software.
The tectono-stratigraphic framework and the subsidence and extension results presented here were the basis for building multidimensional basin and petroleum system models in the LMV and San Jacinto, which were built using Schlumberger's PetroMod software, version 2011, provided by the GFZ Postdam. **Figure C 1** shows two burial history charts extracted from the 3-D model of the LMV, at the locations of two representative wells, one in the northern LMV (Plato depocenter) and one in the southern LMV (San Jorge depocenter). The main subsidence and uplift/shortening episodes are shown in both locations and are discussed in the text.

Detailed description of Oligocene to Recent tectono-stratigraphic sequences in the Lower Magdalena Valley basin

Sequence 5 (Upper Oligocene to lowermost Miocene)

Age: Based on studies of planktonic foraminifera in wells and outcrops, this sequence has been associated to the planktonic zones P.20 to N.6 (M.3), equivalent to an Early Oligocene to Earliest Miocene age. However, recent analyses in the south-western LMV (Planeta Rica-Montería road) suggest that the basal deposits of

this sequence can also be of (upper?) Eocene age. Given that it spans for more than 10 Ma, it can be classified as a 2nd-order cycle (*Vail et al., 1977*), which would correspond to a high rank/low frequency cycle in the hierarchy pyramid of *Catuneanu et al. (2009*).

Contacts: In most of the LMV, the lower contact of the sequence is an unconformity with the crystalline basement, except for the eastern part of the basin, close to the limit with the San Jacinto fold belt, where it is unconformably overlying pre-Oligocene sedimentary sequences (3 and 4, *Mora et al. 2017b*). Biostratigraphic data from outcrops and drillholes (*Duque-Caro, 2000, 2001, 2010, 2012*) shows that the upper part of the sequence of Earliest Miocene age (foraminiferal zones N.4/M.1 to N.6/M.3, spanning from 24 to 17 Ma) has been locally eroded, indicating the existence of a regional Early Miocene unconformity which marks the upper limit of this sequence.

Structural and thickness maps: Integration of outcrop data with detailed reflection-seismic mapping of the Ciénaga de Oro sequence shows that it was deposited throughout the whole San Jacinto fold belt, where it appears to be thicker, and it retrograded to the E and SE, as it gradually filled the pre-existing paleo-topographic basement lows. Seismic data shows that the Oligocene to Lower Miocene deposits gradually filled the proto-San Jorge and Plato depocenters from the W and NW and that the main structural basement features, such as the Sucre, Mojana and Pivijay faults, were actively extending. The El Dificil, Apure and the southeastern Magangué-Cicuco highs were positive relief features on top of which the lower part of the sequence (planktonic zones P.20 to P.22) was not deposited, but where small thicknesses of the upper part of the sequence could have been deposited. Seismic and well data show that the top of the sequence is found at more than 3.5 km in the San Jorge depocenter and at more than 5 km in the deepest Plato depocenter. The sequence exhibits the highest thicknesses in the western part of the LMV, towards the San Jacinto fold belt, where more than 1.5 km would be preserved in local depocenters. This is in agreement with the outcrop measurements which report highest thicknesses (>1 km) in the Alférez and San Jacinto sections in the eastern San Jacinto fold belt (*Guzman et al., 2004*; *Guzman, 2007*). These thickness trends indicate that the Oligocene to Earliest Miocene basin was deeper to the NW and shallower to the SE.

Sequence description: While the upper part of Sequence 5 is not very well preserved due to erosion after the Early Miocene unconformity, the lower part of the sequence is better preserved and displays an onlap pattern to the SE (**Figure 5.6** and **Figure 5.7**). Therefore, the lower part is interpreted as a retrogradational, transgressive package which records the advanced of marine sedimentation from NW to SE, filling initially the lowest areas of the basement paleo-topography. Outcrop and well data (electric logs and cores) show that this sequence displays a fining and deepening-upward pattern (**Figure 5.4**). In the northwestern Magangué-Cicuco high, the lower part of the sequence displays calcareous sandy facies of Upper Oligocene age, which grade to Lower Miocene mudstones. Core analyses of the basal part of the sequence in the northwestern Magangué-Cicuco high (*Salazar, 1993*; *Cross, 2014*) show that it consists of highly bioturbated (Cruziana ichnofacies), sub-litharenites and subarkoses which were deposited in shallow marine, estuarine environments that show more proximal facies to the SE. This is in agreement with the seismic pattern, which shows a clear onlap of the basal strata to the SE, against the crystalline basement (**Figure 5.7**). Sandy, shallow-marine facies are present in the southern, southeastern and eastern LMV, close to the paleo-highs, while mudstone deeper-marine facies are more common towards the San Jacinto fold-belt in the W and NW. In the northern part of the belt (Barranquilla area), several wells have drilled a 600 m-thick mudstone Upper Oligocene succession which indicates distal marine-shelf depositional environments in that area. In the San Jorge depocenter, one well has drilled and sampled the Lower Ciénaga de Oro sequence, which comprises lithic sandstones and mudstones deposited in a shallow-marine environment. In the easternmost part of the Plato depocenter, close to the Santa Marta-Bucaramanga fault zone, the Lower Ciénaga de Oro comprises a relatively thick, mostly sandy succession of continental to transitional origin, which has not been drilled by any well. Seismic images do not provide a clear image of the basement in this area, where it should be found at very high depths, below the thick Upper Oligocene and possibly older succession.

Though the low-frequency global eustatic curve of *Haq et al. (1987*,

Figure 5.2) shows a descending sea-level from Early Oligocene to Early Miocene times, the higher-frequency curves suggest a rising-sea-level trend. Well data shows that most of the sedimentary facies are clastic, except for the Pijiño and Pivijay areas where Oligocene carbonates were described. Based on well and seismic data, we interpret that a maximum-flooding event occurred in Earliest Miocene times, related to deposition of mudstones of the N.4 to N.5 foraminiferal zones. The stratigraphic location of the maximum flooding surface can be seen in some wells in the western Magangué-Cicuco high (**Figure 5.4**), and allows subdividing the sequence into systems tracts (*Brown and Fisher, 1977*; *Catuneanu et al., 2009*). The retrogradational deposits of the lower part of the sequence would be the transgressive systems tract while the locally-preserved aggradational deposits of the upper part of the sequence would be the highstand systems

tract. This sequence corresponds in outcrops to the Carmen Formation (*Duque-Caro, 1979*; *Guzman et al., 2004*; *Guzman, 2007*).
Petrography: Thin-section analyses show that sandy facies of Sequence 5 consist of subarkoses and sublitharenites with calcareous cement, lithics of volcanic, sedimentary (mostly cherts), metamorphic and igneous plutonic rocks (*ICP, 1998*; *Chacon et al., 2001*; *ANH/U. Caldas, 2009, ICP, 2010*). While the lower layers appear to be more lithic than the upper ones, the plagioclase content is higher than the K-feldspar content. Heavy minerals are pyroxene, epidote, tourmaline and zircon (*ICP, 2000*). These rocks were deposited initially in shallow marine environments with relatively high terrestrial supply (Lower Ciénaga de Oro), which gradually changed to deeper marine and more anoxic environments (Upper Ciénaga de Oro, *Salazar, 1993*; *ICP, 2000*; *Guzman, 2007*).

Sequence 6 (Lower to Middle Miocene)

Age: Biostratigraphic analyses from numerous wells (*Duque-Caro, 2000, 2001, 2010, 2012*) indicates that the age of Sequence 6, is lower to middle Miocene (Burdigalian to Serravalian, zones N.7/M.4 to N.11/M.8). Considering that it spans for less than 10 Ma, it can be classified as a 3rd-order cycle (*Vail et al., 1977*), which would correspond to a medium rank/medium frequency cycle in the hierarchy pyramid of *Catuneanu et al. (2009*). Well and seismic data show that within this sequence there are two higher order cycles, a lower, latest early Miocene cycle corresponding to the N.7/M.4 planktonic foraminiferal zone and an upper, earliest middle Miocene cycle, corresponding to the N.8/M.5 to N.11/M.8 planktonic foram zones.
Contacts: Both outcrop and subsurface data indicate that most of the Upper Ciénaga de Oro sequence has been eroded (absence of foraminiferal zones N.4/M.1 to N.6/M.3), evidencing the existence of an Earliest Miocene regional unconformity. Therefore, this Earliest Miocene unconformity is the lower contact of this sequence. Biostratigraphic data also show a regional absence of the N.11 and N.12 plaktonic foram zones (M.8 and M.9), which has been related to a Middle Miocene unconformity that marks the upper contact of this sequence.
Structural and thickness maps: Deposition of this sequence extends farther to the E and SE and begins with retrogradational shallow marine clastics and carbonates which then change to progradational deltaic deposits (**Figure 5.9**). The main two extensional fault families which were actively extending since Late Oligocene times continued to be active but gradually decreased their activity through time. Concerning the lower cycle of the sequence (equivalent to the N.7/M.4 planktonic foram zone), the influence of a pre-existing basement paleo-topography is seen in the thickness maps which show that there was either non-deposition in the paleohighs or that they were covered by shallow water carbonates such as Cicuco, El Difícil and Apure. The upper cycle (N.8/M.5 to N.11/M.8 planktonic foram zones), displays more clastic facies which exhibit pronounced progradational seismic facies and stacking patterns in wells. Our thickness maps data show that average thickness of the sequence is 400-600 m (1200-2000 ft) and that it is thickest in the eastern Plato depocenter where more than 4 km (>12000 ft) of Lower to Middle Miocene deposits are preserved. Several wells (e.g. Arjona, Astrea, Tierrafirme) have drilled this sequence finding mainly transitional to continental sandstones which appear to have been mostly sourced from the Cesar-Ranchería basin in the NE.
Sequence description: The lower cycle of the sequence, of latest Early Miocene age (planktonic zone N.7/M.4) continued filling the paleo-topography with clastic deposits in the low areas (San Jorge and Plato depocenters) and carbonate development in the paleo-highs such as the eastern Magangué-Cicuco, El Difícil and Apure highs (**Figure 5.9** to **Figure 5.11**). These deposits are clearly onlapping the basement towards the E, SE and S in the southern LMV, where they have been studied in electrical logs and cores and are interpreted as shallow-marine retrogradational deposits of the transgressive systems tract of this sequence. The transgressive systems tract is not very thick and is limited at the top by a maximum-flooding surface which marks the onset of high-stand progradation.
North of the Magangué-Cicuco high, the Lower to Middle Miocene sequence is thicker because it has been better preserved from Late Miocene to Recent erosional episodes. In the eastern Plato depocenter, the lower Miocene continental to transitional strata of the lower cycle of Sequence 6 has been considerably eroded by progradational marine clastics of the upper cycle, which were deposited in a steep slope and which comprise deep-water clastic deposits (mud to gravel-rich deposits, *Richards, 2001*). Such erosion formed an impressive submarine canyon which has been related to the proto-Magdalena drainage (*ICP, 2000*; *Bernal et al., 2015c*). Formation of the Algarrobo-Ariguaní pull-apart basin probably started in early Miocene times or possibly earlier, as suggested by seismic data. This sequence correlates with the Alférez Formation (*Duque-Caro et al., 1996*; *Guzman, 2007*) and with the Lower Porquero Formation described in outcrops of the eastern San Jacinto fold belt. The lower part of this sequence which contains carbonates and sandstones, also receives the operational name of "Upper Ciénaga de Oro".
Petrography: The clastic Lower to Middle Miocene facies consist of fine-grained sublitharenites. In the southern Sinú fold-belt (Floresanto-1 well, *ICP. 2009*), a fine-grained, coarsening-upwards succession of

litharenites, feldspathic litharenites and lithic arcoses with sedimentary (mudstones towards the base and cherts towards the top), igneous (volcanic and plutonic) and few metamorphic rock fragments is reported. Interpreted depositional environments are upper bathyal to outer neritic (*Duque-Caro, 2000*). The carbonate facies in the paleohighs comprise bioclastic and red algae wackestones and packstones in the El Dificil area (*Ortiz, 1995*) and reef limestones with multiple transported fossils in the Apure high (*Chacon and Martinez,1994*).

Sequences 7 and 8 (Middle to Upper Miocene-Middle and Upper Porquero)

Sequences 7 and 8 have been related to the N.12/M.9 to N.16/M.13 planktonic zones which correspond to a Middle to Upper Miocene age (Serravallian-Tortonian, *Duque-Caro, 2000, 2001, 2010, 2012*). Both sequences span for less than 10 Ma, so they can be classified as 3rd-order cycles (*Vail et al., 1977*), corresponding to medium rank/medium frequency cycles in the hierarchy pyramid of *Catuneanu et al. (2009*). While the lower contact of this succession is the Middle Miocene unconformity (absence of zones N.11/M.8-N.12/M.9), the upper contact is a regional Late Miocene unconformity which has been widely reported in outcrop and subsurface studies (*Duque-Caro, 1979*; *Hocol, 1993*; *Guzman, 2007*). The sequences exhibit mainly fine-grained facies with progradational stacking patterns, which are best preserved in the depocenters where erosion was less intense. According to *ICP (200*0), while the lower part of Sequence 5 contains more igneous plutonic and sedimentary lithics, the proportion of volcanic rock fragments such as rhyolites, trakites and andesites, increases in younger sequences (6 to 9).

Sequence 9 (Upper Miocene to Lower Pliocene-Tubará)

Age: This sequence contains planktonic forams of the N.17/M.14 to Pl.2 zones (*Duque-Caro, 2000; 2001, 2010, 2012*) which are indicative of an Upper Miocene to Lower Pliocene age (Tortonian to Zanclean). It also corresponds to a 3rd-order cycle of *Vail et al. (1977*) and to a medium/rank/medium frequency cycle of *Catuneanu et al. (2009*), given that it spans for less than 10 Ma.
Contacts: Both contacts of this sequence are major regional unconformities which are closely related to uplift pulses in the eastern Colombian Andes, as will be discussed farther on, and which have been identified in outcrop, well and seismic data (*Duque-Caro,1979*; *Hocol, 1993*; *ICP, 2000*; *Guzman, 2007*). The lower contact corresponds to the Late Miocene unconformity (N.17/M.14 planktonic zone) while the upper contact corresponds to the Middle Pliocene unconformity (Pl.2-Pl.3 zones, *Duque-Caro, 1984*).
Structural and thickness maps: Seismic and well data show that this sequence has been partially eroded in the southern LMV, south of the Magangué-Cicuco high, by a Middle Pliocene tectonic episode. Therefore, it is best preserved to the north of the Magangué-Cicuco high, especially along the Plato depocenter, where it displays thicknesses of more than 2 km (**Figure 5.8** and **Figure 5.10**). However, Pleistocene to Recent uplift in the easternmost Plato depocenter, towards the Santa Marta-Bucaramanga fault, caused the erosion of a great portion of the sequence.
Sequence Description: The Upper Miocene to Lower Pliocene sequence represents the increased progradation to the NNW of continental to shallow-marine deposits along the shelf, until they reached the present-day coastline in latest Miocene to early Pliocene times (**Figure 5.8**). Thick Upper Miocene to Lower Pliocene deposits are also preserved in present-day offshore areas, recording the shifting of the Magdalena River delta (*Romero-Otero et al., 2015*). Reflection-seismic data shows that this sequence is composed of low-angle (0.3-0.6°) and wide (100-200 km) sigmoidal clinoforms which advanced from SSE to NNW, representing the advance of the paleo-Magdalena river. Vertical thicknesses of the Tubará clinoforms are in the order of thousands of meters, and they prograde at rates of 8 to 16km/Ma, two features which are characteristic of shelf-margin clinoforms (*Steel et al., 2008*). In such cases, the clinoforms grow into bathyal depths, suggesting that bathyal facies should be predominant in the NNW. By contrast, the upper parts of the slope and the topsets located towards the SSE would be dominated by continental to shallow-marine shelf deposits (**Figure 5.10**). Despite of the fact that not very much wells have been drilled along the Tubará clinoforms, available well data shows that the Tubará topsets in the SSE exhibit sandy fluvial to deltaic sandstones with coal interbeddings, while muddy deeper-water facies are dominant to the NNW. The clinoform shelf-edge trajectories are initially flat and then appear to be slightly rising (youngest clinoforms to the NNW), indicating low topset accumulation, which is best achieved during intervals of stillstand or falling relative sea level (*Steel et al., 2008*).
Petrography: Sandy fluvio-deltaic facies which are more abundant in the clinoform topsets have been described as fine to coarse-grained sandstones in wells of the Plato depocenter. Petrography analyses show that compositionally they are lithic arkoses and feldspathic litharenites with high contents of volcanic rock fragments and subordinate metamorphic and plutonic rock fragments (*ICP, 2000*). Plagioclase is more

abundant than potassium feldspar, while there is a high content of hornblende. Clinoform topset deposits contain abundant coaly and plant remains indicating high supply from vegetated land areas.

Sequence 10 (Upper Pliocene to Pleistocene - Corpa)

Age: Considering that the deposits of this sequence have been ascribed to continental environments, there are very few studies aiming to properly describe and date the sequence. Taking into account the stratigraphic contacts above the Tubará Late Miocene to Early Pliocene sequence, and below the Quaternary (Late Pleistocene to Recent) deposits, we infer here a Late Pliocene to Early Pleistocene age for this sequence, spanning from 3 to 1.3 Ma (3rd order cycle). However, we recommend detailed palynological studies in order to properly date this sequence.
Contacts: The lower contact above Sequence 9 (Tubará) is an angular unconformity very clearly seen in reflection-seismic data in the Magangué-Cicuco high and southern LMV (**Figure 5.6**). The upper contact is also unconformable below Late Pleistocene to Recent deposits preserved in the main, present-day depocenters of the LMV.
Structural and Thickness maps: We divided the Corpa Sequence into two seismic packages which were mapped and are shown in **Figure 5.11**. The lower package, which we assign to the Late Pliocene, is preserved as a SSW-NNE-trending elliptic depocenter, located south and SW of the Magangué-Cicuco high. The structural map of the top of this lower Corpa package shows that it is more deeply buried to the NW of the San Jorge graben, where it lies at depths in excess of 3 km. However, the thickness map of this package shows that the thickest deposits occur farther south, to the SW of the San Jorge graben where it reaches a thickness of 2 km. The upper Corpa package, which we assign to the Early Pliocene, is forming a round depocenter with its deepest part also located to the NW of the San Jorge graben (**Figure 5.11**). The deepest part of the top of this package is found at a depth of 2.5 km. The thickness map of this package shows that the area where the thickest deposits are preserved (maximum thickness of 2.5 km), coincides with the structurally deepest area.
Sequence Description: The expression of the Corpa Sequence in reflection-seismic data consists of low-angle clinoforms broadly prograding from South to North, which appear to represent the deposits of the paleo-Cauca drainage system, including fluvial channels, lakes and swamps (**Figure 5.11**). In seismic images, the lower Corpa package exhibits an increased Late Pliocene progradation to the north of mostly fluvial deposits, which have been described in drill holes as conglomerates and coarse-grained sandstones which grade upwards to floodplain mudstones. The upper Corpa has been described in exploratory wells as a predominantly muddy succession with minor sandy and conglomeratic beds, representing lacustrine and swampy sedimentation which was preserved in a circular-shaped sag-basin located to the NW of the San Jorge graben (**Figure 5.11**). This sequence is not preserved to the north of the Magangué-Cicuco high, due to erosion/non-deposition. However, it correlates in age with the Popa limestones preserved in the northwestern SJFB.
The internal seismic-stratigraphic architecture of the Corpa Sequence reveals the time when the SJFB started to be uplifted, which appears to be close to the boundary between the Pliocene and Pleistocene. Upper Pliocene seismic reflectors of the lower part of the Corpa Sequence exhibit a divergent pattern towards the W, indicating that the lower Corpa deposits thicken towards the W where there was more accommodation space. By contrast, the upper Corpa seismic reflectors show an onlapping pattern to the W, indicating that the SJFB started to behave as a positive feature in Early Pliocene times (section 3, **Figure 5.6**).
Petrography: There are only outcrop samples available from the Corpa and equivalent units corresponding to Sequence 10 and they exhibit compositional variations according to location. Sandstones were classified as lithic arkoses, feldspathic litharenites and litharenites.

Supplementary Figures for *Chapter 5*:

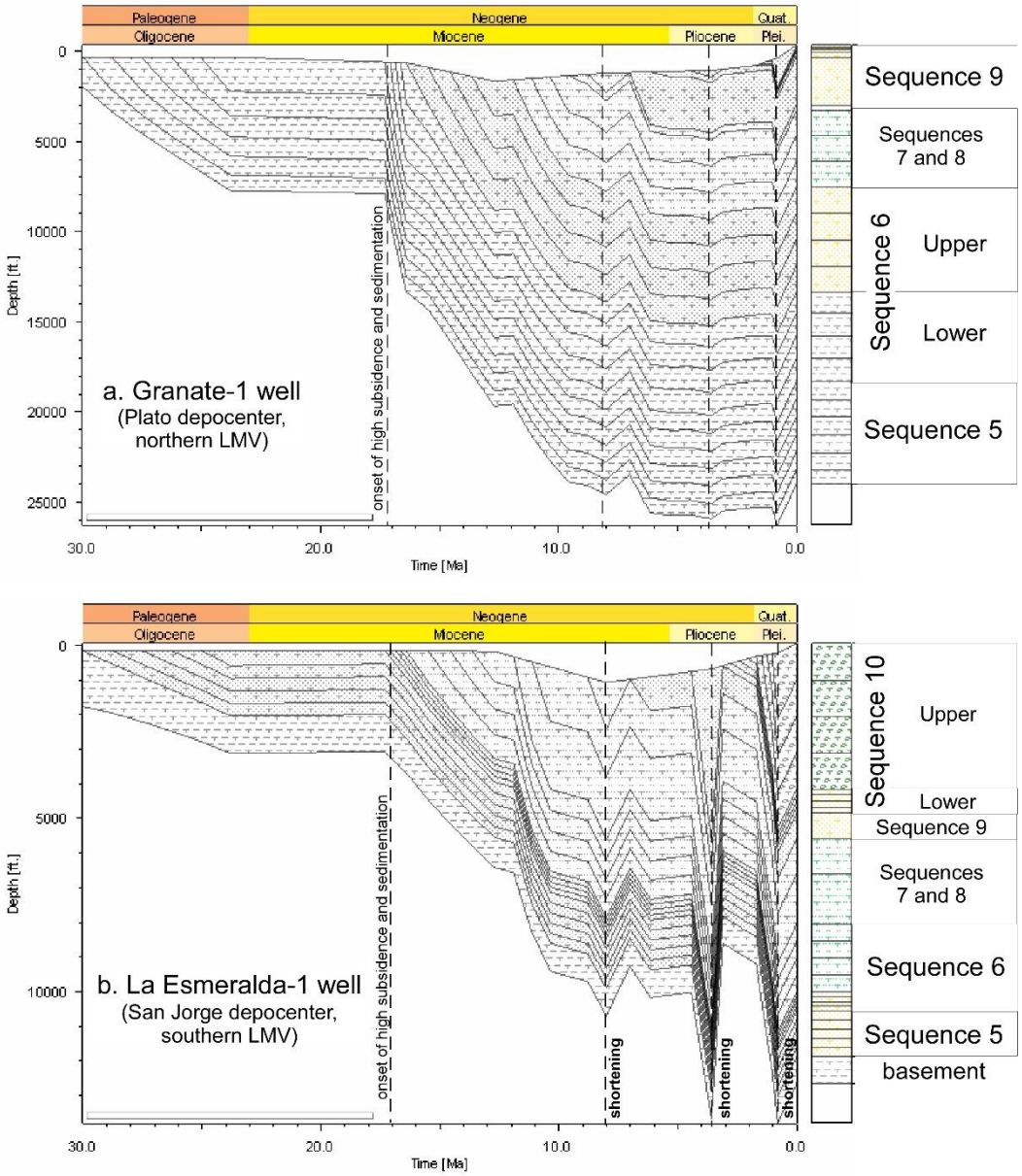

Figure C 1. Burial history charts for representative wells in the LMV, showing the main subsidence and shortening (uplift and erosion) episodes. The charts were extracted from well locations in a 3-D model of the LMV, constructed using the Schlumberger's PetroMod software (v. 2011). a. Granate-1 well, located in the Plato depocenter of the northern LMV. b. La Esmeralda-1 well, located in the San Jorge depocenter of the southern LMV.

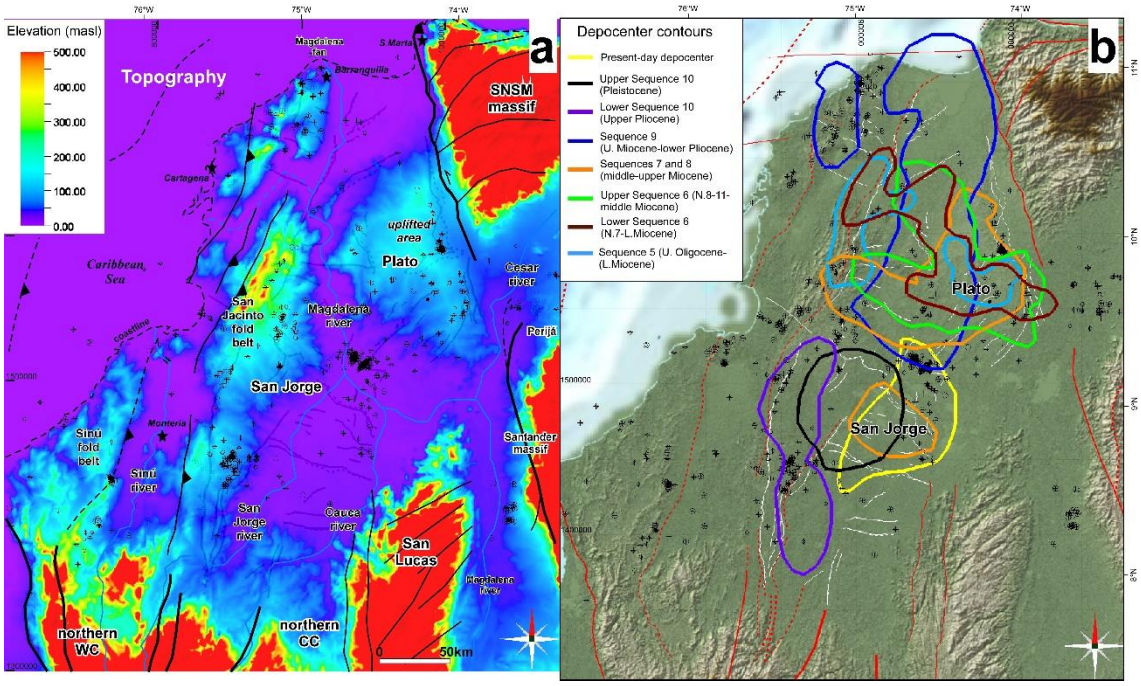

Figure C 2. a. Digital elevation model of the study area, showing the main morphological features. While the San Jorge depocenter continues subsiding, the Plato depocenter became a positive area possibly in Pleistocene times. b. Contours showing the location of the depocenters of each of the studied sequences, based on the isopach maps and illustrating the depocenter migration with time; see text for further explanation.

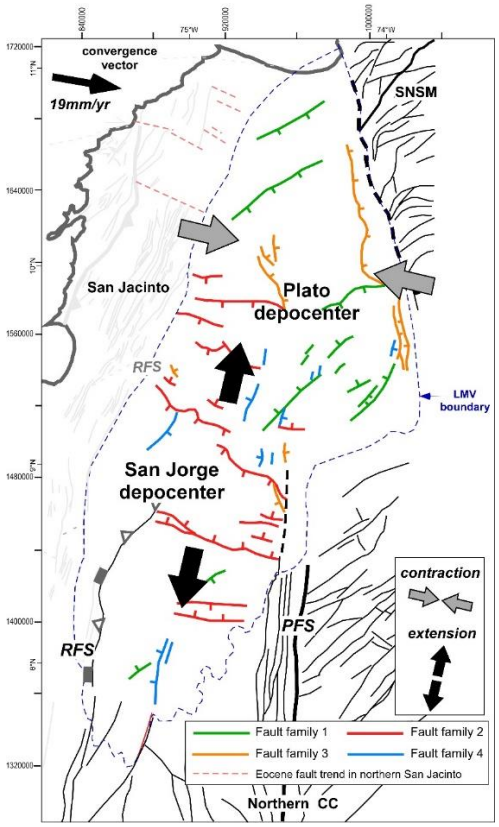

Figure C 3. Basement fault families in the LMV, defined by *Mora et al. (2017a*), and the main stresses according to the plate displacement vector of the Caribbean relative to a fixed South America. NE-SE-trending compression and slight inversion of normal faults that occurred after late Miocene times, would be related to northern Andes "escape" or to collision stages of the Chocó-Panamá block. See text for further explanation.

Appendix D

Supplementary figures for *Chapter 6*:

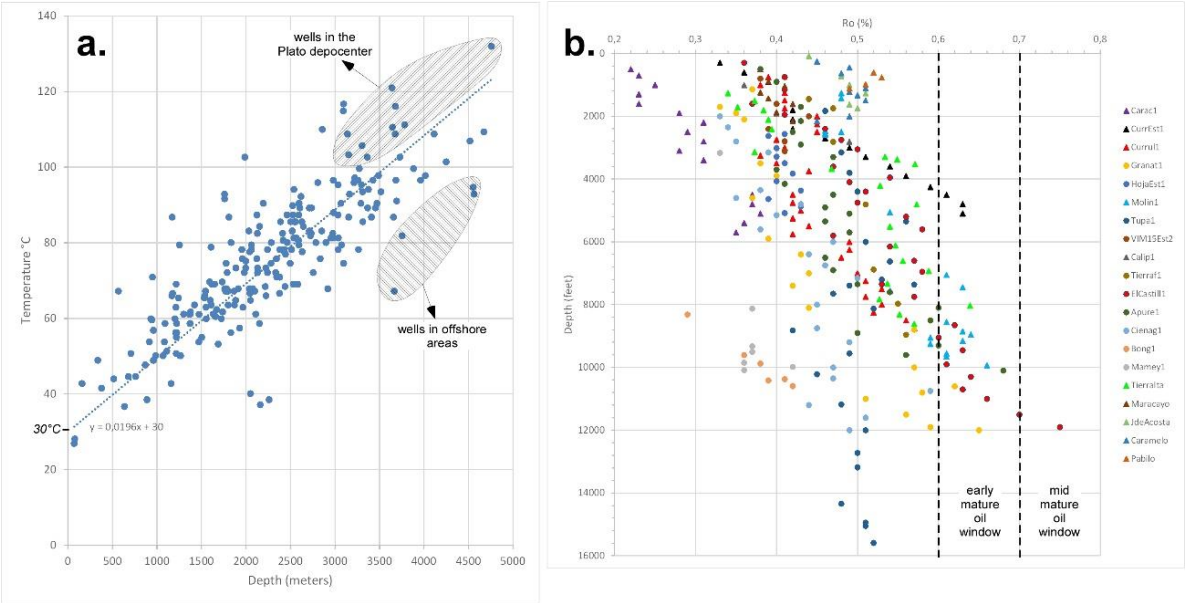

Figure D 1. a). Bottom hole temperatures (BHT) from wells in the study area plotted versus depth; a 10% correction accounting for cooling due to the drilling mud was applied. The best-fit line was set to intersect with the x-axis at the assumed present-day average surface temperature (30°C). The slope of the line corresponds to the average current geothermal gradient in NW Colombia (19.6°C/km). b). Plot of all the available vitrinite reflectance data (Ro) in the LMV and SJFB against depth. Circles are wells in the LMV while triangles are wells in the SJFB. Most of the vitrinite reflectance data is below 0.6% (immature), whereas only samples from the central Plato depocenter in the northern LMV and from the northern SJFB are early to mid-mature.

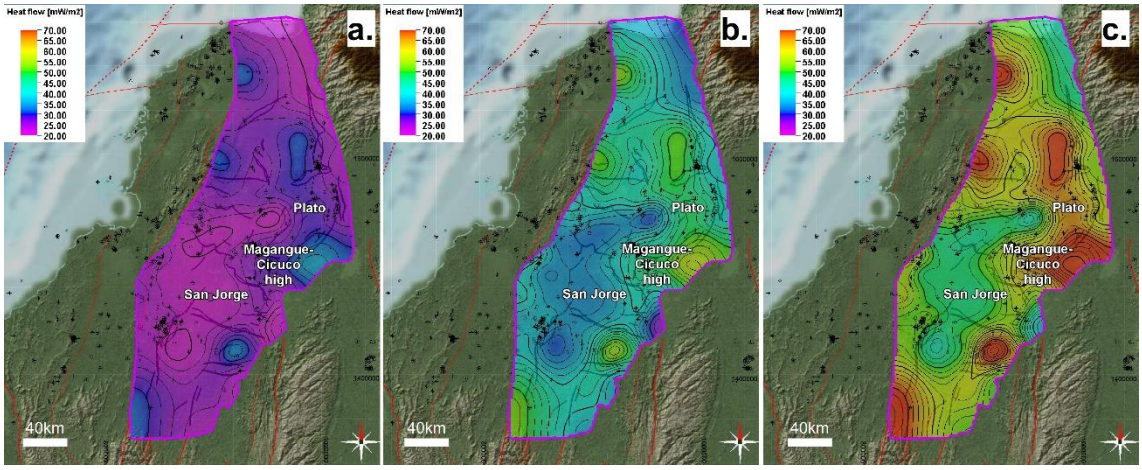

Figure D 2. Different heat flow scenarios that were implemented and tested in the 3-D model. a) Low heat flow, obtained by using a thermal conductivity of 1.2 Wm-1 K-1. b). Mean heat flow, obtained by using a thermal conductivity of 2 Wm-1 K-1. c) High heat flow, obtained after using a thermal conductivity of 2.8 Wm-1 K-1.

Bibliography

Aleman, A., 1983. Geology and Hydrocarbon Evaluation of Northwest Colombia. Internal Report, Gulf Oil E&P Company.

Allen, P. and Allen, J., 2005. Basin Analysis- Principles and Applications. Blackwell Publishing Ltd., 2nd Ed., 549 p.

Allmendinger, R. W., Cardozo, N. C., and Fisher, D., 2013, Structural Geology Algorithms: Vectors & Tensors: Cambridge, England, Cambridge University Press, 289 p.

Altamira, A. and Burke, K., 2015, The Ribbon Continent of South America in Ecuador, Colombia, and Venezuela; In C. Bartolini and P. Mann, eds., Petroleum geology and potential of the Colombian Caribbean Margin: American Association of Petroleum Geologists Memoir 108, 39–84.

Alvarez, E. and Gonzales, H., 1978. Geología y geoquímica del Cuadrángulo I-7 (Urrao). Mapa escala 1:100.000, Ingeominas. Informe 1761, 347 p., Medellín.

Anderson, F. 1926. Original source of oil in Colombia. Bulletin of the American Association of Petroleum Geologists, 382-404.

Anderson, V.J., Horton, B.K., Saylor, J.E., Mora, A., Tesón, E., Breecker, D.O., and Ketcham, R.A., 2016, Andean topographic growth and basement uplift in southern Colombia: Implications for the evolution of the Magdalena, Orinoco, and Amazon river systems: Geosphere, 12/4, 1–22, doi:10.1130/GES01294.1.

Angevine, C. L., Heller, P. L., and Paola, C., 1990, Quantitative sedimentary basin modeling: American Association of Petroleum Geologists Continuing Education Course Note Series, 32, 133 p.

ANH-U. Caldas, 2009. Estudio Integrado de los núcleos y registros obtenidos de los pozos someros tipo “slim holes” en la cuenca del Sinú. Report for the ANH, Bogotá.

ANH, 2011a. Petroleum Geology of Colombia. Cediel, F. (Ed.). Volume 1, Regional Geology-Phanerozoic Granitoid Magmatism in Colombia and the Tectono-magmatic evolution of the Colombian Andes.

ANH, 2011b. Petroleum Geology of Colombia. Cediel, F. (Ed.). Volume 10, Lower Magdalena Basin.

Ares, 2014. Petrografía y Datación Quimioestratigráfica del Cinturón plegado de San Jacinto en el área de Luruaco-Arroyo de Piedra. Internal report for Hocol S.A. and Lewis Energy Colombia, Bogotá.

Arminio, J.F. and Yoris, F. 2006. Exploration Potential of the Pre-Paleogene Succession in the Cicuco High, Lower Magdalena Basin, Colombia. IX Simposio Bolivariano-Exploración Petrolera en Cuencas Subandinas, Cartagena, Colombia.

ATG-ANH, 2009. Cartografía Geológica, levantamiento de Columnas estratigráficas, toma de muestras y análisis bioestratigráficos. Sector de Chalán, Cuenca Sinú-San Jacinto. Public report for the ANH, Bogotá.

ATG, 2017. Cartografía Geológica y Columnas estratigráficas Bloques SN-8, SN-18 & SN-15. Internal report for Hocol, Bogotá.

Avé-Lallemant, H., 1996. Displacement partitioning and arc-parallel extensión in the Aleutian volcanic island arc. Tectonophysics, 256, 279-293.

Avé-Lallemant, H. and Oldow, J., 1988. Early Mesozoic Southward Migration of Cordilleran Transpressional Terranes. Tectonics, 7/5, 1057-1075.

Avé-Lallemant, H. and Oldow, J., 2000. Active displacement partitioning and arc-parallel extension of the Aleutian volcanic arc based on Global Positioning System geodesy and kinematic analysis. Geology, 28/8, 739-742.

Ayala, R.C., Bayona, G., Cardona, A., Ojeda, C., Montenegro, O., Montes, C., Valencia, V. and Jaramillo, C. 2012. The Paleogene Synorogenic succession in the northwestern Maracaibo Block: Tracking intraplate uplifts and changes in sediment delivery systems. Journal of South American Earth Sciences, 39, 93-111.

B&G, 2006. Cartografía Geológica en los Cinturones Plegados Sinú-San Jacinto. Internal report for ANH, Bogotá.

Babault, J., Teixell, A., Struth, L., Van den Driessche, J., Arboleya, M. and Teson, E., 2013. Shortening, structural relief and drainage evolution in inverted rifts: insights from the Atlas Mountains, the Eastern Cordillera of Colombia and the Pyrenees, in Nemčok, M., et al., eds., Thick-Skin-Dominated Orogens: From Initial Inversion to Full Accretion: Geological Society of London Special Publication 377, 315–342, doi: 10 .1144 /SP377 .12.

Barrera, R., Perez, J. and Salazar, C., 2014. Carbones Colombianos: clasificación y caracterización termoquímica para aplicaciones energéticas. rev.ion. 27/2, 43-54.

Barrero, D., Alvarez, J. and Kassem, T., 1969. Actividad Ignea y tectónica en la Cordillera Central. Bol. Geol. Ingeominas, 17, 1-3, 145-173.

Barrero, D., 1979. Geology of the Central Western Cordillera West of Buga and Roldanillo. Publicaciones Geol. Esp. No. 4, Ingeominas, Bogotá.

Bayona, G., Cortes, M., Jaramillo, C., Ojeda, G., Aristizabal, J., Reyes-Harker, A., 2008. An integrated analysis of an orogen-sedimentary basin pair: latest Cretaceous-Cenozoic evolution of the linked Eastern Cordillera orogen and the Llanos foreland basin of Colombia. Geological Society of America Bulletin 120, 1171–1197.

Bayona, G., Montes, C., Cardona, A., Jaramillo, C., Ojeda, G., Valencia, V., 2011. Intraplate subsidence and basin filling adjacent to an oceanic arc-continental collision; a case from the southern Caribbean–South America plate margin. Basin Research 23. http://dx.doi.org/10.1111/j.1365-2117.2010.00495.x.

Bayona, G., Cardona, A., Jaramillo, C., Mora, A., Montes, C., Valencia, V., Ayala, C., Montenegro, O. and Ibañez, M., 2012. Early Paleogene magmatism in the northern Andes: Insights on the effects of Oceanic Plateau–continent convergence. Earth and Planetary Science Letters 331-332, 97-111.

Bayona, G., Cardona, A., Jaramillo, C., Mora, A., Montes, C., Caballero, V., Mahecha, H., Lamus, F., Montenegro, O., Jimenez, G., Mesa, A. and Valencia, V., 2013. Onset of fault reactivation in the Eastern Cordillera of Colombia and proximal Llanos Basin; response to Caribbean–South American convergence in early Palaeogene time. in M. Nemcok, A.

Mora, and J. W. Cosgrove, eds., Thick-skin-dominated orogens: From initial inversion to full accretion: GSL Special Publications 377, 285-314.

Behar, F., Vandenbroucke, M., Tang, Y. and Espitalie, J., 1997. Thermal cracking of kerogen in open and closed systems: determination of kinetic parameters and stoichiometric coefficients for oil and gas generation. Organic Geochemistry 26, 321-339.

Berggren, W. A., Kent, D. V., Swisher, I. I. I., CC, and Aubry, M.-P., 1995, A revised Cenozoic geochronology and chronostratigraphy: Society of Economic Paleontologists and Mineralogists, Special Publication, 54, 129-212.

Bermudez, H., 2016. Esquema estratigráfico de secuencias del registro sedimentario del Cinturón Plegado de San Jacinto, Caribe colombiano. Extended abstract presented at the XII Simposio Bolivariano Exploración Petrolera en Cuencas Subandinas, September 26-28, 2016, Bogotá.

Bernal, R., Mann, P., and Vargas, C., 2015a. Earthquake, tomographic, seismic reflection, and gravity evidence for a shallowly dipping subduction zone beneath the Caribbean Margin of Northwestern Colombia. In C. Bartolini and P. Mann, (eds.), Petroleum geology and potential of the Colombian Caribbean Margin: American Association of Petroleum Geologists Memoir 108, 247–270.

Bernal, Rocío, Sánchez, J., Mann, P. and Murphy, M., 2015b. Along-strike crustal thickness variations of the subducting Caribbean plate produces two distinctive styles of thrusting in the offshore South Caribbean deformed belt, Colombia, in C. Bartolini and P. Mann, eds., Petroleum Geology and Potential of the Colombian Caribbean Margin: American Association of Petroleum Geologists Memoir 108, 295–322.

Bernal, R., Mann, P. and Escalona, A., 2015c. Cenozoic Tectonostratigraphic Evolution of the Lower Magdalena Basin, Colombia: An Example of an Under- to Overfilled Forearc Basin. In C. Bartolini and P. Mann, (eds.), Petroleum geology and potential of the Colombian Caribbean Margin: American Association of Petroleum Geologists Memoir 108, 345–398.

Beroiz, C., Lindberg, F. & Winter, S., 1986. Northwest Colombia Hydrocarbon Evaluation. Chevron Overseas Petroleum Inc., Internal report, California.

Bezada, M.J., Levander, A. and Schmandt, B., 2010. Subduction in the southern Caribbean: Images from finite-frequency P wave tomography. Journal of Geophysical Research., 115, B12333, doi:10.1029/2010JB007682.

Blow, W. H., 1969, Late middle Eocene to Recent planktonic foraminiferal Biostratigraphy, in Bronnimann, P., and Renz, H. H., eds. Proceedings of the First International Conference on Planktonic Microfossils. Geneva, 1967: Leiden, E.J. Brill, 199-421.

Boinet, T., Bourgois, J., Mendoza, H. and Vargas, R., 1989. La Falla de Bucaramanga (Colombia): Su función durante la Orogenia Andina. Geologia Norandina 11, 3-11.

Boschman, L., van Hinsbergen, D., Torsvik, T., Spakman, W and Pindell, J., 2014. Kinematic reconstruction of the Caribbean region since the Early Jurassic. Earth-Science Reviews 138, 102–136.

Bouvier, A., Vervoort, J. D., & Patchett, P. J., 2008. The Lu-Hf and Sm-Nd isotopic composition of CHUR: Constraints from unequilibrated chondrites and implications for the bulk composition of terrestrial planets. Earth and Planetary Science Letters, 273, 1-2, 48–57. http://doi.org/10.1016/j.epsl.2008.06.010

Bowland, C. and Rosencrantz, E., 1988. Upper crustal structure of the western Colombian basin, Caribbean Sea. Geological Society of America Bulletin, 100/4, 534-546.

Boyden, J., Müller, R.D., Gurnis, M., Torsvik, T.H., Clark, J., Turner,M., Ivey-Law, H.,Watson, R., Cannon, J., 2011. Next-generation plate-tectonic reconstructions using GPlates. In: Keller, R., Baru, C. (Eds.), Geoinformatics: Cyberinfrastruture for the Solid Earth Sciences. Cambridge University Press.

Brooks, J., 1990. Classic Petroleum Provinces. In Brooks, J. (Ed.), Classic Petroleum Provinces. Geological Society Special Publication, No. 50, 1-8.

Brown, L. and Fisher, W., 1977. Seismic stratigraphic interpretation of depositional systems: examples from Brazil rift and pull-apart basins. AAPG Memoir, 26, 213-248. American Association of Petroleum Geologists, Tulsa, OK, USA.

Burke, K., 1988, Tectonic evolution of the Caribbean: Annual Review of Earth and Planetary Sciences, 16, 201–230.

Burnham, A. and Sweeney, J., 1989. A chemical kinetic model of vitrinite maturation and reflectance. Geochimica et Cosmochimica Acta. 43, 2649-2657.

Bustamante, C., Cardona, A., Archanjo, C., Bayona, G., Lara, M and Valencia, V., 2017. Geochemistry and isotopic signatures of Paleogene plutonic and detrital rocks of the Northern Andes of Colombia: A record of post-collisional arc magmatism, Lithos http://dx.doi.org/10.1016/j.lithos.2016.11.025

Byrne, D.E., Wang, W.H., and Davis, D.M., 1993, Mechanical role of backstops in the growth of forearcs: Tectonics, 12/1, 123–144, doi: 10 .1029 /92TC00618 .

Caballero, V., Mora, A., Quintero, I., Blanco, V., Parra, M., Rojas, L., Lopez, C., Sánchez, N., Horton, B., Stockli, D. and Duddy, I., 2013a. Tectonic controls on sedimentation in an intermontane hinterland basin adjacent to inversion structures: the Nuevo Mundo syncline, Middle Magdalena Valley, Colombia, in M. Nemcok, A. Mora, and J. W. Cosgrove, eds., Thick-skin-dominated orogens: From initial inversion to full accretion: GSL Special Publications 377, 315-342.

Caballero, V., M. Parra, A. Mora, C. Lopez, L. E. Rojas, and I. Quintero, 2013b. Factors controlling selective abandonment and reactivation in thick-skin orogens: A case study in the Middle Magdalena Valley, Colombia, in M. Nemcok, A. Mora, and J. W. Cosgrove, eds., Thick-skin-dominated orogens: From initial inversion to full accretion: GSL Special Publications 377, 343–367.

Campbell, C.J., 1968, The Santa Marta wrench fault of Colombia and its regional setting. In Fourth Caribbean Geological Conference, 1965: Port of Spain, Trinidad, 247–261.

Cardona, A., Cordani, U. and MacDonald, W., 2006. Tectonic correlations of pre-Mesozoic crust from the northern termination of the Colombian Andes, Caribbean Region. Journal of South American Earth Sciences, 21, 337-354.

Cardona, A., Chew, D., Valencia, V.A., Bayona, Miskovic, A., Ibañez-Mejia, M., 2010a. Grenvillian remnants in the Northern Andes: Rodinian and Phanerozoic paleogeographic perspectives. Journal of South American Earth Sciences 29, 92–104.

Cardona, A., Valencia, V., Bustamante, C., García-Casco, A., Ojeda, G., Ruiz, J.,Saldarriaga, M., Weber, M., 2010b. Tectonomagmatic setting and provenance of the Santa Marta Schists, Northern Colombia: insights on the growth and approach of Cretaceous Caribbean oceanic terranes to the South American continent. Journal of South American Earth Sciences, 29, 784-804.

Cardona, A., Valencia, V., Bayona, G., Duque, J., Ducea, M., Gerhels, G., Jaramillo, C., Montes, C., Ojeda, G., Ruiz, J., 2011. Early subduction orogeny in the Northern Andes: Turonian to Eocene magmatic and provenance record in the Santa Marta massif and Rancheria Basin, Northern Colombia. Terranova 23, 26–34.

Cardona, A., Montes, C., Ayala, C., Bustamante, C., Hoyos, N., Montenegro, O., Ojeda, C., Niño, H., Ramirez, V., Valencia, V., Rincon, D., Vervoort, J. and Zapata, S., 2012. From arc-continent collision to continuous convergence, clues from Paleogene conglomerates along the southern Caribbean–South America plate boundary. Tectonophysics, 580, 58-87.

Cardona, A., Weber, M., Valencia, V., Bustamante, C., Montes, M., Cordani, U. and Muñoz, C., 2014. Geochronology and geochemistry of the Parashi granitoid, NE Colombia: Tectonic implication of short-lived Early Eocene plutonism along the SE Caribbean margin. Journal of South American Earth Sciences, 50, 75-92.

Cardozo, N., and Allmendinger, R. W., 2013, Spherical projections with OSXStereonet: Computers & Geosciences, 51, 193 - 205, doi: 10.1016/j.cageo.2012.07.021

Caro, M., y D. Spratt. 2003. Tectonic evolution of the San Jacinto fold belt. CSEQ Recorder 36-43.

Case, J. and MacDonald, W., 1973. Regional Gravity Anomalies and Crustal Structure in Northern Colombia. Geological Society of America Bulletin 84, 2905-2916.

Catuneanu, O., Abreu, V., Bhattacharya, J., Blum, M., Dalrymple, R., Eriksson, P., Fielding, C., Fisher, W., Galloway, W., Gibling, M., Giles, K., Holbrook, J., Jordan, R., Kendall, C., Macurda, B., Martinsen, O., Miall, A., Neal, J., Nummedal, A., Pomar, L., Posamentier, H., Pratt, B., Sarg, J., Shanley, K., Steel, R., Strasser, A., Tucker, M. and Winker, C., 2009. Towards the standardization of sequence stratigraphy. Earth Science Reviews 92, 1-33.

Cawood, P., Hawkesworth, C. and Dhuime, B., 2012. Detrital zircon record and tectonic setting. Geology, v. 40, No. 10, p. 875-878. doi:10.1130/G32945.1

Cecil, M.R., Gehrels, G., Ducea, M.N., Patchett, P.J., 2011. U–Pb–Hf characterization of the central Coast Mountains batholith: implications for petrogenesis and crustal architecture. Lithosphere 3, 247–260, http://dx.doi.org/10.1130/L134.1

Cediel, F., R. P. Shaw, and C. Cáceres, 2003. Tectonic assembly of the Northern Andean Block. In C. Bartolini, R. T. Buffler, and J. Blickwede, (eds.), The Circum-Gulf of Mexico and the Caribbean: Hydrocarbon habitats, basin formation, and plate tectonics: American Association of Petroleum Geologists Memoir 79, 815– 848.

Cerón, J., Kellogg, J., Ojeda, G., 2007. Basement Configuration of the northwestern South America-Caribbean margin from recent geophysical data. Ciencia, Tecnología y Futuro, 3/3, 25-49.

Chacon, M. and Martinez, N., 1994. Analisis sedimentologico-petrologico de las areniscas perforadas en la parte inferior de los pozos Ligia-1, Guamito-1, Apure-1 y Apure-2, Fm. Porquero, Valle Inferior del Magdalena. Final report for Ecopetrol.

Chacon, M., Cardozo, C. and Vásquez, M., 2001. Estudio petro-sedimentologico de algunas de las unidades arenosas perforadas en el pozo Flor del Monte-1, Valle Inferior del Magdalena. Final report for Ecopetrol.

Chenevart, Ch., 1963. Les dorsales transverses anciennes de Colombie et leurs homologues d'Amérique latine. Eclogae Geologicae Helvetiae, 56/2, 907-927.

Chiarabba, C., De Gori, P., Faccena, C., Speranza, F., Deccia, D., Dionicio, V., Pri-eto, G.A., 2015. Subduction system and flat slab beneath the Eastern Cordillera of Colombia. Geochem. Geophys. Geosyst.17, 16–27. http://dx.doi.org/10.1002/2015GC006048.

Clavijo, J., 1996. Mapa Geológico de Colombia, Plancha 75- Aguachica. Ingeominas, Memoria Explicativa, Bucaramanga, 1. 48p.

Clavijo, J. and Barrera, R, 1999. Geologia de las Planchas 44, Sincelejo y 52, Sahagun. Ingeominas, Bogota.

Clavijo, J., Mantilla, L., Pinto, J., Bernal, L and Perez, A., 2008. Evolución Geológica de la Serranía de San Lucas, Norte del Valle Medio del Magdalena y Noroeste de la Cordillera Central. Boletín de Geologia 30, 1, 45-62.

Clift, P.D., and MacLeod, C.J., 1999, Slow rates of subduction erosion estimated from subsidence and tilting of the Tonga forearc: Geology, v. 27, no. 5, p. 411–414, doi: 10.1130/0091-7613(1999)027<0411:SROSEE>2.3.CO;2.

Clift, P., and Vanucchi, P., 2004. Controls on Tectonic Accretion versus Erosion in subduction zones: Implications for the origin and recycling of the continental crust. Rev. Geophys., 42, RG2001, doi:10.1029/2003RG000127

Clift, P., and Hartley, A., 2007. Slow rates of subduction erosion and coastal underplating along the Andean margin of Chile and Peru. Geology, 35/6, 503-506. doi: 10.1130/G23584A.1.

Cochrane, R., Spikings, R., Gerdes, A., Ulianov, A., Mora, A., Villagómez, D., Putlitz, B. and Chiaradia, M., 2014. Permo-Triassic anatexis, continental rifting and the disassembly of western Pangaea. Lithos 190-191, 383-402.

Cooper, M., Addison, F., Alvarez, R., Coral, M., Graham, R., Hayward, A., Howe, S., Martinez, J., Naar, J., Peñas, R., Pullham, A. and Taborda, A., 1995. Basin Development and Tectonic History of the Llanos Basin, Eastern Cordillera, and Middle Magdalena Valley, Colombia. American Association of Petroleum Geologists Bulletin 79/10, 1421-1443.

Cordani, U.G., Cardona, A., Jimenez, D., Liu, D., Nutman, A.P., 2005. Geochronology of Proterozoic basement inliers from the Colombian Andes: tectonic history of remnants from a fragmented Grenville belt. In: Vaughan, A.P.M., Leat P.T., Pankhurst, R.J. (Eds.), Terrane Processes at the Margins of Gondwana. GSL Special Publication 246, 329–346.

Corredor, F., 2003. Seismic strain rates and distributed continental deformation in the northern Andes and three-dimensional seismotectonics of northwestern South America. Tectonophysics, 362, 147-166.

Cortes, M., and Angelier, J., 2005. Current states of stress in the northern Andes as indicated by focal mechanisms of earthquakes, Tectonophysics, 403, 29–58.

Cross, T. 2014. Core examination summary of the Ecopetrol M-3X core. Internal report for Hocol S.A., Bogotá.

Cuadros, F., Botelho, N., Ordoñez, O. and Matteini, M., 2014. Mesoproterozoic crust in the San Lucas Range (Colombia): An insight into the crustal evolution of the northern Andes. Precambrian Research, 245, 186-206.

Daly, M., 1989. Correlations between Nazca/Farallón Plate kinematics and forearc basin evolution in Ecuador. Tectonics, 8/4, 769-790.

De Freitas, M., Rizzi, J., Duarte, L. and Mora, A., 2003. Neogene Tectonics as a major control on Hydrocarbon plays of the Upper Magdalena Valley, Colombia. Presented at the AAPG Annual meeting, May 11-14, 2003, Salt Lake City, USA.

De Freitas, M., Mora, J.A., Mesa, A., Vélez, V., Martínez, M., Sierra, D. and Serna, L., 2013. New Geologic and Geophysical Constraints in the Assessment of Exploration Plays in the Lower Magdalena Valley, Onshore northern Colombia. Poster presented at the AAPG International Conference and Exhibition, Cartagena, September 8 -11.

De la Parra, F., Mora, A., Rueda, M. and Quintero, I., 2015. Temporal and spatial distribution of tectonic events as deduced from reworked palynomorphs in the eastern Northern Andes. Bulletin of the American Association of Petroleum Geologists, 99/8, 1455–1472

DePorta, J., 1962. Consideraciones sobre el estado actual de la estratigrafía del Terciario en Colombia. Boletin de Geología, Universidad Industrial de Santander, No. 9, 5.43.

Dhuime, B., Hawkesworth, C., & Cawood, P., 2011. When Continents Formed. Science, 331(6014), 154–155. http://doi.org/10.1126/science.1201245

Diaz-Cañas, S., 2015. Marco bioestratigráfico y proveniencia de la Formación Penderisco, y su significado en la formación de un domo marginal a las Fallas de Romeral. BSc. Thesis, Universidad Nacional de Colombia, Bogotá, 57 p.

Dickinson, W.R., 1973, Widths of modern arc-trench gaps proportional to past duration of igneous activity in associated magmatic arcs: Journal of Geophysical Research, 78/17, 3376–3389, doi: 10 .1029/JB078i017p03376 .

Dickinson, W.R., 1974, Plate tectonics and sedimentation, in Dickinson, W.R., ed., Tectonics and Sedimentation: Society of Economic Paleontologists and Mineralogists (SEPM) Special Publication 22, p. 1–27, doi: 10.2110 /pec .74 .22 .0001 .

Dickinson, W. and Seely, D., 1979. Structure and Stratigraphy of Forearc regions. Bulletin of the American Association of Petroleum Geologists 63/1, 2-31.

Dickinson, W. R., 1985. Interpreting provenance relations from detrital modes of sandstones. In G. G. Zuffa (Ed.), Provenance of Arenites (pp. 333–361). Dordrecht, Netherlands: Springer. https://doi.org/10.1007/978-94-017-2809-6_15

Dickinson, W., 1995. Chapter 6: Forearc Basins. In: "Tectonics of Sedimentary Basins". Ingersoll, R. and Busby, C. (eds.), 221-261. Blackwell Science.

Dickinson, W. R., & Gehrels, G. E., 2009. Use of U-Pb ages of detrital zircons to infer maximum depositional ages of strata: A test against a Colorado Plateau Mesozoic database. Earth and Planetary Science Letters, 288, 115–125. http://doi.org/10.1016/j.epsl.2009.09.013

Driscoll, N. W., and J. B. Diebold, 1999, Tectonic and stratigraphic development of the Eastern Caribbean: New constraints from multichannel seismic data, in P. Mann, ed., Caribbean basins: Sedimentary basins of the world 4: Amsterdam, Elsevier Science B.V., 591–626.

Dueñas, H., and Duque-Caro, H., 1981. Geologia del Cuadrangulo F-8. Boletin Geologico. Ingeominas 24/1, 1-35.

Dueñas, H. and Gomez, C., 2013. Bioestratigrafía de las Formación Cansona en la Quebrada Peñitas, Cinturon de San Jacinto: Implicaciones Paleogeográficas. Revista de la Academia Colombiana de Ciencias, Vol. XXXVII, No. 145, 527-539.

Dunham, R.J. 1962. Classification of carbonate rocks according to depositional texture. In: Ham, W. E. (ed.), Classification of carbonate rocks: American Association of Petroleum Geologists Memoir, 108-121

Dumitru, T.A.,1990. Subnormal Cenozoic geothermal gradients in the extinct Sierra Nevada magmatic arc: consequences of Laramide and Post-Laramide shallow-angle subduction. Journal of Geophysical. Research, 95, 4925–4941.

Dumitru, T.A., Gans, P.B., Foster, D.A. & Miller, E.L. (1991) Refrigeration of the western Cordilleran lithosphere during Laramide shallow-angle subduction. Geology, 19, 1145–1148.

Duque-Caro, H., 1972. Ciclos tectonicos y sedimentarios en el norte de Colombia y sus relaciones con la paleoecología. Boletin Geologico Ingeominas, 19/33, 1-23.

Duque-Caro, H., 1979. Major Structural Elements and Evolution of Northwestern Colombia. In "Geological and Geophysical Investigations of Continental Margins", Watkins, J.S., Montadert, L. and Wood Dickerson, P. (eds.). American Association of Petroleum Geologists Memoir 29, Tulsa.

Duque-Caro, H., 1980, Geotectónica y evolución de la región noroccidental Colombiana: Boletín Geológico Ingeominas, 23, 4–37.

Duque-Caro, H., 1984. Structural Style, diapirism, and accretionary episodes of the Sinú-San Jacinto terrane, southwestern Caribbean borderland. Geological Society of America, Memoir 162, 303-316.

Duque-Caro, H., 1991. Contributions to the Geology of the Pacific and the Caribbean Coastal Areas of Northwestern Colombia and South America. PhD Thesis, Princeton University.

Duque-Caro, H., Guzman, G. and Hernandez, R., 1996. Mapa Geológico de la Plancha 38, Carmen de Bolívar. Ingeominas, Bogotá.

Duque-Caro, H., 2000. Analisis bioestratigráficos de 400 muestras de 34 pozos y 16 muestras de superficie de las cuencas de San Jorge, Sinu, Plato y Barranquilla en el Valle Inferior del Magdalena. Internal report for Ecopetrol.

Duque-Caro, H., 2001. Analisis bioestratigráficos de 250 muestras de 5 pozos de las cuencas de San Jorge, Sinu, Plato y Barranquilla en el Valle Inferior del Magdalena. Internal report for Ecopetrol.

Duque-Caro, H., 2010. Analisis microestratigráficos de 36 muestras del pozo Saman Norte-1. Internal report for Hocol S.A., Bogotá.

Duque-Caro, H., 2011a. Microstratigraphic analyses of samples from the Wells Caracoli-1, Manati-1 and Polonuevo-1, Barranquilla Province. Internal report for Hocol S.A., Bogotá.

Duque-Caro, H., 2011b. Microstratigraphic analyses of samples from the Wells Molinero-1, Molinero-2 and Molinero-3X, Barranquilla Province. Internal report for Hocol S.A., Bogotá.

Duque-Caro, H., 2011c. Microstratigraphic analyses of 100 samples from the Wells Guaruco-1, Molinero-2 and Molinero-3X and Tubará-1, Barranquilla Province. Internal report for Hocol S.A., Bogotá.

Duque-Caro, H., 2012a. Microstratigraphic analyses of 92 samples from the Well Bonga-1, San Jorge basin. Internal report for Hocol S.A., Bogotá.

Duque-Caro, H., 2012b. Microstratigraphic analyses of samples from the Well CEST1, Barranquilla Province. Internal report for Hocol S.A., Bogotá.

Duque-Caro, H., 2013a. Microstratigraphic analyses of samples from the Well SamanEst-1, Barranquilla Province. Internal report for Hocol S.A., Bogotá.

Duque-Caro, H., 2013b. Microstratigraphic analyses of samples from the Well C-1, Barranquilla Province. Internal report for Hocol S.A., Bogotá.

Duque-Caro, H., 2014. Microstratigraphic analyses of 39 samples from the Well Calipso-1, Barranquilla Province. Internal report for Hocol S.A., Bogotá.

Ecopetrol/ICP, 2014. Proyecto "Protocolo del Pre-Neógeno del Caribe en las Cuencas Sinú-San Jacinto y Valle Inferior del Magdalena". Internal Reports. Bogotá.

Edgar, N.T., Ewing, J. and Hennion, J., 1971. Seismic Refraction and Reflection in Caribbean Sea. Bulletin of the American Association of Petroleum Geologists, 55/6, 833-870. American Association of Petroleum Geologists, Tulsa, OK, USA.

Ekstrom, G., Dziewonski, A., Maternovskaya, N and Nettles, M., 2005. Global seismicity of 2002: centroid-moment-tensor solutions for 1034 earthquakes. Physics of the Earth and Planetary Interiors 148, 303-326.

English, J. M., Johnston, S. and K. Wang, 2003. Thermal modelling of the Laramide Orogeny: Testing the flat-slab subduction hypothesis, Earth Planet. Sci. Lett., 214/3–4, 619–632.

Erlich, R. N., Villamil, T. and Keens-Dumas, J., 2003. Controls on the deposition of Upper Cretaceous organic carbon– rich rocks from Costa Rica to Suriname. In C. Bartolini, R. T. Buffler, and J. Blickwede, (eds.), The Circum-Gulf of Mexico and the Caribbean: Hydrocarbon habitats, basin formation, and plate tectonics: American Association of Petroleum Geologists Memoir 79, 1–45.

Escalona, A., and Mann, P., 2011. Tectonics, basin subsidence mechanisms, and paleogeography of the Caribbean-South American plate boundary zone: Marine and Petroleum Geology, 28, 8–39.

Espurt, N., Funiciello, F., Martinod, J., Guillaume, B., Regard, V., Faccenna, C. and Brusset, S., 2008. Flat subduction dynamics and deformation of the South American plate: Insights from analog modeling. Tectonics, 27, TC3011, doi:10.1029/2007TC002175.

ESRI/ILEX, 1995. Evaluación Geológica Regional de la Cuenca Sinú-San Jacinto. Technical report for Ecopetrol.

Etayo, F. et al. 1983. Mapa de terrenos geológicos de Colombia. Publicación Geológica Especial No. 14:1-235, Ingeominas. Publicación efectiva, 1986. Bogotá.

Etayo-Serna, F., Renzoni, G. & Barrero, D. 1969. Contornos sucesivos del mar Cretáceo en Colombia. I Congreso Colombiano Geológico. Memorias, p. 217–252. Bogotá.

Ewing, J., Antoine, J. and Ewing, M., 1960. Geophysical Measurements in the Western Caribbean Sea and in the Gulf of Mexico. Journal of Geophysical Research, 65/12, 4087-4126.

Farris, D.W., Jaramillo, C.A., Bayona, G.A., Restrepo-Moreno, S.A., Montes, C., Cardona, A., Mora, A., Speakman, R.J., Glasscock, M.D., Reiners, P., and Valencia , V., 2011, Fracturing of the Panamanian isthmus during initial collision with South America: Geology, 39, 1007–1010, doi:10.1130/G32237.1.

Faure, G. And Mensing, T., 2005. Isotopes, Principles and Applications, 3rd Ed. John Wiley and Sons, New Jersey. 897 p.

Feininger, T., 1970. The Palestina fault, Colombia. Geological Society of America Bulletin, 81, 1201-1216.

Fisher, C.M., Vervoort, J.D., Hanchar, J.M., 2014b. Guidelines for reporting zircon Hf isotopic data by LA-MC-ICPMS and potential pitfalls in the interpretation of these data. Chem. Geol. 363, 125–133, http://dx.doi.org/10.1016/j.chemgeo.2013.10.019

Flinch, J. F., 2003, Structural evolution of the Sinu-Lower Magdalena area (Northern Colombia), in C. Bartolini, R. T. Buffler, and J. Blickwede, eds., The Circum-Gulf of Mexico and the Caribbean: Hydrocarbon habitats, basin formation and plate tectonics: American Association of Petroleum Geologists Memoir 79, 776–796.

Folk, R.L., 1959, Practical petrographic classification of limestones: American Association of Petroleum Geologists Bulletin, 43, 1-38.

Folk, R., 1980. Petrology of Sedimentary Rocks, Hemphill Publishing Co., 170p, Austin.

Forero, O., 1974, The Eocene of northwestern South America [M.S. thesis]: Tulsa, University of Tulsa, 81 p.

Fuller, C.W., Willett, S.D., and Brandon, M.T., 2006, Formation of forearc basins and their influence on subduction zone earthquakes: Geology, 34/2, 65–68, doi:10 .1130 /G21828 .1 .

Gehrels, G.E., Valencia, V.A., Ruiz, J., 2008. Enhanced precision, accuracy, efficiency and spatial resolution of U–Pb ages by laser ablation–multicollector–inductivelycoupled plasma–mass spectrometry. Geochem. Geophys. Geosyst. 9, Q03017,http://dx.doi.org/10.1029/2007GC001805

GEMS Ltda., 2007. Caracterizacion Geoquimica de Rocas y crudos en las cuencas de Cesar-rancheria, Sinu-San Jacinto, Choco y Area de Soapaga (Cuenca Cordillera Oriental). Final report for ANH, Bogotá.

GEMS Ltda., 2014. Evaluación de los Sistemas Petrolíferos en el Bloque SSJN1 del Cinturón Plegado de San Jacinto. Internal report for Hocol S.A. and Lewis Energy Colombia, Bogota.

GEMS Ltda., 2017. Resultados preliminares de análisis geoquímicos a pozos estratigráficos en el Cinturón de San Jacinto. Internal report for Hocol, Bogotá.

Geosearch Ltda., 2006. Cartografía e Interpretación geológica y levantamiento estratigráfico para el Bloque Perdices, Cuenca del Valle Inferior del Magdalena. Internal report for Ecopetrol, Bogotá.

Gleeson, S., Herrington, R., Durango, J., Velásquez, C. and Koll, G., 2004. The Mineralogy and Geochemistry of the Cerro Matoso S.A. Ni Laterite Deposit, Montelíbano, Colombia. Economic Geology, 99, 1197-1213.

Glodny, J., Lohrmann, J., Echtler, H., Gräfe, K., Seifert, W., Collao, S. and Figueroa, O., 2005. Internal Dynamics of a paleoaccretionary wedge: Insights from combined isotope tectonochronology and sandbox modelling of the South-Central Chilean forerarc. Earth and Planetary Science Letters, 231, 23-39.

Gómez, I., 2001. Structural Style and Evolution of the Cuisa Fault System, Guajira, Colombia. University of Houston, 147p.

Gómez, E., Jordan, T., Allmendinger, R., Hegarty, K. and Kelley, Sh., 2005. Syntectonic Cenozoic sedimentation in the northern middle Magdalena Valley Basin of Colombia and implications for exhumation of the Northern Andes. Bulletin of the Geological Association of America, 117/5/6, 547–569; doi: 10.1130/B25454.1; 15 figures; 3 tables; Data Repository item 2005076.

Gomez, J., Nivia, A., Montes, N., Tejada, M., Jimenez, D., Sepulveda, M., Osorio, J., Gaona, T., Diederix, H., Uribe, H. and Mora, M., 2007. Geological Map of Colombia, First edition. Ingeominas (Servicio Geologico de Colombia), Bogota.

Gomez, J., Montes, N., Nivia, A. and Diederix, H., 2015. Mapa Geologico de Colombia. Ingeominas (Servicio Geol. Colomb.), Bogota.

González, H, 1980. Geología de las planchas 167 (Sonsón) y 168 (Salamina): Boletín Geológico, 23, 174 p.

González, H., 2001. Mapa Geológico del Departamento de Antioquia Escala 1:400.000, Memoria Explicativa, Ingeominas, Medellín, 240 pp.

Govers, R. and Wortel, M., 2005. Lithospheric tearing at STEP faults: Response to edges of subduction zones. Earth and Planetary Science Letters, 236, 505-523.

Grosse, E., 1926. El Terciario Carbonifero de Antioquia. D. Reimer-E. Vohsen, Berlin. 361 pp.

Gutscher, M.A., Spakman, W., Bijwaard, H. And Engdahl, E., 2000. Geodynamics of flat subduction: seismicity and tomographic constraints from the Andean margin. Tectonics, 19, 814–833.

Guzman, G., Gomez, E. and Serrano, B., 2004. Geologia de los cinturones del Sinu, San Jacinto y Borde occidental del Valle Inferior del Magdalena, Caribe Colombiano. Ingeominas (Colombian Geological Survey) report, Bogotá.

Guzman, G., 2007. Stratigraphy and Sedimentary Environment and Implications in the Plato Basin and the San Jacinto Belt Northwestern Colombia. PhD Thesis, University of Liege, Belgium.

Haq, B.U., Hardenbol, J. and Vail, P.R., 1987. Chronology of fluctuat¬ing sea levels since the Triassic (250 million years ago to present). Science, 235, 1156-1166.

He, Z., 2000. Multidimensional Burial and Thermal Modeling of the Lower Magdalena Valley (Plato-San Jorge) and Sinu (Alcatraz Area). Final report for Ecopetrol, Bogotá.

Hincapie, S., Cardona, A. and Jimenez, G., 2015. Análisis Paleomagnético de la Formación Barroso en el Departamento de Antioquia: Implicaciones Paleogeográficas. Memoirs of the "XV Congreso Colombiano de Geologia, Bucaramanga".

Hocol S.A., 1993. Lower Magdalena Valley Technical Evaluation Agreement. Phase I Internal report. Cartagena.

Hooghiemstra, H., Wijninga, V.M., and Cleef, A.M., 2006, The paleobotanical record of Colombia: Implications for biogeography and biodiversity: Annals of the Missouri Botanical Garden, 93, 297–325,doi: 10.3417/0026-6493

Hoorn, C., Wesselingh, F., ter Steege, H., Bermudez, M., Mora, A., Sevink, J., Sanmartin, I., Sanchez-Meseguer, A., Anderson, C., Figueiredo, J., Jaramillo, C., Riff, D., Negri, F., Hooghiemstra, H., Lundberg, J., Stadler, T., Särkinen, T., Antonelli, A., 2010. Amazonia through time: Andean uplift, climate change, landscape evolution, and biodiversity: Science, 330, 927–931, doi: 10 .1126 /science .1194585.

Horton, B. K., Parra, M., Saylor, J. E., Nie, J., Mora, A., Torres, V., et al., 2010. Resolving uplift of the northern Andes using detrital zircon age signatures. GSA Today, 20/7, 4–9.

Horton, B., Anderson, V., Caballero, V., Saylor, J., Nie, J., Parra, M. and Mora, A., 2015. Application of detrital zircon U-Pb geochronology to surface and subsurface correlations of provenance, paleodrainage, and tectonics of the Middle Magdalena Valley Basin of Colombia: Geosphere, 11/6, 1790–1811, doi:10.1130/GES01251.1.

Houtz, R. and Ludwig, W., 1977. Structure of Colombia Basin, Caribbean Sea, from Profiler-Sonobuoy measurements. Journal of Geophysical Research, 82/30, 4861- 4867.

Hubach, E., 1957. Estratigrafía de la Sabana de Bogotá y sus alrededores. Bol. Geol., Serv. Geol. Nacl. 5, 93–112.

Ibañez-Mejia, M., Tassinari, C.C.G., Jaramillo-Mejia, J.M., 2007. U-Pb zircon ages of the "Antioquian Batholith": geochronological constraints of Late Cretaceous magmatism in the Central Andes of Colombia. 11th Colombian Geological Congress, Extended Abstracts (11 pp.).

Ibañez-Mejia, M., Ruiz, J., Valencia, V. A., Cardona, A., Gehrels, G. E., & Mora, A. R., 2011. The Putumayo Orogen of Amazonia and its implications for Rodinia reconstructions: New U-Pb geochronological insights into the Proterozoic tectonic evolution of northwestern South America. Precambrian Research, 191, 58–77. http://doi.org/10.1016/j.precamres.2011.09.005

Ibañez-Mejia, M., Pullen, A., Arenstein, J., Gehrels, G., Valley, J., Ducea, M., Mora, A., Pecha, M. and Ruiz, J., 2015. Unraveling crustal growth and reworking processes in complex zircons

from orogenic lower –crust: The Proterozoic Putumayo orogeny of Amazonia. Precambrian Research 267, 285-310.

ICP (Instituto Colombiano del Petróleo), 1998. Análisis petrológico muestras pozos Ayombe 1, Valle Inferior del Magdalena. Internal Report, Piedecuesta, Santander.

ICP (Instituto Colombiano del Petróleo), 2000. Evaluación Regional Integrada Cuenca Valle Inferior del Magdalena. Final Internal Report, Piedecuesta, Santander.

ICP (Instituto Colombiano del Petróleo), 2009. Estudio petrológico de muestras de los pozos Floresanto 1, Jaraguay Norte 1, Jaraguay Norte 2, La Mora 1 y La Risa 1, Valle Inferior del Magdalena. Internal report. Piedecuesta, Santander.

ICP (Instituto Colombiano del Petróleo), 2010. Hallazgos petrológicos y mineralógicos Pozo Saman Norte-1. Internal report. Piedecuesta, Santander.

Ingeominas/ANH, 2008. Mapa Preliminar de Gradientes Geotérmicos de Colombia. Bogotá.

Ingersoll, R., 1988. Tectonics of sedimentary basins. Bulletin of the Geological Society of America, 100, 1704-1719.

Ingersoll, R., 2012. Tectonics of sedimentary basins, with revised nomenclature. In: Busby, C. and Azor, A. (eds.), Tectonics of Sedimentary basins: Recent advances. Blackwell.

James, K.H., 2006. Arguments for and against the Pacific origin of the Caribbean Plate: discussion,finding for an inter-American origin. Geol. Acta 4, 279–302.

Janssen, P., Frankowicz, E. and Steffen, D., 2012. Hydrocarbon potential of Forearc Basins in Asia. AAPG Search and Discovery Article #90155©2012, AAPG International Conference & Exhibition, Singapore, 16-19 September 2012

Jarrard, R., 1986. Terrane motion by strike-slip faulting of forearc slivers. Geology, 14, 780-783.

Jiménez, G., Speranza, F., Faccena, C., Bayona, G. and Mora, A., 2014. Paleomagnetism and magnetic fabric of the Eastern Cordillera of Colombia: Evidence for oblique convergence and nonrotational reactivation of a Mesozoic intracontinental rift, Tectonics, 33, 2233–2260, doi:10.1002/2014TC003532.

Juliao-Lemus, T., de Araujo Carvalho, M., Torres, D., Plata, A. and Parra, C., 2016. Paleoenvironmental reconstruction based on palynofacies analyses of the Cansona Formation (Late Cretaceous), Sinú-San Jacinto Basin, northwest Colombia. Journal of South American Earth Sciences, 69, 103-118.

Karig, D.E., 1974, Evolution of arc systems in the western Pacific: Annual Review of Earth and Planetary Sciences, 2/1, 51–75, doi: 10 .1146 /annurev .ea .02.050174 .000411.

Karig, D.E., and Sharman, G.F., III, 1975, Subduction and accretion in trenches: Geological Society of America Bulletin, 86/3, 377–389, doi: 10 .1130 /0016-7606 (1975)86 <377: SAAIT>2 .0 .CO;2.

Keller, G., and Barron, J. A., 1983, Paleoceanographic implications of Miocene deep-sea hiatuses: Geological Society of America Bulletin, 94, 590-613.

Keller, G., and Barron, J. A., 1987, Paleodepth distribution of Neogene deep-sea hiatuses: Paleoceanography, 2, 697-713.

Kellogg, J. and Bonini, W., 1982. Subduction of the Caribbean Plate and Basement uplifts in the overriding South American plate. Tectonics, 1/3, 251-276.

Kellogg, J. N., 1984. The Cenozoic tectonic history of the Sierra de Perija and adjacent basins. In Caribbean-South American Plate Boundary and Regional Tectonics, W. E. Bonini, R. B. Hargraves, and R. Shagam (eds.), Memoir of the Geological Society of America, 162, 239–261.

Kennan, L. and Pindell, J., 2009. Dextral shear, terrane accretion and basin formation in the Northern Andes: best explained by the interaction with a Pacific-derived Caribbean plate? GSL Special Publication 328, 487-531.

Kobayashi, K., 1995, Role of subducted lithospheric slab in uplift and subsidence of the northwestern Pacific margins: Marine Geology, 127, 119–144, doi:10.1016/0025-3227(95)00007-L.

Kodama, K., Takeuchi, T. and Ozawa, T., 1993. Clockwise tectonic rotation of Tertiary sedimentary basins in Central Hokkaido, northern Japan. Geology, 21, 431-434.

Kroehler, M., Mann, P., Escalona, A. and Christenson, G., 2011. Late-Cretaceous-Miocene diachronous onset of backthrusting along the South Caribbean deformed belt and its importance for understanding processes of arc collision and crustal growth. Tectonics, 30, TC60003.

Ladd, J., M. Truchan, M. Talwani, P. Stoffa, P. Buhl, R. Houtz, A. Mauffret, y G. Westbrook. 1984. Seismic reflection profiles across the southern margin of the Caribbean. In The Caribbean-South American plate boundary and regional tectonics. Geological Society of America Memoir 162, ed. W. Bonini.

Lara, M., Cardona, A., Monsalve, G., Yarce, J., Montes, C., Valencia, V., Weber, M., De La Parra, F., Espitia, D. and Lopez-Martinez, M., 2013. Middle Miocene near trench volcanism in northern Colombia: A record of slab tearing due to the simultaneous subduction of the Caribbean Plate under South and Central America? Journal of South American Earth Sciences, 45, 24-41.

Leal, H. 2011. Phanerozoic Gold Metallogeny in the Colombian Andes: A tectono-magmatic approach. Unpubl. PhD Thesis, Univ. Barcelona, 989p.

Leroy, S., Bitri, A. and Mauffret, A., 1996. Migration velocity analysis based on common-shot-depth migration applied to the seismic data of the Caribbean oceanic plateau. Geophys. J. Int., 125, 199-213.

Levander, A., Bezada, M., Niu, F. and Schmitz, M., 2015. The two subduction zones of the Southern Caribbean: Lithosphere Tearing and Continental Margin Recycling in the East, Flat Slab sybduction and Laramide-style uplifts in the west. AGU Fall Meeting, San Francisco.

Lithosphera Ltda., 2010. Interpretación Gravimétrica Cuantitativa, Región Sinú-San Jacinto y Valle Inferior del Magdalena. Informe interno para Hocol S.A., Bogotá.

Londoño, J., Schiek, C. and Biegert, E., 2015, Basement architecture of the Southern Caribbean Basin, Guajira Offshore, Colombia. In C. Bartolini and P. Mann, (eds.), Petroleum geology and potential of the Colombian Caribbean Margin: American Association of Petroleum Geologists Memoir 108, 85–102.

Llinas, R. 2012. Petrographic analyses of outcrop samples from the SSJN1 block (northern San Jacinto fold belt). Internal report for Hocol S.A., Bogotá.

Macellari, C. 1995. Cenozoic sedimentation and tectonics. In: A. Tankard, R Suarez Soruco y&H. Welsink (eds), Petroleum basins of South America, American Association of Petroleum Geologists Memoir 62, 757-780.

Magnani, M. B., C. A. Zelt, A. Levander, and M. Schmitz (2009), Crustal structure of the South American–Caribbean plate boundary at 67_W from controlled source seismic data, J. Geophys. Res., 114, B02312, doi:10.1029/2008JB005817.

Magoon, L. and Dow, W., 1994. The Petroleum System. Chapter 1 in Magoon, L. and Dow, W. (eds.): The Petroleum System- from source to trap. American Association of Petroleum Geologists Memoir 60. American Association of Petroleum Geologists, Tulsa, OK, USA. 3-24.

Malavé, G., and Suárez, G., 1995. Intermediate-depth seismicity in northern Colombia and western Venezuela and its relationship to Caribbean Plate subduction, Tectonics, 14, 617–628.

Manea, V., Manea, M., Ferrari, L., Orozco, T., Valenzuela, R., Husker, A. and Kostoglodov, V., 2017. A review of the geodynamic evolution of flat slab subduction in Mexico, Peru and Chile. Tectonophysics, 695, 27-52.

Mantilla, A., 2007. Crustal structure of the southwestern Colombian Caribbean Margin. Thesis Dr. rer. nat., Friedrich-Schiller-Universität Jena, Germany.

Mantilla, A.M., Jentszsch, G., Kley, J., Alfonso-Pava, C., 2009. Configuration of the Colombian Caribbean Margin: Constraints from 2D Seismic Reflection Data and Potential Fields Interpretation, Subduction Zone Geodynamics. Springer, Dubai, 247–271.

Masy, J., Niu, F., Levander, A., Schmitz, M., 2011. Mantle flow beneath northwestern Venezuela: seismic evidence for a deep origin of the Mérida Andes. Earth and Planetary Science Letters, 305/3–4, 396–404. http://dx.doi.org/10.1016/j.epsl.2011.03.024.

Matthews, K., Maloney, K., Zahirovic, S., William, S., Seton, M. and Muller, D., 2016. Global plate boundary evolution and kinematics since the late Paleozoic. Global and Planetary Change 146, 226-250. http://dx.doi.org/10.1016/j.gloplacha.2016.10.002

Mauffret, A. and Leroy,S.,1997. Seismic stratigraphy and structure of the Caribbean igneous province. Tectonophysics, 283, 61-104.

Maze, W., 1983. Jurassic La Quinta formation in the Sierra de Perija, Northwestern Venezuela: geology, tectonic environment, paleomagnetic data, and copper mineralization of red beds and volcanics. Unpubl. PhD Thesis, Princeton University.

McArthur, J.M., Howarth, R. and Bailey, T., 2001. Strontium Isotope Stratigraphy: LOWESS Version 3: Best fit to the Marine Sr-Isotope Curve for 0-509 Ma and accompanying Look-up Table for Deriving Numerical Age. The Journal of Geology, 109, 155-170.

McCaffrey, R., 1992. Oblique plate convergence, slip vectors and forearc deformation. Journal of Geophysical Research, 97, 8905-8915.

McKenzie, D., 1978. Some remarks on the development of sedimentary basins. Earth and Planetary Science Letters, 40, 25-32.

Mejía, P., Santa, M., Ordóñez, O., Pimentel., M., 2008. Consideraciones petrográficas, geoquímicas y geocronológicas de la parte occidental del Batolito de Santa Marta. Revista Dyna, 155, 223-236.

Meschede, M., y W. Frisch. 1998. A plate-tectonic model for the Mesozoic and Early Cenozoic history of the Caribbean plate. Tectonophysics, 296, 269-291.

Miall, A.D., 2000. Principles of sedimentary basin analysis. 3rd edition, Springer-Verlag Berlin Heidelberg. 616p.

Molinares, C., Martinez, J.I., Fiorini, F., Escobar, J. and Jaramillo, C., 2012. Paleoenvironmental reconstruction for the lower Pliocene Arroyo Piedras section (Tubará e Colombia): Implications for the Magdalena River - paleodelta's dynamic. Journal of South American Earth Sciences 39, 170-183.

Montes, C., Guzman, G., Bayona German, A., Cardona, A., Valencia, V., Jaramillo Carlos, A., 2010. Clockwise rotation of the Santa Marta massif and simultaneous Paleogene to Neogene deformation of the Plato-San Jorge and Cesar-Rancheria basins. Journal of South American Earth Sciences. 29, 832-848.

Montes, C., Cardona, A., Jaramillo, C., Pardo, A., Silva, J.C., Valencia, V., Ayala, C., Perez-Angel. L.C., Rodriguez-Parra, L.A., Ramirez, V., Niño, H., 2015. Middle Miocene closure of the Central American Seaway. Science, 348, 226-229.

Mora, A., and A. Garcia, 2006, Cenozoic tectono-stratigraphic relationships between the Cesar Subbasin and the southeastern Lower Magdalena Valley Basin of Northern Colombia: AAPG, Search and Discovery Article, 30046. Search and Discovery, v. 30046, p. 1-11.

Mora, A., Parra, M., Strecker, M., Sobel, E., Hooghiemstra, H., Torres, V. and Vallejo, J., 2008. Climatic forcing of asymmetric orogenic evolution in the Eastern Cordillera of Colombia. Bulletin of the Geological Society of America, 120/7/8, 930-949; doi: 10.1130/B26186.1; 13 figures; 3 tables.

Mora, A., B. K. Horton, A. Mesa, J. Rubiano, R. A. Ketcham, M. Parra, V. Blanco, D. Garcia, and D. Stockli, 2010a, Cenozoic deformation migration in the Eastern Cordillera of Colombia interpreted from fission-track results and structural relationships: Implications for hydrocarbon systems: American Association of Petroleum Geologists Bulletin, 94/10, 1543–1580.

Mora, A., Parra, M., Strecker, M., Sobel, E., Zeilinger, G., Jaramillo, C., Ferreira Da Silva, S. and Blanco, M., 2010b. The eastern foothills of the Eastern Cordillera of Colombia: An example of multiple factors controlling structural styles and active tectonics. Bulletin of the Geological Association of America, 122, 11-12: 1846-1864. https://doi.org/10.1130/B30033.1

Mora, J. A., De Freitas, M., Velez, V., 2013. Cenozoic Tectonostratigraphy of the Northern San Jacinto fold belt, Northwestern Colombia. Poster presented at the AAPG International Convention and Exhibition, Cartagena, 8-11 September.

Mora, A., A. Reyes, G. Rodriguez, E. Teson, J. Ramirez-Arias, M. Parra, V. Caballero, J. Mora, I. Quintero, V. Valencia, M. Ibanez-Mejia, B. Horton, and D. Stockli, 2013a, Inversion tectonics under increasing rates of shortening and sedimentation throughout the Cenozoic, in M. Nemcok, A. Mora, and J. Cosgrove, eds., Thick-skin-dominated orogens; from initial inversion to full accretion: GSL Special Publication 377, 411-442.. doi: 10.1144/SP377.6

Mora, A., Blanco, V., Naranjo, J., Sanchez, N., Ketcham, R., Rubiano, J., Stockli, D., Quintero, I., Nemčok, M., Horton, B. and Davila, H., 2013b. On the lag time between internal strain and basement involved thrust induced exhumation: The case of the Colombian Eastern Cordillera. Journal of Structural Geology, 52, 96-118.

Mora, A., Parra, M., Forero, G., Blanco, V., Moreno, N. and Caballero, V., 2015. What drives orogenic asymmetry in the Northern Andes?: A case study from the apex of the Northern Andean Orocline, in C. Bartolini and P. Mann, eds., Petroleum geology and potential of the Colombian Caribbean Margin: American Association of Petroleum Geologists Memoir 108, 547–586.

Mora, A., Ibáñez-Mejía, M., Oncken, O., De Freitas, M., Vélez, V., Mesa, A. and Serna, L. 2017a. Structure and Age of the Lower Magdalena Valley Basement, Northern Colombia: New reflection-seismic and U-Pb-Hf Insights into the termination of the Central Andes against the Caribbean Basin. Journal of South American Earth Sciences 74, 1-26. http://dx.doi.org/10.1016/j.jsames.2017.01.001

Mora, J.A., Oncken, O., Le Breton, E., Ibáñez-Mejía, M., Faccena, C., Veloza, G., Vélez, V., De Freitas, M., Mesa, A., 2017b. Linking Late Cretaceous to Eocene Tectono-stratigraphy of the San Jacinto fold belt of NW Colombia with Caribbean plateau collision and flat subduction. Tectonics, 36, 1-36. doi: 10.1002/2017TC004612

Müller, R.D., Royer, J.-Y., Cande, S.C., Roest, W.R., Maschenkov, S., 1999. New constraints on the Late Cretaceous/Tertiary plate tectonic evolution of the Caribbean. In: Mann, P. (Ed.), Caribbean Basins. Elsevier Science B.V., Amsterdam, The Netherlands, 33–59.

Nie, J., Horton, B., Saylor, J., Mora, A., Mange, M., Garziones, C., Basu, A., Moreno, Ch., Caballero, V. and Parra, M., 2012. Integrated provenance analysis of a convergent retroarc foreland system: U–Pb ages, heavy minerals, Nd isotopes, and sandstone compositions of the Middle Magdalena Valley basin, northern Andes, Colombia. Earth-Science Reviews 110, 111-126.

Nilsen, T.H., and Sylvester, A., 1995. Strike Slip Basins. In Tectonics of sedimentary basins, ed. Busby, C. and Ingersoll, R. 425-457. Blackwell Science.

Niño, Ch., 2005. Sistemas Petroliferos da parte norte da Bacia de Sinu-San Jacinto, Colombia: Uma avaliacao geologica e geoquimica integrada. Masters Thesis at Federal University of Rio de Janeiro, Brazil.

Nivia, A., Marriner, G., Kerr, A. and Tarney, J., 2006. The Quebradagrande Complex: A Lower Cretaceous ensialic marginal basin in the Central Cordillera of the Colombian Andes. Journal of South American Earth Sciences, 21, 423-436.

Noda, A., 2016. Forearc basins: Types, geometries, and relationships to subduction zone dynamics. Bulletin of the Geological Society of America, 128/5/6, 879–895; doi: 10.1130/B31345.1.

Noury, M., Philippon, M., Bernet, M., Paquette, J.L. and Sempere, Th., 2017. Geological record of flat slab-induced extension in the southern Peruvian forearc. Geology, 45/8, 723-726. doi:10.1130/G38990.1

O'Dea, A., H. A. Lessios, A. G. Coates, R. I. Eytan, S. A. Restrepo-Moreno, A. L. Cione, L. S. Collins, A. de Queiroz, D. W. Farris, R. D. Norris, R. F. Stallard, M. O. Woodburne, O. Aguilera, M.-P. Aubry, W. A. Berggren, A. F. Budd, M. A. Cozzuol, S. E. Coppard, H. Duque-Caro, S. Finnegan, G. M. Gasparini, E. L. Grossman, K. G. Johnson, L. D. Keigwin, N. Knowlton, E. G. Leigh, J. S. Leonard-Pingel, P. B. Marko, N. D. Pyenson, P. G.

Rachello-Dolmen, E. Soibelzon, L. Soibelzon, J. A. Todd, G. J. Vermeij, J. B. C. Jackson, 2016. Formation of the Isthmus of Panama. Science Advances 2, e1600883.

Ordóñez, O., Pimentel, M., de Moraes, R. and Restrepo, J., 1999. Rocas Grenvillianas en la Región de Puerto Berrío, Antioquia. Revista de la Academia Colombiana de Ciencias 23/87, 225-232.

Ordoñez, O. and Pimentel, M., 2001. Consideraciones Geocronológicas e Isotópicas del Batolito Antioqueño. Revista de la Academia Colombiana de Ciencias, 25/94, 27-35.

Ordóñez, O. and Pimentel, M., 2002. Rb-Sr and Sm-Nd isotopic study of the Puquí Complex, Colombian Andes. Journal of South American Earth Sciences 15, 173-182.

Ortiz, A., 1995. Sedimentology, Stratigraphy and Reservoir Quality of the Oligocene Limestone at El Dificil, Lower Magdalena Basin, Colombia. MSc. Thesis, Colorado School of Mines.

Osorno, J.F. and Rangel, A., 2015. Geochemical assessment and petroleum systems in the Sinu-San jacinto Basin, northwestern Colombia. Marine and Petroleum Geology, 65, 217-231.

Parra, M., Mora, A., Sobel, E., Strecker, M. and Gonzalez, R., 2009. Episodic orogenic front migration in the northern Andes: Constraints from low-temperature thermochronology in the Eastern Cordillera, Colombia. Tectonics, 28/4. TC4004, doi: 4010.1029/2008TC002423.

Parra, M., Mora, A., Jaramillo, C., Torres, V., Zeilinger, G. and Strecker, M., 2010. Tectonic controls on Cenozoic foreland basin development in the north-eastern Andes, Colombia. Basin Research 22, 874-903.

Parra, M., Mora, A., López, C., Rojas, L. and Horton, B., 2012. Detecting earliest shortening and deformation advance in thrust belt hinterlands: Example from the Colombian Andes. Geology, 40/2, 175–178; doi:10.1130/G32519.1

Parra, D. and Rincón, D., 2014. Foraminferal Assemblaged and Paleoenvironments of the Early to Middle Eocene Succession in the Sinu-San Jacinto basin, Northern South America. Poster presented at the 4th International Paleontological Congress, 28th September to 3rd October, Mendoza, Argentina.

Patchett, P.J., Tatsumoto, M., 1981. A routine high-precision method for Lu–Hf isotope geochemistry and chronology. Contrib. Mineral. Petrol. 75, 263–267, http://dx.doi.org/10.1007/BF01166766

Pennington, W. D., 1981. Subduction of the eastern Panama Basin and seismotectonics of northwestern South America, Journal of Geophysical Research, 86 (B11), 10,753–10,770, doi:10.1029/JB086iB11p10753.

Pepper, A.S. and Corvi, P.J., 1995. Simple kinetic models for petroleum formation: Part III. Modeling an open system. Marine and Petroleum Geology, 12, 417.452.

Peters, K. and Cassa, M.R., 1994. Applied Source Rock Geochemistry. In: Magoon, L. and Dow, W. (eds), The petroleum system-from source to trap. American Association of Petroleum Geologists Memoir 60.

Petters, V., and Sarmiento, R., 1956, Oligocene and lower Miocene Biostratigraphy of the Carmen-Zambrano area, Colombia: Micropaleontology, 2, 7-35.

Petrobras/Ecopetrol, 1996. The Petroleum System of the Lower Magdalena Basin, Colombia: A Geochemical characterization of oils and potential source rocks. Internal report, Bogotá.

Petroscopia S.A. 2013. Petrographic Analysis of fifteen cutting samples from the Curramba Est-1 well, Lower Magdalena Valley basin, Colombia. Internal report, Hocol S.A., Bogotá.

Philippon, M. and Corti, G., 2016. Obliquity along plate boundaries. Tectonophysics, 693, 171-182.

Piedrahita, V., Bernet, M., Chadima, M., Sierra, G., Marin-Ceron, M. and Toro, G., 2017. Detrital zircon fission-track thermochronology and magnetic fabric of the Amagá Formation (Colombia): Intracontinental deformation and exhumation events in the northwestern Andes. Sedimentary Geology 356, 26-42. http://dx.doi.org/10.1016/j.sedgeo.2017.05.003

Pindell, J. L. 1993. Regional synopsis of Gulf of Mexico and Caribbean evolution. In: Pindell, J. L. & Perkins, R. F. (eds) Transactions of the 13th Annual GCSSEPM Research Conference: Mesozoic and early Cenozoic Development of the Gulf of Mexico and Caribbean Region, 251–274.

Pindell, J. and Kennan, L., 2009. Tectonic evolution of the Gulf of Mexico, Caribbean and northern South America in the mantle reference frame: an update. GSL Special Publication 328, 1–55.

Pindell, J., Kennan, L., Maresch, W., Stanek, K., Draper, G., & Higgs, R., 2005. Plate-kinematics and crustal dynamics of circum-Caribbean arccontinent interactions: Tectonic controls on basin development in Proto-Caribbean margins. In H. Avé Lallemant & V. Sisson (Eds.), Caribbean-South American plate interactions, Venezuela, Geological Society of America Special Paper 394, 7–52.

Pinson, W., Hurley, P., Mencher, E and Fairbairn, H., 1962. K-Ar and Rb-Sr Ages of Biotites from Colombia, South America. Geological Society of America Bulletin 73, 907-910.

Piraquive, A., 2016. Cadre structurel, déformations et exhumation des Schistes du Santa Marta: accumulation, et histoire de déformation d'un terrain Caraïbe au nord de la Sierra Nevada de Santa Marta. PhD Thesis, Université Grenoble Alpes/Universidad Nacional de Colombia. 238 p.

Piraquive, A., Pinzon, E., Kammer, A., Bernet, M. and von Quadt, A., 2017. Early Neogene unroofing of the Sierra Nevada de Santa Marta, as determined from detrital geothermochronology and the petrology of clastic basin sediments. Geological Society of America Bulletin, 129/11. https://doi.org/10.1130/B31676.1

Pomar, L., Esteban M., Martinez, W., Espino, D., Castillo, V., Benkovics, L., and Castro Leyva, T., 2015. Oligocene-Miocene carbonates of the Perla field, offshore Venezuela: Depositional model and facies architecture. In: C. Bartolini and P. Mann, (eds.), Petroleum geology and potential of the Colombian Caribbean Margin: American Association of Petroleum Geologists Memoir 108, 647–674.

Poveda, E., Monsalve, G. and Vargas, C., 2012. Crustal thickness estimation beneath the northern Andes (Colombia) from teleseismic receiver functions. Poster presented at the AGU Fall meeting, San Francisco, USA, 3-7 December.

Poveda, E., G. Monsalve, and C. A. Vargas, 2015. Receiver functions and crustal structure of the northwestern Andean region, Colombia, Journal of Geophysical Research, Solid Earth, 120, 2408–2425, doi:10.1002/2014JB011304.

Ramirez, D., Lopez, A., Sierra, G. and Toro, G., 2006. Edad y Proveniencia de las rocas volcánico sedimentarias de la Formacion Combia en el suroccidente antioqueño-Colombia. Boletin de Ciencias de la Tierra, 19, 9-26.

Ramos, V. and Folguera, A., 2009. Andean flat-slab subduction through time. In: Murphy, J. B., Keppie, J. D. & Hynes, A. J. (eds) Ancient Orogens and Modern Analogues. GSL Special Publications, 327, 31–54.

Rangel, A., Gonzalez, S. and Posada, C., 2003. Geoquímica de producción para la reexploración de Areas Cicuco-Boquete, Cuenca Valle Inferior del Magdalena, Colombia. Extended abstract presented at the VIII Simposio Bolivariano Exploración Petrolera en Cuencas Subandinas, Cartagena.

Rangel, A., Osorno, J., Ramirez, J.C., de Bedout, J., Gonzalez, J. and Pabón, M., 2017. Geochemical assessment of the Colombian Oils based on bulk petroleum properties and biomarker parameters. Marine and Petroleum Geology 86, 1291-1309.

Restrepo, J. and Toussaint, J.F., 1988. Terranes and Continental Accretion in the Colombian Andes. Episodes. 11/3. 189-193.

Restrepo, S., Foster, D.A., Kamenov, G., 2007. Formation age and magma sources for the Antioqueño Batholith derived from LA-ICP-MS Uranium–Lead dating and Hafnium-isotope analysis of zircon grains. Geological Society of America, Annual Meeting, Abstracts, 181-28 (Paper).

Restrepo S., Foster, D., Stockli, D. and Parra, L., 2009. Long-term erosion and exhumation of the "Altiplano Antioqueño", Northern Andes (Colombia) from apatite (U–Th)/He thermochronology. Earth and Planetary Science Letters, 278, 1-12.

Restrepo-Pace, P. A. and Cediel, F., 2010. Northern South America basement tectonics and implications for paleocontinental reconstructions of the Americas. Journal of South American Earth Sciences, 29/4, 764–771. http://doi.org/10.1016/j.jsames.2010.06.002

Restrepo, J., Ordoñez, O., Armstrong, R. and Pimentel, M., 2011. Triassic metamorphism in the northern part of the Tahamí Terrane of the central cordillera of Colombia. Journal of South American Earth Sciences 32, 497-507.

Reyes, A., Montenegro, G. and Gómez, P., 2000. Evolución Tectonoestratigráfica del Valle Inferior del Magdalena, Colombia. VII Simposio Bolivariano-Exploración Petrolera en Cuencas Subandinas, 293-309.

Reyes-Harker, A., Ruiz-Valdivieso, C., Mora, A., Ramirez-Arias, J., Rodriguez, G., de la Parra, F., Caballero, V., Parra, M., Moreno, N., Horton, B., Saylor, J., Silva, A., Valencia, V., Stockli, D. and Blanco, V., 2015. Cenozoic paleogeography of the Andean foreland and retroarc hinterland of Colombia. American Association of Petroleum Geologists Bulletin, 99/8, 1407–1453. DOI: 10.1306/06181411110.

Richards, M.T., 2001. Deep Marine Clastic systems. In Emery, D. and Myers, K., (Eds.), Sequence Stratigraphy. Blackwell Science, Oxford, UK.

Ridgway, K., Trop, J. and Finzel, E.,2012. Modification of continental forearc basins by flat-slab subduction processes: a case study from southern Alaska. In: Busby, C and Azor, A., (eds.), Tectonics of Sedimentary basins: Recent Advances. First edition. Blackwell Publishing Ltd.

Rodriguez, G., Zapata, G. and Gómez, J.F., 2010. Memoria de la Geología de la Parte Oriental de la Plancha 114 Dabeiba. Ingeominas, Medellín.

Rodriguez, G., Arango, M.I. and Bermúdez, J.G., 2012. Batolito de Sabanalarga, Plutonismo de Arco en la zona de sutura entre las Cortezas Oceánica y Continental de los Andes del Norte. Boletin de Ciencias de la Tierra 32, 81-98.

Romero-Otero, G., Slatt, R. and Pirmez, C., 2015. Evolution of the Magdalena Deepwater Fan in a Tectonically Active Setting, Offshore Colombia, in C. Bartolini and P. Mann, eds., Petroleum geology and potential of the Colombian Caribbean Margin: American Association of Petroleum Geologists Memoir 108, 675–708.

Ross, M., and Scotese, C., 1988. A hierarchical tectonic model of the Gulf of Mexico and Caribbean region. Tectonophysics, 155, 139–168.

Rossello, E. and Cossey, S., 2012. What is the evidence of subduction in the Caribbean margin of Colombia? Memoirs of the XI Simposion Bolivariano Exploracion en Cuencas subandinas, Cartagena.

Russo, R.M., Speed, R.C., Okal, E.A., Shepherd, J.B., Rowley, K.C., 1993. Seismicity and tectonics of the southeastern Caribbean. J. Geophys. Res. 98 (B8), 14299. http://dx.doi.org/10.1029/93JB00507.

Salazar, A., 1993. Icnología, Facies y Ambiente de depósito de la Formación Ciénaga de Oro en el Pozo Ayombe-1. Report presented to Ecopetrol, Bogotá

Sanchez, C., and Permanyer, A., 2006. Origin and alteration of oils and oil seeps from the Sinú-San Jacinto Basin, Colombia. Org. Geochem. 37, 1831-1845.

Sanchez, J. and Mann, P., 2015. Integrated structural and basinal analysis of the Cesar-Rancheria Basin, Colombia: Implications for it's tectonic history and petroleum systems, in C. Bartolini and P. Mann, eds., Petroleum geology and potential of the Colombian Caribbean Margin: American Association of Petroleum Geologists Memoir 108, 431–470.

Sarmiento, G., Bonilla, G. and Osorio, J., 2016. Evidencias de Vulcanismo Penecontemporáneo en la Formación San Cayetano de la Cuenca Sinu-San Jacinto e Implicaciones en el entorno geológico regional. The Colombian and Venezuelan Caribbean Geology Workshop, May 27, 2016, Universidad Nacional de Colombia, Bogotá.

Saylor, J., Horton, B., Stockli, D., Mora, A., Corredor, J., 2012. Structural and thermochronological evidence for Paleogene basement-involved shortening in the axial Eastern Cordillera, Colombia. Journal of South American Earth Sciences 39, 202-215.

Schepers, G., van Hinsbergen, D., Spakman, W., Kosters, M., Boschman, L. and McQuarrie, N., 2017. South-American plate advance and forced Andean trench retreat as drivers for transient flat subduction episodes. Nature Communications, 8, 15249 doi: 10.1038/ncomms15249.

Sclater, J.G. and Christie, P.A., 1980. Continental stretching: an explanation of the post mid Cretaceous subsidence of the central North Sea basin. Journal of Geophysical Research 85, 3711-3739.

Seely, D.R., Vail, P.R., and Walton, G.G., 1974, Trench slope model, in Burk, C.A., and Drake, C.L., eds., The Geology of Continental Margins: New York, Springer-Verlag, 249–260, doi: 10 .1007 /978 -3 -662 -01141 -6_18.

Silva, A., Mora, A., Caballero, V., Rodriguez, G., Ruiz, C., Moreno, N., Parra, M., Ramirez-Arias, J., Ibañez, M. and Quintero, I., 2013. Basin compartmentalization and drainage evolution during rift inversion: evidence from the Eastern Cordillera of Colombia. In M. Nemcok, A. Mora, and J. Cosgrove, eds., Thick-skin-dominated orogens; from initial inversion to full accretion: GSL Special Publication 377, doi: 10.1144/SP377.6

Silva, A., Paez, L., Rincón, M., Tamara, J., Gomez, P., Lopez, E., Restrepo, S., Mantilla, L. and Valencia, V., 2016. Basement characteristics in the Lower Magdalena Valley and the Sinu and San Jacinto fold belts: Evidence of a Late Cretaceous magmatic arc at the south of the Colombian Caribbean. Ciencia, Tecnología y Futuro, 6/4, 5-36.

Spikings, R.A., Winkler, W., Seward, D., Handler, R., 2001. Along-strike variations in the thermal and tectonic response of the continental Ecuadorian Andes to the collision with heterogeneous oceanic crust. Earth and Planetary Science Letters 186, 57–73.

Spikings, R.A., Crowhurst, P.V., Winkler, W., Villagomez, D., 2010. Syn- and post accretionary cooling history of the Ecuadorian Andes constrained by their in-situ and detrital thermochronometric record. Journal of South American Earth Sciences 30, 121–133.

Spikings, R., Cochrane, R., Villagómez, D., Van der Lelij, R., Vallejo, C., Winkler, W. and Beate, Bernardo, 2015. The geological history of northwestern South America: from Pangaea to early collision of the Caribbean Large Igneous Province (290-75 Ma). Gondwana Research 27, 95-139.

Steckler, M. and Watts, A., 1978. Subsidence of the Atlantic-type continental margin off New York. Earth and Planetary Science Letters, 41, 1-13.

Steel, R., Carvajal. C., Petter, A. and Uroza, C., 2008. Shelf and shelf-margin growth in scenarios of rising and falling sea level. In Hampson, G., Steel, R., Burgess, P. and Dalrymple, R. eds., Recent advances in Models of Siliciclastic shallow-marine stratigraphy. SEPM Special Publication No. 90, 47-71.

Stevens-Goddard, A. and Carrapa, B., 2017. Using basin thermal history to evaluate the role of Miocene–Pliocene flat-slab subduction in the southern Central Andes (27° S–30° S). Basin Research, 1–22, doi: 10.1111/bre.12265.

Stone, B., 1968. Plakntonic foraminiferal zonation in the Carmen-Zambrano area, Colombia. Micropaleontology, 14/3, 363-364.

Sweeney, J. and Burnham, A., 1990. Evaluation of a Simple Model of Vitrinite Reflectance based on chemical kinetics. American Association of Petroleum Geologists Bulletin, 74/10, 1559-1570. Tulsa, OK, USA.

Symithe, S., Calais, E., de Chabalier, J.B., Robertson, R., and Higgins, M., 2015. Current block motions and strain accumulation on active faults in the Caribbean, J. Geophys. Res. Solid Earth, 120, 3748–3774, doi:10.1002/2014JB011779.

Syracuse, E., Maceira, M., Prieto, G., Zhang, H. and Ammon, Ch., 2016. Multiple Plates subducting beneath Colombia, as illuminated by seismicity and velocity from the joint inversion of seismic and gravity data. Earth and Planetary Science Letters 444, 139-149.

Taboada, A., Rivera, L., Fuenzalida, A., Cisternas, A., Philip, H., Bijwaard, H., Olaya, J., Rivera, C., 2000. Geodynamics of the northern Andes: subductions and intracontinental deformation (Colombia). Tectonics, 19/5, 787–813. http://dx.doi.org/10.1029/2000TC900004.

Tatsumi, Y. and Eggins, S. 1995. Subduction Zone Magmatism. Blackwell Science, Frontiers in Earth Sciences, Vol. I, Wiley, 224 pp.

Thery, J.-E., Esquevin, J., Menendez, R., 1977. Signification géotectonique de datations radiométriques dans des sondages de Basse Magdalena (Colombie). Bulletin des Centres de Recherches Exploration-Production Elf-Aquitaine 1, 475–494.

Tissot, B., Durand, B., Espitalié, J. and Combaz, A., 1974. Influence of the nature and diagenesis of organic matter in the formation of petroleum. American Association of Petroleum Geologists Bulletin, 58, 499-506.

Tissot, B. and Welte, D., 1984. Petroleum Formation and occurrence. 2nd edition. Springer Verlag, NY.

Toro, G., Rendon, D. and Montes, L., 2007. Levantamiento de los Andes en el norte de la Cordillera Central de Colombia: Una aproximación geomorfológica, estructural y cronológica (trazas de fisión). Boletin Ciencias de la Tierra, 22, 125-126.

Toussaint, J.F. and Restrepo, J.J., 1994. The Colombian Andes during Cretaceous times. In: Vieweg, S. (Ed.), Cretaceous Tectonics of the Andes, 61-100, Wiesbaden.

Trenkamp, R., Kellogg, J., Freymueller, J. and Mora, H., 2002. Wide plate margin deformation, southern Central America and northwestern South America, CASA GPS observations. Journal of South American Earth Sciences 15, 157-171.

Tschanz, Ch., Marvin, R., Cruz, J., Mehnert, H. And Cebula, G., 1974. Geologic Evolution of the Sierra Nevada de Santa Marta, Northeastern Colombia. Geological Society of America Bulletin 85, 273-284.

Vail, P.R., Mitchum Jr., R.M., Thompson III, S., 1977. Seismic stratigraphy and global changes of sea level, part 3: relative changes of sea level from coastal onlap. In: Payton, C.E. (Ed.), Seismic Stratigraphy — Applications to Hydrocarbon Exploration. Memoir 26, American Association of Petroleum Geologists, 63–81.

Van Benthem, S., Govers, R., Spakman, W. and Wortel, R., 2013. Tectonic evolution and mantle structure of the Caribbean. Journal of Geophysical Research, 118, 3019-3036.

Van der Hammen, T., 1960. Estratigrafía del Terciario y Maestrichtiano continentales y tectogénesis de los Andes Colombianos, Informe No. 1279. Servicio Geológico Nacional, Bogotá. 128 pp.

Van der Hilst, R. D., and Mann, P.,1994. Tectonic implications of tomographic images of subducted lithosphere beneath northwestern South America, Geology, 22, 451–454.

Van der Lelij, R., Spikings, R., Ulianov, A., Chiaradia, M., & Mora, A., 2016. Palaeozoic to Early Jurassic history of the northwestern corner of Gondwana, and implications for the evolution of the Iapetus, Rheic and Pacific Oceans. Gondwana Research, 31, 271–294. http://doi.org/10.1016/j.gr.2015.01.011

Van Hinte, J., 1978. Geohistory Analysis – Application of Micropaleontology in Exploration Geology. Bulletin of the American Association of Petroleum Geologists 62/2, 201-222.

Van Wagoner, J.C., Mitchum Jr., R.M., Campion, K.M., Rahmanian, V.D., 1990. Siliciclastic sequence stratigraphy in well logs, core, and outcrops: concepts for high-resolution correlation of time and facies. American Association of Petroleum Geologists Methods in Exploration Series, 7. 55 pp.

Vargas, L. and Mantilla, M., 2006. Modelo de Carga de Hidrocarburos en el Sector Suroccidental de la Subcuenca de Plato, Valle Inferior del Magdalena, Colombia. Extended abstract presented at the 9th Simposio Bolivariano de Cuencas Subandinas, September, 2006, Cartagena, Colombia.

Vargas, C. and Mann, P., 2013. Tearing and breaking off of subducted slabs as the result of collision of the Panama arc-indenter with northwestern South America. Bulletin of the Seismological Society of America, 103/3, 2025–2046. https://doi.org/10.1785/0120120328

Vargas, Carlos A., Idarraga-Garcia, J. and Salazar, J., 2015. Curie point depths in northwestern South America and the southwestern Caribbean Sea. C. Bartolini and P. Mann, (eds.), Petroleum geology and potential of the Colombian Caribbean Margin: American Association of Petroleum Geologists Memoir 108, 179–200.

Veloza, G., Styron, R., Taylor, M. and Mora, A., 2012. Open-source archive of active faults for northwest South America. GSA Today, 22/10, 4-10.

Vence, E.M., 2008. Subsurface structure, stratigraphy and regional tectonic controls of the Guajira Margin of northern Colombia. MSc. Thesis, U. of Texas at Austin, 128p.

Vervoort, J. D., and Blichert-Toft, J., 1999. Evolution of the depleted mantle: Hf isotope evidence from juvenile rocks through time. Geochimica Et Cosmochimica Acta, 63(3), 533–556.

Vervoort, J., Patchett, P., Soderlund, U., Baker, M., 2004. Isotopic composition of Yb and the determination of Lu concentrations and Lu/Hf ratios by isotope dilution using MC-ICPMS. Geochem. Geophys. Geosyst. 5, Q11002, http://dx.doi.org/10.1029/2004GC000721

Villagómez, D., Spikings, R., Magna, T., Kammer, A., Winkler, W. And Beltrán, A., 2011a. Geochronology, Geochemistry and Tectonic Evolution of the Western and Central Cordilleras of Colombia. Lithos, 125, 875-896.

Villagómez, D., R. Spikings, A. Mora, G. Guzmán, G. Ojeda, E. Cortés, and R. van der Lelij, 2011b, Vertical tectonics at a continental crust-oceanic plateau plate boundary zone: Fission track thermochronology of the Sierra Nevada de Santa Marta, Colombia, Tectonics, 30, TC4004, doi:10.1029/2010TC002835.

Villagómez, D., Spikings, R., 2013. Thermochronology and tectonics of the Central and Western Cordilleras of Colombia: Early Cretaceous–Tertiary evolution of the Northern Andes. Lithos 168, 228–249.

Villamil, T., 1999, Campanian–Miocene tectonostratigraphy, depocenter evolution and basin development of Colombia and western Venezuela: Palaeogeography, Palaeoclimatology, Palaeoecology, v. 153, p. 239–275, doi: 10.1016/S0031-0182(99)00075-9.

Vinasco, C.J., Cordani, U., Gonzalez, H., Weber, M and Pelaez, C., 2006. Journal of South American Earth Sciences 21, 355-371.

Waples, D.,1981. Organic Geochemistry for Exploration Geologists. Burgess Publishing Company, USA. 151p.

Watts, A. and Ryan, W., 1976. Flexure of the Lithosphere and Continental margin basins. Tectonophysics, 36, 25-44.

Weber, M., Cardona, A., Valencia, V., García-Casco, A., Tobón, M., Zapata, S., 2010. U/Pb detrital zircon provenance from Late Cretaceous metamorphic units of the Guajira Peninsula, Colombia: tectonic implications on the collision between the Caribbean arc and the South American margin. Journal of South American Earth Sciences, 29, 805-816.

Weber, M., Gomez, J., Cardona, A., Duarte, E., Pardo, A. and Valencia, V., 2015. Geochemistry of the Santa Fe Batholith and Buritica Tonalite in NW Colombia - Evidence of subduction initiation beneath the Colombian Caribbean Plateau. Journal of South American Earth Sciences, 62, 257-274.

Wernicke, B., 1981. Low-angle normal faults in the Basin and Range province: nappe tectonics in an extending orogen. Nature, 291, 645-648.

Wernicke, B., 1985. Uniform-sense normal simple shear of the continental lithosphere. Canadian Journal of Earth Sciences, 22, 108-125.

Wijninga, V.M., 1996, Palynology and paleobotany of Neogene sediments from the high plain of Bogotá (Colombia): Evolution of the Andean flora from an ecological perspective [Ph.D. thesis]: University of Amsterdam, 370 p.

Woodhead, J.D., Hergt, J.M., 2005. A preliminary appraisal of seven natural zircon reference materials for in situ Hf isotope determination. Geostand. Geoanal. Res. 29, 183–195, http://dx.doi.org/10.1111/j.1751-908X.2005.tb00891.x

Wygrala, B., 1989. Integrated study of an oil field in the southern Po Basin, northern Italy. PhD Thesis, University of Cologne, Germany.

Xie, X., and Heller, P.L., 2009, Plate tectonics and basin subsidence history: Geological Society of America Bulletin, 121/1–2, 55–64, doi: 10 .1130 /B26398 .1.

Yarce, J., Monsalve, G., Becker, Th., Cardona, A., Poveda, E., Alvira, D. and Ordoñez, O., 2014. Seismological observations in Northwestern South America: Evidence for two subduction segments, contrasting crustal thicknesses and upper mantle flow. Tectonophysics, 637, 57-67.

Zachos, J., Pagani, M., Sloan, L.C., Thomas, E., and Billups, K., 2001, Trends, rhythms, and aberrations in global climate 65 Ma to present: Science, v. 292, p. 686–93, doi: 10 .1126 /science.1059412.

Zarifi, Z., J. Havskov, and A. Hanyga (2007), An insight into the Bucaramanga nest, Tectonophysics, 443, 93–105.

List of Figures

List of Tables

Acknowledgements

The present thesis was made possible thanks to Hocol S.A. (Bogotá, Colombia) which provided the database and the financial support to carry out this research in Germany and Colombia. In Hocol, my greatest thanks go to Mario de Freitas, former Exploration Vicepresident at Hocol S.A. and my mentor in Petroleum Geology, from whom I've learned a lot, not only technically but also personally. He was my first boss when I started working in the oil industry with Petrobras and he later asked me to join Hocol, just when I was planning to leave to do a PhD in Canada. Several years after that, I am really glad I accepted his offer because it brought to my life only good things. Working with him in Hocol has been a great professional and personal experience for me and it also allowed me to continue with my initial plans of doing a PhD. In fact, Mario was the person in Hocol who helped and supported me most in my plans to do a PhD. I also became interested in photography and especially in bird watching thanks to him; being a foreigner, he made me much more aware of the real value of the natural and cultural treasures and diversity of my own country.

The investigation was undertaken at Hocol offices in Bogotá, and at the German Research Centre for Geosciences (Deutsches GeoForschungs Zentrum –GFZ), Postdam, Germany. I am extremely grateful to Professor Doctor Onno Oncken for accepting me to come to the GFZ, and for his valuable guidance, supervision and patience during all my PhD. Thanks to him I spent an excellent, fruitful and unforgettable time at the GFZ and in Germany.

Many thanks to Dr. Robert Ondrak (GFZ) who kindly accepted to help me with basin and petroleum system modelling and introduced me to the PetroMod modeling software. Thanks a lot to him for his patience and time.

I also received important feedback for my PhD from external researchers such as Dr. Eline Le Breton (Free University Berlin), Dr. Mauricio Ibáñez-Mejía (U. Rochester), Professor Claudio Faccenna (UniRoma Tre) and Professor Alan Levander (Rice).

I must also thank Franziska Alberg for help kindness and help, especially by arranging everything related to my stay at the GFZ, where I always had a nice and well-equipped office to carry out my research. Antje Schäfer's help and kindness are also acknowledged.

Living and studying in Germany was a wonderful experience in every aspect, especially because of the great people I met, not only from Germany but also from other parts of the world. First of all, it was great meeting all the staff at section 4.1. I was lucky to make friends like my office mates Shaoyang Li and Michael Rudolf, Felix Hoffmann, Jonathan Bedford, Oystein Haug, Io Ioannidi, Sofia Kufner, Malte Ritter and the Chilean colony (Hugo, Marcos, Isabel and Begoña). Thanks to Sofia and Michael for their help with the thesis abstract. I also want to mention other friends I made outside my section and of the GFZ, like Ricardo Ruiz, Iskander Muldashev, Maria Michail and Bo Fang Pen.

Thanks a lot to Wilfried Herr and Heiner Brauer for their help and patience with IT issues.

I want to express my gratitude to many other people from Hocol who contributed to my PhD project. Vickye Vélez supported and helped me a lot with these plans, especially by giving me time for the trip preparation and for finishing my thesis while working at Hocol's offices. I am also very grateful to Claudia Varela, former Human Resources manager at Hocol, who supported this initiative since the very beginning. Elsa Jaimes, Exploration Vicepresident at Hocol, is also acknowledged for her help and support for finishing this PhD. My PhD plans were approved while Alvaro Vargas was president of Hocol S.A., so I thank him very much for that. Eida Tobián and Jaime Martínez are

acknowledged for their help for traveling and living in Germany. I also thank Guillermo Fonseca, current president of Hocol S.A., for his final approval of my PhD plans.

All my colleagues in Hocol's exploration team are also thanked for their help during my absence and for fruitful discussions that contributed greatly to improve my PhD dissertation. In particular, many thanks to Alexis Rosero for keeping me up to date with all the news from Colombia. Jaime Rocha helped me a lot gathering the necessary data and assembling the Petrel project for the trip to Germany. Hernán Carvajal, Jaime López, Diego Quiroga and Mirenchu Gonzalez were also very helpful with data such as GIS, maps, drawings, etc.

Flavio Granados and Patricia Prada helped us a lot with the plane tickets and other logistic matters, while Neida Ortiz and Rocío helped my wife and me with all our health exams, insurances and other issues.

Román Gonzalez, Wilson Zamora, Camilo Higuera and other colleagues from Ecopetrol contributed with discussion, ideas and suggestions to the PhD. I am also grateful to Juan Pablo Arias for his help in structural cross-section construction and restoration.

My decision to come to Germany to do this PhD was greatly influenced by my geologist brother, Andrés Mora, whom I admire and love very much, so I want to thank him for putting me in contact with Prof. Dr. Oncken and for all his help. All my love also goes to the rest of my brothers and sisters (Liliana, Pilar, Rodrigo and Ximena) and to lovely their "kids".

I also have to thank my wife's family (Ramón, Gloria, Felipe, Diana, Hugo and Julio) for supporting us in our plans to live for more than two years away from home and for taking care of everything in Bogotá.

Dr. Luis Vergara encouraged me not only to study geology as an undergraduate career, but also to continue studying and to do a PhD, so I am very grateful to him.

I dedicate this PhD to my wife Alejandra and to my parents, Josué and Zoraida. My dear wife Alejandra put aside her career and work commitments to support and follow me in this adventure in Germany. She sacrificed more than two years of her career to carry out this trip, including the long initial months in which we had to apply and wait for our visas and residence permits to be issued. Then, back in Colombia, she was also very patient with me when I dedicated long working days and nights to finish the PhD. Without her constant love, patience, help and support I would not have successfully finished this PhD. All my love and my gratitude to her. I am also deeply indebted with my parents who dedicated their lives to work hard in order to give their six sons the best education they could.

Finalmente, gracias a Dios por haberme dado esta oportunidad única en la vida.

Zusammenfassung

In dieser Arbeit verwende Ich einen regionalgeologischen und geophysikalischen Datensatz um die Entwicklung des Unteren Magdalena Talbeckens und des San Jacinto Faltengürtels im Nordwesten Kolumbiens von der frühen Kreide bis heute zu rekonstruieren. Meine detaillierte Interpretation von Reflexionsseismik und neuen geochronologischen Analysen zeigen, dass das untere Magdalena Becken die nördliche Verlängerung der Grundgebirgs Terrane der nördlichen Zentral Kordilleren ist. Diese bestehen aus permo-triassischen Metasedimenten welche von spätkreidezeitlichen Granitoiden intrudiert wurden. Die Analyse der Strukturen suggeriert, dass der NO-SW Trend der Störungen im Grundgestein im Unteren Magdalena Becken von einer jurazeitlichen Grabenbildung stammt, während der OSO-WNW Trend während eines spätkreidezeitlichen bis eozänem Blattverschiebungs- und Grabenbildungsphase entstand. Die Sedimente des San Jacinto Faltengürtes aus der der Oberkreide bis zum Untereozän, wurden im sich durch die schiefe Konvergenz der Karibischen und Südamerikanischen Platte bildenden marinen Forearc-Becken abgelagert. Es wird angenommen, das eine unter- bis mitteleozäne Winkeldiskordanz oberhalb der San Cayetano Sequenz, das Ende der Störungsaktivität im Romeral Störungssystem und der Rückgang der vulkanischen Aktivität, den Beginn der flachen Subduktion des Karibischen Plateaus unter die Südamerikanische Platte darstellt, welche vor 56 bis 43 Ma stattfand. Die flache Subduktion dauert bis heute an und ist die Hauptursache für magmatische post-eozäne Ablagerungen und die Bildung des unteren Magdalena Talbeckens. Nach dem Kollaps eines pre-oligozänen magmatischen Bogens, spätoligozäne bis frühmiozäne störungskontrollierte Subsidenz erlaubte die ursprüngliche Verfüllung des unteren Magdalena bei niedriger Sedimentationsrate. Oligozäne bis frühmiozäne Anhebung der Anden Terrane machten eine Verbindung des unteren und mittleeren Magdalena Beckens möglich und führte somit zur Bildung des wichtigsten kolumbianischen Entwässerungssystems, dem Magdalena-Fluss-System. Dieses Flusssystem lieferte enorme Mengen Sediment im mittleren Miozän, während die Störungsaktivität nachließ und schrittweise durch eine setzungskontrollierte Absenkung ersetzt wurde, welche durch die große sedimentäre Auflast verstärkt wurde. Der dramatische Anstieg der Sedimentmenge führte zu einem hohen Sedimenteintrag im Graben und daher zur Bildung von forearc Erhebungen in San Jacinto und eines Akkretionskeils im weiter entfernten Westen. Diese Ergebnisse zeigen die fundamentalen Auswirkungen Veränderungen in Plattenkinematik und Sedimentfluss, auf Forearc-Becken, wie z.B. des unteren Magdalena und San Jacinto, haben.

Meine Ergebnisse und Interpretationen zur Bildung, die zeitliche Entwicklung von der Kreide bis heute, der tektonostratigraphische Aufbau und die Sedimentfüllung des unteren Magdalena Beckens und des San Jacinto Faltengürtels, sind Eingangsparameter für die multidimensionale Becken- und Erdöl-System Modellierung welche ich durchgeführt habe. Ein dreidimensionales Modell des unteren Magdalena Beckens wurde aus Seismikdaten und Bohrungsdaten erstellt, und zur Rekonstruktion der thermischen und Maturitätsentwicklung des Beckens verwendet. Ich habe die stratigrafische Architektur des Beckens rekonstruiert, die verschiedenen Hebungs- und Erosionsphasen implementiert und eine geothermische Gradientenkarte erstellt, welche zur Generierung von Wärmeflusskarten in 3D benötigt wurden. Die Ergebnisse der Modellierung deuten darauf hin, dass die Bildung von Erdöl vor ca. 15 Ma (Mittelmiozän) innerhalb oberoligozäner Schichten im nördlichen Teils des Beckens (Plato-Depocenter) begann, während die Bildung von Kohlenwasserstoffen aus untermiozänen Ursprungsgesteine vor etwa 9 Ma (Mittel-Spätmiozän) begann. Die Maturität wurde durch die schnelle und reichliche Sedimentation von tiefmarinen und deltaischen Sedimenten des Oligozäns und Untermiozäns beeinflusst. Die Bildung aus spätmiozänen Schichten wurde durch episodische Verkürzung und Anhebung während des Pliozän (4-3 Ma) und Pleistozän unterbrochen, obwohl im zentralen Ablagerungsraum die Maturation fortgesetzt wurde. Eine schlechte bis mittelmäßige Qualität der Ursprungsgesteine, wird

scheinbar durch die große Schichtdicke der oligozänen bis untermiozänen Gesteine kompensiert, welche immer noch Kohlenwasserstoffe unterhalb von 3350 m (11000 ft) generieren, vor allem im Zentralbereich der bisherigen Aktivität im nördlichen Teil des unteren Magdalena (Plato-Depocenter). Im Gegensatz dazu, wurde die Maturation in oligozänen und frühmiozänen Ursprungsgesteinen durch die Verkürzungsphasen und einen niedrigen thermischen Gradienten verhindert. Daher werden weitere mögliche Kohlenwasserstoffquellen benötigt, welche das Vorkommen von Dry-Gas in diesem Teil des Beckens erklären. Als mögliche Quellen kommen pre-oligozäne Einheiten, welche im westlichen San Jacinto Depocenter vorliegen, oder Biogenese in Frage. Vorläufige 1D und 2D Modellierung im San Jacinto Faltengürtel, kalibriert mit thermischen Maturitätsdaten, unterstützt die vermutete Beckenentwicklung welche zeigt, dass der San Jacinto als Forearc-Anhöhe agierte und nicht in großer Tiefe lag. Die Ergebnisse aus dieser Arbeit geben neue Einblicke in die Auswirkungen von Plattentektonik und Beckenentwicklung auf Kohlenwasserstoff-Systeme.

Erklärung

Hiermit versichere ich, dass ich die vorliegende Dissertation ohne unzulässige Hilfe Dritter und ohne Benutzung anderer als der angegebenen Literatur angefertigt wurde. Die Stellen der Arbeit, die anderen Werken wörtlich oder inhaltlich entnommen sind, wurden durch entsprechende Angaben der Quellen kenntlich gemacht. Diese Arbeit hat in gleicher oder ähnlicher Form noch keiner Prüfungsbehörde vorgelegen.

Berlin, 15 Dezember 2017

Curriculum Vitae

For reasons of data protection, the Curriculum Vitae is not published in the electronic version.